

Advanced Oxidation Process Models for Optimisation and Decision Making Support in Water Management

This dissertation is submitted for the degree of *Doctor of Philosophy* by

Francesca Audino

Directed by

Prof. Dr. Moisès Graells Sobre

Prof. Dr. Montserrat Pérez Moya



Universitat Politècnica de Catalunya

PhD Program in Chemical Engineering

June 2019

Nothing in life is to be feared, it is only to be understood.

Marie Curie

Declaration

I HEREBY STATE:

1) That in my capacity as the author of the thesis entitled “**Advanced Oxidation Process Models for Optimisation and Decision Making Support in Water Management**” (hereinafter “the thesis”), I am the exclusive owner of the intellectual property rights relating to its content.

2) That this work is original, that its content is lawful and does not violate the interests and rights of third parties as regards industrial property, intellectual property, trade secrets or any other interests and rights that are protected by legal regulations, and that the texts, pictures, images, graphs and other material by third parties contained therein have been duly cited without violating the rights of these third parties.

3) That I am aware that article 14 of Royal Decree 99/2011 of 28 January, which regulates official doctoral studies, states that, once approved, the thesis must be incorporated into an institutional repository that is freely available for consultation.

4) That I have been informed that, in accordance with an agreement by the Interuniversity Council of Catalonia, to meet this legal obligation the thesis will be included in the Theses and Dissertations Online repository (TDX, www.tdx.cat).

5) That I am aware that in exceptional circumstances determined by the programme's academic committee, such as the participation of companies in the programme or school, the existence of confidentiality agreements with companies or the possibility of patents being generated from the content of the thesis, the University guarantees that no publicity relating to these issues will be given during the time required in each case.

6) That as the holder of the rights, I would like the thesis to be disseminated with:

Advanced Oxidation Process Models for Optimisation and Decision Making support in Water Management

CC Attribution - NonCommercial (by-nc) license: Commercial use of the work is not permitted. Derivative works may be generated as long as they are not used commercially.

Declaración

DECLARO

- 1) Que en mi condición de AUTORA de la tesis doctoral denominada **“Advanced Oxidation Process Models for Optimisation and Decision Making Support in Water Management”** (en adelante “la tesis”), me corresponden de forma exclusiva los derechos de propiedad intelectual sobre sus contenidos.
- 2) Que esta obra es original, sus contenidos son lícitos y no perjudican los intereses y derechos de terceros en materia de propiedad industrial, intelectual, secreto comercial o cualquier otro protegido por el ordenamiento, y que los textos, cuadros, imágenes, gráficos u otros materiales obra de terceros que puedan figurar han sido incorporados en base al derecho de cita y sin conculcar los derechos de estos terceros.
- 3) Que me consta que el Real Decreto 99/2011 de 28 de enero, por el que se regulan las enseñanzas oficiales de doctorado establece en el artículo 14 que una vez aprobada, la tesis se debe incorporar a un repositorio institucional para que sea libremente consultable.
- 4) Que me declaro informado/a que para cumplir esta obligación legal la difusión de la tesis se efectuará, por un acuerdo del Consell Interuniversitari de Catalunya, desde el repositorio Tesis Doctorals en Xarxa (TDX, www.tdx.cat).
- 5) Que me consta que en circunstancias excepcionales determinadas por la comisión académica del programa, como pueden ser, entre otras, la participación de empresas en el programa o Escuela, la existencia de convenios de confidencialidad con empresas o la posibilidad de generación de patentes que recaigan sobre el contenido de la tesis, la universidad asegurará la no publicidad de estos aspectos durante el tiempo que sea necesario en cada caso.
- 6) Que como titular de los derechos deseo que la tesis se difunda con:

Advanced Oxidation Process Models for Optimisation and Decision Making support in Water Management

CC Reconocimiento - NoComercial (by-nc): Se permite la generación de obras derivadas siempre que no se haga un uso comercial. Tampoco se puede utilizar la obra original con finalidades comerciales.

Declaració

DECLARO

1) Que en la meua condició d' AUTORA de la tesi doctoral denominada **“Advanced Oxidation Process Models for Optimisation and Decision Making Support in Water Management”** (en endavant “la tesi”), em corresponen de forma exclusiva els drets de propietat intel·lectual sobre els seus continguts.

2) Que aquesta obra és original, els seus continguts són lícits i no perjudiquen els interessos i drets de tercers en matèria de propietat industrial, intel·lectual, secret comercial o qualsevol altre protegit per l'ordenament, i que els textos, quadres, imatges, gràfics o altres materials obra de tercers que hi poden figurar han estat incorporats en base al dret de cita i sense conculcar els drets d'aquests tercers.

3) Que em consta que el Real Decreto 99/2011 de 28 de enero, por el que se regulan las enseñanzas oficiales de doctorado estableix a l'article 14 que un cop aprovada, la tesi s'ha d'incorporar a un repositori institucional per tal que sigui lliurement consultable.

4) Que em declaro informat/da que per complir aquesta obligació legal la difusió de la tesi s'efectuarà, per un acord del Consell Interuniversitari de Catalunya, des del repositori Tesis Doctorals en Xarxa (TDX, www.tdx.cat).

5) Que em consta que en circumstàncies excepcionals determinades per la comissió acadèmica del programa, com poden ser, entre altres, la participació d'empreses en el programa o Escola, l'existència de convenis de confidencialitat amb empreses o la possibilitat de generació de patents que recaiguin sobre el contingut de la tesi, la universitat assegurarà la no publicitat d'aquests aspectes durant el temps que sigui necessari en cada cas

6) Que com a titular dels drets desitjo que la tesi es difongui amb:

Llicència CC Reconeixement - NoComercial (by-nc): Es permet la generació d'obres derivades sempre que no se'n faci un ús comercial. Tampoc es pot utilitzar l'obra original amb finalitats comercials.

Dichiarazione

Dichiaro:

1) Nella mia qualità di autore della tesi dal titolo **“Advanced Oxidation Process Models for Optimisation and Decision Making Support in Water Management”** (di seguito "la tesi"), di essere proprietaria esclusiva dei diritti di proprietà intellettuale relativi al suo contenuto.

2) Che questo lavoro è originale, che il suo contenuto è lecito e non viola gli interessi e i diritti di terzi in materia di proprietà industriale, proprietà intellettuale, segreti commerciali o altri interessi e diritti che sono protetti da norme legali, e che il testo, immagini, foto, grafici e altro materiale di terzi in esso contenuti sono stati debitamente citati senza violare i diritti di queste terze parti.

3) Che sono a conoscenza del fatto che l'articolo 14 del regio decreto n. 99/2011 del 28 gennaio, che disciplina gli studi di dottorato ufficiali, stabilisce che, una volta approvata, la tesi deve essere incorporata in un archivio istituzionale liberamente consultabile.

4) Di essere stato informata che, conformemente ad un accordo del Consiglio Interuniversitario della Catalogna, per adempiere a questo obbligo legale la tesi sarà inclusa nell'archivio Tesi e Dissertazioni Online (TDX, www.tdx.cat).

5) Che sono consapevole che in circostanze eccezionali determinate dal comitato accademico del programma, come la partecipazione di aziende al programma o alla scuola, l'esistenza di accordi di riservatezza con le aziende o la possibilità di brevetti generati dal contenuto della tesi, l'Università garantisce che nessuna pubblicità relativa a questi aspetti sarà data durante il tempo richiesto in ciascun caso.

6) Che come titolare dei diritti, vorrei che la tesi venisse divulgata con:

Licenza CC Attribuzione - Non commerciale (by-nc): l'uso commerciale del lavoro non è permesso. Le opere derivate possono essere generate purché non vengano utilizzate commercialmente.

Acknowledgements

This work was supported by the Spanish "Ministerio de Economía, Industria y Competitividad (MINECO)" and the European Regional Development Fund, both funding the research Project SIGERA (DPI2012-37154-C02-01) and AIMS (DPI2017-87435-R). Francesca Audino, particularly acknowledges the MINECO for the PhD grant [BES-2013-065545].

Agradecimientos

Este trabajo fue apoyado por el "Ministerio de Economía, Industria y Competitividad (MINECO)" y el Fondo Europeo de Desarrollo Regional que han financiado los proyectos de investigación SIGERA (DPI2012-37154-C02-01) y AIMS (DPI2017-87435-R). Francesca Audino, en particular, agradece al MINECO por la beca de doctorado [BES-2013-065545].

Agraïments

Aquest treball va ser recolzat pel "Ministeri d'Economia, Indústria i Competitivitat (MINECO)" i el Fons Europeu de Desenvolupament Regional que han finançat els projectes d'investigació SIGERA (DPI2012-37154-C02-01) i AIMS (DPI2017-87435-R). Francesca Audino, en particular, agraeix al MINECO per la beca de doctorat [BES-2013-065545].

Ringraziamenti

Questo lavoro è stato sostenuto dal Ministero Spagnolo dell'Economia, dell'Industria e della Competitività (MINECO) e dal Fondo Europeo di Sviluppo Regionale, che finanziano entrambi i progetti di ricerca SIGERA (DPI2012-37154-C02-01) e AIMS (DPI2017-87435-R). Francesca Audino, in particolare, ringrazia il MINECO per la borsa di dottorato [BES-2013-065545].

Abstract

The objective of this thesis is contributing to the development of a systematic modelling approach for a more efficient and sustainable water management.

The main aim is introducing Chemical and Process System Engineering methods and tools to provide a contribution to the AOPs (Advanced Oxidation Processes) investigation field by proposing process models that can be exploited to progress towards efficient management strategies for practical AOPs operation and inclusion in wastewater treatment networks.

First, different Advanced Oxidation Processes, namely Fenton, photo-Fenton and VUV photo-oxidation, were investigated and compared for the treatment of paracetamol (PCT) aqueous solution, by evaluating a series of performance indicators. Among the selected AOPs, VUV photo-oxidation and photo-Fenton showed the most promising results. Both processes allowed attaining total removal of the target compound and high mineralization levels.

The second and main part of the thesis was focused on transforming “data into knowledge” by proposing different modelling approaches. The modelling effort focused on Fenton/photo-Fenton processes that showed the need of improving operating conditions.

Accordingly, two practical kinetic models for Fenton and photo-Fenton degradation of organic compounds have been proposed and validated:

- A conventional First Principles Model, based on a line source radiation model with spherical and isotropic emission, developed for the prediction of Fenton and photo-Fenton degradation of PCT and the oxidant (H_2O_2) consumption;
- A general non-conventional First Principles Model, based on a wide-ranging contaminant degradation mechanism considering a variable number of carbon atoms for the characterization of the intermediates.

Both models were experimentally validated and showed that were able to satisfactorily reproduce the system behavior. Particularly, the non-

conventional First Principles Model showed to be a successful modelling approach for the Fenton/photo-Fenton degradation of different wastewater systems composed by single or multiple organic contaminants by means of lumped parameters (e.g. Total Organic Carbon-TOC). Thus, the approach proved to offer practical characterization of complex mixtures of chemicals.

Once process models are proposed and validated, they can be systematically exploited to determine efficient operation modes or design alternatives. Accordingly, the thesis addressed two cases of practical interest: the optimisation of a control recipe and the design of a treatment network.

Particularly, a dynamic optimisation framework for taking advantage of available kinetic models and determining the best hydrogen peroxide dosage profile, was proposed. Economic and environmental objectives and constraints were included to develop a dynamic optimisation problem that was implemented in JModelica and solved using a direct simultaneous optimisation method (IPOPT).

Finally, the combination of cheaper conventional biological processes with more expensive AOPs was explored. A Mixed-Integer Non Linear Programming (MINLP) model for the optimisation of a general wastewater network was proposed based on a superstructure of alternative designs, which was implemented and solved in GAMS. The novel formulation includes the BOD₅/COD ratio method, describing the removal efficiency of BOD₅ and COD of a treatment for modelling the variation of the biodegradability of the influents. This novel formulation allows determining the extent of the AOP treatments when combined with biological treatments, and paves the way for more complex models aimed at solving the trade-off between cost and treatment efficiency.

Resumen

El objetivo de esta tesis es contribuir al desarrollo de técnicas de modelado sistemático para una gestión del agua eficiente y sostenible.

El objetivo principal es contribuir a la investigación de los PAOs (Procesos Avanzados de Oxidación). La tesis introduce métodos y herramientas de Ingeniería de Procesos Químicos y propone modelos que puedan ser explotados para producir estrategias eficientes de gestión y operación de los PAOs, así como para la integración de estos PAOs en redes de tratamiento de aguas residuales.

Primero, se investigaron diferentes PAOs. Se consideraron los procesos Fenton, foto-Fenton y la foto-oxidación VUV, y se compararon en el tratamiento de soluciones acuosas de paracetamol (PCT) adoptando una serie de indicadores de rendimiento (Key Performance Indicators, KPI). Entre los PAOs seleccionados, la foto-oxidación VUV y foto-Fenton produjeron los resultados más prometedores, permitiendo lograr la eliminación total del contaminante y alto nivel de mineralización.

La segunda parte de la tesis se centró en transformar “datos en conocimiento” mediante la propuesta de modelos para los procesos Fenton /photo-Fenton con el fin de mejorar las condiciones operativas de los mismos.

En concreto, se han propuesto y validado dos modelos cinéticos que describen la degradación de compuestos orgánicos por procesos Fenton y foto-Fenton:

- Un Modelo de Principios Básicos convencional, que incluye la modelización de la radiación lineal con emisión esférica e isotrópica, desarrollado para predecir la degradación Fenton y foto-Fenton del PCT y el consumo de oxidante (H_2O_2);
- Un Modelo de Principios Básicos no convencional, que propone un mecanismo de degradación de contaminantes general puesto que considera el número de átomos de carbono del contaminante como la variable de

partida para la propuesta de fragmentación y consiguiente generación de intermedios.

Ambos modelos se validaron experimentalmente y mostraron reproducir satisfactoriamente el comportamiento del sistema. En particular, el Modelo de Principios Básicos no convencional generó resultados prometedores para la degradación Fenton / foto-Fenton de diferentes sistemas (compuestos por uno o más contaminantes orgánicos) por medio de parámetros globales (como el Carbono Orgánico Total). Por tanto, este enfoque ofrece un modelado práctico independiente del contaminante y válido para mezclas complejas de productos químicos.

Una vez propuestos y validados, los modelos de proceso se pueden utilizar sistemáticamente para determinar modos de operación eficientes o alternativas de diseño. En consecuencia, la tesis se dirigió a dos casos de interés práctico: la optimización de una receta de control y el diseño de una red de tratamiento.

En el primer caso, se propuso una estrategia de optimización dinámica para aprovechar los modelos cinéticos disponibles y determinar el mejor perfil de dosificación de peróxido de hidrógeno. Se incluyeron objetivos y limitaciones económicas y ambientales para desarrollar un problema de optimización dinámica que se implementó en JModelica y se resolvió utilizando un método de optimización simultánea directa (IPOPT).

Finalmente, se exploró la combinación de procesos biológicos convencionales, más baratos, con PAOs, más costosos. Se propuso un modelo de Programación no Lineal de Enteros Mixtos (MINLP) para la optimización de una red general de aguas residuales, basado en una superestructura de diseños alternativos, que se implementó y resolvió en GAMS. La nueva formulación incluye la relación BOD_5 / COD , que describe la eficiencia de eliminación de BOD_5 y COD de un tratamiento con el fin de modelar la variación de la biodegradabilidad de los influentes. Esta novedosa formulación permite determinar el alcance de los tratamientos de PAOs cuando se combinan con tratamientos biológicos, y allana el camino para modelos más complejos destinados a resolver el equilibrio entre coste y eficiencia del tratamiento.

Resum

L'objectiu d'aquesta tesi és contribuir al desenvolupament de tècniques de modelatge sistemàtic per a una gestió de l'aigua eficient i sostenible.

L'objectiu principal és contribuir a la investigació dels PAOs (Processos Avançats d'Oxidació). La tesi introdueix mètodes i eines d'Enginyeria de Processos Químics i proposa models que puguin ser explotats per produir estratègies eficients de gestió i operació dels PAOs, així com per a la integració d'aquests PAOs en xarxes de tractament d'aigües residuals.

Primer, es van investigar diferents PAOs. Es van considerar els processos Fenton, foto-Fenton i la foto-oxidació VUV, i es van comparar en el tractament de solucions aquoses de paracetamol (PCT) adoptant una sèrie d'indicadors de rendiment (Key Performance Indicators, KPI). Entre els PAOs seleccionats, la foto-oxidació VUV i foto-Fenton van produir els resultats més prometedors, permetent aconseguir l'eliminació total del contaminant i alt nivell de mineralització.

La segona part de la tesi es va centrar en transformar "dades en coneixement" mitjançant la proposta de models per als processos Fenton / photo-Fenton amb la finalitat de millorar les condicions operatives dels mateixos.

En concret, s'han proposat i validat dos models cinètics que descriuen la degradació de compostos orgànics per processos Fenton i foto-Fenton:

- Un model de Principis Bàsics convencional, que inclou la modelització de la radiació lineal amb emissió esfèrica i isotròpica, desenvolupat per predir la degradació Fenton i foto-Fenton del PCT i el consum d'oxidant (H_2O_2);
- Un model de Principis Bàsics no convencional que proposa un mecanisme de degradació de contaminants general, ja que considera el nombre d'àtoms de carboni del contaminant com la variable de partida per a la proposta de fragmentació i consegüent generació d'intermedis.

Tots dos models es van validar experimentalment i van mostrar la seva capacitat de reproduir satisfactòriament el comportament del sistema. En

particular, el Model de Principis Bàsics no convencional ha generat resultats prometedors per a la degradació Fenton / foto-Fenton de diferents sistemes (compostos per un o més contaminants orgànics) per mitjà de paràmetres globals (com el Carboni Orgànic Total). Per tant, aquest enfocament ofereix un modelatge pràctic, independent del contaminant i vàlid per a mesclades complexes de productes químics.

Un cop proposats i validats, els models de procés es poden utilitzar sistemàticament per determinar maneres d'operació eficients o alternatives de disseny. En conseqüència, la tesi es va dirigir a dos casos d'interès pràctic: l'optimització d'una recepta de control i el disseny d'una xarxa de tractament.

En el primer cas, es va proposar una estratègia d'optimització dinàmica per aprofitar els models cinètics disponibles i determinar el millor perfil de dosificació de peròxid d'hidrogen. Es van incloure objectius i limitacions econòmiques i ambientals per desenvolupar un problema d'optimització dinàmica que es va implementar en JModelica i es va resoldre utilitzant un mètode d'optimització simultània directa (IPOPT).

Finalment, es va explorar la combinació de processos biològics convencionals, més barats, amb PAOs, més costosos. Es va proposar un model de Programació No Lineal Entera Mixta (MINLP) per a l'optimització d'una xarxa general d'aigües residuals, basat en una superestructura de dissenys alternatius, que es va implementar i resoldre en GAMS. La nova formulació inclou la relació BOD_5 / COD , que descriu l'eficiència d'eliminació de BOD_5 i COD d'un tractament per tal de modelar la variació de la biodegradabilitat dels influents. Aquesta nova formulació permet determinar l'abast dels tractaments de PAOs quan es combinen amb tractaments biològics, i aplanar el camí per a models més complexos destinats a resoldre l'equilibri entre cost i eficiència del tractament.

Riassunto

L'obiettivo della presente tesi è contribuire allo sviluppo di tecniche di modellizzazione sistematica finalizzate ad una gestione efficiente e sostenibile delle risorse idriche.

L'obiettivo principale è contribuire allo studio dei POA (Processi di Ossidazione Avanzata). La tesi introduce metodi e strumenti dell'ingegneria dei processi chimici e propone modelli che possano servire per lo sviluppo di strategie efficaci di gestione dei POA nonché per l'integrazione di questi ultimi nelle reti di trattamento delle acque reflue.

In primo luogo, sono stati studiati diversi POA. Nello specifico, sono stati studiati i processi di foto-ossidazione Fenton, photo-Fenton e VUV per il trattamento di soluzioni acquose di paracetamolo (PCT) la cui efficacia è stata confrontata adottando una serie di indicatori di prestazione (Key Performance Indicators, KPI). Tra i POA selezionati, la foto-ossidazione VUV e il processo photo-Fenton hanno prodotto i risultati più promettenti, consentendo di ottenere l'eliminazione totale del contaminante e un alto livello di mineralizzazione.

La seconda parte della tesi si è concentrata sulla trasformazione dei "dati in conoscenza" proponendo modelli finalizzati alla descrizione dei processi Fenton / photo-Fenton e con l'obiettivo ultimo di adoperarli per ottimizzare le condizioni operative di questi ultimi.

In particolare, sono stati proposti e validati due modelli cinetici che descrivono la degradazione dei composti organici per mezzo dei processi Fenton e photo-Fenton:

- Un modello convenzionale, che include la modellizzazione della radiazione basata sull'ipotesi di radiazione lineare ed emissione sferica e isotropica, e in grado di prevedere la degradazione del PCT ad opera dei processi Fenton e photo-Fenton nonché il consumo di ossidante (H_2O_2);
- Un modello non convenzionale, che propone un meccanismo generale di degradazione degli inquinanti basato sul numero di atomi di carbonio del contaminante da degradare a partire dal quale si propone un meccanismo di

frammentazione di quest'ultimo con conseguente generazione di prodotti intermedi.

Entrambi i modelli sono stati validati sperimentalmente e hanno mostrato prestazioni soddisfacenti. In particolare, il modello non convenzionale ha mostrato di poter rappresentare la degradazione Fenton e photo-Fenton di diversi composti organici attraverso l'utilizzo di un parametro globale (come il carbonio organico totale) e quindi di offrire una proposta di modellizzazione pratica indipendente dal contaminante e che può pertanto essere adottata in caso di miscele complesse di prodotti chimici.

Una volta proposti e convalidati, i modelli di processo possono essere utilizzati sistematicamente per determinare modalità operative efficienti o alternative di progettazione.

Di conseguenza, la tesi ha affrontato due casi di interesse pratico: l'ottimizzazione della ricetta di controllo del processo e la progettazione di una rete di trattamento di acque reflue.

Nel primo caso è stata proposta una strategia di ottimizzazione dinamica per sfruttare i modelli cinetici disponibili e determinare il miglior profilo di dosaggio del perossido di idrogeno. Sono stati inclusi obiettivi e limiti economici e ambientali per sviluppare un problema di ottimizzazione dinamica implementato in JModelica che è stato risolto utilizzando un metodo di ottimizzazione simultanea diretta (IPOPT).

Infine, è stata esplorata la combinazione di processi biologici convenzionali, più economici, con i PAO, più costosi. È stato proposto un modello MINLP (Nonlinear Mixed Integer Programming) per l'ottimizzazione di una rete di acque reflue, basato su una struttura attraverso la quale è possibile rappresentare scelte progettuali alternative, che è stato implementato e risolto in GAMS. La nuova formulazione include il rapporto BOD_5 / COD , che descrive l'efficienza di eliminazione di BOD_5 e COD di un trattamento al fine di modellare la variazione della biodegradabilità degli influenti. Questa nuova formulazione consente di determinare le diverse possibilità di combinazione dei PAO con i trattamenti biologici e apre la strada a modelli più complessi volti a risolvere l'equilibrio tra costo ed efficienza del trattamento.

Table of Contents

<i>Declaration</i> _____	<i>VII</i>
<i>Declaración</i> _____	<i>IX</i>
<i>Declaració</i> _____	<i>XI</i>
<i>Dichiarazione</i> _____	<i>XIII</i>
<i>Acknowledgements</i> _____	<i>XV</i>
<i>Agradecimientos</i> _____	<i>XVII</i>
<i>Agraïments</i> _____	<i>XIX</i>
<i>Ringraziamenti</i> _____	<i>XXI</i>
<i>Abstract</i> _____	<i>XXIII</i>
<i>Resumen</i> _____	<i>XXV</i>
<i>Resum</i> _____	<i>XXVII</i>
<i>Riassunto</i> _____	<i>XXIX</i>
<i>Table of Contents</i> _____	<i>XXXI</i>
<i>Acronyms</i> _____	<i>XXXVII</i>
<i>Nomenclature</i> _____	<i>LIII</i>
<i>1 Introduction and thesis scope</i> _____	<i>1</i>
<i>1.1 Chemical process industries: current state and future challenges</i> _____	<i>1</i>
<i>1.2 The water challenge</i> _____	<i>5</i>
<i>1.3 Motivation</i> _____	<i>8</i>
<i>1.4 Thesis objectives</i> _____	<i>8</i>
<i>1.5 Thesis outline</i> _____	<i>9</i>
<i>2 State of the art</i> _____	<i>13</i>
<i>2.1 Regulation context in EU: EU Water Framework Directive</i> _____	<i>14</i>

Advanced Oxidation Process Models for Optimisation and Decision Making support in Water Management

2.2	Sources of pollution	15
2.2.1	Priority substances (PS) and priority hazardous substances (PHS)	16
2.2.2	Contaminants of Emerging Concern (CECs)	17
2.2.2.1	Pharmaceuticals	18
2.2.3	Mixture of contaminants	19
2.3	Water treatment technologies	21
2.3.1	AOPs	25
2.3.1.1	VUV oxidation	27
2.3.1.2	Fenton and photo-Fenton	28
2.4	Mathematical modelling of chemical processes	33
2.4.1	Fenton and photo-Fenton modelling approaches	35
2.5	Supply Chain and Supply Chain Management	37
2.5.1	Optimisation techniques	39
2.5.2	Water Supply Chain and Water Supply Chain Management	41
3	<i>Experimental setting, analytical techniques and mathematical tools</i>	43
3.1	Experimental	44
3.1.1	Experimental set-up	44
3.1.1.1	Fenton/photo-Fenton pilot plant	44
3.1.1.2	VUV photo oxidation pilot plant	49
3.1.2	Reagents and chemicals	50
3.1.3	Analytical techniques	52
3.1.3.1	Total Organic Carbon (TOC) determination	53
3.1.3.2	Model contaminant determination via HPLC (High Performance Liquid Chromatography)	54
3.1.3.3	Hydrogen peroxide determination via spectrophometric technique	57
3.1.3.4	Iron species determination via spectrophometric technique	58
3.1.4	Design of Experiment (DOE)	60
3.1.5	Toxicity tests	61
3.2	Mathematical tools	62
3.2.1	Simulation tools	62
3.2.2	Optimisation tools	63
4	<i>Comparison of effective AOPs</i>	67
4.1	Introductory perspective	68
4.2	Materials and methods	72
4.2.1	Reagents and chemicals	72
4.2.2	Experimental	73

Table of Contents

4.2.2.1	Experimental Design, analytical determinations, pilot plants	73
4.2.2.2	Toxicity tests	77
4.2.3	Modelling	79
4.3	Results and discussion	80
4.3.1	Fenton, photo-Fenton and VUV photo-induced assays	80
4.3.2	Citotoxicity assays	88
4.4	Conclusions	91
4.5	Acknowledgements	92
5	<i>Conventional kinetic study</i>	93
5.1	Introductory perspective	94
5.2	Methodological framework: experimental settings and process modelling	97
5.2.1	Experimental	97
5.2.1.1	Reagent and chemicals	97
5.2.1.2	Analytical determinations	98
5.2.1.3	Experimental set-up	99
5.2.1.4	Experimental procedure	102
5.2.2	Modelling	105
5.2.2.1	Kinetic model	105
5.2.2.2	Reactor model	108
5.2.3	Model fitting and parameter estimation	112
5.3	Results and discussion	113
5.3.1	Experimental results	113
5.3.2	Model fitting	117
5.4	Conclusions	120
5.5	Acknowledgements	121
6	<i>Non-Conventional kinetic study</i>	123
6.1	Introductory perspective	124
6.2	Experimental	126
6.2.1	Reagents and chemicals	126
6.2.2	Analytical determinations	127
6.2.3	Pilot plant	128
6.2.4	Experimental design and protocol	129
6.3	Model development	138
6.4	Implementation of Programmable Structures	142

6.5	Results and discussion	147
6.5.1	Estimation of the kinetic parameters of the general core mechanism (Fenton, photo-Fenton, and inefficient reactions of the free radicals)	148
6.5.2	Estimation of the kinetic parameters of the degradation mechanism for the first target compound (PCT)	150
6.5.3	Estimation of the kinetic parameters of the degradation mechanism for the second target compound (SQX)	156
6.5.4	Estimation of the kinetic parameters of the degradation mechanism for the third target compound (FA)	159
6.6	Conclusions	163
6.7	Acknowledgements	165
7	<i>Recipe optimisation</i>	167
7.1	Introductory perspective	168
7.2	Methodological framework and tools	171
7.2.1	Kinetic model and data	172
7.2.2	Reactor model: H ₂ O ₂ Dosage	176
7.2.3	Dynamic simulation	181
7.2.4	Dynamic optimisation	182
7.2.4.1	Optimisation study based on partial objectives	184
7.2.4.2	Optimisation under economic and environmental considerations	186
7.3	Results and discussion	187
7.3.1	Dynamic simulation results	187
7.3.2	Dynamic optimisation results: optimisation study based on partial objectives	193
7.3.3	Dynamic optimisation results: optimisation under economic and environmental considerations	200
7.4	Conclusions	205
7.5	Acknowledgements	206
8	<i>Water Supply Chain Modelling and Management</i>	207
8.1	Introduction	208
8.2	Methodological framework	210
8.2.1	Problem Statement	210
8.2.2	Model formulation (NLP-MINLP)	210
8.2.2.1	Mixer units	212
8.2.2.2	Splitter units	214
8.2.2.3	Treatment units	215

Table of Contents

8.2.2.4	Objective function _____	217
8.3	Case studies _____	218
8.4	Results and Discussion _____	221
8.5	Conclusions _____	232
8.6	Acknowledgements _____	233
9	<i>Final remarks and future work</i> _____	235
9.1	Conclusions _____	235
9.2	Further work _____	238
	<i>References</i> _____	241
	<i>Appendix A: Scientific production</i> _____	263

Acronyms

Chemical notations

CH_2O_2	Formic acid
$\text{C}_8\text{H}_9\text{NO}_2$	Paracetamol
$\text{C}_{14}\text{H}_{11}\text{N}_4\text{NaO}_2\text{S}$	Sulfaquinoxaline sodium salt
CO_2	Carbon dioxide
e_{aq}^-	Hydrated electrons
Fe^{2+}	Ferrous ion
Fe^{3+}	Ferric ion
Fe^{TOT}	Total iron
$\text{FeSO}_4 \cdot 7\text{H}_2\text{O}$	Iron sulfate

Advanced Oxidation Process Models for Optimisation and Decision Making support in Water Management

Fe(OH)^{2+}	Ferric ion complex
H^\bullet	Radical
H^+	Hydron
HCl	Hydrochloric acid
HNO_3	Nitric acid
HO^-	Hydroxide
HO^\bullet	Hydroxyl radical
H_2O	Water
H_2O_2	Hydrogen peroxide
H_3PO_4	Phosphoric acid
H_2SO_4	Sulphuric acid
I_2	Iodine

Acronyms

$K_2Cr_2O_7$	Potassium dichromate
MeOH	Methanol
Mn^{2+}	Manganese ion
NaOH	Sodium hydroxide
NO_3^-	Nitrate
O_2	Oxygen
O_2^\bullet	Oxygen radical
O_3	Ozone
RMe_2SiCl	Silica
TiO_2	Titanium dioxide
VO_3^-	Ammonium metavanadate
VO_2^{3+}	Peroxovanadium cation

Advanced Oxidation Process Models for Optimisation and Decision Making support in Water Management

Generic symbols

AA	Annual Average
ACN	Acetonitrile
AML	Algebraic Modelling Language
ANN	Artificial Neural Network
AOP	Advanced Oxidation Process
ARGs	Antibiotic Resistance Genes
B	Number of the consecutive breakage steps
BARON	Branch-And-Reduce Optimisation Navigator
BDFs	Backward Differentiation Formulas
BOD ₅	Biochemical Oxygen Demand
BPs	By products

Acronyms

BZQ	Benzoquinone
c_{1DO}	Stoichiometric coefficients in the dissolved oxygen balance
CEC	Contaminant of Emerging Concern
COD	Chemical Oxygen Demand
D	Discharge point
DAEs	Differential Algebraic Equations
DBM	Data Based Model
DCM	Direct Computer Mapping
DMEM	Dulbecco's Modified Eagle Medium
DMSO	Dimethyl Sulfoxide
DO	Dissolved Oxygen

Advanced Oxidation Process Models for Optimisation and Decision Making support in Water Management

DO*	Dissolved Oxygen Saturation Concentration
DOC	Dissolved Organic Carbon
DOE	Design of Experiment
EBMs	Effect-Based Methods
EEA	European Environment Agency
EM	Empirical Model
EPA	Environmental Protection Agency
EQS	European Environmental Quality Standards
EU	European Union
EV	Electrovalve
FA	Formic Acid
FBS	Foetal Bovine Serum

Acronyms

FNC	Fictitious number of carbon atoms
FPM	First Principles Model
FR	Fragments in which an organic compound is decomposed
$g_{1_{DO}}$, $g_{2_{DO}}$	Stoichiometric coefficients in the dissolved oxygen balance
GAMS	General Algebraic Modelling System
GBD	Generalized Benders Decomposition
GRG	Generalized Reduced Gradient Method
HDQ	Hydroquinone
HPLC	High Performance Liquid Chromatography
I	Generic point $I = I(r,z)$ (located at \underline{x}) inside the reactor

Advanced Oxidation Process Models for Optimisation and Decision Making support in Water Management

i	General component
IPOPT	Interior Point Optimizer
j, k	Index of inlet streams and outlet streams
KPI	Performance Indicator
LC50	Concentration of the selected chemical that kills 50% of the tested sample in a given time
LOD	Limit of Detection
LOQ	Limit of Quantification
LP	Linear Programming
LSSE	Line Source Model with Spherical and Isotropic Emission
LVRPA	Local Volumetric Rate of Photon Absorption

Acronyms

LVRPA _{VIRR}	Local Volumetric Rate of Photon Absorption averaged over the reactor volume
M	Parent organic compound present at the beginning of the reaction
MAC	Maximum Allowable Concentrations
MATLAB	MATrix LABoratory
MILP	Mixed-Integer Linear Programming
MINLP	Mixed-Integer Nonlinear Programming
m_{IN}, m_{OUT}	Set of inlet streams into mixer μ and of outlet streams from mixer μ
MO	Multi-Objective Optimisation
MoA	Mode of Action
MTT	(3-(4,5-dimethyl-2-thiazolyl)-2,5-diphenyl-2H-tetrazolium bromide

Advanced Oxidation Process Models for Optimisation and Decision Making support in Water Management

mu	Mixer Unit
MU	Set of mixer units
MX_1	Partially oxidized organic: first intermediate
MX_2	Partially oxidized organic: second intermediate
n	Section in the piecewise function
NC	Number of carbon atoms
NDFs	Numerical differentiation formulas
NDIR	Non Dispersive Infrared
NIR	Near Infrared
NLP	Non Linear Programming
NRWWS	Non-recalcitrant Wastewater
ODEs	Ordinary Differential Equations

Acronyms

OK	Ordinary Kriging
ORP	Oxidation-Reduction Potential
P_i	Generic intermediate compounds
PBS	Phosphate-Buffered Saline
PCT	Paracetamol
PDEs	Partial Differential Equations
PHS	Priority Hazardous Substances
PID	Proportional–Integral–Derivative
PLC	Programmable Logic Controller
PPCP	Personal Care Products
PS	Priority Substances
R	Free Radicals

Advanced Oxidation Process Models for Optimisation and Decision Making support in Water Management

$R_{H_2O_2/PCT}$	Hydrogen peroxide to paracetamol initial molar ratio
RMSE	Root Mean Square Error
R_p	BOD_5 / COD
RTE	Radiative Transfer Equation
RWWS	Recalcitrant wastewater
S	Linear coordinate along Ω
SC	Supply Chain
SCADA	Supervisory Control And Data Acquisition System
SCM	Supply Chain Management
SEM	Semi-Empirical Models
S_{IN}, S_{OUT}	Set of inlet streams into splitter su and set of outlet streams from splitter su

Acronyms

SLP	Successive Linear Programming
SQP	Successive Quadratic Programming
SQX	Sulfaquinoxaline Sodium Salt
SSA	Steady State Approximation
su	Splitter Unit
SU	Set of splitter units
SVR	Support Vector Regression
T	Target compound
TC	Total Carbon
TIC	Total Inorganic Carbon
t_{IN}, t_{OUT}	Set of inlet streams into treatment unit t_u and set of outlet streams from treatment unit t_u

Advanced Oxidation Process Models for Optimisation and Decision Making support in Water Management

TOC	Total Organic Carbon
T_R	Retention time
tu	Treatment Unit
TU	Set of treatment units
$u(t)$	Control Variables
UV	Ultraviolet
VRPA	Volumetric Rate of Photon Absorption
VSVO	Variable-Step, Variable-Order
VUV	Vacuum Ultraviolet
WFD	EU Water Framework Directive
WWTP	Waste Water Treatment Plant

\underline{x}	Position vector accounting for the radius and the axial coordinates of the reactor
x_n	Binary variable indicating whether the removal efficiency of unit t_u for component i is valid for the section n of the piecewise functions
$y(t)$	Decision Variables
$z(t)$	Differential State Variables

Greek symbols

β_i^{tu}	Efficiency of the unit t_u for component i
$\gamma_{H_2O_2/TOC}$	Specific consumption of the oxidizing agent
χ	TOC conversion
χ^{MAX}	Maximum TOC conversion
χ^t	TOC conversion at a specific time

Advanced Oxidation Process Models for Optimisation and Decision Making support in Water Management

χ^τ

TOC conversion at the final time τ

Ω

Solid angle

 Nomenclature

 Nomenclature

Generic symbols

$A(t)$	Amount of H_2O_2 employed at a generic time t	mmol
$A(\tau)$	Total amount of H_2O_2	mmol
C_i^j, C_i^k	Concentration of component i in the inlet stream j and in the outlet stream k	$mg\ L^{-1}$
$[C_i], [i]$	Concentration of the component inside the reactor	$mmol\ L^{-1},$ $mol\ L^{-1}, mg\ L^{-1}$
$[C_i]^0, [i]^0$	Initial concentration of the component	$mmol\ L^{-1},$ $mol\ L^{-1}, mg\ L^{-1}$
$[C_i]^{IN}, [i]^{IN}$	Concentration of the component in the inlet stream to the reactor	$mmol\ L^{-1},$ $mol\ L^{-1}, mg\ L^{-1}$

Advanced Oxidation Process Models for Optimisation and
Decision Making support in Water Management

$[C_i]^t, [i]^t$	Final concentration of the component	mmol L ⁻¹ , mol L ⁻¹ , mg L ⁻¹
$C_M, M=1,2,3$	Unit cost coefficients	Several units
$COST^{tu}$	Specific cost coefficient defined for each treatment unit	Several units
$e_\lambda^a(\underline{x}, t)$	Local Volumetric Rate of Photon Absorption for a monochromatic radiation	Einstein L ⁻¹ s ⁻¹
$F(t)$	Inlet flowrate that produces a variation in the total volume of the reactor	L h ⁻¹
$F(t) V^{-1}$	Dilution factor for the fed-batch operation	h ⁻¹
$f_i(t)$	Molar inlet flowrate for each component i	mmol h ⁻¹
$F_l(t)$	Recirculation flowrate	L min ⁻¹
F^j, F^k	Flowrate of inlet stream j and of outlet stream k	ton h ⁻¹
I	Irradiance	W m ⁻²

Nomenclature

k_{la}	Gas–liquid mass transfer coefficient in the dissolved oxygen balance	h^{-1}
k_l	Kinetic constants for each reaction l	Several units
k_T^i, k_{FR}^i	Kinetic constants for the generic component i relative to the first fragmentation step of the target compound (T), and to the following fragmentation steps of the generated fragments (FR)	Several units
$\kappa_\lambda(\underline{x}, t)$	Volumetric absorption coefficient of the reacting species	cm^{-1}
$\kappa_{T,\lambda}(\underline{x}, t)$	Volumetric absorption coefficient of the medium	cm^{-1}
L_L	Useful length of the lamp	cm
$P_{\lambda,s}$	Lamp spectral power emission	$W\ cm^{-2}$
r	Radius	cm
r_{int}	Internal radius	cm

Advanced Oxidation Process Models for Optimisation and
Decision Making support in Water Management

r_{ext}	External radius	cm
$R_i(\underline{x}, t), r_i$	Reaction rates for each component i	$M L^{-1} s^{-1}$
$R_i^T(\underline{x}, t)$	Thermal reaction rates for each component i	$M L^{-1} s^{-1}$
$[TOC]^\infty$	Limit concentration from which further degradation of the organic matter cannot be attained	$mmol L^{-1}$
T	Temperature	$^\circ C$
t_0	Initial reaction time	s, h
t, t'	Time	s, h
V	Total volume of the reactor	L, cm^3
V_{IRR}	Irradiated volume of the reactor	L, cm^3

Greek symbols

Nomenclature

$\alpha_{\text{Fe(OH)}^{2+}, \lambda}$	Molar absorptivity of ferric ions complex (Fe(OH)^{2+})	$\text{M}^{-1} \text{cm}^{-1}$
λ	Wavelength	nm
Φ	Wavelength-averaged primary quantum yield	M Einstein^{-1}
τ	Final reaction time (reaction span)	s, h
$\sum_{\lambda} e_{\lambda}^a(\underline{x}, t)$	Local Volumetric Rate of Photon Absorption for a polychromatic radiation	$\text{Einstein L}^{-1} \text{s}^{-1}$
$\langle \sum_{\lambda} e_{\lambda}^a(\underline{x}, t) \rangle$	Value of the Local Volumetric Rate of Photon Absorption for a polychromatic radiation, averaged over the reactor volume	$\text{Einstein L}^{-1} \text{s}^{-1}$

1 Introduction and thesis scope

1.1 Chemical process industries: current state and future challenges

The chemical sector is a strategic sector for European Union (EU) since chemical industry virtually supplies all sectors of the economy and provides a significant contribution to EU net exports. In spite of this, as analysed by

Advanced Oxidation Process Models for Optimisation and Decion Making support in Water Mangement

the European Chemical Industry Council-CEFIC (Landscape of the European Chemical Industry, 2018), European Union has lost its top spot in world chemical production to the advantage of Asia, whose chemical sales in 2012 were more than double those of the European Union. Consequently, due to the rapid growth and imposition of Asian countries on the chemicals market along with an increasing market globalization, Europe will be forced to fight against an increasingly strong competition.

Hence, chemical companies and therefore Chemistry and Chemical Engineering as well as all the related process industries (such as agriculture, food, pharmaceuticals, petroleum, etc.), are asked to face new ambitious challenges. The main goal will be to meet the new requirements of a globalized and more competitive market while aiming at a Sustainable Development or rather, as defined by the World Commission on Environment and Development (Brundtland Commission), “the development that meets the needs of the present without compromising the ability of future generations to meet their own needs”.

World chemical sales: geographic breakdown

World chemicals sales (€3,360 billion in 2016)



Source: Cefic Chemdata International 2016

* Rest of Europe covers Switzerland, Norway, Turkey, Russia and Ukraine

** North American Free Trade Agreement

*** Asia excluding China, India, Japan and South Korea

Unless specified, chemical industry excludes pharmaceuticals

Unless specified, EU refers to EU 28

Figure 1.1. Landscape of the European Chemical Industry 2018 provided by European Chemical Industry Council-CEFIC, 2018

Especially, chemical and process industries have now to deal with more complex systems, all them interconnected; they have to consider economic, environmental and social instances; and they have to face the need of continuous improvements in methods, tools and technologies. von Wedel and Marquardt, 2000, well described this concept by proposing the chemical supply chain, shown in Figure 1.2, which identifies the large span of time and space scales ranging from Chemical to Process System Engineering.

The chemical supply chain defines a complex system composed by different components that are mutually influenced and that act on different time and space scales (multi-scale problem). A full understanding of the system is not possible by simply splitting the global system into a set of independent components. A new integrated, multidisciplinary and multi-scale system approach is required. Therefore, it is necessary to redefine the role of Chemistry, Chemical and Process Systems Engineering, so to give response to these new needs and new challenges.

The National Research Council and its Board on Chemical Sciences and Technology (BCST) have provided a report named Beyond the molecular frontiers, Challenges for Chemistry and Chemical Engineering (Beyond the Molecular Frontier, 2003) with the aim of reviewing Chemistry and Chemical Engineering current state and future challenges, from molecular-level to industrial-scale level, or else, considering all the levels of the chemical supply chain.

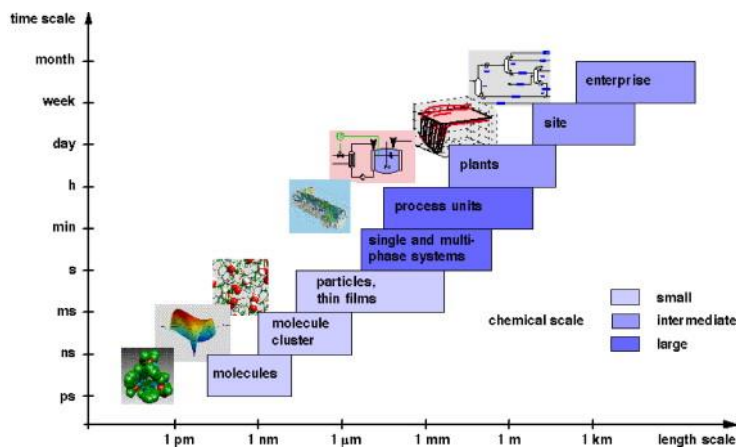


Figure 1.2. The chemical supply chain (von Wedel and Marquardt, 2000)

Advanced Oxidation Process Models for Optimisation and Decision Making support in Water Management

This report identifies some grand challenges that the chemical sector must face and some of the major are listed below:

- Learn how to synthesize and manufacture any new substance that can have scientific or practical interest, using compact synthetic schemes and processes with high selectivity for the desired product, and with low energy consumption and benign environmental effects in the process;
- Understand and control how molecules react over all time scales and the full range of molecular size, so to design new reactions and manufacturing processes;
- Understand the complex chemistry of the earth, including land, sea, atmosphere, and biosphere, so to maintain its livability;
- Develop unlimited and inexpensive energy (with new ways of energy generation, storage, and transportation) to pave the way to a truly sustainable future;
- Revolutionize the design of chemical processes to make them safe, compact, flexible, energy efficient, environmentally benign, and conducive to the rapid commercialization of new products;
- Develop reliable computer methods to calculate the detailed pathways by which reactions occur in both ground states and excited states, taking full account of molecular dynamics as well as quantum and statistical mechanics;
- Invent new algorithms to globally optimise at the worldwide level the use of raw materials, energy, and environmental impact of chemical processes.

To face the above mentioned challenges, new methods and supporting tools that can solve a variety of very complex mathematical models involving a large number of variables, are required.

Chemical and Process Systems Engineering play a major role in providing new conceptual approaches as well as in developing computational procedures for the simulation, design and operation of systems ranging from atoms and molecules to industrial scale processes.

The task of Chemical Engineering is to analyse the subsystem at the scale level that ensures an adequate representation of its complexity. Then, it is necessary to propose models that can simplify the complexity of the lower level in order to pursue the efficient integration of the lower level solutions

into the definition of the upper level problem and vice versa (scale-up and scale-down).

On the other hand, Process Systems Engineering is the study of all the processes (Chemistry or Biochemistry, batch or continuous, dedicate or general purpose, micro-scale or macro-scale) used in manufacturing. Its main goal is the understanding and development of tools for the synthesis, analysis, optimisation, evaluation, design, control, scheduling, and operation of Chemical Process Systems according to new social and economic instances.

The enhancement in methods and tools of Chemical and Process Systems Engineering, will allow facing another important economic and environmental challenge: the water challenge. Actually, chemical industries are, on one hand, one of the biggest water-consuming industry and, on the other, one of the biggest provider of water treatment materials and technologies.

1.2 The water challenge

Water is essential for life and for sustainable development, since it is also an essential resource for urban, industrial and agricultural sectors. It seems to be the only infinite resource in the world (covering 70% of the earth's surface). However, most of the water is saltwater and only 2.5% of the total volume of water on earth is freshwater. Moreover, of all the world freshwater resources, less than 1%, is available to humans at reasonable costs (such as through lakes, rivers and shallow aquifers, regularly renewed by the global water cycle).

Furthermore, the rapid growth of world population (between 1959 and 2000, the world's population increased from 2.5 billion to 6.1 billion people), the industrial development, and the inefficient use of water resources have led to an increase of water demand, to the subsequent overexploitations of aquifers, and to an increase of water pollution.

Therefore, nowadays, several regions in the world have no access to waters suitable for human uses and the problem of water scarcity is expected to get worse in the coming decades.

Advanced Oxidation Process Models for Optimisation and Decision Making support in Water Management

Hence, water scarcity is a major problem to be addressed, involving urban, industrial and agricultural sectors, and that needs a fast response.

A novel integrated approach considering all the actors (urban, agriculture and industry) involved in the whole water cycle management (water supply, water use, and wastewater treatment and reuse/recycle) has to be established. The main challenge is to enable a sustainable water management that can provide economic, environmental and social benefits to all the contributing sectors.

Water symbiotic strategies can become really relevant to improve sustainable water management, since it accounts for the possibility to use the effluents of Waste Water Treatment Plants (industrial and/or urban) as a potential, valuable resource for one or several other industries or that can be used for agricultural purposes.

As highlighted by the European Environment Agency (EEA), in the sustainable development context, efficient water use is closely linked to efficient use of other resources such as energy, chemicals, materials and land. Water is used in energy and food production; energy and materials are needed for water treatment; energy, food and industrial production are important drivers for water pollution and over abstraction.

Hence, an important challenge to be addressed concerns the development of more economic and cleaner water networks (Boix et al., 2011) aiming at reducing both freshwater consumptions and wastewater production, through a more efficient exploitation of the water resources (in order to reduce the great gap between use and consumption).

Another important factor to be considered is the need of improving wastewater treatment efficiency at a sustainable cost. This will allow to meet the stricter regulations both for discharge into the environment and for water reuses and to face the problem of the increasing release of more toxic and non biodegradable contaminants (above all by industrial and agricultural activities) that damage or resist conventional biological wastewater treatments.

Conventional water and wastewater treatments have been long established in removing many chemical and microbial contaminants of concern to public health and the environment. However, the effectiveness of these processes has become limited in the last years for two main reasons:

- Much stricter regulations (expanded scope of regulated contaminants and lowered maximum contaminant levels) have been implemented;
- An increasing number of new organic substances in very low concentrations (micropollutants) have been detected, thanks to more powerful analytical instrumentals, in wastewater, natural water and even ground water, so showing the inefficiency of conventional treatments.

Among these new organic substances there are the Contaminants of Emerging Concern (CECs), a group of organic substances that may be candidates for future regulations, depending on the results of the investigation concerning their effects on human health, aquatic life forms and their presence in the environment. Detergents, pharmaceutical products and its metabolites, personal care products, flame retardants, antiseptics, fragrances, industrial additives, steroids and hormones, are classified as particularly relevant emerging contaminants.

The main characteristic of CECs is that they are hardly biodegradable or toxic and so they can resist or even damage conventional biological treatments, causing several possible ecological problems (acute and chronic toxicity, microbial community inhibition in sewage systems, microbiological resistance and the occurrence of antibiotic resistance genes (ARGs), etc...).

Advanced Oxidation Processes (AOPs) seem the only feasible option for such biologically persistent wastewater (Oller et al., 2011) because they rely on the formation of highly reactive and non-selective free radicals (above all hydroxyl radical, HO^{*}) that are able to mineralize almost any organic contaminant.

However, the notable costs due to chemical and energy consumption have prevented the development of real successful applications in waste water treatment plants (WWTPs), as they still cannot compete with the cheaper and easier manageable biological treatments.

To improve the performance of the overall system a possible option could be to apply the AOPs before (pre-treatment, to increase biodegradability) or after (post-treatment, to improve the quality of the water) a biological treatment.

However, a recent review by (Oller et al., 2011), showed that the AOP field needs the development of more accurate economic models for the estimation of the cost of the combined systems as well as the improvement in the degradation kinetics and reactor modelling.

Also, the literature review highlighted that a great effort was made in studying the AOPs following an experimental approach, but less studies have been devoted to seeking for the optimal design, operational and control as well as the automation of AOPs (Moreno-Benito et al., 2013), (Ortega-Gómez et al., 2012).

1.3 Motivation

The present work was inspired by the idea of contributing to the development of a systematic modelling approach that can allow a more efficient and sustainable water management.

On one hand, the thesis aimed at providing a contribution to the AOPs investigation field by:

- proposing process models that can be exploited to progress in process control and automation strategies for practical AOPs applications;
- Including AOPs in the modelling and optimisation of general wastewater treatment networks.

On the other hand, Chemical and Process System Engineering methods and tools were applied to address AOPs investigation.

1.4 Thesis objectives

Accordingly, the specific objectives of this work are outlined as follows:

- A.** To quantitatively study and compare, different AOPs by selecting a model contaminant and adopting appropriate performance indicators (KPIs).

B. To propose different process modelling approaches in order to investigate their potentiality in the modelling and optimisation of a wastewater network including both conventional and non-conventional (e.g. AOPs) wastewater treatment technologies.

- These approaches are required to provide a compromise solution between unaffordable First Principle Models (FPMs) and oversimplified Empirical Models (EMs) and Data based Models (DBMs).

C. Based on the previous, to develop, fit and validate (by using experimental data) practical kinetic models to cover different needs:

- First, to provide deeper understanding of the Fenton and photo-Fenton mechanisms for simple, single-contaminant, systems;

- Second, to address the Fenton and photo-Fenton degradation of multiple target compounds by means of lumped parameters offering practical characterization of complex mixtures of organic species.

D. To develop a dynamic model-based optimisation methodology, aimed at decision-making and focusing on both economic and environmental factors, for systematically determining the best H₂O₂ dosing strategies.

E. To develop an optimisation model for wastewater networks including both conventional and non-conventional technologies (e.g. AOPs) and taking into consideration the effect of the interrelations between the different inlet contaminants (mixture of organic compounds).

1.5 Thesis outline

This work is divided into four main parts as represented in Figure 1.3.

Two chapters compose **the first part**. An **introduction chapter** that gives a general overview motivating the work. A **state of the art chapter** describing the current state of the water pollution and wastewater treatments (conventional and non-conventional), of the methods and tools employed in AOPs modelling and optimisation strategies, and in the Water Supply Chain Modelling and Management.

The second part consists of two chapters describing the experimental study including experimental setting and methodologies as well as the mathematical tools. **Chapter 3** describes the methodological framework of the present study, or rather the experimental setting, the analytical techniques and the mathematical tools. **Chapter 4** describes the study and comparison of different AOPs (Fenton, photo-Fenton, Vacuum Ultraviolet VUV photo-induced oxidation) that was used to raise conclusions and select the AOP to be investigated as main case study (e.g. photo-Fenton process) of the thesis.

The third part is the modelling and optimisation at a process unit level and a plant unit level. Particularly, the modelling and optimisation at a process unit level is faced in **Chapters 5 and 6**, which describe a conventional and a non-conventional kinetic study, respectively. On the other hand, **Chapter 7** faces the recipe optimisation problem, with the aim of investigating the use of available models for process control. Finally, in **Chapter 8** the modelling and optimisation at an upper level or rather the plant unit level is faced. In this case, the knowledge acquired from the previous experimental and modelling study at a process level of the AOP under study is used to address a novel Water Supply Chain Modelling and Management approach that can also include AOP treatment and not just conventional treatments as usual.

The last **Chapter 9** presents the conclusions as well as the discussion on the open issues and future work.

Introduction and Thesis Scope

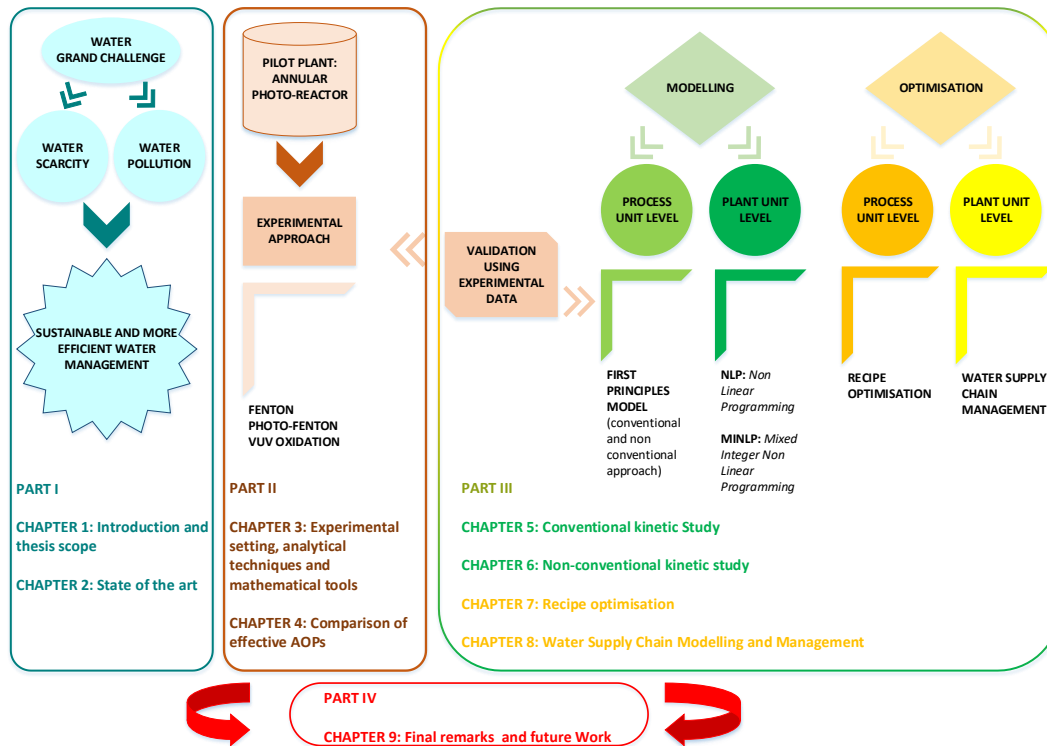


Figure 1.3.Thesis outline

Advanced Oxidation Process Models for Optimisation and Decision Making support in Water Management

The following Table 1.1 is finally listing the nine chapters composing the thesis with the specific titles and colors used to identify them.

Table 1.1 Legend of the nine chapters composing the thesis

Legend of the chapters composing the thesis	
1	Chapter 1: Introduction and Thesis Scope
2	Chapter 2: State of the Art
3	Chapter 3: Experimental Setting, Analytical Techniques and Mathematical Tools
4	Chapter 4: Comparison of Effective AOPs
5	Chapter 5: Conventional Kinetic Model
6	Chapter 6: Non-Conventional Kinetic Model
7	Chapter 7: Recipe Optimisation
8	Chapter 8: Water Supply Chain Modelling and Management
9	Chapter 9: Final Remarks and Future Work

2 State of the art

The following chapter presents a review of the different sources of contamination, of the different contaminants and of the available water treatment technologies.

More specifically, Advanced Oxidation Processes (AOPs) and especially Vacuum Ultraviolet VUV photo-oxidation, Fenton and photo-Fenton processes are described, being the AOPs specifically investigated in the present work.

Starting from a general overview of the different process modelling approaches a deep focus was paid in the main approaches that can be found

in literature for modelling Fenton and photo-Fenton processes, the main case study of the thesis, on which is based the modelling effort of the present work.

Finally, the different modelling and optimisation approaches for water treatment networks were also reviewed in order to present an overview that can be useful for a deeper understanding of the novel approach presented in Chapter 8.

2.1 Regulation context in EU: EU Water Framework Directive

A vast number of chemical compounds enter aquatic habitats in different concentrations and can cause direct effect (toxic) on aquatic biota and indirect effect on human health (via food and drinking water consumption).

The water issue related to water pollution and water stress is one of the main concern of European community. This was also confirmed by a representative opinion poll Eurobarometer in all 25 EU countries (Flash Eurobarometer 344, Attitudes of Europeans Towards Water – Related Issues, TNS Political & Social at the request of Directorate General for Environment, 2012) that showed that nearly half (47%) of the respondents are worried about water pollution and are demanding additional measures to address water problems in Europe.

As a result, on 23 October 2000, the Directive 2000/60/EC of the European Parliament and of the Council establishing a framework for the Community action in the field of water policy, abbreviated in the “EU Water Framework Directive” or also WFD, was adopted and several amendments have been introduced since then.

This legislation is widely considered the most ambitious European environmental legislation to date.

The entry into force of this legislation marked the beginning of a new era for European water management based on an holistic approach focusing on understanding and integrating all the different aspects related to the water environment to be effective and sustainable (Teodosiu C. et al., 2003).

The main purpose of this Directive was the protection of European waters by providing a framework allowing enhancing the status of the water bodies as well as preventing further contamination. Particularly, good chemical status is defined in terms of compliance with European environmental quality standards (EQS) for priority substances (PS). The EQS are defined as “the environmental threshold concentrations in water, sediment or biota that should not be exceeded in order to protect the environment and human health” while PS are those “substances posing a significant risk to or via the aquatic environment at EU level”.

The WFD is based on a six-year cycle and at first no deadline extensions were planned for the accomplishment of all WFD environmental objectives that consequently had to be met by 2015. Nevertheless, it appeared necessary to grant extensions for some Member States in order to attain all the WFD environmental objectives by the end of the second and third management cycles, which extend from 2015 to 2021 and 2021 to 2027 respectively (European Commission, 2012a).

2.2 Sources of pollution

According to the above mentioned Directive 2000/60/EC, it is possible to distinguish between point sources of pollution and non-point sources of pollution. The first ones are associated with a point location and include wastewater, industry, mining, contaminated land, agriculture point, waste management, and aquaculture. The second ones are associated with land-use activities and include urban drainage (including runoff), agriculture diffuse and forestry. Non-point sources are more difficult to identify, because they cannot be traced back to a particular location.

According to the United States Environmental Protection Agency (EPA), water pollution can be divided in six main categories:

- Urban wastewater discharges, including domestic wastewater or the mixture of domestic wastewater with industrial wastewater and/or run-off rain water;
- Domestic wastewater, including wastewater from residential settlements which originates mainly from human metabolism and from household activities;

Advanced Oxidation Process Models for Optimisation and Decision Making support in Water Management

- Industrial discharges, including any wastewater discharged from premises used for carrying on any trade or industry, other than domestic wastewater and run-off rain water;
- Discharges from farms, manure and slurry providing suspended solids, organic matter, nitrogen and phosphorus;
- Agricultural wastewater discharges, waters carrying fertilizers, pesticides and salts;
- Others, such as mining which release destructive substances like copper, cadmium and lead, boats which release hydrocarbons.

However the US EPA also establishes the importance of considering a new group of contaminants, Contaminants of Emerging Concern (CECs), including pharmaceuticals and personal care products (PPCPs).

In this regard, European commission, in the context of the WFD, identified a list of priority substances (PS), including the priority hazardous substances (PHS), or rather “persistent, toxic and liable to bioaccumulate, or that give rise to an equivalent level of concern” and states the importance of monitoring a new group of pollutants, the so called Emerging Contaminants.

The following sections present a more detailed description of such new sources of water pollution.

2.2.1 Priority substances (PS) and priority hazardous substances (PHS)

The Directive 2455/2001/EC, established the list of priority substances (PS), including the priority hazardous substances (PHS), that became the Annex X of WFD.

This Directive 2455/2001/EC amends Directive 2000/60/EC that specifies that specific measures must be adopted to reduce or even, in the case of priority hazardous substances, to cease the discharges, emissions and losses into the aquatic environment, within 20 years after their adoption at Community level. The final purpose is achieving concentrations approaching

background values for naturally occurring substances and close to zero for man-made synthetic substances.

The first list presented in the Directive 2455/2001/EC comprised 33 substances of which 11 were classified as priority hazardous substances while 14 substances were identified as being subject to later review.

This first list was then replaced by Annex II of the Directive on Environmental Quality Standards EQSD Directive 2008/105/EC, also known as the Priority Substances Directive, which set environmental quality standards (EQS) for the substances in surface waters (river, lake, transitional and coastal) and confirmed their designation as priority or priority hazardous substances. In this case the list included the EQS for 33 PS and groups of PS and 8 so called “other pollutants”.

Moreover, annual average (AA) EQS and maximum allowable concentrations (MAC) EQS defined in order to protect against long-term exposure and short-term peak concentrations, respectively, are listed in Annex I to Directive 2008/105/EC.

The Commission is required to review the list of substances designated as PS and PHS every six years as established by Article 16(4) of the WFD, amended by Directive 2013/39/EU.

The first review process was done between 2007 and 2011 (Directive 2013/39/EU amending Directive 2008/105/EC) and resulted in 12 new PS or PS groups, 6 of which are identified as PHS.

Directive 2013/39/EU also set up the so-called Watch List (WL) mechanism for surface water, to obtain more monitoring data for substances suspected of posing a risk at EU level. The first WL was established by Commission Decision 2015/495/EU and comprises 10 substances/groups of substances, including Diclofenac, 17-Alpha-ethinylestradiol and 17- Beta-estradiol.

2.2.2 Contaminants of Emerging Concern (CECs)

Moreover, Directive 2013/39/EU also states the importance of monitoring a new group of pollutants, the so called Emerging Contaminants or as defined

by the United States Environmental Protection Agency (US EPA), Contaminants of Emerging Concern (CECs). CECs are a group of unregulated chemicals, including pharmaceuticals and personal care products (PPCPs), that, thanks to more powerful techniques, are increasingly being detected at low concentrations (ng L^{-1} to $\mu\text{g L}^{-1}$) in surface waters, ground waters and even drinking waters. The main characteristic of this group of pollutants is that they are hardly biodegradable and consequently resist treatment by conventional sewage treatment plants so that are continuously discharged into the environment. Their continuous introduction into the environment cannot be compensated neither by high rates of transformation and/or removal so that they do not need to be persistent to cause negative effects on the aquatic environment (Pal et al., 2010).

These substances may be included in future environmental regulations depending on the results of the investigations on their potential ecotoxicological and toxicological effects. Particularly, Directive 2013/39/EU defines the importance of studying the risks of environmental effects from medicinal products so to evaluate the effectiveness of the current legislation in protecting the human health and the environment. Another important factor is to provide a high-quality monitoring information on the concentration of substances in the aquatic environment, with a focus on emerging pollutants.

The main CECs are: pharmaceuticals, personal care products, synthetic musk fragrances, sun-screen agents, insect repellents, surfactants and metabolites, flame retardants, industrial additives and agents, gasoline additives, disinfection by-products and pesticides.

In the following section a brief but more detailed description of the pharmaceuticals is presented because the present study addressed the treatment of different pharmaceuticals by using several Advanced Oxidation Processes (AOPs). Especially a widely used antipyretic and analgesic (paracetamol) and a drug used in veterinary medicine (sulfaquinoxaline sodium salt) were selected as main model compounds of the present work.

2.2.2.1 Pharmaceuticals

The pharmaceuticals (including psychiatric drugs, anticonvulsant drugs, analgesics and anti-inflammatory drugs, β -blockers, steroids and hormones,

X-Ray contrast agents, lipid regulators), enter the environment through several paths as shown in Figure 2.1. Particularly, human actions classified as involuntary (e.g. excretion through the body into the sewage system) and purposeful (disposal of medicines into the refuse waste and/or down the drain) are the main responsible of the introduction of pharmaceuticals into the environment. Another important source is the excreted manure, which contains the mixture of metabolite/unchanged pharmaceutical coming from the medicines administered to the farmed animals. The latter, being often used as fertilizer, allows the pharmaceuticals to reach the soil. Moreover, the pharmaceuticals can also reach the environment through the sludge of the Waste Water Treatment Plants, also often used as fertilizer.

Finally, soil leaching and groundwater recharge caused by heavy precipitation, are the main modes of transportation for pharmaceuticals through the soil and into the aquatic environment but also industrial spills and aquaculture play a major role.

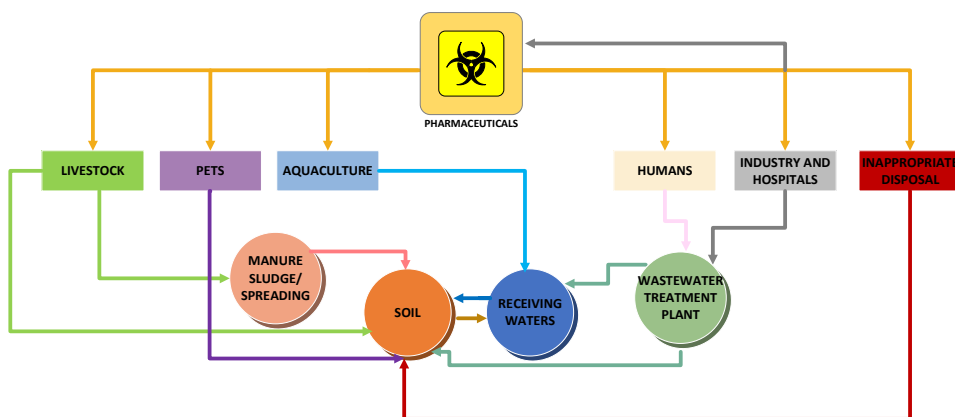


Figure 2.1. Sources of pharmaceuticals in the environment defined by *Boxall, 2004*

2.2.3 Mixture of contaminants

Finally, a report named “Modes of action of the current Priority Substances list under the Water Framework Directive and other substances of interest” has been recently published (2018). This report establishes the need of a new

Advanced Oxidation Process Models for Optimisation and Decision Making support in Water Management

holistic approach through which it can be possible the assessment of the chemical and ecological status of the water by not only focusing on the risk posed by individual chemicals but also on their effects in combination (interactions between chemicals).

It has become increasingly clear that the approach followed up to now and based on the regulation of single substances cannot adequately take under control the risks arising from the great number of chemicals in the aquatic environment (including Contaminants of Emerging Concern CECs, metabolites and transformation products).

For this reason the Commission acknowledges the need to consider the potential toxic effects of mixtures of chemicals (EC COM(2012)252, 7th EAP).

The toxicity of mixtures depends on the chemical reactivity and on the bioavailability of the compounds. Particularly, the risks associated with the environmental pollutants can be better understood by understanding their mode of action (MoA). According to the EC Scientific Committees, “a MoA is a plausible hypothesis about measurable key events by which a chemical exerts its biological effects”.

Especially, the MoA is basically the process initiated by the interaction of the toxicant with the receptor and which causes molecular, biochemical, physiological and/or anatomical changes in the organism that can result in sub-lethal and lethal effects.

A number of more or less specific modes of action (MoAs) have been identified, such as photosynthesis inhibition, endocrine disruption, oxidative stress, activation of metabolizing/detoxifying pathways, induction of stress proteins, inhibition of growth, perturbed lysosomal stability, genotoxicity, histopathological changes.

The understanding of the MoA allows linking the exposure to chemicals to their effects in the aquatic environment. From this it is also possible the development of effect-based methods (EBMs) than can be used for monitoring the MoA and for assessing the combined effects of chemicals. These effect-based methods include biomarkers (biomarkers of exposure and biomarkers of effect) and bioassays:

“A biomarker of exposure is a xenobiotic substance or its metabolite(s), or the product of an interaction between a xenobiotic agent and some target

molecule(s) or cell(s) that is measured within a compartment of an organism”.

“Biomarkers of effect are defined as any measurable biochemical, physiological, or other alteration within an organism that, depending on magnitude, can be recognized as an established or potential health impairment or disease”.

“Bioassays are those EBMs, which measure the toxicity of environmental samples under defined laboratory conditions, at cellular and individual organism levels (in vitro and in vivo, respectively)”.

This report opens the way to new and interesting investigation research lines. Following the conventional approach that was focused on the risk posed by individual chemicals, also the modelling approaches were mainly based on the description of the degradation path of a single pollutant. However, considering the new awareness about the risk produced by the interaction between the different chemicals, novel modelling approaches should be also proposed and investigated. Especially, there is the need of modelling approaches that can be generalizable solutions that can describe the degradation of any pollutants as well as of mixtures of pollutants. For this reason Chapter 6 addresses a preliminary proposal of a First Principle Model of medium complexity that can allow describing the photo-Fenton degradation of any organic compounds regardless of its structure and chemical formula. However in Chapter 5 is also proposed a conventional First Principle Model describing the photo-Fenton degradation of the PCT and the consumption of the oxidant (H_2O_2).

2.3 Water treatment technologies

To struggle contamination of water bodies and meet the regulations, different technologies are available.

The selection of the most appropriate technologies will depend on the wastewaters to be treated.

Usually wastewaters are treated in Wastewater Treatment Plants (WWTPs), in which various treatment steps including physical, biological and eventually

Advanced Oxidation Process Models for Optimisation and Decision Making support in Water Management

chemical processes, are carried out for the removal of physical, biological and chemical contaminants.

Generally a WWTP comprises a set of subsequent treatment stages, namely pre-treatments, primary, secondary and eventually, tertiary treatments. The treatment efficiency of each step is measured by measuring some indicators of the water pollution that, according to the Guide Extensive wastewater treatment process, are defined as follows:

- **Biochemical Oxygen Demand- BOD₅:** is a measurement of the pollution by organic matter. It is expressed in milligrams of oxygen per day and per p.e. (population equivalents defined as organic biodegradable load that has a five-day biochemical oxygen demand of 60 grams of oxygen per day). It corresponds to the quantity of oxygen that is needed to oxidise the discharges of polluted effluents produced on average by each inhabitant in a watercourse or by a given agglomeration. This measurement is carried out according to standardised tests after five days of oxidation of the organic matter, hence the term BOD₅.
- **Chemical Oxygen Demand-COD:** represents the quantity of oxygen consumed, expressed in milligrams per liter, by the chemically oxidizable matter contained in a discharge. According to the standard method, this is the oxidation by an excess of potassium dichromate (K₂Cr₂O₇) in a fermenting and acidic medium, of the chemically oxidizable matter contained in a discharge. COD is a valuable parameter indicating the presence of pollution in wastewater. It represents the major part of the organic compounds but also oxidizable mineral salts (sulphides, chlorides, etc.). Industrial wastewater can frequently reach COD values of several grams per litre.
- **Suspended Solids-SS:** all of the mineral and (or) organic particles that are present as suspended solids in natural or polluted water.

Below are briefly described all the steps comprising a general WWTP:

- **Pre-treatments** involve physical processes for the removal of coarse solids, grit and sand, grease and fat with the aim of avoiding the damage of mechanical parts (e.g. pumps) of the different treatment lines.
- **Primary treatments**, based on physical processes that take place into a quiescent basin where heavy solids can settle to the bottom while oil, grease and lighter solids float to the surface. The primary treatment step allows reducing the

suspended solids of the incoming wastewaters by at least 20% and the BOD₅ by at least 50%.

- Secondary treatment is the step following the primary treatment and allows the treatment of urban wastewater by a process generally involving biological treatment with a secondary settlement. It is based on the use of indigenous, water-borne micro-organisms in a managed habitat for the removal of dissolved and suspended biological matter. The subsequent separation process allows the removal of the micro-organisms and solids that have been generated through biological activity. The secondary treatment step removes almost all the suspended solids and 85-90% of biological oxygen demand (BOD₅). After this treatment, sewage can be discharged into the environment or it can be sent to a tertiary treatment.
- Tertiary treatments, refer to several types of treatments or different functions and are used when the aim is attaining a treatment level of higher quality than the one provided by a secondary treatment. Generally, these treatments are used when stricter regulations must be met for example in order to allow the discharge into a highly sensitive or fragile ecosystem (estuaries, low-flow rivers, coral reefs). Tertiary treatment technologies can be used to remove nitrogen and phosphorus that are poorly removed by the secondary treatments, or can involve physical-chemical separation techniques such as carbon adsorption, flocculation/precipitation, and membranes.

Additionally, the concern regarding persistent and hardly biodegradable pollutants, such as PHS and CECs has produced a great research effort in the development and implementation of Advanced Oxidation Processes (AOPs). For this reason, in the following sections, an overview of the AOPs is presented. Especially, a detailed description of Vacuum Ultraviolet VUV photo-induced oxidation and above all Fenton and photo-Fenton processes, being the latter the selected main case study of the present work, was provided.

It must be noted that a literature review of the AOPs field, reveals that different indicators are generally used to assess quantitative performance of the AOPs in the degradation of organic compounds. Especially, measurements of the evolution of the organic compound and of the Total Organic Carbon-TOC that represents the amount of carbon in the organic compound, are usually performed. The TOC is a lumped parameter that gives

an indirect measure of all the organic compounds and as a consequence gives an indication of the sample mineralization.

Furthermore, in the AOPs field, another important key performance indicator is given by the toxicity tests of the treated water, performed during and at the end of the treatment. These toxicity tests are required in order to ensure the safe application of AOPs since they can lead to the formation of more toxic intermediates than the parent compound. Generally, the toxicity of the produced effluents have been tested on bacteria such as, *Vibrio* Fishery (Miralles-Cuevas et al., 2014) and *E. coli* bacteria (Pérez-Moya et al., 2007).

In this context, the present study in the subsequent Chapter 4, addresses the use of the evolution of PCT concentration, TOC conversion, and cytotoxicity results as key performance indicators to compare different AOPs (Fenton, photo-Fenton and VUV photo-induced oxidation) in the degradation of paracetamol (PCT) in aqueous solution.

However, in this work, cytotoxicity assays based on the use of cell lines culture (e.g. VERO and COS-1 cells, epithelial-like and fibroblast-like cells, respectively, both isolated from an African green monkey kidney) and aiming at detecting cytotoxicity or cell viability following exposure to the produced effluent, were tested. The cytotoxicity assays based on the use of cell lines culture were selected with the aim of addressing a more general case by testing a system with a higher sensitivity than the bacteria commonly employed.

Cytotoxicity assays are widely used in vitro toxicology studies and the most common are the LDH leakage, the neutral red and the MTT assays. In the present study the MTT assays were performed because they have been often used to detect cytotoxicity following exposure to toxic substances (Almazan et al., 2000) and the validity of this method has been tested on several cell lines (Mosmann, 1983).

The MTT (3-[4,5-dimethylthiazol-2-yl]-2,5-diphenyltetrazolium bromide) is a water soluble tetrazolium salt, converted to an insoluble purple formazan by cleavage of the tetrazolium ring by succinate dehydrogenase within the mitochondria. The insoluble purple formazan product accumulates in healthy cells because it is impermeable to the cell membranes (Fotakis and Timbrell, 2006).

In the following sections a description of the main AOPs with a deep focus on the AOPs investigated in the present work, such as VUV photo-oxidation, Fenton and photo-Fenton processes, is addressed.

2.3.1 AOPs

The AOPs are a group of chemical processes all characterized by the capability of exploiting the high reactivity of free radicals (e.g. HO[•] radicals) in driving oxidation reactions that can allow pollutant remediation and organic matter mineralization (Andreozzi et al., 1999). The HO[•] radicals are extremely reactive and attack the most part of organic molecules with a constant rate in the order of 10⁶–10⁹ L mol⁻¹ s⁻¹ (Ross and Farhatziz, 1977), (Hoigné and Bader, 1983).

Hence, the AOPs have been used at various scales for different applications such as the destruction of micropollutants (Prieto-Rodríguez et al., 2013), (Ortega-Gómez et al., 2013), and specific pollutants (Nichela et al., 2013), (Babuponnusami and Muthukumar, 2012), sludge treatment (Pham et al., 2010), (da Rocha et al., 2010), (Tokumura et al., 2009), increase of biodegradability of recalcitrant wastewaters (Vilar et al., 2012), mineralization of organic matter (Ji et al., 2011), and color and odour removal (Tokumura et al., 2013).

The HO[•] radicals are also characterized by a little selectivity of attack that promotes flexibility of such processes enabling the treatment of several pollutants.

As a consequence, AOPs are nowadays considered to be the only feasible option for the treatment of refractory or toxic substances that can resist or damage conventional secondary biological treatments (Oller et al., 2011).

However, the chemical oxidation for the complete mineralization of the organic matter is not a viable solution because the intermediates by-products become more resistant during the oxidation process so requiring a greater reaction time that would led to an increase of the reagents and energy consumption and consequently of the operational cost. On the contrary the conventional biological processes are easier manageable and cheaper technologies.

Hence, with the aim of containing the operational costs, the combination of the conventional biological processes with the AOPs has been proposed as a potential attractive alternative. The AOPs can be used as pre-treatments, to convert the persistent or toxic contaminants into more biodegradable substances. Particularly, in this case, the aim is to define the minimum pretreating time that can allow reaching the desired level of mineralization that ensures the generation of biodegradable substances that can be treated with the subsequent biological treatment step, and avoiding unnecessary consumption of chemicals and energy.

Moreover, the AOPs can also be used as post-treatment step following the secondary treatment with the aim of attaining a treatment level of higher quality.

The main different possibilities given by AOPs (Andreozzi et al., 1999) are listed below:

- **Fenton ($\text{H}_2\text{O}_2/\text{Fe}^{2+}$) and Fenton-like ($\text{H}_2\text{O}_2/\text{Fe}^{3+}$):** the production of HO^\bullet radicals by Fenton reagent occurs by means of addition of H_2O_2 to Fe^{2+} salts.
- **Photo assisted Fenton ($\text{H}_2\text{O}_2/\text{Fe}^{2+}$ (Fe^{3+})/UV):** it's an extension of the Fenton process. The use of a UV-VIS light irradiation at wavelength values higher than 300 nm allows the photolysis of Fe^{3+} complexes and the consequent regeneration of Fe^{2+} leading to an increase of the degradation rate of organic pollutants.
- **$\text{H}_2\text{O}_2/\text{Fe}^{3+}$ - oxalate:** it's an improvement of photo-assisted Fenton processes. The irradiation of ferrioxalate in acidic solution led to the generation of CO_2 and Fe^{2+} , free or complexed with oxalate, which can provide a continuous source of Fenton's reagent by reaction with H_2O_2 .
- **Photocatalysis ($\text{TiO}_2/h\nu/\text{O}_2$):** the photocatalytic processes are based on the use of oxygen as oxidizing agent and of a semiconductor metal oxide as catalyst. The initiating event is the absorption of the radiation with the formation of electron-hole pairs ($\text{TiO}_2 \xrightarrow{h\nu} e^- + h^+$). The formed electrons have a high reducing power which allows the generation of the superoxide radical ion $\text{O}_2^{\bullet-}$ by reducing some metals and dissolved oxygen, whereas remaining holes can oxidize adsorbed H_2O or HO^- to reactive HO^\bullet radicals.
- **Peroxozone ($\text{O}_3/\text{H}_2\text{O}_2$) and Peroxone combined with Ultraviolet light (O_3/UV ; $\text{O}_3/\text{H}_2\text{O}_2/\text{U}$):** Hoigné and Bader, 1983 showed OH^- ion has the role of initiator

of the process of ozone decomposition in aqueous solution that develops through the formation of HO[•] radicals. Moreover, the addition of hydrogen peroxide to the ozone aqueous solution can enhance the O₃ decomposition allowing the formation of HO[•] radicals.

- **Mn²⁺ catalysed ozonation of oxalic acid (Mn²⁺/Oxalic acid/ozone):** This system can be used to enhance ozone decomposition for the production of HO[•] radicals. The Mn²⁺ catalysed ozonation of oxalic acid develops according to a radical mechanism at pH >4.0 at which Mn(III)-dioxalate and Mn(III)-trioxalate are formed. Then the oxidation process proceeds presumably through the formation of HO[•] radicals.
- **Peroxidation combined with Ultraviolet light (H₂O₂/UV):** The irradiation of the pollutant solution containing H₂O₂ with a UV light source with λ < 280 nm led to the homolytic cleavage of H₂O₂ ($H_2O_2 \xrightarrow{h\nu} 2HO^{\bullet}$).
- **Vacuum Ultraviolet VUV photo-induced oxidation:** Is the process that led to the generation of hydroxyl radicals by photolysing the water through the use of higher energies of the Vacuum Ultraviolet or VUV (λ < 190nm).

The AOPs using an irradiation source which in general is a Ultraviolet (UV) light, are photochemical AOPs. UV light refers to the region of the electromagnetic spectrum between visible light and X-rays, with a wavelength falling between 400 and 10 nanometres.

Below are analysed more in detail the processes that have been used in this study, or rather water photolysis in Vacuum Ultraviolet (VUV) and above all the Fenton/photo-Fenton processes, being the latter the main case study of the present work.

2.3.1.1 VUV oxidation

Vacuum Ultraviolet VUV photo-induced oxidation is the process that uses the higher energies of the Vacuum Ultraviolet or VUV (λ < 190 nm) as a mean to generate hydroxyl radicals by photolysing water.

The photochemical reaction known as homolysis of water is shown in the following Equation 2.1:



The chemical bond dissociation leads to the formation of the main reactive and non-selective species, or rather the HO^\bullet radicals, as well as of H^\bullet , H^+ and hydrated electrons e_{aq}^- .

The VUV photo-induced technology does not require chemical additives and this represents its main advantage. Moreover it can be described as a completely unselective oxidation that relies on the use of high light-energy density. Finally it also provides flexibility as scalable process.

This photochemical process has shown a great potential in achieving the oxidation and mineralization of several organic pollutants.

Particularly, relevant studies have investigated the use of VUV photo-induced oxidation for the treatment of:

- solvents (e.g. 1,1,1-trichloroethane) in concentrations between 1.0 and 24.9 mg L^{-1} (Oppenländer et al., 1995);
- phenols (e.g. 2,4-dichlorophenol) in concentrations in the order of 100.0 mg L^{-1} (Oppenländer et al., 1995), (Oppenländer, 1997), (Oppenländer and Gliese, 2000);
- several organic contaminants such as 3-amino-5-methylisoxazole (Gonzalez and Braun, 1995) and 1,2-dichloroethene (Oppenländer et al., 1995) in concentrations of 49.0 and 20.0 mg L^{-1} , respectively.

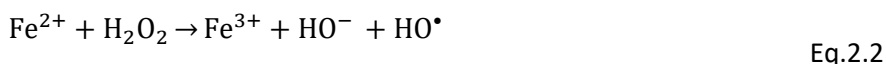
2.3.1.2 Fenton and photo-Fenton

The photo-Fenton process is a photochemical AOP that uses UV/VIS radiation as a means to generate the non-selective and highly reactive free radicals, mainly HO^\bullet , in presence of an oxidant (H_2O_2) and a catalyst (Fe^{2+}).

The **Fenton reaction** is an old reactive system proposed by Fenton in 1894 (Fenton, 1894).

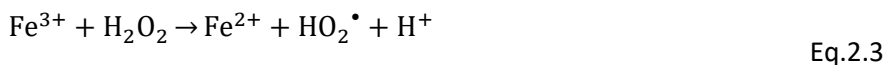
It can be divided in two stages:

- A first stage (Equation 2.2) leads to the formation of HO• by the addition of hydrogen peroxide (H₂O₂) to ferrous ion salts (Fe²⁺). This is the faster stage and presents a kinetic constant of $k = 63.0\text{-}76.0 \text{ L mol}^{-1} \text{ s}^{-1}$ (Chen and Pignatello, 1997), (Gallard and De Laat, 2000), (Kang et al., 2002), (Kusic et al., 2006), (Simunovic et al., 2011).



$$k = 63.0\text{-}76.0 \text{ L mol}^{-1} \text{ s}^{-1}$$

- In the second stage (Equation 2.3), the regeneration of ferrous ions is possible by the reaction of ferric ion with hydrogen peroxide. This stage is slower and presents a kinetic constant of $k = 0.01\text{-}0.02 \text{ L mol}^{-1} \text{ s}^{-1}$ (Chen and Pignatello, 1997), (Gallard and De Laat, 2000), (Kang et al., 2002), (Kusic et al., 2006), (Simunovic et al., 2011).



$$k = 0.01\text{-}0.02 \text{ mol}^{-1} \text{ s}^{-1}$$

However, the use of a UV-VIS light source at wavelength higher than 300 nm and acid medium (pH= 2.8) causes the photolysis of ferric ions (Fe³⁺) complexes (Fe(OH)²⁺) which allows the Fe²⁺ regeneration and the formation of hydroxyl radicals, with a consequent strong increase of the degradation rate of organic pollutants. This process is described as the **photo-assisted Fenton process** (Kiwi et al., 1993), (Pulgarin and Kiwi, 1996) and is described by the following reaction:



$$\phi = 0.21 \text{ mol Einstein}^{-1}$$

The photo-Fenton reaction (Equation 2.4) is described by a quantum yield (the ratio of the number of photons emitted to the number of photons absorbed) $\phi = 0.21 \text{ mol Einstein}^{-1}$, as defined by (Bossmann et al., 1998).

Particularly, the Fe^{3+} hydroxyl complexes are the ones that in mildly acidic solution, absorb light appreciably in the UV and into the visible region. Especially, $\text{Fe}(\text{OH})^{2+}$, due to its high absorption coefficient, is the most important specie that undergoes photoreduction to give HO^{\bullet} and Fe^{2+} .

Among the AOPs, Fenton and photo-Fenton processes have attracted widespread attention in the scientific community and many applications of both Fenton and photo-Fenton processes for the treatment of many kinds of wastewaters, can be found.

Two recent reviews on Fenton-like processes for organic wastewater treatment by Wang et al., 2016 and on photo-Fenton processes for the treatment of recalcitrant wastewaters by Rahim Pourn et al., 2015 have stressed that such processes have been mostly applied for the treatment of high strength organic wastewaters.

Particularly, in the case of the Fenton-like processes many applications can be found for the treatment of several wastewaters such as olive-oil mill (Bianco et al., 2011), textile (Arslan-Alaton, 2007), laboratory (Benatti et al., 2006), pesticide (Badawy et al., 2006), cosmetic (Bautista et al., 2007), dye (Kušić et al., 2007), (Ramirez et al., 2005), fermentation brine from green olives (Rivas et al., 2003), pharmaceutical (Tekin et al., 2006), cork cooking, (Pintor et al., 2011), pulp mill (Catalkaya and Kargi, 2007), and phenolic (Lopez et al., 2005).

Conversely, regarding photo-Fenton process, efficient applications can be found mainly for the treatment of pharmaceuticals and pharmaceutical wastewaters (Trovó et al., 2012), (Jordá et al., 2011), agrochemicals (Zhang and Pagilla, 2010), (Silva et al., 2012) and petroleum refinery waters (da Rocha et al., 2013), (Sun et al., 2008).

However, photo-Fenton process also proved to be able to efficiently remove micropollutants (Jung et al., 2012), (De la Cruz et al., 2013), (Pablos et al., 2013) and CECs as well (Miralles-Cuevas et al., 2014). Moreover, it is of added interest, because of the possibility of exploit solar irradiation as a photon source, with removal rates over 99% (Klamerth et al., 2013).

Hence, in the last years a remarkable experimental effort has been made for a better understanding of the photo-Fenton process as a whole. Several studies performed at both laboratory and pilot plant scale addressed the investigation of the key process efficiency parameters.

Especially, **pH, Fenton reagents concentration and Fenton reagents ratio, contaminant load and presence of other inorganic ions are some of the main factors affecting the photo-Fenton process efficiency** (Pignatello et al., 2006), (Zapata et al., 2010), (Rahim Pouran et al., 2015).

Regarding the **pH influence**, the range $2.5 < \text{pH} < 3.0$ -4.0 ensures that the $\text{Fe}(\text{OH})^{2+}$ is present at appreciable concentration so allowing the reduction of Fe^{3+} to Fe^{2+} (Fenton-like reaction) at an appreciable rate (Pignatello, 1992), (Pignatello et al., 1999), (Pignatello et al., 2006). However, above pH 3.0, due to precipitation of the catalyst, Fenton reaction rates tend to decrease anyway.

Fenton reagents ratio ($\text{H}_2\text{O}_2:\text{Fe}^{2+}$) was proved to be one of the most significant factors (Gulkaya et al., 2006). However, many different ratios can be found in literature as a function of the matrix and of the contaminant load (e.g. Ramirez et al., 2005 reported ratios ranging between 5:1 and 20:1, while Pignatello et al., 2006 reported ratios ranging between 100:1 and 1000:1).

The **presence of inorganic ions** such as phosphate, sulfate, organosulfonate, fluoride, bromide, and chloride ions, can inhibit at different levels, depending on their concentrations, the Fenton and photo-Fenton oxidations of organic compounds. This inhibition may be due to precipitation of the catalyst, scavenging of HO^\bullet , or to the formation of less reactive complex with Fe^{3+} (Pignatello et al., 2006).

Several studies also pointed out the **importance of the H_2O_2 dosage** (Ince, 1999), (Yamal-Turbay et al., 2012) in the improvement of the process performance, since it can avoid or reduce the activation of inefficient reactions scavenging hydroxyl radicals ($\text{H}_2\text{O}_2 + \text{HO}^\bullet \rightarrow \text{O}_2$, $\text{HO}^\bullet + \text{HO}^\bullet \rightarrow \text{O}_2$). The more efficient use of the hydrogen peroxide allows reducing the operational costs that are mainly due to the oxidant and energy consumption. An excess of Fe^{2+} can scavenge hydroxyl radicals ($\text{Fe}^{2+} + \text{HO}^\bullet \rightarrow \text{Fe}^{3+} + \text{OH}^-$) as well (Huston and Pignatello, 1999).

Moreover, high values of the oxidant concentration result to be toxic for several microorganism. This factor must be taken into account in the case of the combination with conventional biological treatments with the aim of avoiding the damage of the microbial system.

Some works have finally shown the possibility of using **easy measurable variables**, e.g. oxidation reduction potential (ORP) and dissolved oxygen (DO) concentration, **as a way of developing further process monitoring and control applications** (Santos-Juanes et al., 2011), (Prieto-Rodríguez et al., 2013), (Tokumura et al., 2011).

Especially, variation in dissolved oxygen concentration has shown to be related to the hydrogen peroxide decomposition: an increase of DO concentration is a signal of the activation of inefficient reactions that led to the decomposition of H_2O_2 while the decrease in DO concentration is a signal of a lack of hydrogen peroxide.

Hence, Ortega-Gómez et al., 2012 proposed to use the measurements of dissolved oxygen concentration as a mean of developing a process controller through which ensuring the proper and automatic dosage of hydrogen peroxide, focusing on minimizing its consumption and maximizing the pollutant mineralization rate.

However, further investigation is needed for the development of robust and feasible dosage strategies of the oxidant.

Another open issue is the influence of the matrix. Most of the published works relate to DEIONISED water and even ultra-pure water. Real wastewaters can contain different substances in different concentrations as well as carbonates and humic acids that can scavenge hydroxyl radicals (Bautitz and Nogueira, 2007) or substances like the quinones that can enhance the photo-Fenton performance (Pignatello et al., 2006).

It is finally interesting to highlight that photo-Fenton process and above all solar photo-Fenton has also been successfully used in combination with aerobic biological systems for the treatment of different wastewaters. Especially:

- A solar photocatalytic-biological pilot-plant system was used for the treatment of α -methylphenylglycine, a biorecalcitrant industrial compound, (Oller et al., 2007a); of five pesticides (methomyl, dimethoate, oxamyl, cymoxanil and

pyrimethanil) (Oller et al., 2007b); and of a saline industrial wastewater containing around 600.0 mg L⁻¹ of a α -methylphenylglycine and 400.0-600.0 mg L⁻¹ of dissolved organic carbon (Oller et al., 2007c).

- A conventional sequencing batch reactor integrating photo-Fenton and biological treatment, has been used for the treatment of a commercial homo-bireactive dye (125.0 mg L⁻¹) by García-Montaña et al., 2006.

It is worth noting that the experimental information must be exploited and transformed in knowledge by proposing practical process models than can allow the implementation of real applications.

Hence, in the following sections an overview of the possible modelling approaches is presented, with a deep focus on those proposed for modelling Fenton and photo-Fenton processes (being the latter the main case study of this work).

2.4 Mathematical modelling of chemical processes

A mathematical model is a “representation of the essential aspects of an existing system (or a system to be constructed) which presents knowledge of that system in a usable form” (Eykhoff, 1974).

According to the model attributes, it is possible to distinguish between:

- Stochastic or deterministic models: if the model contains elements of randomness or not, respectively;
- Continuous models: usually based on ordinary differential equations or partial differential equations in order to represent natural phenomena;
- Discrete models: usually related to decision-making processes;
- Linear or non-linear models: depending on whether the system of equations is linear or non linear, respectively;
- Steady state or unsteady state models: depending on whether the process variables are constant with time or change with time, respectively;

Advanced Oxidation Process Models for Optimisation and Decision Making support in Water Management

- Lumped parameter (described by Ordinary Differential Equations ODEs) or distributed parameter (described by Partial Differential Equations PDEs) models.

For a proper modelling, it is important to know which of the following categories the chemical process under study falls:

- Continuous (the process inputs and outputs flow continuously throughout the duration of the process and process variables can be mainly considered constant apart from small fluctuations around an average value and transitory start-ups and shutting down);
- Batch (the feed is fed into a vessel at the beginning of the process and removed when the process ends. Also reactants are added at the beginning of the process without further additions during the process evolution);
- Semi-continuous (a process which is neither batch nor continuous process).

The process modelling approaches can be mainly grouped in:

- First principles models (based on physical theory);
- Data-based models (strictly based on empirical descriptions);
- Semi-Empirical Models (based on both physical theory and empirical descriptions).

In order to develop a process model, the following main phases must be followed:

- A problem definition phase that comprises:
 - Formulation of the model objectives, of the evaluation criteria and of the development costs;
 - Selection of the key variables and of the physical principles to apply and of the Parameter Estimation technique to be used.
- A design phase based on:
 - Development of the model (from reality observation and real data);

- Parameters Estimation (by using real data) / Computer simulation.
- An evaluation phase providing:
 - Validation of the model;
 - Application of the model.

Where the parameter estimation is an optimisation problem searching for those parameters that minimize a cost function which measures the goodness of the fit of the model with respect to a given experimental data set (Moles et al., 2003).

2.4.1 Fenton and photo-Fenton modelling approaches

Despite the extensive experimental work, the mathematical modelling of Fenton and photo-Fenton processes, is still under development. The description of the degradation mechanism and of the by-products involved is a very difficult task.

Specifically, mainly three different approaches have been proposed:

- First Principles Models (FPMs);
- Data Based Models (DBMs);
- Semi-Empirical Models (SEMs).

Some FPMs rely on the detailed kinetic modelling of Fenton and photo-Fenton processes and follow the scheme proposed by Kang et al., 2002 based on three main group of reactions (an inorganic chemistry core, interactions between target compounds, intermediates and Fenton reactants and finally the interactions between iron species and the intermediates). The works by Jeong and Yoon, 2005, Ortiz de la Plata et al., 2010, and Simunovic et al., 2011, that rely on the description of all the elementary steps of the process, are representative examples of this kind of FPMs.

Moreover, following the work initiated by Cassano et al., 1995 and Alfano et al., 1986, FPMs based on rigorous radiation models to compute the spatial distribution of the absorbed photons inside the reactor (Conte et al., 2012), (Farias et al., 2007) have also been proposed. A recent work describing a mechanistic model of solar photo-Fenton has also been proposed by Soriano-Molina et al., 2018.

On the other hand, in the area of DBMs, it is possible to find models that rely on a complete empirical approach based on the use of regression models (Kusic et al., 2006) eventually coupled with the design of experimental techniques (Pérez-Moya et al., 2008). Moreover, in the DBMs area, Artificial Neural Networks (ANN) (Göb et al., 2001), Support Vector Regression (SVR) (Shokry et al., 2015) and Ordinary Kriging (OK) (Shokry et al., 2015) have been also used.

Conversely, a SEM model using a lumped parameter (TOC) as a mean of process performance, has been proposed by Cabrera Reina et al., 2012. This model explicitly takes into account the light influence (as a component of the process) and was then improved by Cabrera Reina et al., 2015 by including the effect of the Volumetric Rate of Photon Absorption (VRPA).

The accuracy and completeness of FPMs ensures the understanding of the chemical process, however the resulting computational effort might be unaffordable. Moreover, the complex nonlinear nature of the Fenton and photo-Fenton systems makes it difficult to develop a comprehensive FPM including all the involved reaction mechanisms in more general cases so limiting their application for process monitoring and control. Conversely, among the DBMs the regression models tend to usually oversimplify the complex nonlinear behaviour of such processes, and are characterized by limited capabilities of correlation of larger sets of process variables. Conversely, the DBMs based on the use of advanced techniques can better capture the nonlinear system behaviours but are not based on a physical description and understanding of the chemical process.

The process model can also be integrated into upper level models (e.g. water network) so to allow the optimisation of the whole system.

Hence in the following sections an overview of the techniques to solve different optimisation problems, focusing on the problem of the water treatment network optimisation, is presented.

2.5 Supply Chain and Supply Chain Management

The concept of a Supply Chain (SC) refers to the network of interdependent entities (including retailers, distributors, transporters, production and storage facilities and suppliers) that constitutes the processing and distribution channels of a product, from the sourcing of its raw materials to its delivery to the end consumer (Beamon, 1998).

Conversely, the Supply Chain Management (SCM) concept was defined by The Council of Supply Chain Management Professionals (CSCMP), as follows:

“Supply Chain Management encompasses the planning and management of all activities involved in sourcing and procurement, conversion, and all logistics management activities. Importantly, it also includes coordination and collaboration with channel partners, which can be suppliers, intermediaries, third-party service providers, and customers. In essence, supply chain management integrates supply and demand management within and across companies. Supply Chain Management is an integrating function with primary responsibility for linking major business functions and business processes within and across companies into a cohesive and high-performing business model. It includes all of the logistics management activities noted above, as well as manufacturing operations, and it drives coordination of processes and activities with and across marketing, sales, product design, and finance and information technology.”

Supply Chain Management can be applied at three major levels namely, strategic planning, tactical planning, and production scheduling that will be detailed below and that can be observed in the following Figure 2.2:

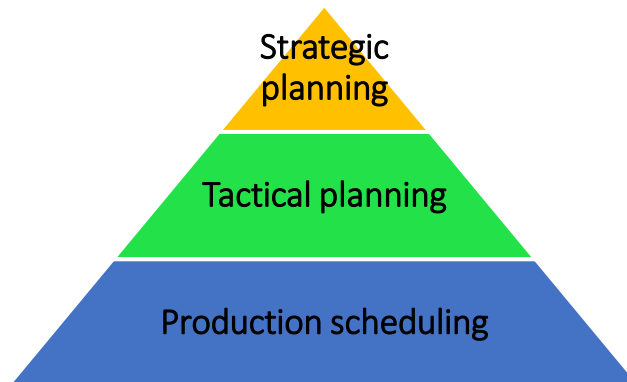


Figure 2.2 Hierarchical levels of the Supply Chain Management

- Strategic planning, or long term planning, is a long term planning (time horizon of years). Issues addressed at this level include choosing the site and purpose of business facilities; creating a network of reliable suppliers, transporters, and logistics handlers; long-term improvements and innovations to meet client demands; inventory and product management throughout its life cycle. The SC design problem has its origins in the location and planning problem that has been studied in Operations Research since the mid-1950s (Heragu, 2006).
- Tactical planning or medium-term planning is a medium-term planning (time horizon of months). Common concerns include procurement contracts for necessary materials and services, production schedules and guidelines to meet quality, safety, and quantity standards; transportation and warehousing solutions, including outsourcing and third-party options; inventory logistics, including storage and end-product distribution; adopting best practices in comparison to competitors.
- Production scheduling or short-term planning is a short-term decision making (scheduling horizons in days or weeks), and aims at determining the allocation of resources along time in order to achieve a specific amount of production optimally in compliance with a specific objective function. Scheduling decisions include batch-sizing, assignment of tasks to equipment units, and sequencing of tasks.

In order to address the above listed optimization problems the technique presented in the following section can be employed.

2.5.1 Optimisation techniques

The techniques to solve optimisation problems are mainly classified in deterministic and stochastic techniques. The selection of the proper technique to be used depends on the nature of the problem to be addressed.

Deterministic techniques can ensure global optimality of the solution within a specific tolerance. They can be classified in continuous and discrete optimisation techniques:

- Continuous optimisation techniques can solve Linear and Non-linear problems:
 - Linear Programming (LP), refers to problems in which both the objective function and the constraints are linear. The most common methods to solve LP problems are simplex and interior points.
 - Non Linear Programming (NLP), refers to problems involving minimization (or maximization) of a nonlinear objective function. The most common algorithms designed for NLP optimisation include Newton-Raphon methods, conjugate gradient methods or quasi-Newton methods (Broyden method) and successive quadratic programming (SQP) for quadratic optimisation problems.
- Discrete optimisation techniques can solve Mixed Integer Linear and Non-Linear problems:
 - Mixed-Integer Linear Programming (MILP), refers to problems that are linear in the objective function and in constraints and in which the objective function depends on two sets of variables, x and y ; where x is a vector of continuous variables and y is a vector of integer variables;
 - Mixed-Integer Nonlinear Programming (MINLP), refers to problems involving discrete variables in which some of the functions are nonlinear. The main algorithms for MINLP problems include Branch and Bound, Generalized Benders Decomposition, Outer-Approximation and Extended Cutting Plane.

Stochastic techniques cannot ensure global optimality but provide with approximations. These techniques are used to solve large scale problems for which it is difficult to find a solution through deterministic techniques, due

Advanced Oxidation Process Models for Optimisation and Decision Making support in Water Management

to computational complexity. Usually are used in order to model and solve optimisation problems under uncertainty related to the presence of unknown parameters.

In the following Table 2.1 are summarized the most common optimisation methods used for each of the above mentioned optimisation problem:

Table 2.1. Most common optimisation methods for LP, NLP, MILP, MINLP problems

Optimisation problem	Optimisation method
LP - Linear Programming	Simplex Method; Barrier Methods (Primal-Dual Interior-Point Method).
NLP - Non Linear Programming	Penalty, Barrier and Augmented Lagrangian Methods; Successive Linear Programming (SLP); Successive Quadratic Programming (SQP); Generalized Reduced Gradient Method (GRG).
MILP - Mixed Integer Linear Programming	Branch and Bound Method; Outliner linearization (LP relaxation); Exhaustive Enumeration Algorithm; Cutting-plane method.

MINLP - Mixed Integer Non Linear Programming	Branch and Bound Method; Outer approximation; Generalized Benders decomposition (GBD).
--	--

Finally **multi-objective optimisation problems**, concerning the trade-off between multiple conflicting objectives (e.g. economic, environmental and social instances) can be also addressed. In this case the proposed mathematical model will be optimized by using different objective functions. The solution of a multi-objective optimisation problem will provide a set of the so called **Pareto frontiers solutions** (Messac et al., 2003). The mathematical methods used to solve a multi-objective optimisation problem are mainly, meta-heuristic and e-constraint methods.

2.5.2 Water Supply Chain and Water Supply Chain Management

Water Supply Chain and Waste Water Supply Chain allow the conceptualization of the succession of events to be addressed in the water management, from where water is accessed (the source) through the various uses and reuses, to where it is disposed.

Several works have addressed the problem of the water treatment network optimisation, starting by Mishra et al., 1975 that stated the need of systematic design tools for wastewater treatment systems. The first approach was to describe centralized system and then decentralized ones. The first approach relies on the treatment of all the different streams (urban and different industrial effluents coming from different production plants) in a common facility. Conversely in the decentralized approach streams can be treated separately or partially mixed, so to reduce the flowrate to treat and consequently the capital costs.

The solution obtained following a decentralized approach, showed to be the best design option (McLaughlin L. A., et al., 1992) because it allowed reducing the flowrate to be treated, which turned into a decrease of the investment cost. Moreover, it avoids the total mixing of the streams to be treated which led to a decrease of the concentration of the contaminant to be removed, and which in turn led to an increase of the operational cost.

Three main approaches have been followed in the water allocation problems, such as, graphical methodology based on superstructures of alternative designs (Takama et al., 1980), (Wang and Smith, 1994a), (Wang and Smith, 1994b), (Wang and Smith, 1995), (Kuo and Smith, 1997), (Manan et al., 2006), mathematical programming (Feng et al., 2008) and mass exchange networks (Shafiei et al., 2004).

NLP and MILP models have been proposed for single pollutant networks while MINLP for more complex networks.

Especially, Boix et al., 2011 addressed the multi-objective and multi-contaminant optimisation problem for the optimal design of an industrial water networks solved with a MINLP. Rubio-Castro et al., 2012 have proposed a MINLP to find the optimal reconfiguration of a multi-plant network. (Koleva et al., 2015) proposed a MILP model for the synthesis and optimisation of water purification flowsheets, where both individual units and their interconnections are optimized.

Moreover, fixed rates for the treatment units and independent components have been usual assumptions (Galan and Grossmann, 1998), (Karuppiah and Grossmann, 2006). However, Yang et al., 2014 recently made an important contribution to this investigation area by replacing the traditional fixed recovery treatment units with unit-specific short-cut models, developed for the best available techniques selected for the removal of major pollutant groups.

However, the recent need of combining conventional biological systems and Advanced Oxidation Processes (AOPs) and of considering also the interrelations between the different inlet components (mixture of substances interacting), has paved the way to new modelling and optimisation challenges in the Water Supply Chain Management area.

3 Experimental setting, analytical techniques and mathematical tools

This chapter presents an overview of the experimental settings and analytical methods that have been used to acquire data that helped the overall understanding of the AOPs under study. An overview of the mathematical tools that allowed the transformation of the collected data into information and knowledge in the subsequent step of modelling and optimisation at a process and plant level, is also given.

3.1 Experimental

This section presents a first detailed description of the pilot plant that was used to perform Fenton and photo-Fenton experiments being the photo-Fenton process selected as the main case study of the thesis, according to the experimental results described in the following Chapter 4. This pilot plant was designed by the CEPIMA (Center for Process and Environmental Engineering, Universitat Politècnica de Catalunya, Barcelona Spain) investigation group as part of the activities developed under Project EHMANN (EXPANDING THE HORIZONS OF MANUFACTURING: SOLVING THE INTEGRATION PARADOX. Project EHMANN DPI2009-09386, funded by the European Union, European Regional Development Fund 2007-13 and the Spanish Ministry of Science and Innovation-MCINN). Then, a brief description of the pilot plant used to perform the VUV photo-oxidation assays is presented as well. The latter was designed by the Institute for Interfacial Engineering and Biotechnology (Fraunhofer, Germany), collaborating with the CEPIMA investigation group.

Finally, the experimental part is concluded by presenting the materials, with a deep focus on the selected target compounds that were used to perform the required experiments, including toxicity tests, for obtaining the desired experimental data to be used in the subsequent modelling step. Then, a final description of the applied analytical techniques, of the design of experiment technique, and of the cytotoxicity technique used in this study, is presented as well.

3.1.1 Experimental set-up

3.1.1.1 Fenton/photo-Fenton pilot plant

The pilot plant that has been used to perform Fenton and photo-Fenton experiments is a flexible installation that can allow investigating different AOPs, such as UV-photolysis, Fenton and photo-Fenton.

The installation is a 15.0-L system composed by a glass jacketed tank that can act as reservoir and as photoreactor because it has a lamp holder axially

located, and a glass annular reactor which also has a lamp holder axially located. These two reactors can work individually or can be combined.

In the present study the selected configuration of the pilot plant was the one using the glass jacketed tank as reservoir and the glass annular reactor as photoreactor.

A Philips Actinic BL TL-DK 36 W/10 1SL lamp (UVA-UVB) has been used as radiation source.

In Figure 3.1 it is possible to observe the spectrum of the lamp considering a Pyrex envelope.

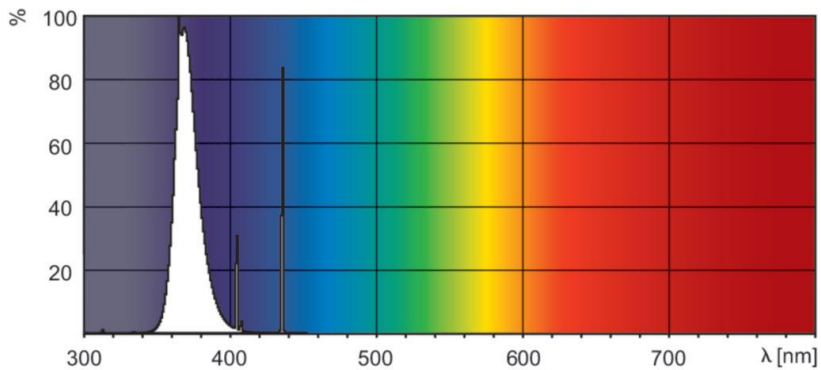


Figure 3.1. Spectrum of a Philips Actinic BL TL-DK 36 W/10 1sl lamp

A picture of the glass annular photoreactor with its specifications as well as the characteristic of the lamp are presented in the following Figure 3.2.



REACTOR

Irradiated volume: 1.5 L

Irradiated height: 130.0 mm

Outer cylinder (*Outer diameter: 150.0 mm, Inner diameter: 130.0 mm*)

Inner cylinder (*Outer diameter: 70.0 mm, Inner diameter: 63.6 mm*)

IRRADIATION SYSTEM

Lamp: Philips Actinic BL TL-DK 36 W/10 1SL lamp (UVA-UVB): (*diameter: 28.0 mm, length: 589.8 mm*)

Figure 3.2. Annular photoreactor and irradiation system

The incident photon power, $E = 3.36 \times 10^{-4}$ Einstein min^{-1} (300 and 420 nm) was measured by Yamal-Turbay et al., 2015 using potassium ferrioxalate actinometry (Murov et al., 1993).

The following Figure 3.3 presents a schematic view of the pilot plant with the different components that will be described below.

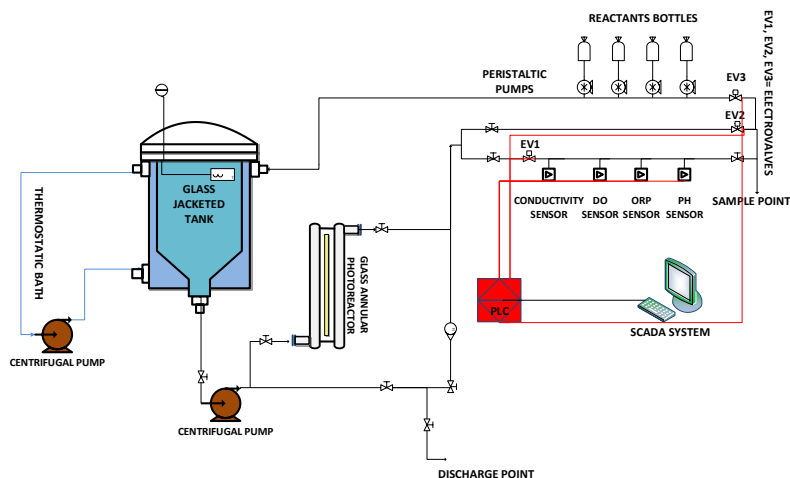


Figure 3.3. Schematic view of the pilot plant

The recirculation flowrate through the tank reactor and the annular photo-reactor is possible thanks to a centrifugal pump (Iwaki Magnet Pump, MD-30RZ-220, 1-16HP-220V) connected to a variable frequency inverter (Eurotherm, CFW-10 series) that allows varying the flowrate from 2.0 to 15.0 L min⁻¹ so to ensure working under perfect mixing conditions. The recirculation flowrate through the system is measured by a rotameter (Tecfluid 6001/PVC 3/4").

Moreover, four peristaltic pumps (Watson Marlow, OEM 313 24V) for the possible dosage of the reactants are also available.

Two electro valves (Hunter PGV-101G-B 1"), indicated as EV2 and EV3 in Figure 3.3, are located before the pumping line composed by the peristaltic pumps.

The pilot plant is also equipped with a measuring line in which sensors of pH, dissolved oxygen, conductivity and oxidation-reduction potential (ORP), are allocated.

The flowrate flowing through this measuring line is kept at 1.0 mL min⁻¹ through a proportional electro-valve (mPm L20-J2), named EV1 in Figure 3.3. While a flowmeter (DIGMESA 04 – 16 L min⁻¹, 800 p/L), connected to a

Advanced Oxidation Process Models for Optimisation and Decision Making support in Water Management

Eurotherm 2132i indicator ($4 - 16 \text{ L min}^{-1}$) allows the measurement of the recirculation flowrate through this measuring line.

Moreover, a UV sensor probe (sglux UV_Surface_A_4-20mA_cable) for surface measurements with a highest sensitivity range of 1 nW cm^2 is located at the external surface of the annular photoreactor. This sensor allows continuous measurements and collection (each second) of UV radiation. It is used to guarantee that the experiments belonging to a same design of experiments are characterized by the same intensity of radiation.

Finally, a temperature probe PT-100 is also located inside the tank reactor and it is connected to a Eurotherm 2132i indicator.

Regarding the temperature of the system it must be noted that it can be kept constant thanks to a thermostatic bath.

The characteristics of each of the sensors installed are presented in the following Table 3.1.

Table 3.1. Sensors installed in the 15.0-L pilot plant

SENSORS IN THE MEASURING LINE	
pH probe	Hamilton Polilyte HTVP 120 (0-14 pH units), connected to a Eutech alpha pH 500 indicator
Conductivity probe	4 ring conductivity sensor (0.1 microSiemens to 1,000 milliSiemens) connected to a Eutech CON 500 LCD indicator
ORP probe	Hamilton Polilyte RX120 ($\pm 2000 \text{ mV}$) Connected to a Eutech alpha pH 500 indicator
Dissolved Oxygen probe	Hamilton Oxysens (40 ppb to 40 ppm (DO) or 0.8 to 1000 mbar (pO_2)) connected to a Knick Stratos EVO A402 indicator)
OTHER SENSORS	
UV sensor probe	Sglux UV_Surface_A_4-20mA_cable for surface measurements
Temperature probe	PT-100 connected to a Eurotherm 2132i indicator

With the aim of allowing process control, the pilot plant is equipped with a Programmable Logic Controller (PLC) connected to a WonderwareR InTouchR

software, that allows data acquisition from in/out modules connected to the installation (e.g. sensors) and data management from an OPC (OLE for Process Control) server throughout a SCADA (Supervisory Control And Data Acquisition) system.

One of the advantage of the connection with a PLC-SCADA system is the possibility of programming the dosage of the Fenton reactants (H_2O_2 , $\text{Fe}^{2+}/\text{Fe}^{3+}$). A stepwise dosage strategy is programmed via a PID (Proportional–Integral–Derivative) programmed through InTouchR software, and requires the definition of the amount of reactant to be dosed during a specific time interval.

3.1.1.2 VUV photo oxidation pilot plant

The pilot plant designed by the Institute for Interfacial Engineering and Biotechnology (Fraunhofer, Germany) is equipped with:

- four flat lamp reactor systems, each containing a Xenon Excimer Flat Lamp emitting VUV at 172 nm and connected to a
- 2.0-L jacketed glassware reservoir tank.

A magnetically coupled centrifugal pump Sondermann BGR 1.5 (Sondermann, Köln, Germany) is used to control the recirculation flowrate through the flat lamp reactors and the reservoir tank and can be varied between 0.8 and 4.2 L min⁻¹.

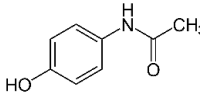
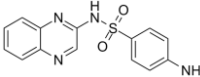
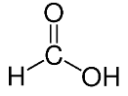
The irradiated volume (V_{IRR}) of this system is given by the product of the lamp surface (310.0 cm²) for the effective absorbing path (3.6×10^{-3} cm) resulting in a value of 1.1 cm³ or rather 1.1×10^{-3} L.

For more specifications please refer to Toro Santamaria et al., 2017.

3.1.2 Reagents and chemicals

In the present study, three different organic substances were selected as model contaminants: paracetamol, sulfaquinoxaline sodium salt and formic acid and their characteristics are specified in the following Table 3.2.

Table 3.2. Selected model contaminants

Name (abbreviation used in the thesis)	Chemical structure	Formula	Molecular weight (g mol ⁻¹)	Provider
Paracetamol 98% purity (PCT)		C ₈ H ₉ NO ₂	151.17	Sigma-Aldrich (St. Louis, MO, USA)
Sulfaquinoxaline sodium salt 95% purity (SQX)		C ₁₄ H ₁₁ N ₄ NaO ₂ S	332.32	Sigma-Aldrich (St. Louis, MO, USA)
Formic acid 98% purity (FA)		CH ₂ O ₂	46.03	Honeywell Fluka (Morris Plains, NJ, USA)

Paracetamol (PCT) was selected as model pollutant since it is one of the top 200 pharmaceuticals prescribed overall the world, being widely used as antipyretic and analgesic. Therefore, PCT is continuously released by hospital waste (Langford and Thomas, 2009), as well as by consumer use and disposal (according to Muir et al., 1997, PCT is excreted in 58-68% during therapeutic treatment). As a consequence, it has been detected in the effluents of sewage treatment plants in µg L⁻¹ (Ternes, 1998), in natural water sources, e.g. at concentrations higher than 65 µg L⁻¹ in the Tyne River (UK) (Antunes

et al., 2013), and even in groundwater at concentration ranging between $\mu\text{g L}^{-1}$ and ng L^{-1} (De Gusseme et al., 2011).

Sulfaquinoxaline sodium salt (SQX) is usually used to prevent coccidiosis in poultry, swine, and sheep and hence it represents a potential food contaminant in animal products. Significant levels of Sulfonamides have been detected in rivers, groundwater and soil, particularly coming from the wastewaters of animal farms and hospitals (Baran et al., 2011). The SQX consists of a sulfa group and a quinoxaline group. The latter is the one that has shown mutagenic and carcinogenic activities. Moreover, the presence of low concentrations of sulfonamides in the environment has shown to be responsible of the formation of strains of antibiotic-resistant bacteria (Novo et al., 2013), (Hoff et al., 2014).

Formic acid (FA) has been selected as by-product of the degradation of many hazardous organic compounds. It belongs to the group of carboxylic acids, being an organic compound that contains a carboxylic group, and that are hardly degradable even by chemical oxidation.

Moreover all the experiments performed in the present study (Fenton, photo-Fenton, VUV photo-oxidation) used a deionised water with a conductivity lower than $1.25 \mu\text{S}$ that was provided by Adesco S.A. (Barcelona, Spain).

Particularly, regarding Fenton and photo-Fenton experiments the following reagents were also used:

- Reagent-grade hydrogen peroxide (H_2O_2) 33% w/v from Panreac (Barcelona, Spain) was used as the oxidant;
- Iron sulfate ($\text{FeSO}_4 \cdot 7\text{H}_2\text{O}$) from Merck (Kenilworth, NJ, USA), was adopted as the ferrous ion (Fe^{2+}) source;
- Hydrogen chloride HCl 37% from J.T. Baker Inc. (Phillipsburg, NJ, USA) was used to adjust the initial pH.

Regarding the analytical techniques applied in this study, the HPLC (High Performance Liquid Chromatography) analysis for the detection of the model compounds, were carried out using HPLC gradient grade methanol, MeOH,

purchased from J.T. Baker Inc. (Phillipsburg, NJ, USA) and filtered milli Q grade water as HPLC mobile phases.

Conversely, measurements of iron species required the following reagents:

- High purity (>99%) ascorbic acid from Riedel de Haën (Seelze, Germany);
- 0.2% 1,10-phenanthroline from Scharlab (Barcelona, Spain);
- Sodium acetate anhydrous from Panreac (Barcelona, Spain);
- 95%–98% sulfuric acid, from Panreac (Barcelona, Spain).

Finally to perform cytotoxicity assays using cell line cultures the following reactants were required:

- Dulbecco's Modified Eagle Medium (DMEM), purchased from Gibco® (Thermo Fisher Scientific, Madrid, Spain);
- Phosphate-Buffered Saline (PBS) purchased from Gibco® (Thermo Fisher Scientific, Madrid, Spain);
- Foetal bovine serum (FBS) purchased from Gibco® (Thermo Fisher Scientific, Madrid, Spain);
- (3-(4,5-dimethyl-2-thiazolyl)-2,5-diphenyl-2H-tetrazolium bromide (MTT) purchased from Sigma-Aldrich (St. Louis, MO, USA).
- Dimethyl sulfoxide (DMSO) purchased from Sigma-Aldrich (St. Louis, MO, USA).

3.1.3 Analytical techniques

This section is dedicated to the description of the analytical techniques and of the equipment that were used in the present study to characterize the performance of the investigated AOPs.

Particularly, measurements of the Total Organic Carbon (TOC) and of the concentration of the model contaminants were performed in both Fenton/photo-Fenton experiments and VUV photo-oxidation assays.

Conversely, during Fenton and photo-Fenton assays, the measurements of the concentration of the Fenton reagents (H_2O_2 , iron species) were also required.

3.1.3.1 Total Organic Carbon (TOC) determination

The Total Organic Carbon (TOC) represents the amount of carbon in the organic compound. It is a lumped parameter that gives an indirect measure of all the organic compounds in the water sample. The TOC is of high interest because it is virtually impossible to detect and follow the degradation of each intermediate formed during the treatment. Hence the TOC is used to evaluate the mineralization of the organic matter in the water sample, or rather as an indicator of water quality.

The analysis of TOC is attained via the analysis of Total Carbon (TC) and Total Inorganic Carbon (TIC): the difference between TC and TIC results in TOC.

The TC analysis is based on the combustion of the aqueous sample in a tube filled with platinum catalyst on an aluminum spheres support that is heated and maintained at a temperature of 680.0 °C. In this way, the carbon in the sample is oxidized to CO_2 . The CO_2 is then swept by a CO_2 free carrier gas (purified air) flowing at a controlled flowrate ($150.0 \text{ mL min}^{-1}$) onto a dehumidifier where it is cooled and dried. Finally the CO_2 reaches a non dispersive infrared (NDIR) detector that analyzes the signal produced by the absorbance of the CO_2 which is then evaluated by the equipment's software. The NDIR detector signal generates a peak, the area of which is proportional to the concentration of TC.

The measurement of Total Inorganic Carbon (TIC) is attained by mixing the sample with a 25% w/v phosphoric acid (H_3PO_4) in a reaction chamber. The acidified sample is then sparged with the free carrier gas so to attain the decomposition of the carbonates and bicarbonates into CO_2 , which is then

dehumidified and analysed by the non dispersive infrared (NDIR) detector and evaluated by the equipment's software.

The quantification is done via a linear relationship between peak area and carbon concentration (for TC and TIC) obtained by preparing standard solutions in ultra-pure water (Milli-Q® system).

In the present work the TOC analysis were carried out by using a Shimadzu TOC-VCSH/CSN analyser (Shimadzu; Kyoto, Japan).

Due to the measuring time limitation (each measure lasts 15.0 min), samples were taken each 15.0 min and were refrigerated after extraction in order to slow down any further degradation of the organic matter.

Regarding the calibration curves, the TC measurement was calibrated using potassium hydrogen phthalate standard solutions while TIC measurement was calibrated by sodium carbonate/sodium hydrogen carbonate standards.

Especially, for the TC quantification, two calibration curves ranging from 0.0-20.0 mg L⁻¹ ([TC]= 0.4238 * PEAK_AREA - 0.2207, R²= 0.99), and 0.0-50.0 mg L⁻¹ ([TC]= 0.4278 * PEAK_AREA - 0.1892, R²= 0.99.), were obtained. Conversely, the TIC quantification has been possible by using two linear calibration curves, ranging from 0.0-5.0 mg L⁻¹ ([TIC]= 0.0249 * PEAK_AREA - 0.307, R²= 0.99), and 0.0-10.0 mg L⁻¹ ([TIC]= 0.0247 * PEAK_AREA - 0.3533, R²= 0.99).

These calibration curves cover the range of minimum and maximum TOC concentrations adopted in the experimental study of this work.

The measurement errors for this equipment resulted to be 0.23 mg L⁻¹ for TC and for TIC 0.04 mg L⁻¹.

3.1.3.2 Model contaminant determination via HPLC (High Performance Liquid Chromatography)

High Performance Liquid Chromatography (HPLC) has been used to detect and quantify the concentration of the model contaminants in the water sample.

The HPLC is a technique that allows the separation of the components of a sample, driven by a mobile phase and forced by mechanical pumping to pass through a separation column filled with a porous medium that is the stationary phase (solid particles typically smaller than 2 μm). The separation of the individual components in a water sample occurs in the stationary phase. Then the separated components are detected at the exit of the column by a detector. The majority of organic compounds, as absorb light in the UV or visible regions of the electromagnetic spectrum, can be analysed by The UV/VIS detector which uses light in the visible and adjacent (near-UV and near-infrared (NIR)) ranges. Then, thanks to a linear relation between peak area and concentration is possible to achieve the required value of concentration.

The time that a substance takes to pass through the separation column and reach the infra-red detector is known as retention time (T_R) and it depends on several factors such as the pressure, the nature and temperature of the stationary phase, and the composition of the mobile phase.

The equipment used in this study is an HPLC Agilent 1200 series (Agilent Technologies, Santa Clara, CA, USA) consisting of four modules: a mobile phase degasser, a quaternary pump, a heating oven and a UV diode (UV-DAD) array detector. A manual injector allows the mixing of the sample with the mobile phase. This mixture is then carried out by the quaternary pump throughout the stationary phase towards the UV-DAD array detector.

As stationary phase an Akady 5 μm C-18 150 \times 4.6 mm column was used, or rather silica (RMe_2SiCl) with a side chain alkyl group (R) such as $\text{C}_{18}\text{H}_{37}$.

The mobile phase was a mixture of ultra-pure solvents (Milli-Q[®] water) and organic solvents like methanol (MeOH).

Specific chromatographic conditions have been used to detect each of the model contaminants of this study and are presented in Table 3.3.

In all cases an isocratic method based on a constant mobile phase composition throughout the separation process was applied.

The methods are programmed by a Chem-StationR software that also allows data acquisition and processing.

Table 3.3. Chromatographic conditions used to detect each of the model contaminants selected in the present study

	PCT	SQX
Mobile phase	25% H ₂ O 75% MeOH	55% MeOH 45%, 0.1% (v/v) formic acid
Stationary phase	Akady 5 µm C-18 150.0×4.6 mm	Akady 5 µm C-18 150.0×4.6 mm
T, °C	25.0	25.0
Flow, mL min⁻¹	0.4	1.5
λ, nm	243	250
T_R, min	9.0	2.0

Samples were taken at specific time intervals depending on the degradation rate of each model contaminant so to be able to capture the evolution of the concentration during the treatment span and were previously treated with methanol (in proportion 50:50) in order to stop further degradation of the organic matter.

To quantify the concentration of the model contaminants specific calibration curves have been prepared according to the maximum concentration to be detected.

In the case of PCT a nine points calibration curve was used [0.0, 0.5, 2.5, 5.00, 10.0, 20.0, 30.0, 40.0, 50.0 mg L⁻¹]. The corresponding equation is [PCT]= 0.0048 * PEAK_AREA + 0.0697, R²= 0.99.

The concentration of sulfaquinoxaline was quantified by preparing a seven points calibration curve [2.5, 5.0, 10.0, 20.0, 30.0, 40.0, 60.0 mg L⁻¹]. The corresponding equation is [SQX]= 0.0188 * PEAK_AREA + 0.8366, R²= 0.99.

Finally, the concentration of formic acid, being composed by only one carbon atom, was not followed by HPLC but only by TOC measurements.

The experimental error of the measurement technique resulted to be 0.15 mg L⁻¹.

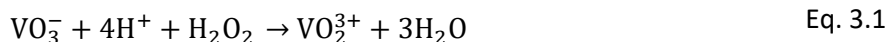
3.1.3.3 Hydrogen peroxide determination via spectrophotometric technique

The hydrogen peroxide is the oxidant consumed during the treatment of water by Fenton and photo-Fenton process. The measurement of the residual concentration of hydrogen peroxide and consequently its consumption during the treatment span allows evaluating the efficiency of the chemical oxidation of the organic matter. It is also possible to raise conclusions about the additional requirement of hydrogen peroxide to attain the desired mineralization level and/or model contaminant degradation.

Several methods are available for the determination of the hydrogen peroxide, such as iodometric or permanganate titration. The first one is more time-demanding and less reliable (due to the volatilization and hydrolysis of I₂) than the second one which on the contrary cannot be used in case of performing Fenton and photo-Fenton experiments because of the interference with the ferrous ion.

Hence, the spectrophotometric method proposed by Nogueira et al., 2005 was used in this study, having the advantages to be economic and fast.

The method is based on the measurement of the absorbance at 450 nm of the peroxovanadium cation (VO₂³⁺) that originates from the reaction between hydrogen peroxide and ammonium metavanadate in acidic medium:



An excess of ammonium vanadate was always added in order to ensure that all of the hydrogen peroxide reacts with the ammonium metavanadate.

The final concentration of peroxovanadium is equal to the initial concentration of hydrogen peroxide as can be deduced by stoichiometry of the reaction in Equation 3.1.

The absorption at 450 nm is proportional to the $[\text{VO}_3^-]$ which allows its quantification by UV-visible spectrophotometry.

A U-2001 UV-VIS spectrophotometer (Hitachi, Tokyo, Japan) was used to determine the concentrations of hydrogen peroxide during Fenton and photo-Fenton experiments. Samples were taken each 5.0 min during the first 30.0 min of reaction and then each 15.0 min until the end of the treatment. Usually, 1.0 mL of sample was mixed with 1.1 mL of ammonium metavanadate and then taken to 10.0 mL.

The hydrogen peroxide concentration was quantified using a ten points calibration curve [1.3, 2.6, 13.2, 26.4, 39.6, 52.8, 66.0, 75.6, 99.0, 113.4 mg L⁻¹]. The corresponding equation is $[\text{H}_2\text{O}_2] = 125.8 * \text{ABSORBANCE} + 0.58$, $R^2 = 0.99$.

This curve was defined considering that Nogueira et al. 2005 evaluated that despite the linear range of the calibration curve is up to 5.0 mmol L⁻¹ (corresponding to 170.0 mg L⁻¹) it is possible to determine higher concentrations of the hydrogen peroxide after proper dilution in order to avoid absorbance values > 1.5.

3.1.3.4 Iron species determination via spectrophotometric technique

Iron is the driving catalyst of the homogeneous photo-Fenton reaction. In order to ensure the use of the iron as a catalyst or rather, ensuring the reduction of Fe^{3+} to Fe^{2+} (Fenton-like reaction) at an appreciable rate (Pignatello, 1992), (Huston and Pignatello, 1999), (Pignatello et al., 2006), and avoiding its precipitation, pH must be maintained in the range $2.5 < \text{pH} < 3.0-4.0$.

This means that to ensure the correct measurement of the iron a fast, simple and robust method is required.

A reliable method is the spectrophotometric method (ISO 6332) with 1,10-phenanthroline, based on the measurement of the absorbance of the stable orange-red colored chelate complex that ferrous iron forms with 1,10-phenanthroline. This complex does not change color between pH 3.0 and 9.0 and has a molar extinction coefficient of $11720.0 \pm 60.0 \text{ L mol}^{-1} \text{ cm}^{-1}$ at 510 nm. Although this range is large enough to ensure the quantitative formation of the desired complex, a buffer solution is used in order to maintain the pH between 3.0 and 3.5.

The presence in the solution of other oxidizing agents (as H_2O_2) that can oxidize ferrous ion (Fe^{2+}) to ferric ion (Fe^{3+}) which does not form complexes with phenanthroline, can interfere with the iron measurements.

In order to avoid the interference of hydrogen peroxide, ascorbic acid is used, which destroys H_2O_2 and reduces any Fe^{3+} to Fe^{2+} , so that the iron measured is the total iron present in the dissolved form in the sample.

The ISO 6332 method has been used in this study to determine the concentrations of the iron species ($[\text{Fe}^{2+}]$, $[\text{Fe}^{3+}]$, $[\text{Fe}^{\text{TOT}}]$) during Fenton and photo-Fenton experiments, by a U-2001 UV-VIS spectrophotometer (Hitachi, Tokyo, Japan).

Total iron concentration (Fe^{TOT}) was measured using ascorbic acid to convert all ferric ions (Fe^{3+}) to ferrous ions (Fe^{2+}), while ferrous ion is measured without the addition of ascorbic acid. Finally, ferric ion concentration is determined through the iron balance ($[\text{Fe}^{3+}] = [\text{Fe}^{\text{TOT}}] - [\text{Fe}^{2+}]$).

To quantify the concentration of the iron species that were used in a maximum concentration of 10.0 mg L^{-1} in all the experiments, a five points calibration curve [$0.5, 2.5, 5.0, 7.5, 10.0, 12.5 \text{ mg L}^{-1}$] was determined. The corresponding equation is $[\text{Fe}^{2+}] = 6.8 * \text{ABSORBANCE} + 0.09$, $R^2 = 0.99$.

3.1.4 Design of Experiment (DOE)

In the present work, the set of experiments to be performed was determined by applying the so called **Design of Experiment (DOE) technique**, also referred to as **Designed Experiments** or **Experimental Design**.

The DOE allows designing a set of experiments to collect the desired information such as which are the process inputs that have a significant impact on the process outputs, or the target level of those inputs that can produce a desired output.

The DOE analyzes three aspects of a process:

- **Factors:** these are the inputs to the process and can be classified as either controllable or uncontrollable variables;
- **Levels:** are the settings of each factor in the study;
- **Response:** represent the outputs of the experiment.

The Design of Experiment (DOE) techniques are used with the aim of improving processes and products by:

- Comparing possible alternatives;
- Identifying the significant inputs (Factors) affecting an output (Response) and avoiding considering not relevant information;
- Obtaining an optimal process output (Response);
- Reducing Variability;
- Minimizing, maximizing, or targeting an Output (Response);
- Improving process or product robustness, or rather the feasibility under varying conditions;
- Balancing tradeoffs when different factors require to be optimized.

One factor or multi factors experiments can be designed. Multi-factor experiments are designed to evaluate multiple factors set at multiple levels. One possible approach is the full factorial experiment, in which each factor is tested at each level in every possible combination with the other factors and their levels.

In the present work a 2² factorial design, with two factors each taking two levels and four treatment combinations in total, was used to design the experiments to be performed.

3.1.5 Toxicity tests

Cytotoxicity measurements at planned intervals were performed to determine the real environmental outcome of the AOPs under study.

In the present study cytotoxicity tests based on cell lines culture were carried out. Particularly, VERO and COS-1 cells, both cell lines isolated from an African green monkey kidney but with a different morphology, were selected and tested. Especially, the morphology of VERO cells corresponds to epithelial-like cells while the morphology of COS-1 cells corresponds to fibroblast-like cells (ATCC®, city, state abbrev, USA).

Cytotoxicity was assessed by measuring the viability of the cells exposed to the model contaminant and possible by-products.

In the present study the MTT assays were performed because they have been often used to detect cytotoxicity following exposure to toxic substances (Almazan et al., 2000) and the validity of this method has been tested on several cell lines (Mosmann, 1983).

The specific procedure followed for its determination is detailed in the following Chapter 4.

3.2 Mathematics tools

In this final section the tools used in this work for simulation and optimisation addressed in Chapters 5-8, are presented.

3.2.1 Simulation tools

The simulation of the First Principles Model describing the photo-Fenton degradation of PCT and addressed in Chapter 5 was performed using MATLAB.

MATLAB short for MATrix LABoratory and it is a fourth-generation programming language and a numerical computing environment.

It has several built-in functions for a wide variety of computations as well as several toolboxes designed for specific scientific disciplines, including solution of Ordinary and Partial Differential Equations, optimisation, statistics and data analysis.

Particularly, there are several ODEs (Ordinary Differential Equations) solvers, each based on a specific algorithm, available in MATLAB. These solvers solve two types of first-order ODEs:

- Explicit ODEs of the form $y' = f(t, y)$.
- Linearly implicit ODEs of the form $M(t, y) y' = f(t, y)$, where $M(t, y)$ represents a nonsingular mass matrix and can be time or state-dependent, or it can be a constant matrix.

There are solvers for non-stiff (ode45, ode23, ode113) and stiff (ode15s, ode23s, ode23t, ode23tb) problems. Also an ODE solver (ode15i) is available for fully implicit problems in the form $f(t, y, y') = 0$ and for Differential Algebraic Equations (DAEs) of index 1.

In the present work the simulation analysis were performed by solving a system of Ordinary Differential Equations (ODEs) using the following ODE solver:

- ODE45, based on an explicit Runge-Kutta (4,5) formula, or rather the Dormand-Prince pair. It is a single-step solver, or rather in computing $y(t_n)$, it needs only the solution at the immediately preceding time point, $y(t_{n-1})$.

It must be noted that for modelling and simulation of the First Principles Model of medium complexity describing Fenton and photo-Fenton degradation of the model compound as well as TOC and H_2O_2 evolution, faced in Chapter 6, a non-conventional methodology was adopted. This methodology is named Direct Computer Mapping (DCM) (Csukás et al., 1999), (Csukás et al., 2013) based Programmable Structure (Varga and Csukas, 2017). It has been already tried and validated for dynamic simulation based analysis of multi-scale, hybrid processes in a broad range of applications (from cellular signaling based biosystems to agri-food and environmental process systems (Varga et al., 2016), (Varga et al., 2017), (Varga and Csukas, 2017). This methodology allows building the process model from the definition of unified state (describing the actual state of the process) and transition (describing the actual transformations, transportations and rules) elements.

More specifications can be found in the following Chapter 6.

3.2.2 Optimisation tools

In the present work, the optimisation was addressed at two different levels: the optimisation of a control recipe faced in Chapter 7 and the design of a treatment network faced in Chapter 8.

The dynamic optimisation of the fed-batch photo-Fenton system addressed in Chapter 7 was carried out by using JModelica.org open source platform (Åkesson et al., 2010).

A direct approach, namely direct simultaneous optimisation method, was applied for solving the dynamic optimisation problem. This method is based on orthogonal collocation on finite elements (a fully implicit Runge-Kutta method), and relies on the discretization of both control and state variables by polynomials, whose coefficients become the decision variables of a very large-scale NLP problem.

The CasADi algorithm based on direct collocation and implemented in Python was used for computing function derivatives and IPOPT (Interior Point Optimizer) solver was used for solving the resulting NLP problem.

The simulation environment of JModelica.org open source platform uses Assimulo that is a standalone Python package for solving ordinary differential equations (ODEs) and differential algebraic equations (DAEs). Among the different supported solvers, the CVode solver was selected to run the dynamic simulation. The CVode (Åkesson et al., 2010) is a variable-order, variable-step, multi-step algorithm for solving ordinary differential equations of the form shown in Equation 3.2:

$$\frac{dy}{dt} = f(t, y), \quad y(t_0) = y_0 \quad \text{Eq. 3.2}$$

It includes the Backward Differentiation Formulas (BDFs), suitable for stiff problems, but also the Adams-Moulton formulas for non-stiff systems.

Finally, to solve the optimisation of a general wastewater network, the General Algebraic Modelling System (GAMS) was adopted.

GAMS can be used for large-scale modelling applications and to model and solve linear, nonlinear, and mixed-integer optimisation problems. For this reason is extensively used by multinational companies as well as universities and research institutions in several areas, including energy and chemical industries, economic modelling and agricultural planning.

GAMS was the first Algebraic Modelling Language (AML) and is formally similar to commonly used fourth-generation programming languages. It is connected to more than 25 optimisation solvers.

Particularly, the BARON solver or rather a Branch-And-Reduce Optimisation Navigator that can provide global solutions was adopted in this study (Tawarmalani and Sahinidis, 2005).

Moreover, it must be noted that to perform the estimation of the kinetic parameters of the conventional kinetic model presented in Chapter 5, one of the least squares (model fitting) algorithm available in MATLAB has been used.

Particularly, least squares, in general, is the problem of finding a vector x that is a local minimizer to a function that is a sum of squares, possibly subject to some constraints.

Several Optimisation Toolbox™ solvers are available for different type of functions and of constraints.

Particularly, the lsqnonlin optimisation toolbox, for nonlinear least-squares (nonlinear data-fitting) problems, and using a Levenberg-Marquardt algorithm was used in this study to solve the model fitting problem.

4 Comparison of effective AOPs

In the present chapter the performance of different AOPs (Fenton, photo-Fenton and VUV photo-induced oxidation) in the degradation of a pharmaceutical (paracetamol (PCT) in aqueous solution) has been presented.

The quantitative performance of the AOPs was addressed in terms of evolution of PCT concentration, Total Organic Carbon (TOC) conversion, and cytotoxicity results.

4.1 Introductory perspective

The increasing sensitivity of analytical instruments has allowed the detection of a growing number of new organic substances in wastewater, natural water and groundwater. Particularly, special attention has recently been paid to Contaminants of Emerging Concern (CECs) a group of chemicals including pharmaceuticals and personal care products that resist treatment by conventional Waste Water Treatment Plants (WWTPs) and accordingly require alternative and more effective treatment processes.

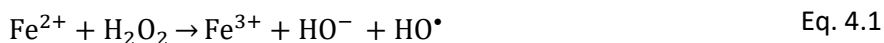
Several studies have reported the presence of persistent pharmaceuticals in effluents from conventional WWTPs and in surface waters affected by such effluents (Ternes, 1998), (Daughton and Ternes, 1999), (Heberer et al., 2002), (Joss et al., 2005), (Jones et al., 2007). Other studies have reported the presence of pharmaceuticals also in groundwaters, the major source of drinking waters (Heberer et al., 1997).

Advanced Oxidation Processes (AOPs) have been widely investigated as a promising and effective alternative for the removal of such Contaminants of Emerging Concern (CECs).

Particularly, several studies have addressed the use of photo-Fenton process for the removal of microcontaminants (Miralles-Cuevas et al., 2014) and the treatment of several kinds of industrial wastewaters (e.g. pharmaceuticals, olive-oil, cork, dye, and pesticides wastewaters) with a high organic content (Wang et al., 2016). The photo-Fenton process has attracted widespread attention in the scientific community because of the possibility of using solar light for its activation but also because it can be combined with conventional and cheaper biological processes to develop innovative, efficient and cost effective treatments (Rahim Pouran et al., 2015).

The photo-Fenton process results from the photo-induced enhancement of the Fenton process. The Fenton process (Fenton, 1894) occurs by means of the addition of hydrogen peroxide to Fe^{2+} salts (see Equations (4.1) to Equation (4.3)) while the photo-Fenton process occurs by the additional use of UV-VIS light irradiation at wavelength higher than 300 nm (Kiwi et al., 1993), (Pulgarin and Kiwi, 1996), which produces the photolysis of Fe^{3+}

complexes and subsequently causes a faster Fe^{2+} regeneration (see Equation (4.4)):



The extensive experimental work dedicated in the last decades to the understanding of the photo-Fenton process has revealed the importance of the Fenton reagent ratio ($\text{H}_2\text{O}_2:\text{Fe}^{2+}$) as one of the most significant factors for the enhancement of its performance (Gulkaya et al., 2006).

Furthermore, several studies (Prieto-Rodríguez et al., 2011), (Yamal-Turbay et al., 2012), (Yamal-Turbay et al., 2013) have also shown the importance of developing an efficient hydrogen peroxide dosage strategy aimed at avoiding or limiting the activation of inefficient reactions scavenging hydrogen peroxide:



Photochemical AOPs, as the photo-Fenton process, are processes that use UV/VIS radiation as a means to generate hydroxyl radicals in presence of oxidants and/or photo-catalysts. However, hydroxyl radicals can also be generated by photolysing water using the higher energies of the Vacuum Ultraviolet or VUV ($\lambda < 190\text{nm}$); in such a case, the process is known as VUV photo-induced oxidation.

A literature review reveals the great potential of VUV photo-induced oxidation for achieving the oxidation and mineralization of organic

pollutants. Particularly, relevant studies have investigated the use of VUV photo-induced oxidation for the treatment of solvents, e.g. 1,1,1-trichloroethane, in concentrations between 1.0 and 24.9 mg L⁻¹ (Oppenländer et al., 1995); of phenols, e.g. 2,4-dichlorophenol, in concentrations in the order of 100.0 mg L⁻¹ (Oppenländer et al., 1995), (Oppenländer, 1997), (Oppenländer and Gliese, 2000); and also the treatment of organic contaminants such as 3-amino-5-methylisoxazole (Gonzalez and Braun, 1995) and 1,2-dichloroethene (Oppenländer et al., 1995) in concentrations of 49.0 and 20.0 mg L⁻¹, respectively.

The photochemical reaction known as homolysis of water is shown in Equation (4.6):



The chemical bond dissociation leads to the formation of H⁺, H[•] hydrated electrons e_{aq}⁻, and the main reactive and non-selective species that is the HO[•] radical.

The VUV photo-induced technology is an interesting alternative to other AOPs as well as a solution suitable to be combined with conventional treatments due to several advantages such as: i) no requirement of chemical additives, ii) completely unselective oxidation, iii) high light-energy density, and vi) flexibility as scalable process.

The present study investigates the performance of different AOPs (Fenton, photo-Fenton and VUV photo-induced oxidation) in the degradation of paracetamol (PCT) in aqueous solution.

The quantitative performance of the AOPs was addressed by:

- Measuring the evolution of PCT concentration, aimed at estimating the time at which PCT concentration decays below a threshold (HPLC limit detection),
- Measuring and modelling, following a Semi-Empirical Modelling approach, the Total Organic Carbon (TOC) conversion, aimed at estimating and comparing the limits of sample mineralization,

- Measuring cytotoxicity at planned intervals (trading-off the effort of this analysis and the information produced), aimed at determining the real environmental outcome of the treatment.

Paracetamol was selected as model contaminant because it is one of the most frequently prescribed analgesics and antipyretics worldwide. It has been detected in concentrations up to $11.3 \mu\text{g L}^{-1}$ in European WWTPs effluents (Ternes, 1998), (Kolpin et al., 2002), (Rabiet et al., 2006), (Jones et al., 2007), (De Gusseme et al., 2011), (Antunes et al., 2013), but also in natural waters in concentrations greater than $65.0 \mu\text{g L}^{-1}$ in the Tyne River, UK (Ternes, 1998), (Dalgic et al., 2016).

In all cases, the initial concentration of the target compound was fixed to 0.26 mmol L^{-1} (40.00 mg L^{-1}) corresponding and to an initial TOC concentration of 2.16 mmol L^{-1} (25.92 mg L^{-1}), which is a value higher than that of the concentrations observed in wastewaters and surface waters (Ternes, 1998), (Rabiet et al., 2006), (Jones et al., 2007), (De Gusseme et al., 2011), (Antunes et al., 2013). This higher concentration was fixed with the aim of simulating the treatment of a real-wastewater characterized by higher PCT concentrations, as also studied by other authors. For example, a recent study (Dalgic et al., 2016) addressed the Fenton treatment of a paracetamol wastewater of a pharmaceutical industry characterized by a PCT concentration between 37.0 and 294.0 mg L^{-1} . Finally, this value also simplifies the monitoring of PCT and TOC concentrations along the treatment span.

In all cases, deionised water was set as the water matrix in order to study the pure and specific degradation of paracetamol and its by-products, as well as their effect on the toxicity evolution. This also prevents the interference of other organic substances that are present in a real wastewater matrix with an uncertain composition.

In the case of Fenton and photo-Fenton processes, the effects of Fenton reagents (H_2O_2 and Fe^{2+}) and the effects of H_2O_2 dosage were also analysed for further insight and discussion. Especially, low (2.78 mmol L^{-1} of H_2O_2 and 0.09 mmol L^{-1} of Fe^{2+} – 94.5 mg L^{-1} and 5.0 mg L^{-1} respectively) and high ($11.12 \text{ mmol L}^{-1}$ of H_2O_2 and 0.18 mmol L^{-1} of Fe^{2+} – 378.0 mg L^{-1} , and 10.0 mg L^{-1} respectively) concentrations of the Fenton reactants were studied.

Besides, an additional, illustrative photo-Fenton experiment based on a dosage strategy of the oxidant was performed. This additional experiment was aimed at comparing the performance of the VUV photo-induced and the photo-Fenton process. Indeed, the dosage of the oxidant led to a continuous generation of the HO[•] radicals as in the case of VUV photo-induced oxidation experiments. On the contrary, in the case of a photo-Fenton experiment without H₂O₂ dosage, the generation of HO[•] radicals occurs mostly at the beginning of the assay.

4.2 Materials and methods

4.2.1 Reagents and chemicals

Paracetamol (PCT) 98% purity purchased from Sigma-Aldrich (St. Louis, MO, USA) was used as target compound. Reagent-grade hydrogen peroxide (H₂O₂) 33% w/v from Panreac Química SLU (Barcelona, Spain) and iron sulfate (FeSO₄·7H₂O) from Merck (Kenilworth, NJ, USA), adopted as the ferrous ion (Fe²⁺) source, were used as Fenton reagents. HPLC gradient grade methanol, MeOH, purchased from J.T. Baker Inc. (Phillipsburg, NJ, USA) and filtered milli Q grade water were used as HPLC mobile phases. High purity (>99%) ascorbic acid from Riedel de Haën (Seelze, Germany), 0.2% 1,10-phenanthroline from Scharlab SL (Barcelona, Spain), sodium acetate anhydrous and 95%–98% sulfuric acid, both from Panreac Química SLU (Barcelona, Spain), were used to perform measurements of iron species. Hydrogen chloride HCl 37% from J.T. Baker Inc. (Phillipsburg, NJ, USA) was used to adjust the initial pH. Deionised water with a conductivity lower than 1.25 μs was provided by Adesco S.A. (Barcelona, Spain) and was used as water matrix in all experiments.

Dulbecco's Modified Eagle Medium (DMEM), Phosphate-Buffered Saline (PBS) and foetal bovine serum (FBS) purchased from Gibco® (Thermo Fisher Scientific, Madrid, Spain), (3-(4,5-dimethyl-2-thiazolyl)-2,5-diphenyl-2H-tetrazolium bromide (MTT) and dimethyl sulfoxide (DMSO) reagents purchased from Sigma-Aldrich were used to perform cytotoxicity assays using cell line cultures.

4.2.2 Experimental

4.2.2.1 Experimental Design, analytical determinations, pilot plants

The Fenton, photo-Fenton and VUV photo-induced assays were all performed in batch mode with recirculation and fixing the reaction time to 120.0 min for the treatment of a PCT water solution with an initial concentration of $[PCT]^0 = 0.26 \text{ mmol L}^{-1}$ corresponding to an initial TOC concentration of $[TOC]^0 = 2.16 \text{ mmol L}^{-1}$.

The experiments summarized in Table 4.1 were set up and performed. Particularly, the design of experiments was composed of:

- a set of preliminary blank experiments for Fenton (dark conditions, or rather with an irradiated volume $V_{IRR} = 0.0 \text{ L}$) and photo-Fenton (irradiated conditions, or rather with an irradiated volume $V_{IRR} = 1.5 \text{ L}$) processes, investigating the role of the oxidant under dark (BLANK_1) and irradiated (BLANK_3) conditions, the role of the catalyst under dark (BLANK_2) and irradiated (BLANK_4) conditions, and the direct photolysis of the PCT molecule (BLANK_5);
- a set of Fenton experiments based on the use of low (FENTON_LOW) and high (FENTON_HIGH) concentrations of the Fenton reagents;
- a set of photo-Fenton experiments based on the use of low (PHOTO-FENTON_LOW) and high (PHOTO-FENTON_HIGH) concentrations of the Fenton reagents;
- a photo-induced oxidation experiment (VUV_PHOTO INDUCED).

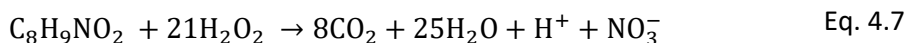
Table 4.1. Design of experiments performed for an initial PCT concentration of $[PCT]^0 = 0.26 \text{ mmol L}^{-1}$ corresponding to an initial TOC concentration of $[TOC]^0 = 2.16 \text{ mmol L}^{-1}$

Advanced Oxidation Process Models for Optimisation and
Decision Making support in Water Management

Experiments	[H ₂ O ₂] ⁰ mmol L ⁻¹	[Fe ²⁺] ⁰ mmol L ⁻¹	pH	T °C	λ nm	V _{IRR} L
BLANK_1	11.12	0.00	2.8±0.2	28.0±2	300-420	0.0
BLANK_2	0.00	0.18	2.8±0.2	2.8±0.2	300-420	0.0
BLANK_3	11.12	0.00	2.8±0.2	2.8±0.2	300-420	1.5
BLANK_4	0.00	0.18	2.8±0.2	2.8±0.2	300-420	1.5
BLANK_5	0.00	0.00	2.8±0.2	2.8±0.2	300-420	1.5
FENTON_LOW	2.78	0.09	2.8±0.2	2.8±0.2	300-420	0.0
FENTON_HIGH	11.12	0.18	2.8±0.2	2.8±0.2	300-420	0.0
PHOTO-FENTON_LOW	2.78	0.09	2.8±0.2	2.8±0.2	300-420	1.5
PHOTO-FENTON_HIGH	11.12	0.18	2.8±0.2	2.8±0.2	300-420	1.5
VUV_PHOTO INDUCED	0.00	0.00	5.0±0.2	25.0±2	172	1.1×10 ³

The maximum initial concentration of Fe²⁺ was set to the maximum legal value in wastewaters in Spain (DOGC). The initial concentration of H₂O₂ was changed between half (low doses) and twice (high doses) the stoichiometric

value (5.56 mmol L⁻¹) required for the total mineralization of 0.26 mmol L⁻¹ of PCT, considering H₂O₂ as the only oxidant in the media (Equation (4.7)):



An additional illustrative photo-Fenton experiment including H₂O₂ dosage was also performed (coded as PHOTO-FENTON_DOSAGE).

In this case, the initial concentration of PCT was fixed to 0.26 mmol L⁻¹ and the initial concentration of ferrous ion was set to 0.18 mmol L⁻¹. The total amount of hydrogen peroxide to be added during the experiment (A(τ), being τ the final reaction time) was fixed to 11.12 mmol L⁻¹ in order to evaluate the effect of a high dose of the oxidant. Particularly, an initial amount of 4.0 mL of hydrogen peroxide (2.58 mmol L⁻¹) was added at the beginning of the assay. Then, 5.0 mL (3.24 mmol L⁻¹) were added during the first 5.0 min (corresponding to a flowrate of 1.0 mL min⁻¹) while 8.0 mL (5.18 mmol L⁻¹) were added during the following 55.0 min (corresponding to a flowrate of 0.2 mL min⁻¹). Hence, the total dosage time was 60.0 min.

Regarding the experimental protocol followed to perform Fenton and photo-Fenton assays, the glass reservoir was first filled with 10.0 L of deionised water. After 10.0 min of recirculation, 4.9 L of deionised water in which PCT was previously dissolved were added and were recirculated during 15.0 min with the aim of ensuring a good homogenization of the matrix. After that, a sample was taken to measure the initial concentrations of TOC and PCT ([TOC]⁰, [PCT]⁰). Once pH was adjusted to 2.8±0.2, the remaining 0.1 L of deionised water, in which Fe²⁺ was previously dissolved, were poured into the reactor and, after 10.0 min of recirculation, a sample was taken to measure the initial concentrations of the iron species ([Fe²⁺]⁰, [Fe³⁺]⁰, [Fe^{TOT}]⁰). For the photo-Fenton experiments, H₂O₂ was added 10.0 min after the light was switched on in order to ensure the lamp to stabilize.

Contrariwise, the VUV_PHOTO-INDUCED experimental protocol consisted in filling the four tank reservoirs with 2.0-L of deionised water in which PCT had been previously dissolved (initial pH= 5.0±0.5). Then, after 15.0 min of recirculation and homogenization, a sample was taken so to measure [TOC]⁰ and [PCT]⁰, and the Xenon Excimer Flat Lamps were switched on in order to start the assay.

During Fenton and photo-Fenton experiments, pH was continuously monitored and it resulted to lay in the range $\text{pH} = 2.8 \pm 0.2$, which is the range defined by (Pignatello et al., 2006) as the range ensuring the use of the iron as a catalyst or rather, ensuring the reduction of Fe^{3+} to Fe^{2+} (Fenton-like reaction) at an appreciable rate (Pignatello, 1992) and avoiding its precipitation. Temperature was also continuously monitored and checked to lay in the range $T = 28.0 \pm 2.0$ °C. On the other hand, performing the photo-induced experiments required no pH adjustment; after the addition of PCT, pH naturally remained in the 5.0 ± 0.5 range. Temperature remained at a value of 25.0 ± 2.0 °C.

Concentration measurements of PCT, by-products (BPs), Total Organic Carbon (TOC), H_2O_2 and iron species (Fe^{2+} , Fe^{3+} , Fe^{TOT}) were carried out during the experiments. The PCT and by-products concentrations ($[\text{PCT}]$, $[\text{BPs}]$) were determined using an HPLC Agilent 1200 series with UV-DAD (Agilent Technologies, Santa Clara, CA, USA) and the samples were previously treated with methanol (in proportion 50:50) in order to stop further degradation of the organic matter. The HPLC analysis used an Akady 5 μm C-18 150 \times 4.6 mm column maintained at 25.0 °C as stationary phase and a mixture of methanol:water (25:75) flowing at 0.4 mL min^{-1} as mobile phase. The diode array detector was set at 243 nm.

TOC concentration ($[\text{TOC}]$) was measured with a VCHS/CSN TOC analyzer (Shimadzu; Kyoto, Japan). Samples were refrigerated after extraction in order to slow down any further degradation of the organic matter.

Finally, during Fenton and photo-Fenton experiments, the concentrations of hydrogen peroxide ($[\text{H}_2\text{O}_2]$) and iron species ($[\text{Fe}^{2+}]$, $[\text{Fe}^{3+}]$, $[\text{Fe}^{\text{TOT}}]$) were determined with a U-2001 UV-VIS spectrophotometer (Hitachi, Tokyo, Japan). Standard methods (Nogueira et al., 2005) (ISO 6332:1988) were followed to ensure the proper determination of oxidant and catalyst concentrations, respectively. Particularly, the spectrophotometric technique by Nogueira et al., 2005 is based on the measurement of the absorption at 450 nm of the complex formed after reaction of H_2O_2 with ammonium metavanadate. The 1,10-phenanthroline method (ISO 6332:1988) used to analyze the evolution of iron species follows ISO 6332 and is based on the absorbance measurements of the Fe^{2+} -phenanthroline complex at 510 nm. Total iron concentration ($[\text{Fe}^{\text{TOT}}]$) is measured using ascorbic acid to convert all ferric ions (Fe^{3+}) to ferrous ions (Fe^{2+}); then, ferric ion concentration is determined through the iron balance ($[\text{Fe}^{3+}] = [\text{Fe}^{\text{TOT}}] - [\text{Fe}^{2+}]$).

Fenton and photo-Fenton assays were performed in a 15.0 L pilot plant composed by a glass jacketed reservoir tank and a glass annular photo-reactor (Termo Fisher Scientific, Barcelona, Spain) equipped with an Actinic BL TL-DK 36 W/10 1SL lamp (UVA-UVB) (Barcelona LED, Barcelona, Spain) with an irradiated volume of 1.5 L. A pumping system allows keeping a constant recirculation flow of 12.0 L min^{-1} , which ensures perfect mixing. The incident photon power, $E = 3.4 \times 10^{-4} \text{ Einstein min}^{-1}$ (300 and 420 nm), was measured by (Yamal-Turbay et al., 2015) using potassium ferrioxalate actinometry (Murov et al., 1993). Continuous pH and temperature measurements are given by on-line sensing equipment, while a flowmeter ensures the on-line control of the recirculation flowrate. The pilot-plant is also equipped with four peristaltic pumps controlled by a PLC system connected to a SCADA system allowing the dosage of the reactants during the experiments. For more specifications, please refer to Yamal-Turbay et al., 2015 and Audino et al., 2019. Photo-induced oxidation experiments were performed in a pilot plant equipped with four Flat Lamp reactor systems, each containing a Xenon Excimer Flat Lamp emitting VUV at 172 nm and connected to a 2.0-L jacketed glassware reservoir tank. A magnetically coupled centrifugal pump Sondermann BGR 1.5 (Sondermann, Köln, Germany) is used to control the flowrate that can be varied between 0.8 and 4.2 L min^{-1} . The irradiated volume (V_{IRR}) is given by the product of the lamp surface (310.0 cm^2) for the effective absorbing path ($3.6 \times 10^{-3} \text{ cm}$) resulting in a value of 1.1 cm^3 or rather $1.1 \times 10^{-3} \text{ L}$. Hence, the photochemical reaction (see Equation (4.6)) only takes place in a volume that corresponds to the 0.056% of the total volume of 2.0 L. This pilot plant was developed at the Institute for Interfacial Engineering and Biotechnology (Fraunhofer, Germany) and for more information please refer to Toro Santamaria et al., 2017.

4.2.2.2 Toxicity tests

The safe application of the treatments under study for the removal of PCT was also investigated. Toxicity tests based on the use of specific bacteria (*E. coli* and *S. aureus* bacteria) were performed and all the studied AOPs resulted to be environmentally friendly. The results agree the observations reported by other authors who tested the toxicity of the produced effluents on the *Vibrio* Fishery bacteria (Trovó et al., 2012).

Hence, a system with a sensitivity higher than the one based on the use of specific bacteria was selected with the purpose of addressing a more general case study. In particular, the cytotoxicity tests based on cell lines culture were carried out. Particularly, VERO and COS-1 cells were selected and tested. Both cell lines were isolated from an African green monkey kidney but their morphology is different. The morphology of VERO cells corresponds to epithelial-like cells while the morphology of COS-1 cells corresponds to fibroblast-like cells (ATCC[®], Manassas, VA, USA).

The cells were cultured in a DMEM medium (supplemented with 100.00 U/mL penicillin, 100.00 $\mu\text{g mL}^{-1}$ streptomycin and 10%-v/v FBS at 37.0 °C) and a wet atmosphere containing 5% CO₂ and 95% air. In order to allow the formation of monolayers, VERO and COS-1 cells were seeded in culture plates of 96 wells 24 hours before performing the assay. Cells with viability greater than 95% were seeded at a density of 10⁴ cells/well.

Aqueous samples of PCT were taken before, during and after the treatment by Fenton, photo-Fenton and VUV photo-induced AOPs and were evaluated at serial one-third dilutions. Specifically, 150.0 μL of each PCT dilution and 150.0 μL of culture medium were added to each well in order to obtain 300.0 μL on the cell monolayer in each well. In all cases, the pH of the samples was adjusted to 7.2–7.4.

Additionally, two controls were performed: i) a control of maximum cell growth achieved culturing the cells in medium alone (300.0 μL of culture medium) and ii) a control to evaluate the effect of the aqueous dilution of the medium achieved by adding 150.0 μL of water and 150.0 μL of culture medium. Then, the plates were incubated for 24 hours under culture conditions. The samples were evaluated in triplicate on independent plates.

Cytotoxicity was assessed by measuring the viability of the cells exposed to PCT and possible by-products. The viability was determined by the MTT method. First, after 24 h of culture, the media were aspirated and plates were washed with PBS (100.0 μL /well). Then, 50.0 μL of culture medium supplemented with 5.00 mg mL^{-1} MTT reagent were added to each well. The plates were incubated for 3 h in culture conditions to allow the formation of formazan crystals in the viable cells. The quantification was performed solubilizing the formazan crystals in a DMSO/methanol/water mixture (20/70/10%-v) using 100.0 μL /well, and the absorbance at 570 nm was measured with a microplate reader (Biochrom, Cambridge, UK).

4.2.3 Modelling

The Semi-Empirical Model by Pérez-Moya et al., 2011 summarized in Equations (4.8)-(4.12), has been adopted in order to rate the progress of the degradation of organic matter through a lumped parameter such as the TOC.

The term “semi-empirical” refers to a model that represents a balanced approach between detailed first-principles modelling and pure empirical modelling (e.g. response surface). On one hand this model describes the degradation of the model contaminant by measuring a lumped parameter such as the concentration of TOC. On the other hand, the model has been expressed in terms of physically meaningful factors with the aim of overcoming the limitations of pure statistical modelling.

Especially, the model describes the degradation as follows:

$$\frac{d[\text{TOC}]}{dt} = -k ([\text{TOC}] - [\text{TOC}]^\infty) \quad \text{Eq.4.8}$$

where k is a kinetic constant (min^{-1}) and $[\text{TOC}]^\infty$ represents the limit concentration (mmol L^{-1}) from which, regardless the reaction time, and under specific conditions, further degradation of the organic matter cannot be attained.

By integrating the Equation (4.8), the analytical expression of the TOC evolution under given initial conditions can be derived and results in:

$$[\text{TOC}] = [\text{TOC}]^\infty + k ([\text{TOC}]^0 - [\text{TOC}]^\infty) e^{-kt} \quad \text{Eq.4.9}$$

where $[\text{TOC}]^0$ represents the initial TOC concentration (mmol L^{-1}).

TOC evolution in Equation (4.9) can be also expressed in terms of conversion (χ) as follows:

$$\chi = \chi^{\text{MAX}} (1 - e^{-kt}) \quad \text{Eq.4.10}$$

$$\chi = \frac{[\text{TOC}]^0 - [\text{TOC}]^t}{[\text{TOC}]^0} \quad \text{Eq.4.11}$$

$$\chi^{\text{MAX}} = \frac{[\text{TOC}]^0 - [\text{TOC}]^{\infty}}{[\text{TOC}]^0} \quad \text{Eq.4.12}$$

Hence, this allows characterizing the process performance by determining two parameters: the maximum conversion χ^{MAX} and the kinetic constant k . For more details, please refer to (Pérez-Moya et al., 2011).

4.3 Results and discussion

4.3.1 Fenton, photo-Fenton and VUV photo-induced assays

Concerning Fenton and photo-Fenton processes, results of the preliminary blank assays (not shown) revealed that, when disregarding first the catalyst and then the oxidant, PCT and TOC remained almost constant, and that the adopted UV radiation (300–420 nm) was not able to appreciably photolyze PCT.

Before starting analyzing the processes performance in terms of TOC and PCT evolution, the evolution of iron species is presented for Fenton and photo-Fenton experiments (see Figure 4.1). Particularly, Figure 4.1 shows the evolution of the concentrations of Fe^{2+} , Fe^{3+} and total iron in the case of FENTON_HIGH (Figure 4.1-a) and PHOTO-FENTON_HIGH (Figure 4.1-b) experiments.

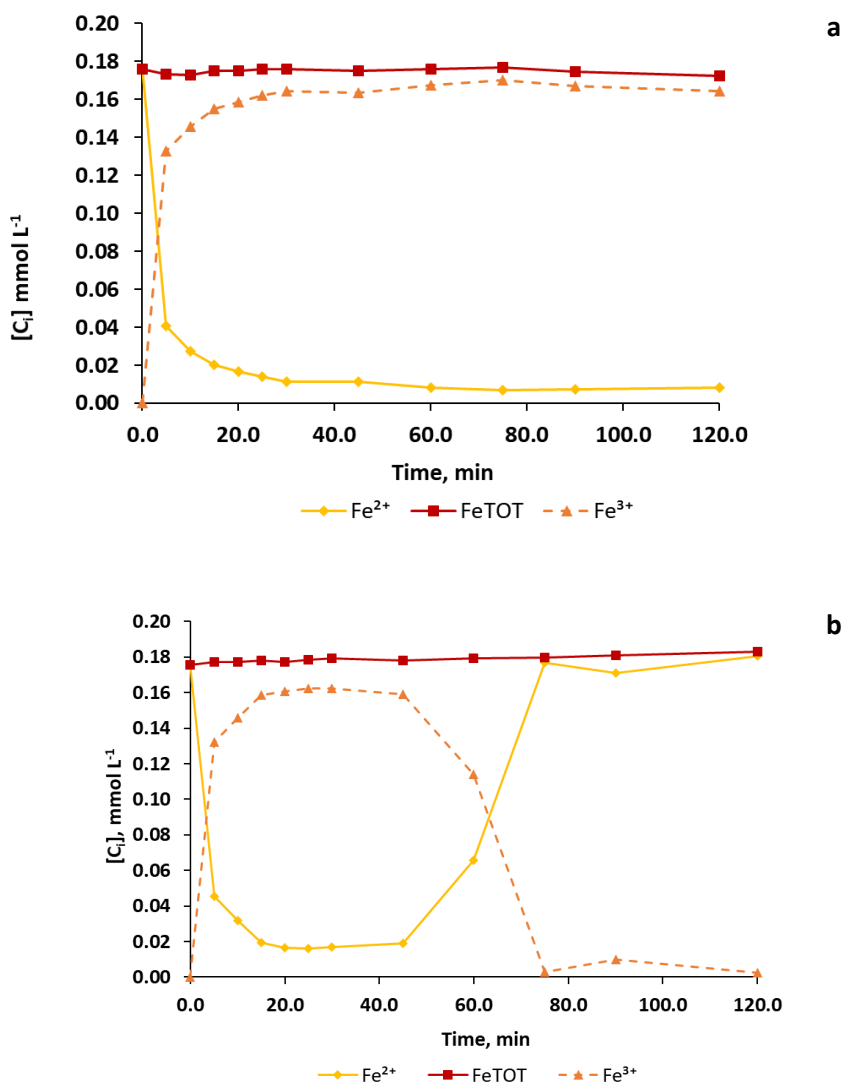


Figure 4.1. Evolution of the measured concentration of Fe²⁺ (◇,◆) and total iron (□,■) represented by a continuous line and of the calculated concentration of Fe³⁺ (Δ,▲), represented by a dashed line, during **a**) Fenton (empty symbols) and **b**) photo-Fenton (solid symbols) experiments performed with high concentrations of the Fenton reagents.

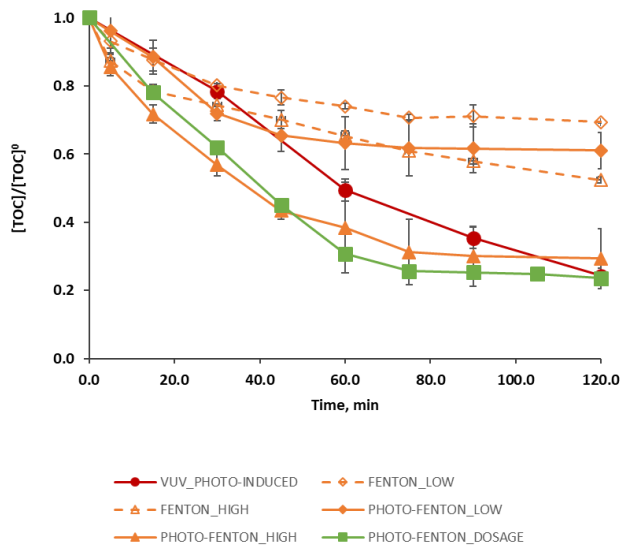
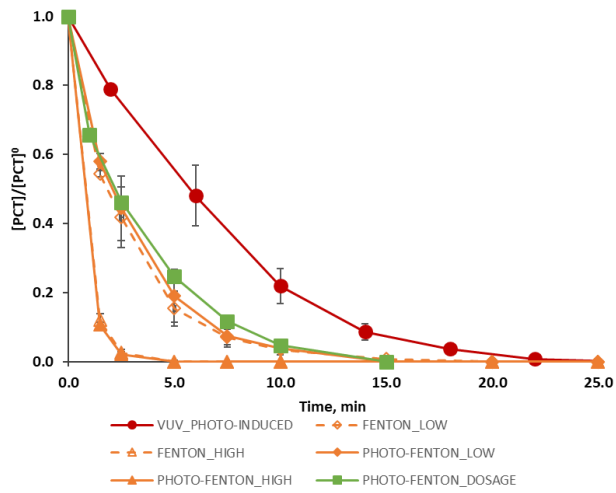
During the first minutes of the reaction, both cases (FENTON_HIGH and PHOTO-FENTON_HIGH) show a fast increase of Fe^{3+} concentration together with a fast decrease of Fe^{2+} concentration. In the FENTON_HIGH (Figure 4.1-a), Fe^{3+} and Fe^{2+} concentrations reach stable values around 0.17 mmol L^{-1} and 0.01 mmol L^{-1} , respectively. Conversely, the PHOTO-FENTON_HIGH case (Figure 4.1-b) presents a different behavior. After 45.0 min, when hydrogen peroxide is depleted (see Figure 4.2-c), the concentration of Fe^{3+} decreases while the concentration of Fe^{2+} increases up to a value of about 0.17 mmol L^{-1} . Hence, Fe^{2+} becomes the main iron species in solution.

This different behavior can be explained by analyzing the Fenton and photo-Fenton kinetics together with the different hydrogen peroxide evolution. In the Fenton case, the fastest reaction is the Fenton reaction (Equation (4.1)), which generates Fe^{3+} from Fe^{2+} with a kinetic constant in a range of $63.0 \div 76.0 \text{ mol L}^{-1} \text{ s}^{-1}$ (Simunovic et al., 2011). On the other hand, the only reaction generating Fe^{2+} (Equation (4.3)) has a kinetic constant in the range of $1.0 \times 10^{-2} \div 2.0 \times 10^{-2} \text{ mol L}^{-1} \text{ s}^{-1}$ (Simunovic et al., 2011). In the PHOTO-FENTON_HIGH case, unlike the FENTON_HIGH case, for which H_2O_2 concentration never drops to zero, the concentration of H_2O_2 reaches a null value. As a consequence, the Fenton reaction (Equation (4.1)) is no longer effective unless further Fe^{2+} is supplied (Equation (4.3) and Equation (4.4)). The generation of Fe^{2+} is here particularly enhanced by the photo-Fenton reaction (Equation (4.4)) under a convenient light source (quantum yields $\bar{\Phi} = 0.21 \pm 0.04 \text{ mol Einstein}^{-1}$) (Simunovic et al., 2011). Conversely, in the PHOTO-FENTON_DOSAGE case, the change from Fe^{3+} to Fe^{2+} was not observed (results not shown). In this case, higher concentrations of Fenton reagents were used and, as a consequence, H_2O_2 was never depleted.

Finally, constant total iron concentration can be ensured because all the experiments were performed under a pH range (2.8 ± 0.2) that prevents its precipitation, which is in accordance with the remarks reported by other authors (Pignatello, 1992), (Pignatello et al., 2006) and which was experimentally confirmed as well.

Subsequently, with the aim of discussing the performance of the different treatments studied, Figures 4.2 (a, b, and c) present results in terms of the evolution of PCT and TOC (normalized concentrations) and H_2O_2 (mmol L^{-1}), the latter, in the case of Fenton and photo-Fenton assays, with and without H_2O_2 dosage.

Comparison of effective AOPs



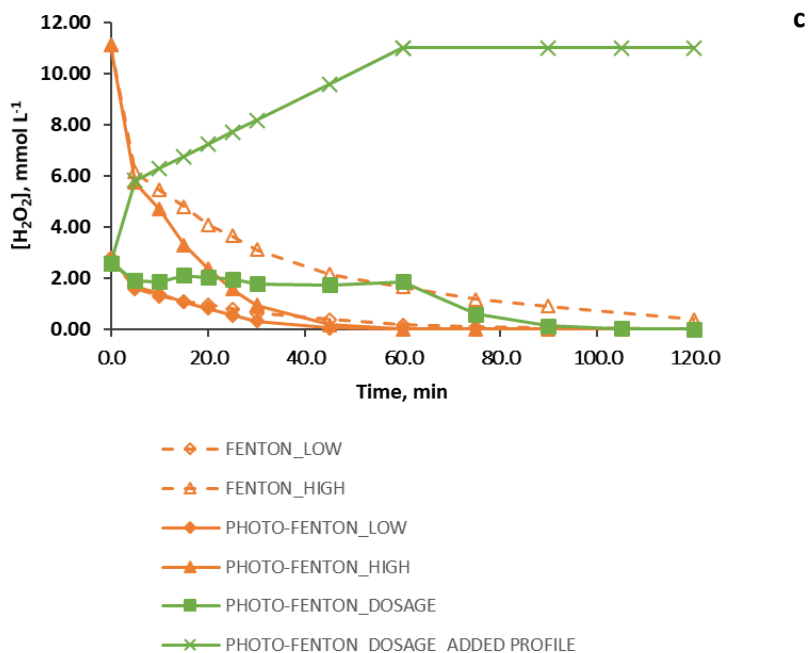


Figure 4.2. Evolution of the degradation of **a)** PCT (normalized values), **b)** TOC (normalized values) and **c)** H_2O_2 (concentration, mmol L^{-1}) for different processes: photo induced advanced oxidation (\bullet); Fenton, using low and high concentrations of Fenton reagents (\diamond, Δ); photo-Fenton using low and high concentrations of Fenton reagents ($\blacklozenge, \blacktriangle$); and photo-Fenton process following a H_2O_2 dosage strategy (\blacksquare). Figure 4.2-c also shows the profile of the added hydrogen peroxide during the reaction span (concentration values, mmol L^{-1}). The error bars display the standard deviation for the set of three experiments.

Figure 4.2-a allows concluding that all the treatments efficiently removed PCT. The model compound was not detected by HPLC within a minimum time of 2.5 min and a maximum time of 20.0 min. PHOTO-FENTON_LOW and PHOTO-FENTON_HIGH assays led to the best results: PCT concentration decayed beyond the HPLC detection limit in 2.5 min. Conversely, the VUV_PHOTO-INDUCED produced a slightly slower decrease of the PCT during the time, and in this case PCT concentration decayed below the HPLC detection limit in about 20.0 min.

It is worth noting that for all the studied treatments, TOC concentration after 20.0 minutes of reaction (maximum time at which PCT is no longer detected) was lower than that established by wastewater disposal regulations or than that required by a subsequent biological treatment. However, although all the AOPs under study allowed the efficient removal of PCT, none of them attained the complete mineralization of the organic matter within the 120.0 min reaction span.

Particularly, VUV_PHOTO-INDUCED and PHOTO-FENTON_DOSAGE experiments (Figure 4.2-b) obtained the best results in terms of final TOC conversion for the studied time span χ^{τ} (being τ the final reaction time). In both cases, a final TOC conversion of about 77% was attained, that is a 6% more if compared with the final TOC conversion reached in the case of the PHOTO-FENTON_HIGH experiment (71%). It is important to observe that such improvement was obtained also without the enhancement introduced by a convenient dosage. Hence, even better results could be expected if H_2O_2 dosage was approached by systematic optimisation (Audino et al., 2019). Furthermore, the VUV_PHOTO-INDUCED case also indicates that if the reaction time would had been extended (> 120.0 min), organic matter degradation would have continued, and higher levels of mineralization would have been attained. Conversely, for the PHOTO-FENTON_DOSAGE case study the TOC reached a stable value starting from a reaction time of 75.0 min so showing that an increase in reaction time would not lead to an increase in mineralization level.

This result is consistent with the hydrogen peroxide evolution observed during the experiment (Figure 4.2-c). As a matter of fact, Figure 4.2-c reveals that when hydrogen peroxide dosage stops (at 60.0 min), the concentration of H_2O_2 in the reactor quickly drops to zero, thus determining the end of the organic matter degradation.

The analysis of the experimental results solely in terms of PCT removal is not enough for sensibly deciding one AOP out of the rest. For this reason, the Semi-Empirical Model by Pérez-Moya et al., 2011 introduced in Section 4.2.3 was adopted with the aim of aiding decision making. Such a model allows deriving the maximum conversion χ^{MAX} and the kinetic constant k for each treatment, and conveniently displays them as means to describe the process performance. Thus, Figure 4.3 displays the kinetic constant k_i as a function of the maximum attainable conversion χ_i^{MAX} , with $i =$ VUV_PHOTO-INDUCED,

FENTON_LOW, FENTON_HIGH, PHOTO-FENTON_LOW, PHOTO-FENTON_HIGH, PHOTO-FENTON_DOSAGE.

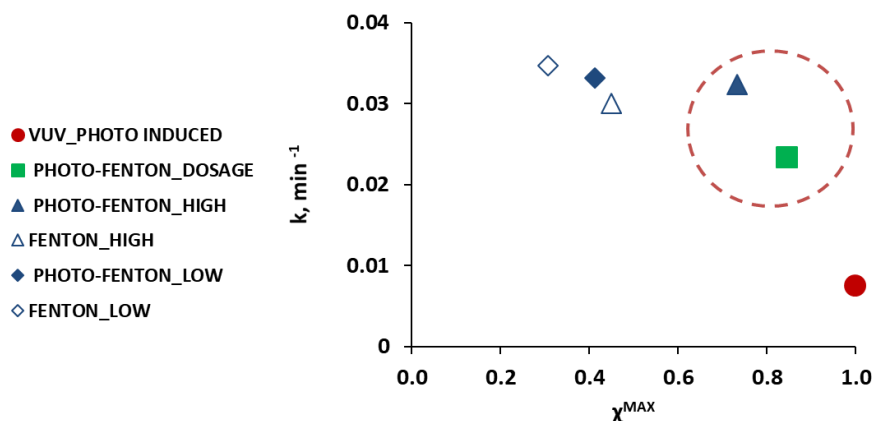


Figure 4.3. Reaction rate as a function of the maximum attainable conversion evaluated for photo induced advanced oxidation process (●); Fenton (◇) and photo-Fenton (◆) process without H_2O_2 dosage using low concentrations of the Fenton reagents; Fenton (Δ) and photo-Fenton (\blacktriangle) process without H_2O_2 dosage using high concentrations of the Fenton reagents; and photo-Fenton process following a H_2O_2 dosage strategy (■).

The results, as displayed in Figure 4.3, highlight that the photo induced advanced oxidation process is the only one that allows attaining the total organic matter mineralization ($\chi^{\text{MAX}} = 100\%$ in 200.0 min), but it is the process with the lowest kinetic constant ($k = 0.7 \times 10^{-2} \text{ min}^{-1}$). The low rate of this process is a consequence of the insufficient illuminated volume of the pilot plant ($V_{\text{IRR}} = 1.1 \times 10^{-3} \text{ L}$), which suggests that increasing this volume would lead to increasing the kinetic constant and to reaching total mineralization in less time. On the contrary, FENTON_LOW and PHOTO-FENTON_LOW show the highest kinetic constants (3.5×10^{-2} and $3.3 \times 10^{-2} \text{ min}^{-1}$, respectively) but only a 30% and a 41% maximum TOC conversion, respectively.

The area highlighted in Figure 4.3 by a red dashed circle represents the area where the intermediate solutions are located. Particularly, the PHOTO-FENTON_HIGH and PHOTO-FENTON_DOSAGE experiments can be considered a compromise solution, since they allow reaching 73% and 84%

maximum TOC conversion with a kinetic constant of 3.2×10^{-2} and $2.3 \times 10^{-2} \text{ min}^{-1}$, respectively.

Thus, in order to solve the trade-off between TOC conversion and kinetics, toxicity tests are considered to provide complementary results for further decision making support. This is connected with the analysis of the by-products (BPs) generated during the treatments presented in Figure 4.4.

For all the AOPs under study, HPLC analysis allowed detecting two main by-products that were identified as hydroquinone (HDQ) and benzoquinone (BZQ) (retention time for HDQ= 7.0 min, retention time for BZQ= 10.0 min). Since Fenton and photo-Fenton experiments produced similar results in this regard, for the sake of simplicity Figure 4.4 only considers photo-Fenton, which gave just a slightly faster BPs degradation than that of the Fenton case. Besides, Figure 4.4 only presents the evolution of BZQ in order to allow a better display of the results.

Figure 4.4 shows that a slightly faster decrease of BZQ was obtained by the PHOTO-FENTON_HIGH process compared to that of the FENTON_HIGH process: particularly, BZQ was no longer detected after 5.0 and 15.0 min, respectively. Contrariwise, when PHOTO-FENTON_DOSAGE assay was performed, BZQ was no longer detected after 15.0 min while, when VUV_PHOTO-INDUCED experiment was performed, BZQ concentration decayed below the HPLC detection limit in 22.0 min.

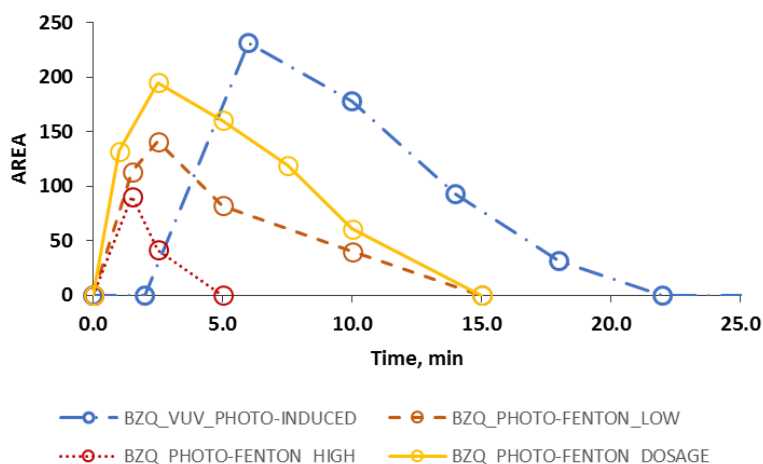


Figure 4.4. Evolution (HPLC AREA) of the degradation intermediate BZQ (○) during photo induced oxidation process (line and dots), photo-Fenton process using high (dotted line) and low (dashed line) concentrations of the Fenton reactants and without dosing the hydrogen peroxide, and photo-Fenton process following a H₂O₂ dosage strategy (solid line)

It is worth noting that in the VUV_PHOTO-INDUCED case, the HO• radicals, which are responsible of the degradation of the organic matter, are formed only in the illuminated volume (1.1×10^{-3} L), which is also much lower than the illuminated volume of the Fenton/photo-Fenton pilot plant (1.5 L). Thus, increasing this volume would improve the kinetics of the process. Contrariwise, the presence of Fenton reaction (see Equation (4.1)) in the Fenton and photo-Fenton process, ensures the generation of HO• radicals in all the volume of the reactor (both dark and irradiated).

It is also important to remark that the detected by-products show coherence with the literature related to the Fenton and photo-Fenton degradation of PCT (Trovó et al., 2012), (Moctezuma et al., 2012) and, in addition, the analytical results obtained in this work point that the same intermediates were generated during the photo-induced AOP.

Regarding Fenton and photo-Fenton experiments, another important factor is the presence of chemical additives in high concentrations that allows a faster generation of HO• radicals if compared with the VUV photo induced AOP. Actually, when hydrogen peroxide was dosed, and so when a lower concentration of H₂O₂ was present in the reactor at the beginning of the assay, the photo-Fenton process performance in terms of TOC, PCT, and BPs evolution, approaches the performance recorded by the photo induced AOP.

4.3.2 Citotoxicity assays

Even though all the AOPs under study generate hydroxyl radicals and the same by-products, the global kinetics are different and other side reactions could lead to different by-products and/or to different amounts of the same by-products and this could affect the toxicity of the samples during and after the processes. For this reason, it is important to test the toxicity of the target compound and of the treated solution during and at the end of the treatment.

Initially, the toxicity study was carried out in *E. coli* and *S. aureus* bacteria. However, both bacteria were capable of metabolizing PCT and taking advantage of it as a carbon source during its growth (data not shown). In this sense, the toxicity study has used the culture system of eukaryotic cell lines for offering greater sensitivity to PCT and its by-products to produce cellular injury.

Hence, toxicity tests based on cell lines culture were performed by using VERO and COS-1 cells (epithelial-like and fibroblast-like cells, respectively). First, the value of the LC50, or rather the concentration of the selected chemical that kills 50% of the tested cell in a given time, was evaluated for PCT with both line cells. Particularly, the LC50 of PCT resulted to be very high (> 1000.0 mg L⁻¹) for both line cells under study, and this result shows that PCT is tolerated by both cells. Figure 4.5 shows the results of the cytotoxicity assays performed to check the viability of all the treatments under study.

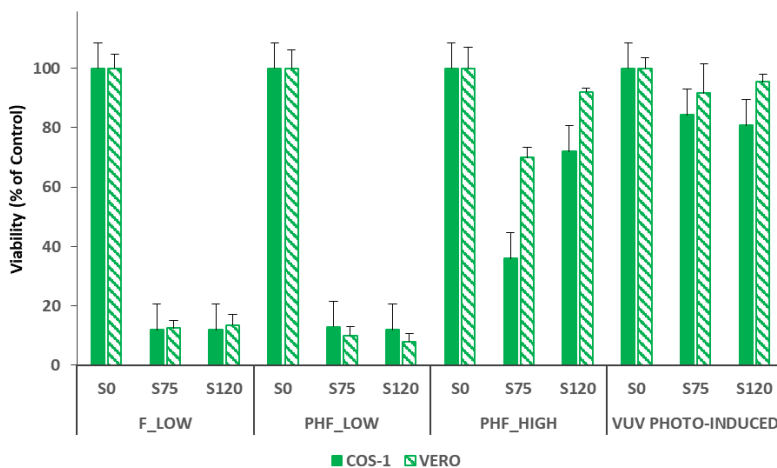


Figure 4.5. Results of the cytotoxicity assays performed using COS-1 (full symbols) and VERO (slashed symbols) and tested on samples taken after 0.0 (S0), 75.0 (S75) and 120.0 (S120) minutes of reaction

Particularly, results are presented for samples (S0) taken before adding the Fenton reagents (or rather before starting the VUV_PHOTO-INDUCED treatment, thus containing only PCT in a concentration of 0.26 mmol L⁻¹), after 75.0 min of reaction (S75) and at the end of each treatment (S120).

Cytotoxicity tests performed using samples S0 and S120 allow evaluating the toxicity of the target compound in the initial concentration set for this study and the safe application of the treatments under study for PCT removal, respectively. Moreover, the presence of possible toxic by-products was analysed by taking samples after 75.0 min of reaction. In this way, it was possible to ensure that, in case of Fenton and photo-Fenton treatments, with the exception of FENTON_HIGH (for which a residual H_2O_2 concentration of about 0.38 mmol L^{-1} was detected at the end of the experiment), H_2O_2 is no longer present in solution. Actually, hydrogen peroxide could be toxic for the cells and may affect the toxicity tests preventing to determine if the toxicity depends on a toxic compound or the oxidant. For this reason, cytotoxicity results obtained for the FENTON_HIGH case are not shown.

Both COS-1 and VERO cells were not affected by PCT in the initial concentration of 0.26 mmol L^{-1} (see results of S0 samples in Figure 4.5). A strong increase of cells mortality (about 85%) was observed when both S75 and S120 samples of the FENTON_LOW and PHOTO-FENTON_LOW experiments were tested. Hence, this case reveals that it is not possible to ensure the safe application of Fenton and photo-Fenton treatments for the PCT removal for mild Fenton reagent loads. The final TOC conversion values attained by applying FENTON_LOW (31%) and PHOTO-FENTON_LOW (39%) treatments also confirm this result.

On the contrary, the PHOTO-FENTON_HIGH treatment is able to finally generate a non-toxic effluent (S120) that can be safely discharged into the aquatic environment, despite the formation of more toxic by-products during the process (highlighted by a 70% mortality of the COS-1 cells, and a 25% mortality of the VERO cells, when S75 samples were tested). A 25% mortality of the COS-1 cells, and a 10% mortality of the VERO cells was recorded when S120 samples were tested. This result is consistent with the higher mineralization value reached at the end of the treatment (71%). The slightly different result obtained using COS-1 and VERO cells can be explained by considering that both cell types have different morphological characteristics (e.g. VERO cells, as epithelial cells, have a large contact surface during cellular spreading, whereas COS-1 cells such as fibroblasts have an adhesion to the surface by focal contacts).

Finally, regarding the VUV_PHOTO-INDUCED treatment, all the cytotoxicity assays using both VERO and COS-1 cells confirm the safe application of this treatment for the removal of PCT. For both cell types, Figure 4.5, shows a

percentage of mortality similar to the control when both S75 and S120 samples were analysed. Moreover, despite the fact Figure 4.5 only shows the results for samples S0, S75 and S120, the toxicity assays for the VUV_PHOTO-INDUCED treatment were performed also using samples taken after 5.0, 15.0, 20.0, 25.0, 30.0, 45.0, 60.0, and 120.0 min. Furthermore, it is worth noting that, for all the samples, the mortality of both cell types was similar to the control. Since the intermediates detected for VUV_PHOTO-INDUCED, Fenton and photo-Fenton treatments are the same, this result can be probably due to the kinetics of the reactions, which in this case can lead to the generation of a certain amount of intermediates whose total balance determines a non-toxic solution. Alternatively, no more toxic by-products could be formed beyond those generated (even if not detected) during the Fenton and photo-Fenton processes. This can be related to the continuous generation of hydroxyl radicals during the VUV_PHOTO-INDUCED treatment; or rather, HO[•] are not generated mostly at the beginning of the process, as it occurs in the Fenton and photo-Fenton cases instead. Hence, interesting further work could be testing the toxicity of the photo-Fenton treatment when dosing H₂O₂, because also in this case, as shown in the previous sections, there is a continuous generation of the hydroxyl radicals during the process.

These results allow concluding that, unlike Fenton and photo-Fenton processes, the VUV_PHOTO-INDUCED treatment can be safely stopped when it is convenient (e.g. according to the desired percentage of TOC conversion and/or PCT removal).

4.4 Conclusions

On the one hand, photo-induced oxidation resulted to be a very promising treatment. It allows the efficient removal of the model compound (which was no longer detected after 20.0 min) and it could allow the total organic matter mineralization by increasing the reaction time span to 200.0 min. Moreover, cytotoxicity assays revealed the feasibility of the VUV photo-induced treatment for PCT removal as well as the possibility to stop this process at any convenient time because it was never possible to detect any increase of toxicity.

The bottleneck of the photo-induced oxidation is the kinetics of the process, which is likely due to the illuminated volume ($V_{IRR} = 1.1 \times 10^{-3} \text{L}$) employed, much lower than the illuminated volume of the Fenton/photo-Fenton pilot plant ($V_{IRR} = 1.5 \text{L}$). Therefore, further investigation is required to address the reactor design with the aim of increasing the irradiated volume.

On the other hand, the photo-Fenton process using high concentrations of Fenton reagents demonstrated good performance in terms of both PCT removal and organic matter mineralization. However, cytotoxicity results highlighted that only after 120.0 min of reaction it was possible to generate a non-toxic effluent, so showing that it is not possible to stop such process at any convenient time and that is mandatory to monitor the cytotoxicity evolution.

4.5 Acknowledgements

This work was supported by the Spanish “Ministerio de Economía, Industria y Competitividad (MINECO)” and the European Regional Development Fund, both funding the research Project AIMS (DPI2017-87435-R). Francesca Audino, particularly acknowledges the MINECO for the PhD grant [BES-2013-065545]. German authors also want to thank the Institute for Interfacial Engineering and Biotechnology, Fraunhofer.

5 Conventional kinetic study

By the analysis of the results presented in Chapter 4, it was decided to go deeper into the study of the photo-Fenton process since it showed a good performance in terms of model contaminant removal and TOC mineralization when using high concentrations of Fenton reagents and allowing generating a non-toxic effluent after 120.0 min of reaction.

This chapter addresses the proposal of a kinetic model for the photo-Fenton degradation of a pharmaceutical (the paracetamol (PCT)) that can be a compromise solution between the unaffordable complexity of the First Principles Model (FPMs) and the oversimplification of the Empirical Models (Ems) and Data Based Models (DBMs).

5.1 Introductory perspective

In the last decades, a notable effort has been made to investigate the main aspects of the Advanced Oxidation Processes (AOPs). AOPs are a group of chemical processes all characterised by the capability of exploiting the high reactivity of HO[•] radicals in driving oxidation reactions that are suitable for achieving pollutant remediation and mineralization (Andreozzi et al., 1999). Hence, AOPs represent a convenient application to wastewater treatment, also considering the possibility to combine the biological treatment with an oxidative degradation of toxic or refractory substances (Oller et al., 2011).

Especially, they can be adopted for the treatment of the so-called Contaminants of Emerging Concern (CECs). CECs are a group of chemicals, including pharmaceuticals and personal care products (PPCPs), which are increasingly being detected at low concentrations (ng L⁻¹ to µg L⁻¹) in surface water, ground waters and even drinking waters, and that may be included in future environmental regulations depending on the results of the investigations on their effects on the human health and environment (Environmental Protection Agency-EPA). This shows that conventional sewage treatment plants are not able to remove this kind of contaminants.

According to the current legislation, the Directive 2013/39/EU of the European Parliament and of the Council of 12 August 2013 amending Directives 2000/60/EC and 2008/105/EC, an important factor to be taken into account is the CECs monitoring as well as the reinforcement of the risk assessment of pharmaceutical products (Ribeiro et al., 2015).

Regarding pharmaceuticals, in the last two decades, a large variety of drugs (analgesics, anti-inflammatory, antibiotics, etc.) coming from domestic, industrial, hospital and health centres wastewaters or from landfill leachates, have been detected in soils, surface waters, ground waters and drinking waters.

Particularly, the photo-enhanced Fenton process has proved to be highly efficient in degrading CECs (Miralles-Cuevas et al., 2014) as well as strength organic wastewaters (Rahim Pouran et al., 2015). As a matter of fact, the review by (Wang et al., 2016) highlighted several industrial applications of the photo-Fenton process that has been used to treat different kinds of wastewaters such as olive-oil mill, textile, pesticide, cosmetic, dye,

fermentation brine, green olives, pharmaceutical, cork cooking, pulp mill and phenolic wastewaters.

The Fenton reaction is an old reactive system proposed by Fenton, 1894, that occurs by means of addition of hydrogen peroxide (H_2O_2) to ferrous ion salts (Fe^{2+}) and that leads to the formation of free radicals, mainly HO^\bullet . The photo-assisted Fenton process (Kiwi et al., 1993), (Pulgarin and Kiwi, 1996) represents an extension of the Fenton process obtained by using a UV-VIS light source. Under irradiated conditions and acid medium ($\text{pH}= 2.8$), the photolysis of ferric ions (Fe^{+3}) complexes ($\text{Fe}(\text{OH})^{2+}$) occurs, allowing the Fe^{+2} regeneration and the formation of an additional hydroxyl radical leading to a strong increase of the degradation rate of organic pollutants.

A large experimental effort has led to an extensive knowledge on photo-Fenton process. Several works, at both laboratory and pilot plant scale, have investigated the key process efficiency parameters, such as H_2O_2 consumption, processing time and mineralization rate, as well as the effect of factors like temperature, pH, dissolved ion concentration and dissolved organic carbon (DOC) on such parameters (Andreozzi et al., 2000), (Pignatello et al., 2006), (Farias et al., 2007), (Zapata et al., 2010). Conversely, despite the extensive experimental work, the mathematical modelling is still under development. Specifically, concerning photo-Fenton kinetics modelling, mainly three different approaches have been proposed: First Principles Models (FPMs), Empirical Models (EMs), and Data Based Models (DBMs). FPMs rely on the description of all the elementary steps of the process. The works by Kang et al., 2002, Jeong and Yoon, 2005, and Ortiz de la Plata et al., 2010, are representative examples of FPMs. On the other hand, EMs rely on a complete empirical approach based on the use of regression models (Kusic et al., 2006) eventually coupled with the design of experiment techniques (Pérez-Moya et al., 2008). Finally, in the area of DBMs, Artificial Neural Networks (ANN) (Göb et al., 2001), Support Vector Regression (SVR) (Shokry et al., 2015) and Ordinary Kriging (OK) (Shokry et al., 2015) have been used. While, currently, EMs and DBMs are unable to fully capture the complexity and nonlinear nature of such processes, the accuracy and understanding that might provide FPMs is unaffordable. Moreover, few works have addressed the modelling of the radiation field inside the photoreactor that requires the evaluation of the Local Volumetric Rate of Photon Absorption (LVRPA) (Cassano et al., 1995), (Conte et al., 2016).

Thus, the present study aims at presenting a kinetic model that can be a compromise solution between the unaffordable complexity of the FPMs and the oversimplification of the EMs and DBMs, without disregarding the assessment of the LVRPA effect.

Paracetamol (PCT) was selected as model pollutant since it is one of the top 200 pharmaceuticals prescribed overall the world, being widely used as antipyretic and analgesic. Therefore, PCT is continuously released by hospital waste (Langford and Thomas, 2009), as well as by consumer use and disposal (according to Muir et al., 1997, PCT is excreted in 58-68% during therapeutic treatment). As a consequence, it has been detected in the effluents of sewage treatment plants in $\mu\text{g L}^{-1}$ (Ternes, 1998), in natural water sources at concentrations higher than $65.0 \mu\text{g L}^{-1}$ in the Tyne River (UK) (Antunes et al., 2013) and even in groundwater at concentration ranging between $\mu\text{g L}^{-1}$ and ng L^{-1} (De Gusseme et al., 2011).

However, another issue is the treatment of real paracetamol wastewaters that are characterized by high levels of PCT, Total Organic Carbon (TOC) and Chemical Oxygen Demand (COD) concentrations. A recent work by (Dalgic et al., 2017) showed that the Fenton process can be an effective pre-treatment of a real paracetamol wastewater of the pharmaceutical industry characterized by a PCT concentration between 37.0 and 294.0 mg L^{-1} . Previously, Rad et al., 2015 also investigated the use of photo-Fenton process in industrial applications. Particularly, these authors analysed the effect of different operational parameters on the photo-Fenton process including the phenol and paracetamol initial concentrations ranging between 20.0 and 100.0 mg L^{-1} . Cabrera Reina et al., 2012 proposed a model to track the photo-Fenton degradation of paracetamol present at high initial concentration (4.0 - 25.0 mmol L^{-1} of TOC) or rather simulating an industrial wastewater.

In the present work, the experimental data set used to study the kinetic model was based on an initial concentration of PCT ($[\text{PCT}]^0$) of 40.0 mg L^{-1} (e.g. industrial wastewater). The initial H_2O_2 concentration ($[\text{H}_2\text{O}_2]^0$) was varied between half and twice the stoichiometric dose to achieve mineralization of 40.0 mg L^{-1} of PCT and the initial ferrous ion concentrations ($[\text{Fe}^{2+}]^0$) between 5.0 and 10.0 mg L^{-1} (being the latter the maximum value allowed in wastewaters in Spain).

Reaction rates for PCT and H_2O_2 were obtained and then ordinary differential equations (ODEs) were used for describing component mass balances inside

the reactor. A line source radiation model with spherical and isotropic emission (LSSE model) was adopted in order to derive the equation describing the variation of LVRPA with the absorbing species.

Experimental and predicted concentrations of PCT and H₂O₂ were compared by implementing a non-linear least-squares regression procedure in MATLAB and root mean square errors (RMSE) were calculated to test model reliability.

5.2 Methodological framework: experimental settings and process modelling

The general methodology consists of an experimental part and a modelling section including model fitting (parameter estimation), that are detailed in the following sections.

5.2.1 Experimental

The experimental step provides the data that will be used in the final optimisation procedure to estimate the kinetic constants of the proposed model.

5.2.1.1 Reagent and chemicals

Paracetamol (PCT) 98% purity purchased from Sigma-Aldrich (St.Louis, MO, USA) was used as target compound. Reagent-grade hydrogen peroxide (H₂O₂) 33% w/v from Panreac Química SLU (Barcelona, Spain) and iron sulfate (FeSO₄·7H₂O) from Merck (Kenilworth, NJ, USA), adopted as the ferrous ion (Fe²⁺) source, were used as Fenton reagents. HPLC gradient grade methanol, MeOH, purchased from J.T. Baker Inc. (Phillipsburg, NJ, USA) and filtered milli Q grade water were used as HPLC mobile phases. High purity (>99%) ascorbic acid from Riedel de Haën (Seelze, Germany), 0.2% 1,10-phenanthroline from Scharlab SL (Barcelona, Spain), sodium acetate anhydrous and 95%–98% sulfuric acid, both from Panreac Química SLU (Barcelona, Spain), were used to

perform measurements of iron species. Hydrogen chloride HCl 37% from J.T. Baker Inc. (Phillipsburg, NJ, USA) was used to adjust the initial pH. Deionised water with a conductivity lower than $1.25 \mu\text{S}$ was provided by Adesco S.A. (Barcelona, Spain) and was used as water matrix in all experiments.

5.2.1.2 Analytical determinations

Measurements of PCT, Total Organic Carbon (TOC), H_2O_2 , and iron species concentrations were performed. TOC concentration ($[\text{TOC}]$) was measured with a Shimadzu VCHS/CSN TOC analyser (Shimadzu; Kyoto, Japan) and samples were taken each 15.0 min until the end of the experiment. PCT concentration ($[\text{PCT}]$) was determined using an HPLC Agilent 1200 series with UV-DAD (Agilent Technologies, Santa Clara, CA, USA). The measurement method is the one described by Yamal-Turbay et al., 2015. All the samples, taken at 0.0, 1.5, 2.5, 5.0, 7.5, 10.0 and 15.0 min, were treated with 0.1 M methanol (in proportion 50:50) to stop reaction and further degradation of PCT. Hydrogen peroxide concentration ($[\text{H}_2\text{O}_2]$) was determined with a Hitachi U-2001 UV-VIS spectrophotometer (Hitachi, Tokyo, Japan) and using the spectrophotometric technique described by Nogueira et al., 2005. This technique is based on the measurement of the absorption at 450 nm of the complex formed after reaction of H_2O_2 with ammonium metavanadate. In this case, samples were taken each 5.0 min until a reaction time of 30.0 min and then each 15.0 min until the end of the assay.

The iron species (Fe^{2+} , Fe^{TOT}) were analysed using the 1,10-phenanthroline method following ISO 6332:1988, based on the absorbance measurements of the Fe^{2+} -phenanthroline complex at 510 nm. To measure total iron concentration ($[\text{Fe}^{\text{TOT}}]$), ascorbic acid must be used so to convert all the ferric ions (Fe^{3+}) to ferrous ions (Fe^{2+}). Then, for difference, ferric ion concentration could be determined ($[\text{Fe}^{3+}] = [\text{Fe}^{\text{TOT}}] - [\text{Fe}^{2+}]$). In this case, samples were taken each 5.0 min until a reaction time of 30.0 min and then each 15.0 min until the end of the assay.

Table 5.1 shows the experimental errors evaluated for all measurement techniques and for a PCT concentration range of $[0.0-40.0] \text{ mg L}^{-1}$, a Total Carbon (TC) concentration range of $[0.0-50.0] \text{ mg L}^{-1}$, a Total Inorganic Carbon (TIC) concentration range of $[0.0-10.0] \text{ mg L}^{-1}$, and a H_2O_2 concentration range of $[0.0-150.0] \text{ mg L}^{-1}$.

Table 5.1. Experimental errors of the measurement techniques

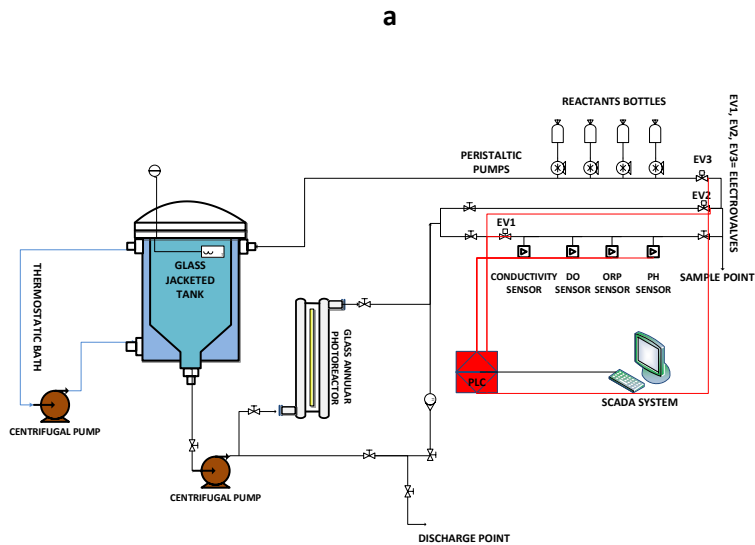
MEASUREMENT EQUIPMENT	MEASURED SPECIES	ERROR (mg L ⁻¹)
HPLC Agilent 1200 series with UV-DAD	PCT [0.0-40.0] mg L ⁻¹	0.15
Shimadzu VCHS/CSN TOC analyser	TC [0.0-50.0] mg L ⁻¹	0.23
	TIC [0.0-10.0] mg L ⁻¹	0.04
Hitachi U-2001 UV-Vis spectrophotometer	H ₂ O ₂ [0.0-150.0] mg L ⁻¹	1.43

5.2.1.3 Experimental set-up

A 15.0 L system composed by a 9.0-L glass jacketed reservoir tank and a 6.0-L glass annular photoreactor (Termo Fisher Scientific, Barcelona, Spain) equipped with an Actinic BL TL-DK 36 W/10 1SL lamp (UVA-UVB) (Barcelona LED, Barcelona, Spain) was used to perform Fenton and photo-Fenton experiments. The irradiated volume is 10% of the total volume (that is 1.5 L). The incident photon power, $E = 3.36 \times 10^{-4}$ Einstein min⁻¹ (300 and 420 nm) was measured by Yamal-Turbay et al., 2015 using potassium ferrioxalate actinometry (Murov, et al., 1993). In addition, the experimental device is also equipped with a pH sensor and a flowmeter for the control of the

Advanced Oxidation Process Models for Optimisation and Decision Making support in Water Management

recirculation flowrate and a thermostatic bath for the temperature control, which is measured by a temperature sensor placed inside the 9.0-L tank. In Figure 5.1, a schematic view (Figure 5.1-a) and a picture of the experimental set-up (Figure 5.1-b) with its specifications (Table 5.2) are shown. For more details of the experimental system, you can refer to Yamal-Turbay et al., 2015.



b



Figure 5.1. Experimental set-up. **a)** Schematic view, **b)** Picture

Table 5.2. Experimental device specifications

TANK REACTOR

Total volume, L 9.0

ANNULAR REACTOR

Total volume, L 6.0

Irradiated volume, L 1.5

Advanced Oxidation Process Models for Optimisation and Decision Making support in Water Management

Annular irradiated height, mm		130.0
Outer cylinder	Outer diameter, mm	150.0
	Inner diameter, mm	140.0
Inner cylinder	Outer diameter, mm	70.0
	Inner diameter, mm	63.6

IRRADIATION SYSTEM

Actinic BL TL-DK 36 W/10 1SL

Diameter, mm	28.0
Length, mm	589.8

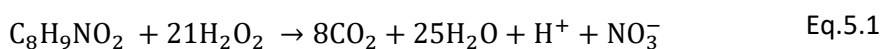
5.2.1.4 Experimental procedure

Fenton and photo-Fenton assays were performed in batch mode with recirculation, changing initial concentrations of hydrogen peroxide ($[H_2O_2]^0$) and ferrous ion ($[Fe^{2+}]^0$) for the same value of the initial concentration of PCT ($[PCT]^0$).

The value of the initial PCT concentration was set to 40.0 mg L^{-1} in order to investigate Fenton and photo-Fenton treatment of a real paracetamol wastewater characterized by higher PCT concentrations (Dalgic et al., 2017).

The maximum value of the initial concentration of Fe²⁺ was set taking into account the maximum legal value in wastewaters in Spain (DOGC), 10.0 mg L⁻¹, while half of such value was set as the minimum value to be investigated.

Also, to select the initial concentration of H₂O₂, the stoichiometric dose to achieve total mineralization when H₂O₂ is considered to be the only oxidant in the media (Equation (5.1)) and when [PCT]⁰= 40.0 mg L⁻¹, was calculated and resulted in a value of 189.0 mg L⁻¹. Then, a range between half and twice the stoichiometric dose (94.5 and 378.0 mg L⁻¹, respectively) was selected.



Eighteen experiments were carried out (Table 5.3) by testing three different values of [H₂O₂]⁰ (94.5, 189.0, and 378.0 mg L⁻¹) and [Fe²⁺]⁰ (5.0, 7.5, and 10.0 mg L⁻¹), for the same value of [PCT]⁰ set to 40.0 mg L⁻¹ (corresponding to [TOC]⁰= 25.4 mg L⁻¹) and under dark and irradiated conditions. Hence three hydrogen peroxide to paracetamol initial molar ratios (R_{H₂O₂/PCT} = 10.5, 21.0, 42.0) were investigated.

Table 5.3. Design of experiments

ID	[Fe ²⁺] ⁰ (mg L ⁻¹)	[H ₂ O ₂] ⁰ (mg L ⁻¹)	Irradiation	R _{H₂O₂/PCT}
E1	5.0	94.5	NO	10.5
E2	5.0	189.0	NO	21.0
E3	5.0	378.0	NO	42.0
E4	7.5	94.5	NO	10.5

Advanced Oxidation Process Models for Optimisation and
Decion Making support in Water Mangement

E5	7.5	189.0	NO	21.0
E6	7.5	378.0	NO	42.0
E7	10.0	94.5	NO	10.5
E8	10.0	189.0	NO	21.0
E9	10.0	378.0	NO	42.0
E10	5.0	94.5	YES	10.5
E11	5.0	189.0	YES	21.0
E12	5.0	378.0	YES	42.0
E13	7.5	94.5	YES	10.5
E14	7.5	189.0	YES	21.0
E15	7.5	378.0	YES	42.0
E16	10.0	94.5	YES	10.5
E17	10.0	189.0	YES	21.0
E18	10.0	378.0	YES	42.0

Regarding the experimental protocol, the glass reservoir was first filled with 10.0 L of distilled water and then, after 15.0 min of recirculation, 4.9 L of distilled water in which PCT was previously dissolved, were added. Once pH was adjusted to 2.8 ± 0.2 , the remaining 0.1 L of distilled water, in which Fe^{2+} was previously dissolved, were filled and the light was switched on (in case of experiments performed under irradiated conditions). Finally, H_2O_2 was added and the initial sample was taken. The total reaction time was fixed to 120.0 min. To ensure perfect mixing conditions, according to the results obtained by Yamal-Turbay et al., 2015, the recirculation flowrate was set to 12.0 L min^{-1} .

5.2.2 Modelling

The modelling section starts by proposing a kinetic model followed by the reactor model that allows describing, by the means of a set of ODEs, the mass balances into the photoreactor (isothermal conditions).

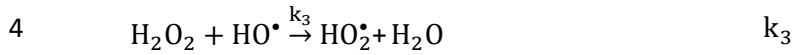
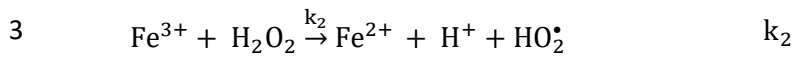
5.2.2.1 Kinetic model

The kinetic model proposed for the Fenton and photo-Fenton degradation of PCT (see Table 5.4) is based on the general Fenton/photo-Fenton reaction scheme proposed by Sun and Pignatello, 1993a, Sun and Pignatello, 1993b, Brillas et al., 2000, and Pignatello et al., 2006.

Table 5.4. Reaction mechanism of Fenton and photo-Fenton PCT degradation

ID	Reaction steps	Kinetic constants
1	$\text{Fe}^{2+} + \text{H}_2\text{O}_2 \xrightarrow{k_1} \text{Fe}^{3+} + \text{HO}^- + \text{HO}^\bullet$	k_1
2	$\text{Fe}^{3+} + \text{H}_2\text{O} \xrightarrow{\overline{\Phi}} \text{Fe}^{2+} + \text{H}^+ + \text{HO}^\bullet$	$\overline{\Phi}$

Advanced Oxidation Process Models for Optimisation and Decision Making support in Water Management



where $\overline{\Phi}$ refers to the wavelength-averaged primary quantum yield that was taken from Bossman et al. (Bossmann et al., 1998) and P_i represents the generic intermediate compound generated by the hydroxyl radical (HO^\bullet) attack to PCT.

The proposed model is based on the following assumptions (Conte et al., 2012):

- only the hydroxyl radicals (HO^\bullet) are taken into account as oxidant species;
- the steady-state approximation (SSA) can be applied to the highly reactive species (HO^\bullet);
- low ferrous ion concentrations were selected so the hydroxyl radical attack to Fe^{2+} can be neglected;
- the radical-radical termination steps are negligible compared to the propagation steps;
- the oxygen concentration is always in excess.

Hence, the kinetic constants accounting for Fenton and Fenton-like reactions, and the hydroxyl radical attack to hydrogen peroxide and paracetamol (k_1 , k_2 , k_3 and $k_{\text{PCT_OH}}$ respectively) were the parameters to be estimated. Subsequently, the following reactions rates for the reactive species PCT, H_2O_2 , Fe^{2+} and Fe^{3+} were derived:

$$\begin{bmatrix} R_{\text{PCT}}(\underline{x}, t) \\ R_{\text{H}_2\text{O}_2}(\underline{x}, t) \\ R_{\text{Fe}^{2+}}(\underline{x}, t) \\ R_{\text{Fe}^{3+}}(\underline{x}, t) \end{bmatrix} = \begin{bmatrix} R_{\text{PCT}}^T(\underline{x}, t) \\ R_{\text{H}_2\text{O}_2}^T(\underline{x}, t) \\ R_{\text{Fe}^{2+}}^T(\underline{x}, t) \\ R_{\text{Fe}^{3+}}^T(\underline{x}, t) \end{bmatrix} + \overline{\Phi} \sum_{\lambda} e_{\lambda}^a(\underline{x}, t) \begin{bmatrix} 1 \\ -\delta \\ -\frac{1}{\rho} \\ 1 \\ -1 \end{bmatrix} \quad \text{Eq. 5.2}$$

Where:

$$\delta = \frac{k_3 [\text{H}_2\text{O}_2]}{k_1 [\text{PCT}]} + 1 \quad \text{Eq.5.3}$$

$$\rho = \frac{k_{\text{PCT_OH}} [\text{PCT}]}{k_3 [\text{H}_2\text{O}_2]} + 1 \quad \text{Eq.5.4}$$

Here $\overline{\Phi}$ is the wavelength-averaged primary quantum yield, $\sum_{\lambda} e_{\lambda}^a(\underline{x}, t)$ the LVRPA extended to polychromatic radiation by performing the integration over all useful wavelengths λ (300-420 nm), and \underline{x} the position vector accounting for the radius and axial coordinates of the reactor.

It should be noted that the general reaction rate expression can be expressed as follows (in matrix notation):

$$[\mathbf{R}(\underline{x}, t)] = [\mathbf{R}^T(\underline{x}, t)] + \overline{\Phi} \sum_{\lambda} e_{\lambda}^a(\underline{x}, t) \boldsymbol{\tau}(\underline{x}, t) \quad \text{Eq.5.5}$$

The first term on the right-hand side of Equation (5.2) corresponds to the thermal reaction rate that gives the i-component degradation by the Fenton reaction, taking place in the total volume V, and is given by Equations (5.6) and (5.7):

$$\begin{bmatrix} R_{PCT}^T(\underline{x}, t) \\ R_{H_2O_2}^T(\underline{x}, t) \\ R_{Fe^{2+}}^T(\underline{x}, t) \\ R_{Fe^{3+}}^T(\underline{x}, t) \end{bmatrix} = k_1[Fe^{2+}][H_2O_2] \begin{bmatrix} -\frac{1}{\delta} \\ -\left(1 + \frac{1}{\rho}\right) \\ -1 \\ +1 \end{bmatrix} + \gamma \begin{bmatrix} 0 \\ -1 \\ +1 \\ -1 \end{bmatrix} \quad \text{Eq.5.6}$$

Where:

$$\gamma = k_2[Fe^{3+}][H_2O_2] \quad \text{Eq.5.7}$$

On the other hand, the second term on the right-hand side of Equation (5.2) corresponds to the i-component degradation by the radiation-activated reaction occurring inside the irradiated liquid volume (V_{IRR}).

5.2.2.2 Reactor model

The mass balances and initial conditions for the well-stirred annular photoreactor are given by the following set of first order, ordinary differential equations:

$$\frac{d[C_i]}{dt} = R^T(t) + \frac{V_{IRR}}{V} \bar{\Phi} \left\langle \sum_{\lambda} e_{\lambda}^a(\underline{x}, t) \right\rangle_{V_{IRR}} \tau(\underline{x}, t) \quad \text{Eq.5.8}$$

With the initial conditions:

$$[C_i] = [C_i]^{t_0} \quad t_0 = 0$$

Where: Eq.5.9

$[C_i]$ = symbol referring to the concentration of the generic component i

$[C_i]^0$ = symbol referring to the initial concentration of the generic component i

Note that the required reaction rate expressions to be replaced in Equation 5.8 are given by Equations (5.2)-(5.4) and Equations (5.6) and (5.7).

Therefore, based on the previous considerations, the following ODEs system gives the mass balance equations of the reactor model for each species (PCT, H_2O_2 , Fe^{2+} and Fe^{3+}):

$$\frac{d[PCT]}{dt} = \left[\left(k_1 [Fe^{2+}][H_2O_2] \left(-\frac{1}{\delta} \right) \right) + \left[\frac{V_{IRR}}{V} \left(\bar{\Phi} \left\langle \sum_{\lambda} e_{\lambda}^a(\underline{x}, t) \right\rangle_{V_{IRR}} \right) \right] \right] \quad \text{Eq.5.10}$$

$$\frac{d[H_2O_2]}{dt} = \left[\left(k_1 [Fe^{2+}][H_2O_2] \left(-\left(1 + \frac{1}{\rho} \right) \right) - \gamma \right) + \left[\frac{V_{IRR}}{V} \left(\bar{\Phi} \left\langle \sum_{\lambda} e_{\lambda}^a(\underline{x}, t) \right\rangle_{V_{IRR}} \right) \right] \right] \quad \text{Eq.5.11}$$

$$\frac{d[Fe^{2+}]}{dt} = [(-k_1 [Fe^{2+}][H_2O_2] + \gamma)] + \left[\frac{V_{IRR}}{V} \left(\bar{\Phi} \left\langle \sum_{\lambda} e_{\lambda}^a(\underline{x}, t) \right\rangle_{V_{IRR}} \right) \right] \quad \text{Eq.5.12}$$

$$\frac{d[Fe^{3+}]}{dt} = - \frac{d[Fe^{2+}]}{dt} \quad \text{Eq.5.13}$$

Here $\langle \sum_{\lambda} e_{\lambda}^a(\underline{x}, t) \rangle_{V_{IRR}}$ is the LVRPA averaged over the irradiated reactor volume (V_{IRR}). The latter depends on the spatial photon distribution within the annular photoreactor and, consequently, on the physical properties and

the geometrical characteristics of the lamp-reactor system. To compute it, a radiation model must be previously introduced. Specifically, a line source model with spherical and isotropic emission (LSSE model) was adopted (Alfano et al., 1986), (Braun et al., 2007). The LSSE model allows calculating $LVRPA_{VIRR}$ as a function of the radiation absorbing specie.

First, the following equation for the evaluation of the LVRPA for cylindrical coordinates has been solved using the numerical integration function in MATLAB:

$$e_{\lambda}^a(\underline{x}, t) = \kappa_{\lambda}(\underline{x}, t) \frac{P_{\lambda,s}}{2\pi L_L} \int_{\theta_1}^{\theta_2} \exp \left[-\frac{\kappa_{T,\lambda}(\underline{x}, t)(r_i - r_{int})}{\cos \theta} \right] d\theta \quad \text{Eq.5.14}$$

where $P_{\lambda,s}$ is the lamp spectral power emission (provided by the lamp supplier), $\kappa_{\lambda}(\underline{x}, t)$ the volumetric absorption coefficient of the reacting species, $\kappa_{T,\lambda}(\underline{x}, t)$ the volumetric absorption coefficient of the medium, r the radius, and L_L the useful length of the lamp. To compute the radiation absorbed in a generic point $l = l(r, z)$ (located at \underline{x}) inside the reactor, it was necessary to estimate the limiting angles of integration (trigonometrically defined), that is:

$$\left\langle \sum_{\lambda} e_{\lambda}^a(\underline{x}, t) \right\rangle_{V_{IRR}} = \frac{2\pi}{V_{IRR}} \int_0^L \int_{r_{int}}^{r_{ext}} e_{\lambda}^a(\underline{x}, t) r dr dz \quad \text{Eq.5.15}$$

To solve Equation (5.14), it was considered that ferric ions present in solution as ferric ions complex ($Fe(OH)^{2+}$) are the dominant ferric species at pH 2.8 and the principal absorbing specie; here it was also assumed that radiation absorption of hydrogen peroxide and ferrous ion is negligible for wavelengths greater than 300 nm. Under these hypotheses, $\kappa_{T,\lambda}(\underline{x}, t)$ can be calculated as follows:

$$\kappa_{T,\lambda}(\underline{x}, t) = \sum_i \alpha_{i,\lambda} [C_i] \cong \alpha_{Fe(OH)^{2+},\lambda} [Fe(OH)^{2+}] \quad \text{Eq.5.16}$$

where $\alpha_{\text{Fe(OH)}^{2+},\lambda}$ is the molar absorptivity of ferric ions complex (Fe(OH)^{2+}) and $[\text{Fe(OH)}^{2+}]$ is the concentration of the latter that can be considered equal to the concentration of Fe^{3+} .

Finally, after evaluating LVRPA at each point inside the irradiated volume, it is possible to compute the averaged value of the LVRPA over the irradiated reactor volume and polychromatic radiation, solving the following equation:

$$\left\langle \sum_{\lambda} e_{\lambda}^a(\underline{x}, t) \right\rangle_{V_{\text{IRR}}} = \frac{2\pi}{V_{\text{IRR}}} \int_0^L \int_{r_{\text{int}}}^{r_{\text{ext}}} e_{\lambda}^a(\underline{x}, t) r \, dr \, dz \quad \text{Eq.5.17}$$

where r_{int} and r_{ext} are the internal and external radius of the annular photoreactor. In addition, in this case the numerical integration function in MATLAB was used to solve Equation (5.17).

In this way, it was possible to estimate the value of LVRPA averaged over the irradiated reactor volume for a specific set of values of $[\text{Fe}^{3+}]$ (Table 5.5):

Table 5.5. Values of LVRPA averaged over the irradiated reactor volume, calculated for a specific set of iron concentration

$[\text{Fe}^{3+}], (\text{mg L}^{-1})$	$\left\langle \sum_{\lambda} e_{\lambda}^a(\underline{x}, t) \right\rangle_{V_{\text{IRR}}}, (\text{Einstein cm}^{-3} \text{ s}^{-1})$
0.0	0.0
2.5	3.5×10^{-10}
5.0	$7.1\text{E} \times 10^{-10}$
7.5	9.5×10^{-10}

5.2.3 Model fitting and parameter estimation

A nonlinear multivariate and multiparameter optimisation procedure was implemented in MATLAB in order to minimize the sum of the squared differences between the experimental and model values of PCT and H_2O_2 normalized concentrations.

The first step is to solve numerically the ODEs system given by Equations (5.8) and (5.9). For this purpose, an Ordinary Differential Equation (ODE) solver in MATLAB was used. Especially, ode15s solver stiff differential equations which is a variable-step, variable-order (VSVO) solver based on the numerical differentiation formulas (NDFs), was selected. Then, the values of the kinetic constants (k_1 , k_3 , k_4 , k_{PCT_OH}) were estimated minimizing the sum of the squared differences between the model values (calculated by solving the ODEs system) and the experimental values of PCT and H_2O_2 . For this purpose, the Levenberg-Marquardt least-squares algorithm available in the Optimisation Toolbox of MATLAB was used. The whole set of experimental data (E1-E18, Table 5.3) was used for the parameter estimation. Additionally, the root mean square errors (RMSEs) were calculated to test model reliability (see Figure 5.2).

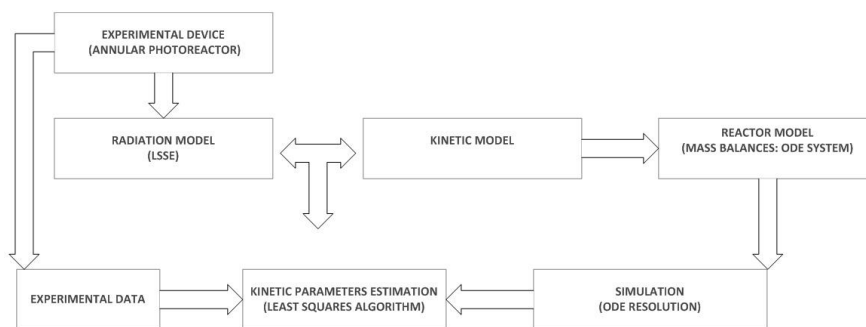


Figure 5.2. Flow diagram of the methodological framework followed to estimate the parameters of the proposed kinetic model

5.3 Results and discussion

5.3.1 Experimental results

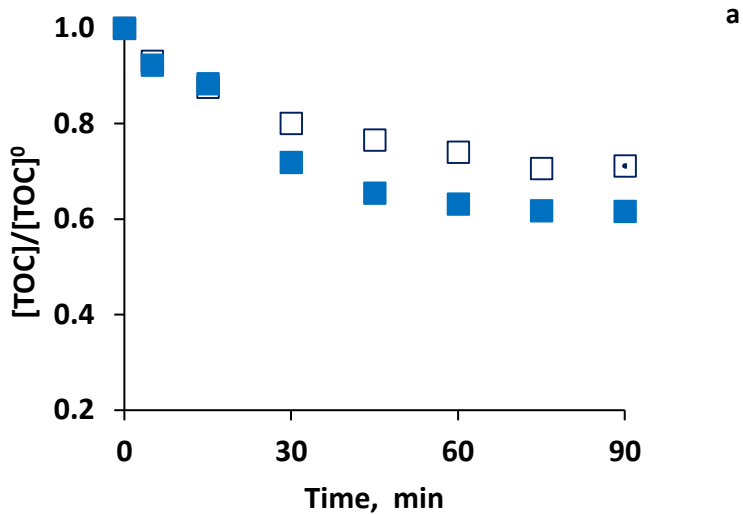
Paracetamol was not detected by the HPLC analyses under all investigated conditions after a maximum time of 15.0 min (E1, Table 5.3) and a minimum time of 2.5 min (E18, Table 5.3) (results not shown). Especially, for the highest value of $[\text{H}_2\text{O}_2]^0$, and considering dark conditions and increasing $[\text{Fe}^{2+}]^0$ from 5.0, to 7.5 and 10.0 mg L^{-1} (experiments E3, E6 and E9, Table 5.3), PCT total removal was obtained in 15.0, 10.0 and 5.0 min, respectively. In addition, for this dark conditions and considering the minimum concentration of oxidizing agent ($[\text{H}_2\text{O}_2]^0 = 94.5 \text{ mg L}^{-1}$), the reaction time necessary to achieve complete PCT destruction is reduced by 66% by doubling the initial catalyst concentration from 5.0 to 10.0 mg L^{-1} (E1 and E7 tests respectively, Table 5.3). On the other hand, for the highest value of $[\text{H}_2\text{O}_2]^0$ and irradiating system (experiments E12, E15 and E18, Table 5.3), the PCT total conversion was obtained in only 10.0, 7.5 and 2.5 min, respectively. Hence, considering irradiated conditions, by doubling the initial concentration of the catalyst, it is possible to reduce by up to 75% the time necessary for the complete destruction of the contaminant. Therefore, it was possible to confirm the beneficial effect of using higher doses of catalyst to reduce the reaction times necessary to achieve complete removal of the contaminant. This effect is of greater relevance for lower concentrations of oxidizing agent.

Although TOC was not introduced as a kinetic model component, it represents an important measurement to analyze the process performance. Hence, the performance of each experiment was also evaluated in terms of reached mineralization levels at a specific time (TOC conversion, χ^t). In Figure 5.3 the TOC experimental evolution obtained using the minimum (Figure 5.3-a) and maximum (Figure 5.3-b) concentrations of oxidizing agent and catalyst, is shown.

In Figure 5.3-a, it can be observed that TOC conversion reaches asymptotic values in both experiments. Specifically, $\chi^{75 \text{ min}} = 29.3\%$ and $\chi^{60 \text{ min}} = 33\%$ for E1 and E10, respectively. However, these maximum conversion levels are associated with reaction times in which the oxidant agent is no more detected (75.0 and 60.0 min for E1 and E10, respectively). Although the

Advanced Oxidation Process Models for Optimisation and Decision Making support in Water Management

TOC conversions obtained in both cases are similar, the use of radiation allowed reducing the reaction time by 20%. Therefore, even in the case of achieving the total removal of the contaminant (15.0 min of reaction) with the minimum concentrations of reagents, the level of mineralization reached is not significant. This is in accordance with the theoretical levels of oxidant agent doses required to achieve complete mineralization of the system (see Equation (5.1)).



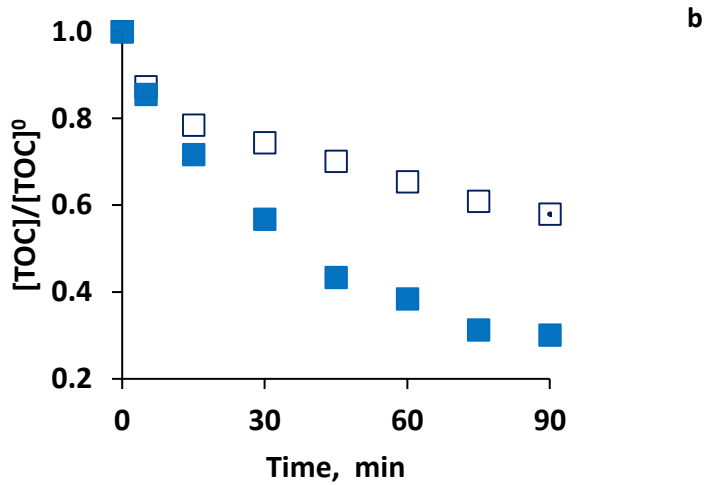


Figure 5.3. Normalized experimental concentrations of TOC, obtained under dark (□) and irradiated(■) conditions and considering the lowest and highest initial concentrations of Fe^{2+} and H_2O_2 ($[\text{Fe}^{2+}]^0$ and $[\text{H}_2\text{O}_2]^0$) experiments E1 and E10 **a)** and experiments E9 and E18 **b)**, respectively

Furthermore, in Figure 5.3-b it can be appreciated an asymptotic value of $\chi^{75 \text{ min}} = 68.5\%$ (depletion of H_2O_2) in the case of the assay E18. This value was the highest level of mineralization that was reached for the whole set of performed experiments. Nevertheless, under the same maximum concentrations of the reagents, the dark reaction (E9), for which H_2O_2 was detected until the end of the assay (120.0 min), only reached $\chi^{120 \text{ min}} = 45.6\%$.

Finally, in order to conclude the study regarding the mineralization performance of the system, the specific consumption of the oxidizing agent, $\gamma_{\text{H}_2\text{O}_2/\text{TOC}}$, was evaluated as follows:

$$\gamma_{\text{H}_2\text{O}_2/\text{TOC}} = \frac{[\text{H}_2\text{O}_2]^0 - [\text{H}_2\text{O}_2]^\tau}{[\text{TOC}]^0 - [\text{TOC}]^\tau} \quad \text{Eq.5.18}$$

where τ is the time at which the oxidizing agent consumption occurred or the final reaction time. In Figure 5.4 a multiple bar chart shows the radiation effect on $\gamma_{H_2O_2/TOC}$ obtained for several initial concentrations of the oxidant (94.50, 189.00 and 378.00 mg L⁻¹) and of the catalyst (5.00 and 10.00 mg L⁻¹).

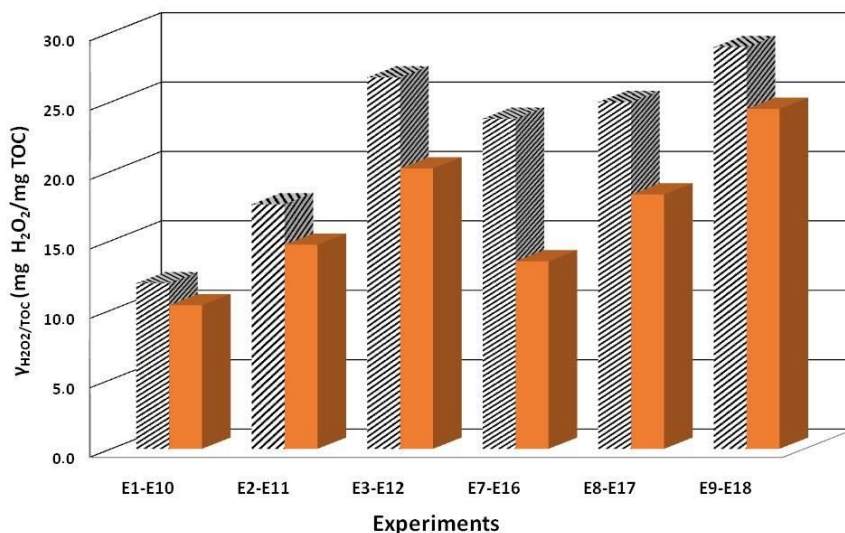


Figure 5.4. Specific consumption of the oxidizing agent as a function of the experiments performed with $[Fe^{2+}]^0 = 5.0$ and 10.0 mg L⁻¹ and for the three different investigated values of $[H_2O_2]^0$ (94.5, 189.0, 378.0 mg L⁻¹) under non irradiated (striped bar chart) and irradiated conditions (solid bar chart)

First of all, it must be noted that for all the investigated conditions, the $\gamma_{H_2O_2/TOC}$ results are always higher for non-irradiated conditions than for irradiated ones. This result highlights a less efficient consumption of H_2O_2 under non-irradiated conditions. Moreover, it is possible to observe that the increase in the initial concentration of the catalyst led to an increase of the gap between the H_2O_2 specific consumption obtained under non-irradiated and irradiated conditions.

It is worth noting that, although the experiment E10 ($[Fe^{2+}]^0 = 5.0$ mg L⁻¹ and $[H_2O_2]^0 = 94.5$ mg L⁻¹), carried out under irradiated conditions, showed to be the most efficient one, only allowed to reach a final TOC conversion of 39%. However, experiment E12 ($[Fe^{2+}]^0 = 5.0$ mg L⁻¹ and $[H_2O_2]^0 = 378.0$ mg L⁻¹), also

performed under irradiated conditions, despite being less efficient than E10, allowed to obtain a final TOC conversion of 74%. This result presents great environmental and economic significance since, according to the level of mineralization required by the system, it would allow knowing the dose of oxidizing agent and necessary reaction time. Hence, this result shows that if, from one hand, the increase of the initial concentration of the oxidant led to a less efficient consumption of the latter; from the other hand, it allows reaching higher levels of mineralization.

5.3.2 Model fitting

The experimental data were used to perform the fitting of the proposed kinetic model. The values of the kinetic parameters accounting for the Fenton and Fenton-like reactions (k_1 and k_3 respectively) and for hydroxyl radical attack to hydrogen peroxide and paracetamol (k_4 and k_{PCT_OH} respectively) were estimated and are shown in Table 5.6.

Table 5.6. Estimated values of the kinetic parameters

$k_1, M^{-1}s^{-1}$	$k_2, M^{-1}s^{-1}$	$k_3, M^{-1}s^{-1}$	$k_{PCT_OH}, M^{-1}s^{-1}$
147.29	3.16	7.00×10^7	3.58×10^9

It is worth noting that the estimated values of the kinetic parameter k_3 and k_{PCT_OH} are within the range of values found in the specific literature (Simunovic et al., 2011), (De Laurentiis et al., 2014). Conversely, the values of the kinetic parameters k_1 and k_2 result to be slightly higher than those found in the literature ($63.00-76.00 M^{-1} s^{-1}$ and $0.01-0.02 M^{-1} s^{-1}$, respectively) (Simunovic et al., 2011).

In Figure 5.5 the comparison between experimental and predicted concentrations of H_2O_2 and PCT obtained for dark (Figure 5.5-a) and irradiated conditions (Figure 5.5-b), is shown.

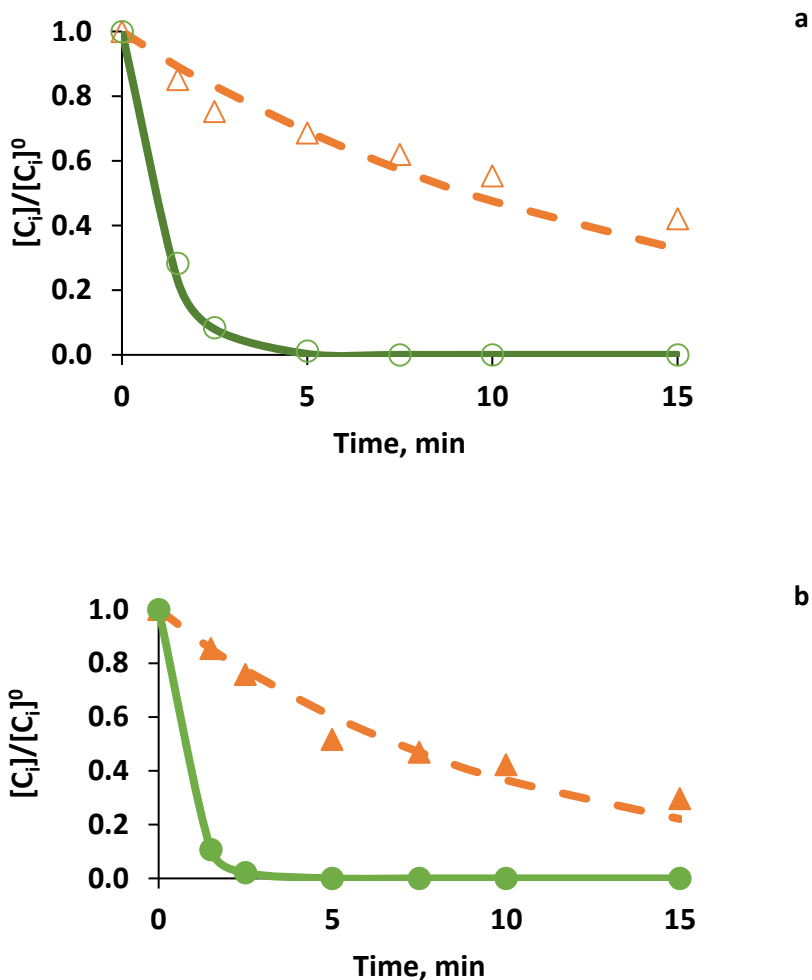


Figure 5.5. Experimental concentrations of paracetamol (\circ, \bullet) and hydrogen peroxide (Δ, \blacktriangle) and predicted concentrations of paracetamol (—) and hydrogen peroxide (- -). Dark (\circ, Δ) and irradiated (\bullet, \blacktriangle) conditions. **a)** Experiment E6 ($[\text{Fe}^{2+}]^0 = 7.5 \text{ mg L}^{-1}$ and $[\text{H}_2\text{O}_2]^0 = 378.0 \text{ mg L}^{-1}$), and **b)** experiment E18 ($[\text{Fe}^{2+}]^0 = 10.0 \text{ mg L}^{-1}$ and $[\text{H}_2\text{O}_2]^0 = 378.0 \text{ mg L}^{-1}$)

Firstly, using the same initial concentration of H_2O_2 under dark conditions and moving from $[\text{Fe}^{2+}]^0 = 7.5 \text{ mg L}^{-1}$ (Figure 5.5-a) to $[\text{Fe}^{2+}] = 10.0 \text{ mg L}^{-1}$ (data not

shown), it was observed that the time at which PCT is no more detected by HPLC remained the same, approximately 5.0 min in both cases. However, it was observed that the irradiated condition (Figure 5.5-b) led to the complete PCT removal in only 2.5 min. Hence, under these experimental conditions, the photo-Fenton process allowed to reach a 50% decrease in the total PCT removal time.

In order to test the model reliability, the root mean square error (RMSE) was calculated by the expression:

$$RMSE_i = \sqrt{\sum_k (y_{ik} - y_{ik}^*)^2 / n_i} \quad \text{Eq.5.19}$$

root mean square error of the i^{th} variable

y_{ik} , value of the k^{th} measurement of the i^{th} variable

y_{ik}^* , value of the k^{th} estimation of the i^{th} variable (model prediction)

$i = 1, 2, \dots, I$, i^{th} element of the set of measured variables

The only measurements considered are the normalized concentration of PCT and H_2O_2 ($I= 2$).

In Table 5.7, the values of RMSE, calculated considering: i) the whole set of experiments (E1 to E18); ii) the experiments performed only under dark conditions (E1 to E9); and iii) the experiments performed only under irradiated conditions (E10 to E18), are shown.

Table 5.7. Root mean square errors (RMSE)

	Dark and irradiated conditions	Dark conditions	Irradiated conditions
PCT	6.80%	7.64%	5.84%
H₂O₂	9.67%	9.75%	9.59%

The proposed model showed a relatively good agreement with the experimental data. The lowest values of RMSE (for normalized PCT and H₂O₂ concentration) were obtained in case of considering only the experiments carried out under irradiated conditions. However, considering the complete set of performed tests, the obtained errors are consistent (RMSE_{PCT}= 6.80% and RMSE_{H₂O₂}= 9.67%) and, therefore, the kinetic model is able to satisfactorily reproduce the system behaviour.

5.4 Conclusions

The Fenton and photo-Fenton degradation of paracetamol and the consumption of hydrogen peroxide have been investigated in a well-stirred annular reactor placed inside the loop of a batch recycling system. Total removal of paracetamol was achieved for all the analysed operating conditions, with a maximum removal time of 15.0 min. Moreover, for each concentration of iron and oxidizing agent, no significant differences were observed in the removal times required for both dark and irradiated tests. However, it should be mentioned that the reaction times were always lower for the irradiated operating conditions, with a minimum required time of 2.5 min.

In addition, the use of radiation allowed a significant enhancement of the process performance leading to a more efficient consumption of the oxidizing agent. For all the evaluated operating conditions, the values of the “specific consumption of the oxidant agent” ($\gamma_{H_2O_2/TOC}$) obtained for Fenton

process were always higher than the corresponding values observed for photo-Fenton system.

Furthermore, the performance of each experiment was also evaluated in terms of reached mineralization levels at a specific reaction time. The highest level of mineralization achieved considering the whole set of experiments was $\chi^{75 \text{ min}} = 68.5\%$, conversion value obtained at the time when the oxidizing agent had been completely consumed.

A kinetic model for predicting Fenton and photo-Fenton degradation of paracetamol and hydrogen peroxide consumption has been proposed. Results have shown that the proposed kinetic model is able to capture the complex and nonlinear nature of such processes and incorporate the effect of the Local Volumetric Rate of Photon Absorption on the reactor behaviour.

Kinetic parameters, accounting for the Fenton and photo-Fenton reaction and for the HO^\bullet attack to PCT and H_2O_2 were estimated. Considering the values of the root mean square error (RMSE) obtained for the complete set of experimental runs ($\text{RMSE}_{\text{PCT}} = 6.80\%$ and $\text{RMSE}_{\text{H}_2\text{O}_2} = 9.67\%$), it was possible to conclude that the proposed kinetic model is able to satisfactorily reproduce the system behaviour.

This kinetic model is the starting point for the development of a more complex model that also takes into account the generation of intermediate compounds and the evolution of the Total Organic Carbon, and their main effects on the reaction rate of the photo-Fenton system.

5.5 Acknowledgements

This work was supported by the Spanish “Ministerio de Economía, Industria y Competitividad (MINECO)” and the European Regional Development Fund, both funding the research Project AIMS (DPI2017-87435-R). Francesca Audino, particularly acknowledges the MINECO for the PhD grant [BES-2013-065545]. Also, the authors acknowledge the financial support from the Universidad Nacional del Litoral (UNL, Project PIC50420150100009LI), Consejo Nacional de Investigaciones Científicas y Técnicas (CONICET, Project

Advanced Oxidation Process Models for Optimisation and Decision Making support in Water Management

PIP-20150100093), and Agencia Nacional de Promoción Científica y Tecnológica of Argentina (ANPCyT, Project PICT-2015-2651).

6 Non-Conventional kinetic study

As also highlighted in the previous chapter, First Principles Models (FPMs) can ensure accuracy and completeness and allow the understanding of the chemical process. However, to the best of our knowledge, as for the model proposed in the previous chapter, all these models have been proposed, trained and validated for a specific target compound.

Hence, the major challenge remains an approximately unified, causally established coupling between the general photo-Fenton system and the decontamination of the quite different organic compounds.

In this chapter, a novel modelling approach of medium complexity that can allow describing the photo-Fenton degradation of any organic compounds regardless of its structure and chemical formula has been proposed and validated.

6.1 Introductory perspective

A notable experimental effort has been spent in the last years in investigating the Advanced Oxidation Processes (AOPs). AOPs are considered to be an effective alternative that can be combined with conventional secondary methods for the treatment of toxic and recalcitrant wastewaters, and for the removal of the Contaminants of Emerging Concern (CECs) (Andreozzi et al., 1999), (Pablos et al., 2013), (Giannakis et al., 2015), (Miklos et al., 2018). Particularly, photo-Fenton process has proved to be of added interest, because of the possibility of developing efficient and cost effective treatment systems by exploiting both solar energy and its combination with biological technologies (Rahim Pouran et al., 2015). Furthermore, it has shown to be highly efficient for the treatment of both high-strength organic wastewaters (Rahim Pouran et al., 2015) and micropollutants (Miralles-Cuevas et al., 2014), (Villegas-Guzman et al., 2017).

Nevertheless, the transition from a pure experimental to a model-based approach is needed for the development of practical applications. The literature review reveals that the proposed models can be enclosed in two main categories: First Principles Models (FPMs) and Empirical Models. Some FPMs rely on the detailed kinetic modelling of Fenton and photo-Fenton processes (Simunovic et al., 2011) and follow the scheme proposed by Kang et al., 2002 based on three main group of reactions (an inorganic chemistry core, interactions between target compounds, intermediates and Fenton reactants and finally the interactions between iron species and the intermediates). Then, following the work by Alfano et al., 1986 FPMs based on rigorous radiation models to compute the spatial distribution of the absorbed photons inside the reactor (Farias et al., 2007), (Conte et al., 2012), have also been proposed. Moreover, a recent work describing a mechanistic model of solar photo-Fenton has been developed by Soriano-Molina et al., 2018.

Regarding the Empirical Models, works proposing the use of response surface platform for regression models (Pérez-Moya et al., 2008) and multivariate Data Based Modelling (Shokry et al., 2015) can be found.

Furthermore, an alternative semi-empirical solution that explicitly takes into account the light influence (as a component of the process) was proposed by Cabrera Reina et al., 2012. In spite of the accuracy and completeness of FPMs that ensures the understanding of the chemical process, the resulting computational effort might be unaffordable. Moreover, the complex nonlinear nature of the Fenton and photo-Fenton systems makes it difficult to develop a comprehensive FPM including all the involved reaction mechanisms in more general cases so limiting their application for process monitoring and control. However, the Empirical Models tend to usually oversimplify the complex nonlinear behaviour of such processes, and are characterized by limited capabilities of correlation of larger sets of process variables. Conversely, the DBMs based on the use of advanced techniques can better capture the nonlinear system behaviours but are not based on a physical description and understanding of the chemical process.

Nevertheless, to the best of our knowledge, all these models have been proposed, trained and validated for a specific target compound.

As a consequence, the major challenge remains an approximately unified, causally established coupling between the general photo-Fenton system and the decontamination of the quite different organic compounds.

Hence, the aim of this work is to propose and validate a novel modelling approach of medium complexity that can allow describing the photo-Fenton degradation of any wastewater containing single or multiple organic compounds. For this purpose, the proposed model was formulated in order to be able to describe the photo-Fenton degradation of the target compound and of the oxidant but also the TOC evolution, being the latter a lumped parameter that is used to define the overall quality of the water.

A general degradation mechanism, depending on the number of carbon atoms in the molecule to be decomposed, has been proposed and coupled with well-known Fenton and photo-Fenton kinetics representing the core mechanism of the proposed model.

The model was previously proposed, trained and validated selecting paracetamol (PCT, $C_8H_9NO_2$) as target compound, being the most widely used antipyretic and analgesic. Then the proposed methodology was validated using two additional model compounds. As second model compound was selected the sulfaquinoxaline sodium salt (SQX, $C_{14}H_{11}N_4NaO_2S$), that is a potential food contaminant in animal products. Finally formic acid (FA, CH_2O_2), that is a by-product of the degradation of many hazardous organic compounds and belongs to the group of carboxylic acids that are hardly degradable even by chemical oxidation (Salazar et al., 2017) was chosen as third target compound.

In this work a non-conventional methodology named Direct Computer Mapping (DCM) (Csukás et al., 1999), (Csukás et al., 2013) based Programmable Structures (Varga and Csukas, 2017), (Varga et al., 2017) was used for modelling and simulation based analysis of the experimental system.

6.2 Experimental

6.2.1 Reagents and chemicals

Paracetamol 98%, sulfaquinoxaline sodium salt 95% purity purchased from Sigma-Aldrich (St. Louis, MO, USA), and formic acid 98% purchased from Honeywell Fluka (Morris Plains, NJ, USA) were used as target compounds. Reagent-grade hydrogen peroxide (H_2O_2) 33% w/v from Panreac Química SLU (Barcelona, Spain) and iron sulfate ($FeSO_4 \cdot 7H_2O$) from Merck (Kenilworth, NJ, USA), adopted as the ferrous ion (Fe^{2+}) source, were used as Fenton reagents. HPLC gradient grade methanol, MeOH, purchased from J.T. Baker Inc. (Phillipsburg, NJ, USA) and filtered milli Q grade water were used as HPLC mobile phases. High purity (>99%) ascorbic acid from Riedel de Haën (Seelze, Germany), 0.2% 1,10-phenanthroline from Scharlab SL (Barcelona, Spain), sodium acetate anhydrous and 95%–98% sulfuric acid, both from Panreac Química SLU (Barcelona, Spain), were used to perform measurements of iron species. Hydrogen chloride HCl 37% from J.T. Baker Inc. (Phillipsburg, NJ, USA) was used to adjust the initial pH. DEIONISED water with a conductivity lower than $1.25 \mu S$ was provided by Adesco S.A. (Barcelona, Spain) and was used as water matrix in all experiments.

6.2.2 Analytical determinations

Measurements of Total Organic Carbon concentrations ([TOC]) were performed with a Shimadzu VCHS/CSN TOC analyzer (Shimadzu; Kyoto, Japan) and samples were taken each 15.0 min (being the measuring time of the equipment of 15.0 min) and refrigerated after extraction in order to slow down any further degradation of the organic matter.

Target compounds concentrations were measured with an HPLC Agilent 1200 series with UV-DAD array detector (Agilent Technologies, Santa Clara, CA, USA). Particularly, PCT concentration ([PCT]) was determined by using an Akady 5 μm C-18 150 \times 4.6 mm column, maintained at 25.0 $^{\circ}\text{C}$ as stationary phase, and a mixture of methanol:water (25:75) flowing at 0.4 mL min^{-1} as mobile phase. The diode array detector was set at 243 nm. Under these conditions, retention time was 9.0 min. Samples were taken at 0.0, 1.5, 2.5, 5.0, 7.5, 10.0 and 15.0 min and were previously treated with methanol (in proportion 50:50) in order to stop further degradation of PCT.

For the determination of SQX concentration ([SQX]), the same Akady 5 μm C-18 150 \times 4.6 mm column, kept at 25.0 $^{\circ}\text{C}$, was used as stationary phase, while methanol and 0.1% (v/v) formic acid (55:45, v/v) were used as the mobile phase flowing at 1.5 mL min^{-1} . In this case, the diode array detector was set at 250 nm. Under these conditions, retention time was 2.0 min. In this case, samples were taken at 0.0, 2.0, 5.0, 10.0, 15.0, 20.0, 25.0, 30.0, 45.0, 60.0, 75.0, 90.0, 120.0 min and were previously treated with methanol (in proportion 50:50) in order to stop the oxidation reactions.

In the case of formic acid, FA, only the TOC concentration was followed during the treatment span.

Finally, measurements of H_2O_2 and iron species concentrations were performed with a Hitachi U-2001 UV-VIS spectrophotometer (Hitachi, Tokyo, Japan). Hydrogen peroxide concentration ($[\text{H}_2\text{O}_2]$) was determined following the spectrophotometric technique described by Nogueira et al., 2005. This technique is based on the measurement of the absorption at 450 nm of the complex formed after reaction of H_2O_2 with ammonium metavanadate. In this case, samples were taken each 5.0 min until a reaction time of 30.0 min and then each 15.0 min until the end of the assay.

The iron species (Fe^{2+} , Fe^{3+} , Fe^{TOT}) were analysed using the 1,10-phenanthroline method following ISO 6332:1988, based on the absorbance measurements of the Fe^{2+} -phenanthroline complex at 510 nm. To measure total iron concentration, ascorbic acid must be used so to convert all the ferric ions (Fe^{3+}) to ferrous ions (Fe^{2+}). Then, for difference, ferric ion concentration could be determined. In this case, samples were taken each 5.0 min until a reaction time of 30.0 min and then each 15.0 min until the end of the assay.

6.2.3 Pilot plant

The pilot plant that was used to perform Fenton and photo-Fenton assays is a 15.0-L system composed by an annular photo-reactor with an irradiated volume (V_{IRR}) of 1.5 L and connected to a glass jacketed reservoir tank, both provided by Termo Fisher Scientific, Barcelona, Spain.

The annular photo-reactor is equipped with an Actinic BL TL-DK 36 W/10 1SL lamp (UVA-UVB) provided by Barcelona LED, Barcelona, Spain, and the incident photon flux, measured by Yamal-Turbay et al., 2015 using potassium ferrioxalate actinometry (Murov et al., 1993), resulted in $E = 3.36 \times 10^{-4}$ Einstein min^{-1} (300 and 420 nm). The pilot plant is also equipped with sensors (conductivity, dissolved oxygen, oxidation reduction potential and pH probes) connected to a programmable logic controller (PLC) that allows data acquisition and process control and to a SCADA system allowing data management.

Finally, a flowmeter is available for the control of the recirculation flowrate.

A schematic view of the pilot plant is shown in the following Figure 6.1.

Non-conventional kinetic study

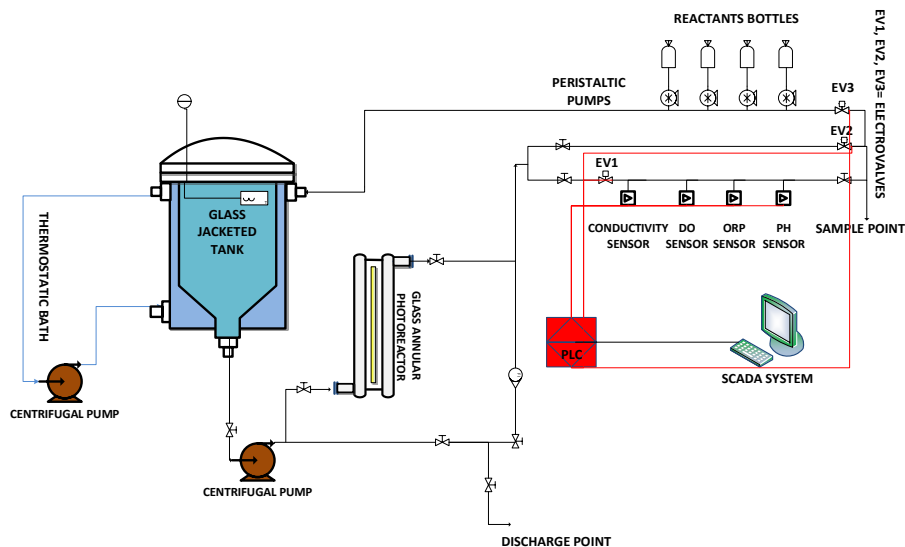


Figure 6.1. Schematic view of the pilot plant

6.2.4 Experimental design and protocol

As first instance, a set of blank assays without any target compound (BLANK 1-4 in Table 6.1) was carried out in order to help the estimation of the kinetic parameters referring to the Fenton and photo-Fenton mechanisms in the proposed simplified First Principles Model. Particularly, in this case the initial concentration of ferrous ion $[\text{Fe}^{2+}]^0$ was set to 10.0 mg L^{-1} (corresponding to 0.18 mmol L^{-1}), or rather to the maximum legal value in wastewaters in Spain [DOGC]. The initial concentration of hydrogen peroxide $[\text{H}_2\text{O}_2]^0$ was set to 378.0 mg L^{-1} , corresponding to $11.12 \text{ mmol L}^{-1}$. The latter was chosen being the highest value of the oxidant concentration among the ones used to perform the experiments with the target compounds that will be detailed in the following sections.

Advanced Oxidation Process Models for Optimisation and Decision Making support in Water Management

Table 6.1. Set of blank assays performed without any target compound

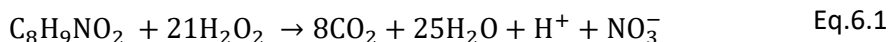
ID	$[\text{H}_2\text{O}_2]^0$	$[\text{Fe}^{2+}]^0$	pH	T	λ	V_{IRR}
	mmol L^{-1}	mmol L^{-1}		$^{\circ}\text{C}$	nm	L
BLANK_1	11.12	0.00	2.8±0.2	28.0±2.0	300-420	0.0
BLANK_2	11.12	0.00	2.8±0.2	28.0±2.0	300-420	1.5
BLANK_3	11.12	0.18	2.8±0.2	28.0±2.0	300-420	0.0
BLANK_4	11.12	0.18	2.8±0.2	28.0±2.0	300-420	1.5

Then, a set of experiments using paracetamol (PCT $\text{C}_8\text{H}_9\text{NO}_2$) as target compound was carried out to estimate the kinetic constants referring to the degradation mechanism.

Particularly, Fenton (dark conditions, $V_{\text{IRR}} = 0.0$ L) and photo-Fenton (irradiated conditions, $V_{\text{IRR}} = 1.5$ L) experiments were performed fixing the initial concentration of PCT, $[\text{PCT}]^0 = 40.00 \text{ mg L}^{-1}$, corresponding to 0.26 mmol L^{-1} and to an initial TOC concentration $[\text{TOC}]^0 = 25.92 \text{ mg L}^{-1}$, and changing the initial concentrations of ferrous ion $[\text{Fe}^{2+}]^0$ and hydrogen peroxide $[\text{H}_2\text{O}_2]^0$.

The value of the initial PCT concentration is higher than that found in wastewaters and surface waters (Ternes, 1998), (Kolpin et al., 2002), (Lapworth et al., 2012), but it allows simulating the treatment of a real paracetamol wastewater characterized by higher PCT, TOC and Chemical Oxygen Demand (COD) concentrations (Dalgic et al., 2016), (Cabrera Reina et al., 2012).

The stoichiometric value of hydrogen peroxide ion concentration to achieve total mineralization of 0.26 mmol L^{-1} of PCT, when H_2O_2 is considered to be the only oxidant in the media, is 5.56 mmol L^{-1} (Equation (6.1)):



In this case, a 2² factorial design was applied in order to define the set of experiments to be performed. The two selected factorials were the Fenton reagents (Fe²⁺ and H₂O₂).

The initial ferrous ion concentration was varied between 0.18 mmol L⁻¹ as maximum value of the factorial design (+1), and half such value, 0.09 mmol L⁻¹, as minimum value of the factorial design (-1), and one and a half times less, 0.13 mmol L⁻¹, as central value of the factorial design (0).

The initial hydrogen peroxide ion concentration was varied between half and twice (2.78-11.12 mmol L⁻¹) the stoichiometric dose as maximum and minimum value of the factorial design (-1, +1). The stoichiometric dose (5.56 mmol L⁻¹) corresponds to the central value of the factorial design (0).

The resulting design of experiment in the case of PCT is presented in the following Table 6.2 in which are reported all the specific conditions (pH, T, λ, and V_{IRR}) of the experiments that were performed. Especially, the experiments from EXP1_PCT to EXP9_PCT, are the experiments performed under dark conditions while those from EXP10_PCT to EXP_18_PCT, are the ones performed under irradiated conditions.

Moreover, a set of preliminary standard blank assays was also performed and it is presented in Table 6.2 as well. The aim was to check the role of the oxidant (BLANK 5 and BLANK 7 experiments in Table 6.2) and the role of the catalyst (BLANK 6 and BLANK 8 experiments in Table 6.2) under both dark and irradiated conditions and the possible direct photolysis of PCT (BLANK 9 experiment in Table 6.2).

Table 6.2. Design of experiments comprising the assays using PCT (C₈H₉NO₂) as target compound

Design of experiments performed for an initial PCT concentration of [PCT]⁰= 0.26 mmol L⁻¹ corresponding to an initial TOC concentration of [TOC]⁰= 25.92 mg L⁻¹

Advanced Oxidation Process Models for Optimisation and
Decision Making support in Water Management

ID	[H ₂ O ₂] ⁰	[Fe ²⁺] ⁰	pH	T	λ	V _{IRR}
	mmol L ⁻¹	mmol L ⁻¹		°C	nm	L
BLANK_5	11.12	0.00	2.8±0.2	28.0±2.0	300-420	0.0
BLANK_6	0.00	0.18	2.8±0.2	28.0±2.0	300-420	0.0
BLANK_7	11.12	0.00	2.8±0.2	28.0±2.0	300-420	1.5
BLANK_8	0.00	0.18	2.8±0.2	28.0±2.0	300-420	1.5
BLANK_9	0.00	0.00	2.8±0.2	28.0±2.0	300-420	1.5
EXP1_PCT	2.78	0.09	2.8±0.2	28.0±2.0	300-420	0.0
EXP2_PCT	2.78	0.13	2.8±0.2	28.0±2.0	300-420	0.0
EXP3_PCT	2.78	0.18	2.8±0.2	28.0±2.0	300-420	0.0
EXP4_PCT	5.56	0.09	2.8±0.2	28.0±2.0	300-420	0.0
EXP5_PCT	5.56	0.13	2.8±0.2	28.0±2.0	300-420	0.0
EXP6_PCT	5.56	0.18	2.8±0.2	28.0±2.0	300-420	0.0
EXP7_PCT	11.12	0.09	2.8±0.2	28.0±2.0	300-420	0.0

Non-conventional kinetic study

EXP8_PCT	11.12	0.13	2.8±0.2	28.0±2.0	300-420	0.0
EXP9_PCT	11.12	0.18	2.8±0.2	28.0±2.0	300-420	0.0
EXP10_PCT	2.78	0.09	2.8±0.2	28.0±2.0	300-420	1.5
EXP11_PCT	2.78	0.13	2.8±0.2	28.0±2.0	300-420	1.5
EXP12_PCT	2.78	0.18	2.8±0.2	28.0±2.0	300-420	1.5
EXP13_PCT	5.56	0.09	2.8±0.2	28.0±2.0	300-420	1.5
EXP14_PCT	5.56	0.13	2.8±0.2	28.0±2.0	300-420	1.5
EXP15_PCT	5.56	0.18	2.8±0.2	28.0±2.0	300-420	1.5
EXP16_PCT	11.12	0.09	2.8±0.2	28.0±2.0	300-420	1.5
EXP17_PCT	11.12	0.13	2.8±0.2	28.0±2.0	300-420	1.5
EXP18_PCT	11.12	0.18	2.8±0.2	28.0±2.0	300-420	1.5

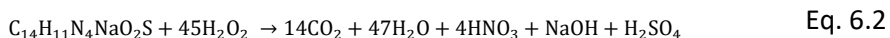
Then, a new target compound, the sulfaquinoxaline sodium salt (SQX, $C_{14}H_{11}N_4NaO_2S$), was used for validating the novel modelling approach that was proposed for the PCT.

The aim was proving that the proposed methodological approach allows obtaining a generalizable solution that can be used to describe the photo-Fenton degradation of any kind of target compound.

In this case, to estimate the kinetic constants of the relative degradation mechanism, a set of six experiments, three Fenton (dark conditions) and three photo-Fenton (irradiated conditions), was performed.

The initial concentrations of SQX was fixed to 25.00 mg L⁻¹ corresponding to 0.08 mmol L⁻¹ and to an initial concentration of TOC, [TOC]⁰= 13.72 mg L⁻¹. The initial concentration of ferrous ion was also fixed and set to 0.18 mmol L⁻¹. Conversely, the initial concentration of hydrogen peroxide was varied.

Again, a 2² factorial design was applied. The initial concentration of hydrogen peroxide was varied between the stoichiometric value (3.47 mmol L⁻¹, as minimum factorial value, -1) to achieve total mineralization of 0.08 mmol L⁻¹ of SQX (according to the stoichiometric reaction shown in Equation (6.2)) and one and half times (5.24 mmol L⁻¹, as central factorial value, 0) and twice (6.94 mmol L⁻¹ as maximum factorial value, +1) such value.



The resulting design of experiment in the case of SQX is shown in Table 6.3 in which all the specific conditions (pH, T, λ, and V_{IRR}) of the experiments that were performed, are reported. Especially, the experiments from EXP1_SQX to EXP3_SQX, are the experiments performed under dark conditions while those from EXP4_SQX to EXP6_SQX, are the ones performed under irradiated conditions.

In addition, as for PCT, a set of five preliminary standard blank assays was performed in order to check the possible direct photolysis of SQX (BLANK ASSAY 14 in Table 6.3). The role of Fenton reagents under both dark (BLANK ASSAY 10 and 11 in Table 6.3) and irradiated conditions (BLANK ASSAY 12 and 13 in Table 6.3) was investigated as well.

Table 6.3. Design of experiments comprising the assays using SQX (C₁₄H₁₁N₄O₂S) as target compound

Design of experiments performed for an initial SQX concentration of [SQX]⁰= 0.08 mmol L⁻¹ corresponding to an initial TOC concentration of [TOC]⁰= 13.72 mg L⁻¹

Non-conventional kinetic study

ID	[H ₂ O ₂] ⁰ mmol L ⁻¹	[Fe ²⁺] ⁰ mmol L ⁻¹	pH	T °C	λ nm	V _{IRR} L
BLANK_10	6.94	0.00	2.8±0.2	28.0±2.0	300-420	0.0
BLANK_11	0.00	0.18	2.8±0.2	28.0±2.0	300-420	0.0
BLANK_12	6.94	0.00	2.8±0.2	28.0±2.0	300-420	1.5
BLANK_13	0.00	0.18	2.8±0.2	28.0±2.0	300-420	1.5
BLANK_14	0.00	0.00	2.8±0.2	28.0±2.0	300-420	1.5
EXP1_SQX	3.47	0.18	2.8±0.2	28.0±2.0	300-420	0.0
EXP2_SQX	5.24	0.18	2.8±0.2	28.0±2.0	300-420	0.0
EXP3_SQX	6.94	0.18	2.8±0.2	28.0±2.0	300-420	0.0
EXP4_SQX	3.47	0.18	2.8±0.2	28.0±2.0	300-420	1.5
EXP5_SQX	5.24	0.18	2.8±0.2	28.0±2.0	300-420	1.5
EXP6_SQX	6.94	0.18	2.8±0.2	28.0±2.0	300-420	1.5

Finally, the modelling approach was validated using a third model compound, the formic acid (FA, CH₂O₂). In this case, a set of four experiments, two Fenton

(dark conditions) and two photo-Fenton (irradiated conditions), was performed.

The initial concentrations of FA was fixed to 40.00 mg L⁻¹ corresponding to 0.87 mmol L⁻¹ and to an initial concentration of TOC, [TOC]⁰= 10.43 mg L⁻¹. The initial concentration of ferrous ion was also fixed and set to 0.09 mmol L⁻¹. Conversely, the initial concentration of hydrogen peroxide was changed between the stoichiometric value (0.88 mmol L⁻¹) to achieve total mineralization of 0.87 mmol L⁻¹ of FA (according to the stoichiometric reaction shown in Equation (6.3)) and twice (1.76 mmol L⁻¹) such value.



Additionally, another photo-Fenton experiment was performed by increasing the initial concentrations of ferrous ion and hydrogen peroxide to 0.18 mmol L⁻¹ and 4.41 mmol L⁻¹, respectively, so to test the effect of higher concentrations of the Fenton reagents.

The resulting design of experiment in the case of FA is shown in Table 6.4 in which are reported all the specific conditions (pH, T, λ, and V_{IRR}) of the experiments that were performed. Especially, the experiments from EXP1_FA to EXP2_FA, are the experiments performed under dark conditions while those from EXP3_FA to EXP5_FA, are the ones performed under irradiated conditions.

Table 6.4. Design of experiments comprising the assays using FA (CH₂O₂) as target compound

Design of experiments performed for an initial FA concentration of [FA]⁰= 0.87 mmol L⁻¹ corresponding to an initial TOC concentration of [TOC]⁰= 10.43 mg L⁻¹

ID	[H ₂ O ₂] ⁰	[Fe ²⁺] ⁰	pH	T	λ	V _{IRR}
	mmol L ⁻¹	mmol L ⁻¹		°C	nm	L

Non-conventional kinetic study

EXP1_FA	0.88	0.09	2.8±0.2	28.0±2.0	300-420	0.0
EXP2_FA	1.76	0.09	2.8±0.2	28.0±2.0	300-420	0.0
EXP3_FA	0.88	0.09	2.8±0.2	28.0±2.0	300-420	1.5
EXP4_FA	1.76	0.09	2.8±0.2	28.0±2.0	300-420	1.5
EXP5_FA	4.41	0.18	2.8±0.2	28.0±2.0	300-420	1.5

All the experiments were performed during 120.0 min in batch mode with recirculation and ensuring perfect mixing conditions by setting the recirculation flowrate to 12.0 L min⁻¹.

Particularly, pH was continuously monitored in order to ensure that it was inside the range (2.5<pH< 3.0-4.0) that, according to Pignatello, 1992, Pignatello et al., 1999, and Pignatello et al., 2006, avoids iron precipitation and ensures the reduction of Fe³⁺ to Fe²⁺ (Fenton-like reaction) at an appreciable rate. Temperature was also continuously monitored and it was checked that was inside the range T= 28.0 ±2.0 °C.

Regarding the experimental protocol, the glass reservoir was first filled with 10.0 L of deionised water and then, after 10.0 min of recirculation, 4.9 L of deionised water in which the model contaminant was previously dissolved, were added and recirculated during 15.0 min with the aim of ensuring a good homogenization of the matrix. After that, a sample was taken to measure the initial concentrations of TOC and the target compound. Then, after the pH was adjusted to 2.8±0.2, the remaining 0.1 L of deionised water, in which Fe²⁺ was previously dissolved, were filled. After 10.0 min more of recirculation, another sample was taken with the aim of checking the initial concentration of the iron species ([Fe²⁺]⁰, [Fe³⁺]⁰, [Fe^{TOT}]⁰). Finally, in case of performing photo-Fenton experiments, the light was switched on 10.0 min before starting the experiment in order to allow the lamp to stabilize. The final step

is the addition of hydrogen peroxide that makes the experiments to start and that was added manually and all the once.

6.3 Model development

The aim of the developed model is to obtain a rationally simplified, but easily configurable and generally usable approach that can be applied in different wastewaters systems containing single or multiple targets. Hence, the photo-Fenton degradation of the target compound and of the oxidant was taken into account together with the TOC evolution, being the latter a lumped parameter that is used to define the overall quality of the water.

The modelling hypotheses of the proposed simplified First Principle Approach are listed below:

H1: Definition of a Fenton system, initiated by mixing H_2O , H_2O_2 , and Fe^{2+} , and described by a set of kinetic reactions involving these compounds, as well as Fe^{3+} , O_2 , free radicals (at least HO^\bullet and HO_2^\bullet) and ions (at least H^+ and OH^-).

H2: Introduction of an additional general reaction for the generation of HO^\bullet in the lighted photo-Fenton system.

H3: A fictitious first order reaction model was used to describe the inefficient reactions of the free radicals.

H4: The simplified general degradation mechanism of targeted organic compounds and of their fragments may be interpreted as the series of consecutive breakage steps, comprising second order binary reaction of the target and its fragments with free radicals. The number of these steps is formally (and algorithmically) determined by the number of carbon atoms in the molecule to be decomposed. It was assumed that in the decomposition steps the targeted compounds and their fragments interact basically with free radical HO^\bullet (main oxidant specie) as also proposed by other authors [e.g.(Conte et al., 2012)].

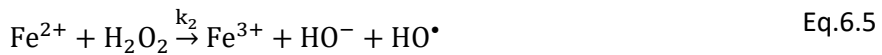
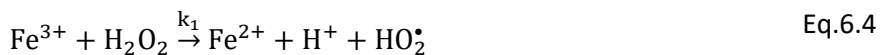
H5: it was supposed a faster initial rate of the degradation mechanism based on the hypothesis that the by-products are more hardly degradable than the parent compound.

H6: it was assumed that the concentration of the TOC can be calculated from the fictitious number of carbon atoms in the fragments originating from the parent compound. The number of fragments depends on the number of carbon atoms in the starting molecule.

H7: In order to avoid infeasible stiffness that can be generated by the competitive reactions (e.g. of the different components with HO•) proportional rates, normalized by the summarized rate of the reactions competing for radical (HO•) were assumed.

Accordingly the hypotheses based simplified principles can be summarized as follows:

P1: the target invariant free radical production of Fenton process is described by the H₂O₂ driven Fe reaction cycle:



P2: the target invariant light initialized free radical production of photo-Fenton process was described as follows:



The kinetic parameter k_0 of photo-Fenton reaction was determined in line with data of Cabrera Reina et al., 2012 who proposed the following reaction scheme explicitly containing the UV irradiance (I):

$$r_0 = k_0 [\text{Fe}^{3+}] I \quad \text{Eq.6.7}$$

P3: the inefficient reaction of the free radicals HO^\bullet was described by a fictitious first order reaction, heuristically introduced:

$$r_{\text{elimination}}: \frac{\Delta[\text{HO}^\bullet]}{\Delta t} = -k_{\text{elimination}} [\text{HO}^\bullet] \quad \text{Eq.6.8}$$

Kinetic parameter $k_{\text{elimination}}$ is to be identified and validated.

In addition, there is an evident auxiliary equilibrium reaction:



which was calculated according to the controlled pH and for a pH= 2.8 the change for $[\text{H}^+]$ resulted in $1.6\text{E}-3 \text{ mol L}^{-1}$.

P4: the degradation mechanism of targeted compounds (T) and their fragments (FR) was described by the series of consecutive breakage steps, comprising second order binary reaction of the target and its fragments with free radicals HO^\bullet . The number of these steps is formally (and algorithmically) determined by the number of carbon atoms in the molecule to be decomposed, as follows:



Therefore, the reaction rate can be calculated as follows:

$$\frac{d[\text{FR}_b]}{dt} = 2r_{b-1} - r_b = 2 [\text{FR}_{b-1}][\text{HO}^\bullet]k_{b-1} - [\text{FR}_b][\text{HO}^\bullet]k_b \quad \text{Eq.6.12}$$

with the initial conditions $[\text{FR}_0] = [\text{T}]$ and $[\text{FR}_b] = 0$

while $b = 1, 2, \dots, B$, and B is the number of the consecutive breakage steps, which can be calculated from the number of carbon atoms NC according to constraints:

$$B-1 < \log_2 NC \leq B \quad \text{Eq.6.13}$$

P5: it was assumed that breakage steps can be characterized by two, target specific parameters, as follows:

$k_{\text{target}} = k_0$ ($b = 0$) for the first breakage step of the targeted compound, and

$k_{\text{fragment}} = k_b$ ($B = 1, 2, \dots, B$) for all following fragmentation steps.

The target specific, temperature dependent parameters k_{target} and k_{fragment} have to be estimated and validated for the various targets, individually.

P6: the concentration of the TOC was calculated from the fictitious number of carbon atoms FNC_b in the subsequent fragments FR_b . The fictitious number of carbon atoms were calculated using the number of carbon atoms in the starting molecule, as follows:

$$FNC_b = NC/2^b; \quad b = 0, 1, 2, \dots, B \quad FNC_0 = T \text{ (target)} \quad \text{Eq.6.14}$$

The approximate concentration of TOC can be calculated from these values as follows:

$$[TOC] = \sum_{b=0}^B FNC_b c_b \quad \text{Eq.6.15}$$

Where c_b is the concentration of each of the produced fragment.

P7: As a robust solution the modified, proportional rates, normalized by the summarized rate of the reactions, competing for radical (HO^*) were described as follows:

$$r_{i,\text{mod}} = \frac{r_i}{r_{\text{elimination}} + \sum_{b=0}^B r_b} * r_i \quad \text{Eq.6.16}$$

where the inefficient reactions of the free radicals HO^\bullet ($r_{\text{elimination}}$ according to P3) also participate in this competition.

Hence, the developed model presents two main steps: a core mechanism (Fenton, photo-Fenton, and inefficient reactions of the free radicals, defined by hypothesis H1, H2, and H3 and described by Equations (6.4)-(6.8) and a general contaminant degradation mechanism (usable for different target compounds, defined by hypothesis H4, H5, H6 and described by Equations (6.10)-(6.15)).

6.4 Implementation of Programmable Structures

The non-conventional methodology named Direct Computer Mapping (DCM) (Csukás et al., 1999), (Csukás et al., 2013) based Programmable Structures (Varga et al., 2017), (Varga and Csukas, 2017) was applied for modelling and simulation based analysis of the experimental system. The method has been already tried and validated for dynamic simulation based analysis of multi-scale, hybrid processes in a broad range of applications (from cellular signaling based biosystems to agri-food and environmental process systems (Varga et al., 2016), (Varga et al., 2017).

Particularly, in the present work, in order to follow the real hydro-dynamical conditions as well as to support possible future scaling-up of the process, it was assumed to consider the compartmentalization of the pilot plant into a circular set of four parts:

- compartment [1] the tank reactor of 9.00 L, where the H_2O_2 reactant is fed and mixed with the previously mixed solution of the target compound and Fe^{2+} ;
- compartment [2] of 2.25 L, connecting compartments [1] and [3];
- compartment [3] of 1.50 L, representing the irradiated volume of the annular reactor;

- compartment [4] of 2.25 L, connecting compartments [3] and [4].

Particularly it must be noted that:

- The compartment [1] is associated with the feeding of H_2O_2 that was taken into account although during the experiments the hydrogen peroxide was added all at once, because it was observed that short term dosage of H_2O_2 better fits the experimented behavior of the system;
- The reaction in Equation (6.6) was taken into account only in the compartment [3] which is the only one associated with the irradiated volume of the pilot plant;
- All the other reactions were taken into account in the whole set of compartments ([1]-[4]).

The Direct Computer Mapping based Programmable Structures methodology is implemented in declarative, logical programming, and supports the easy generation of various model structures from the description of a network and from two general functional meta-prototypes.

The main feature of this technique consists of building the process model from unified state (describing the actual state of the process) and transition (describing the actual transformations, transportations and rules) elements, executing the local programs, described in the respective prototype elements.

In the actual model implementation the following state and transition prototypes were defined:

- two state prototypes: one for the general Fenton components (core mechanism) and another one for the target related components (a general contaminant degradation mechanism) including a total of 10 state elements;
- six transition prototypes: one for the Fenton system (Equations (6.4) and (6.5)), one for photo-Fenton reaction (Equation (6.6)), one for pH related dissociation equilibrium of water (Equation (6.9)), one for target decomposition (Equations (6.10)-(6.15)), one for H_2O_2 feeding and for recirculation of the water ensured by a recycle pumping between the compartments.

Figure 6.2 presents the programmable structure that was generated for the specific case study of PCT and starting from the general state and transition meta-prototypes (see e.g. in Varga et al., 2017).

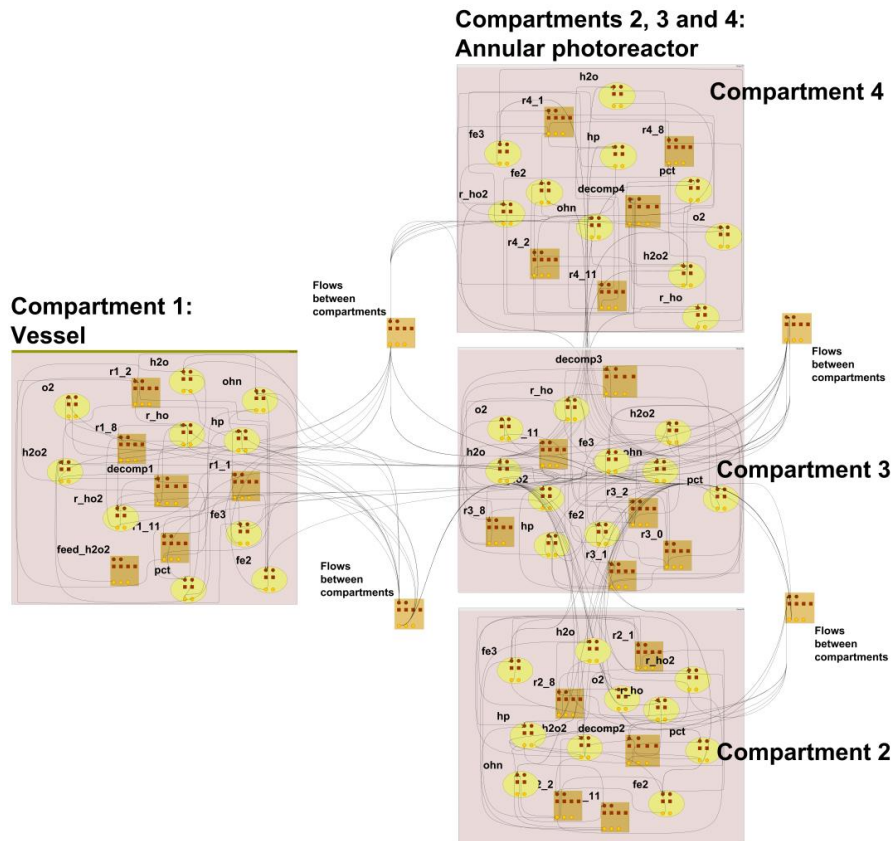


Figure 6.2. The generated structure (the expert interface) of the model, specific for PCT

All the specific state elements and transition elements are summarized in Table 6.5:

Table 6.5. The state and transitions elements defined for the generated structure of the model

10 STATE ELEMENTS

Symbolic notations used in the model	Description
[fe2]	Fe ²⁺
[fe3]	Fe ³⁺
[hp]	H ⁺
[ohn]	OH ⁻
[h2o]	H ₂ O
[h2o2]	H ₂ O ₂
[r_ho]	HO [•]
[o2]	O ₂
target_compound	Actually used organic compound
f1, f2, f3, ...fB	Fragments

6 TRANSITION ELEMENTS

Symbolic notations used in the model	Description
---	--------------------

Advanced Oxidation Process Models for Optimisation and Decision Making support in Water Management

trans	Fenton reactions (Equations (6.4)-(6.5))
photo	Photo-Fenton reaction (Equation (6.6))
phcont	pH related dissociation equilibrium of water (Equation (6.9))
decomp	Target decomposition (Equations (6.10)-(6.15))
feed_h2o2	Feeding of H ₂ O ₂
pump1, pump2, pump3, pump4	Recycle pumping between the compartments

It must be noted that the target molecule and the modeled fragments generating from it contribute to the TOC value.

The generated expert interface (Figure 6.2) needs to be initialized and programmed where:

- The programming is the action of providing copies of the meta-prototypes to prepare the model specific prototypes, containing the local programs, called by the state and transition elements.
- Initialization means the determination of the initial values and optional parameters for the actual state and transition elements, as well as to declare references for the respective prototypes via the GraphML interface. Nevertheless, the initialization can also be modified through a case specifically generated (Excel based) user interface. Starting from the programmed and initialized structure, the general modules of the DCM/PS kernel generate and execute the actualized program, while the results appear in the (Excel based) user interface.

6.5 Results and discussion

Once the model was formulated and the experimental designs were proposed for the selected model compounds, it was possible to proceed to the model training and validation step.

First, the estimation of the kinetic parameters of the core mechanism was carried out by using the data of the blank assays performed without target compounds.

Then, the model was trained and validated by using PCT as target compound.

Finally the methodology was validated by estimating the kinetic parameters of the specific degradation mechanisms of the other targets by using the proper experimental data set.

In the following sections, illustrative examples of the simulation results compared with experimental data are presented in the case of the core mechanism (using the experimental data obtained performing the assays without target compound) and for each of the three selected targets and resulting values of the Root Mean Square Errors (RMSEs) are reported.

Particularly, the root mean square errors (RMSEs) were calculated by the following expression:

$$RMSE_i = \sqrt{\sum_k (y_{ik} - y_{ik}^*)^2 / n_i}$$

root mean square error of the i^{th} variable

y_{ik} , value of the k^{th} measurement of the i^{th} variable

y_{ik}^* , value of the k^{th} estimation of the i^{th} variable (model prediction)

$i = 1, 2, \dots, I$, i^{th} element of the set of measured variables

The only measurements considered are the normalized concentration of the model components: target compound, TOC, and H_2O_2 ($I=3$).

6.5.1 Estimation of the kinetic parameters of the general core mechanism (Fenton, photo-Fenton, and inefficient reactions of the free radicals)

In this step, the kinetic parameters k_0 , k_1 , k_2 , and $k_{elimination}$ of reactions in Equations (6.6), (6.4), (6.5) and (6.8), respectively, were determined by using the experimental data of the assays performed without target compounds (BLANK_1-4, Table 6.1).

As initialization values for k_0 , k_1 and k_2 the ones available in literature were adopted. Conversely, $k_{elimination}$ was set as a free parameter to be estimated.

Especially:

- The initialization value for k_1 was adopted from Simunovic et al., 2011 referring to a range $k_2=63.0-76.0\text{ L mol}^{-1}\text{ s}^{-1}$;
- The initialization value for k_2 was adopted from Walling and Goosen, 1973 referring to a range $k_2=0.1-11.7\text{ L mol}^{-1}\text{ s}^{-1}$;
- The initialization value for k_0 was calculated from Cabrera Reina et al., 2012 using Equation (6.7) and considering in our case second time units and $I=36\text{ W m}^2$.

The final estimated values of the kinetic parameters are reported below:

Table 6.6. Estimated values of the kinetic parameters of the core mechanism (Fenton, photo-Fenton, and inefficient reactions of the free radicals)

k_0, s^{-1}	$k_1, \text{L mol}^{-1}\text{ s}^{-1}$	$k_2, \text{L mol}^{-1}\text{ s}^{-1}$	$k_{elimination}, \text{s}^{-1}$
5.6E-2	50.0	62.0	7.5E-2

The following Figure 6.3 shows the comparison between measured and calculated results of hydrogen peroxide, obtained for the blank experiments without any target compound, named BLANK_3 and BLANK_4 (Table 6.1) referring to dark and irradiated conditions, respectively.

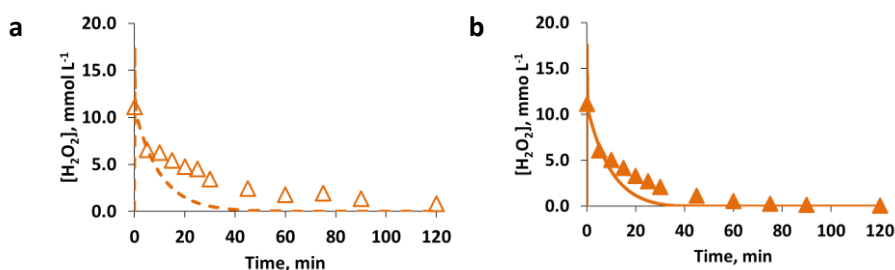


Figure 6.3. Evolution of measured (symbols) and calculated (line) concentrations of hydrogen peroxide in case of blank experiments performed without target compound ($[\text{Fe}^{2+}]^0 = 0.18 \text{ mmol L}^{-1}$, $[\text{H}_2\text{O}_2]^0 = 11.12 \text{ mmol L}^{-1}$), under **a**) dark (empty symbol and dashed line) conditions and **b**) irradiated (solid symbol and solid line).

As can be observed from the experimental results in Figure 6.3, the use of radiation determines a small, but characteristic increase of hydrogen peroxide consumption (e.g. after 10.0 min, in case of using radiation a 55% H₂O₂ consumption was observed, conversely a 44% consumption was experimented under dark conditions). The proposed mechanism core, with the relative estimated kinetic parameters, is able to describe this behavior even if it slightly overestimates the H₂O₂ consumption

The RMSEs resulted in 22.74% and 12.10% in the case of dark and irradiated conditions, respectively.

6.5.2 Estimation of the kinetic parameters of the degradation mechanism for the first target compound (PCT)

In this step two kinetic parameters needed to be estimated, namely

- $k_{\text{target}}^{\text{PCT}}$ [L(mmol s)⁻¹] for the first degradation step of the target compound;
- $k_{\text{fragments}}^{\text{PCT}}$ [L(mmol s)⁻¹] for the following degradation steps of the fragments.

Conversely, the kinetic parameters of the core mechanisms (k_0 , k_1 , k_2 and $k_{\text{elimination}}$) were assumed equal to those estimated in the previous step and presented in Table 6.6.

The parameter estimation was carried out using a subset of the experiments reported in Table 6.2, or rather: EXP1_PCT, EXP4_PCT, EXP5_PCT, EXP9_PCT, EXP10_PCT, EXP13_PCT, EXP14_PCT, and EXP18_PCT. The remaining experiments were used for model validation.

It must be noticed that, the parameter estimation strategy was tuned in order to give priority to a best fitting of TOC and H₂O₂ rather than the target. This hypothesis was assumed due to the importance of describing the evolution of the TOC as a lumped parameter that gives an indication of the water quality in concordance with the main aim of developing a model that can be applied in different wastewaters systems containing single or multiple targets.

The specific PCT degradation mechanism and the estimated values of the relative kinetic parameters are summarized in the following Table 6.7.

Table 6.7. Degradation mechanism and estimated values of the relative kinetics for
PCT



Degradation mechanism

Formal fragmentation	8→4→2→1
TOC value	TOC= 8·c ₁ +4·c ₂ +2·c ₃
Number of carbon atoms, NC	NC= 8
Number of the consecutive breakage steps, B	B= 4

Target specific model parameters

$$k_{\text{target}}^{\text{PCT}} = 1.50\text{E}3 \text{ L mol}^{-1}\text{s}^{-1}$$

$$k_{\text{fragments}}^{\text{PCT}} = 0.15\text{E}3 \text{ L mol}^{-1}\text{s}^{-1}$$

As can be observed by the estimated values of the kinetic parameters in Table 6.7, the rate of the first degradation step resulted of one order magnitude higher than the rate of the subsequent degradation steps.

An illustrative case of the model training carried out using EXP4_PCT and EXP_13_PCT (see Table 6.2) is shown in Figure 6.4. Specifically, the comparison of the simulated and measured data for the different model components (PCT, TOC, H₂O₂) obtained in the case of using [PCT]⁰= 0.26 mmol L⁻¹; [Fe²⁺]⁰= 0.09 mmol L⁻¹; [H₂O₂]⁰= 5.56 mmol L⁻¹ under dark and irradiated conditions, respectively, is reported.

Advanced Oxidation Process Models for Optimisation and Decision Making support in Water Management

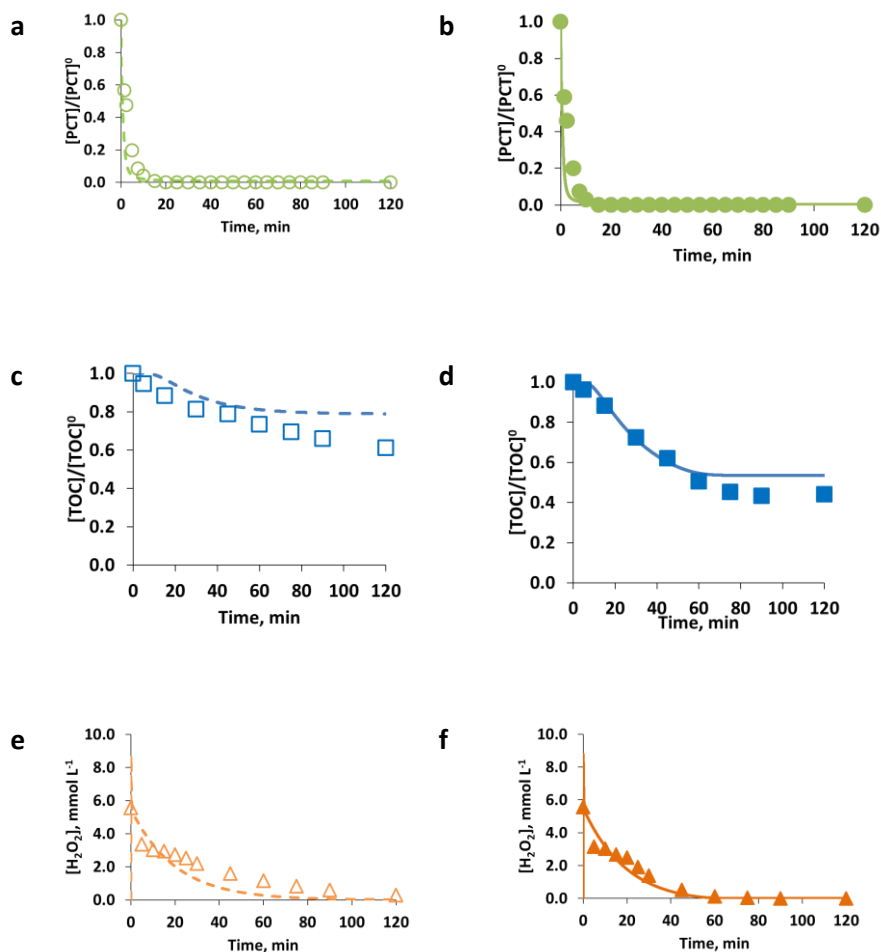


Figure 6.4. Model training results: Comparison of measured (symbols) and simulated (lines) values of PCT (circle, **a and b**), TOC (square, **c and d**) presented as normalized values, and H₂O₂ (triangle, **e and f**) presented as concentration values (mmol L⁻¹), obtained for [PCT]⁰= 0.26 mmol L⁻¹; [Fe²⁺]⁰= 0.09 mmol L⁻¹; [H₂O₂]⁰=5.56 mmol L⁻¹ under dark (empty symbols and dashed lines, **a, c, e**) and irradiated (solid symbols and lines, **b, d, f**) conditions

Model results in terms of PCT concentrations show a similar behavior under dark and irradiated conditions, as also shown by experimental results. Particularly, modelling and experimental results showed a fast initial

stepwise degradation of PCT that slows down later on by the decreased Fe^{3+} concentration and finally it decays below the HPLC detection limit in about 15.0 min under both dark and irradiated conditions.

On the other hand, the effect of radiation was more evident by observing the TOC mineralization.

Particularly, experimental results of the assay performed under irradiated conditions show that after 30.0 min a 28% TOC conversion was reached, conversely, under dark conditions only 19% TOC conversion was attained.

The model is able to represent this behavior: under irradiated conditions and after 30.0 min of reaction the model estimates a TOC conversion of 29%, while under dark conditions TOC conversion after 30.0 min resulted to be 12%.

Moreover, despite the greater differences can be observed during the first steps of the reaction, the radiation allowed attaining also an enhancement of the final TOC conversion. Under dark conditions, it was possible to attain a maximum TOC conversion of 39%, on the contrary, the use of radiation led to a final TOC conversion of 56%.

The model can describe also this behavior and in fact calculates a final TOC conversion of 22% in case of dark conditions and of 47% in case of irradiated conditions.

Finally, Figure 6.4-f shows that the similar results in terms of H_2O_2 consumption were observed under dark and irradiated conditions and this behavior was well described by the model. In this case, under dark conditions and after 10.0 min of reaction, the model estimates a 40% H_2O_2 consumption against a 46% real H_2O_2 consumption. Conversely, under irradiated conditions, the model estimates a 43% H_2O_2 consumption against a 45% real H_2O_2 consumption.

Moreover, for the sake of completeness, an illustrative example of the fragments evolution is presented in Figure 6.5. The latter shows the simulated values of the fragments concentrations compared with the simulated evolution of PCT and TOC concentration in the case of EXP13_PCT or rather in the case of using $[\text{PCT}]^0 = 0.26 \text{ mmol L}^{-1}$; $[\text{Fe}^{2+}]^0 = 0.09 \text{ mmol L}^{-1}$;

$[\text{H}_2\text{O}_2]^0 = 5.56 \text{ mmol L}^{-1}$ and irradiated conditions. We did not measure the intermediates formed during the reactions, however the sum of the PCT and fragments concentrations multiplied by the proper number of carbon atoms gives the simulated value of TOC, which is then compared with the experimental data of TOC concentrations.

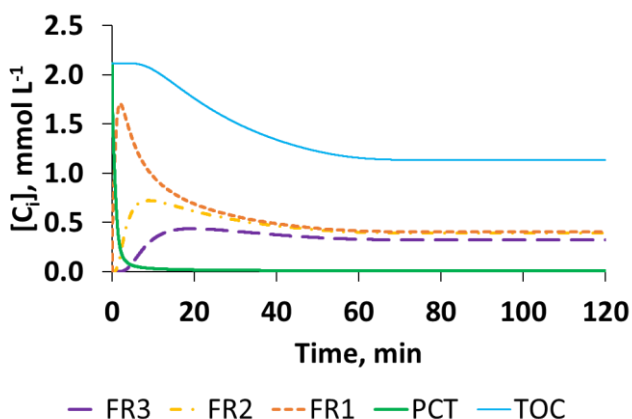


Figure 6.5. Simulated concentrations of the TOC, PCT and of the fragments originating from PCT (C_i , $i = \text{PCT, TOC, FR1, FR2, FR3}$, expressed as mmol L^{-1}) in the case of using $[\text{PCT}]^0 = 0.26 \text{ mmol L}^{-1}$; $[\text{Fe}^{2+}]^0 = 0.09 \text{ mmol L}^{-1}$; $[\text{H}_2\text{O}_2]^0 = 5.56 \text{ mmol L}^{-1}$ and irradiated conditions.

Regarding the fragments evolution, it can be seen that the fragments concentration after a first rapid increase starts to decrease and then reaches an asymptotic value. Particularly, after 120.0 min of reaction fragments FR1, FR2 and FR3 reach a constant concentration of about 0.10, 0.19 and 0.32 mmol L^{-1} , respectively.

Finally, an illustrative case of the model validation carried out using EXP6_PCT and EXP15_PCT experiments (see Table 6.2) is presented in Figure 6.6. Specifically, the comparison of the simulated and measured data for the different model components (PCT, TOC, H_2O_2) obtained in the case of using $[\text{PCT}]^0 = 0.26 \text{ mmol L}^{-1}$; $[\text{Fe}^{2+}]^0 = 0.18 \text{ mmol L}^{-1}$; $[\text{H}_2\text{O}_2]^0 = 5.56 \text{ mmol L}^{-1}$ under dark and irradiated conditions, respectively, is reported.

Non-conventional kinetic study

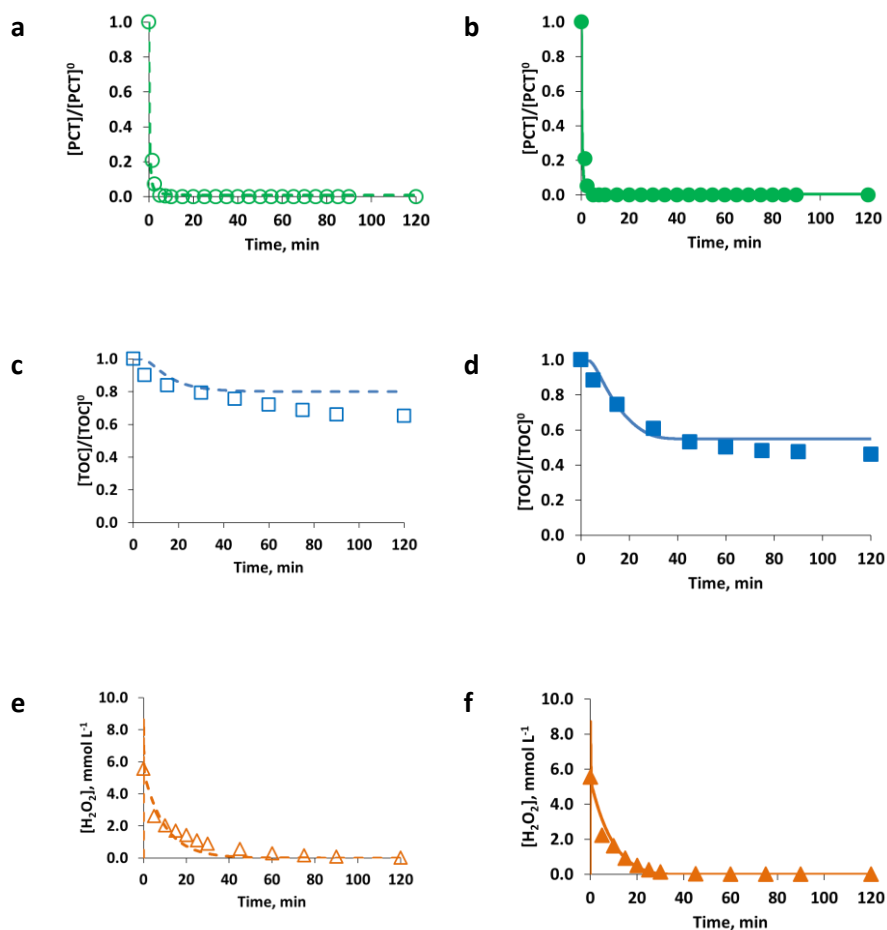


Figure 6.6. Model validation results: Comparison of measured (symbols) and simulated (lines) values of PCT (circle, **a and b**), TOC (square, **c and d**) presented as normalized values, and H_2O_2 (triangle, **e and f**) presented as concentration values ($mmol L^{-1}$), obtained for $[PCT]^0 = 0.26 mmol L^{-1}$; $[Fe^{2+}]^0 = 0.18 mmol L^{-1}$; $[H_2O_2]^0 = 5.56 mmol L^{-1}$ under dark (empty symbols and dashed lines, **a,c,e**) and irradiated (solid symbols and lines, **b,d,f**) conditions

The Root Mean Square Error (NRSME) values that resulted in 30% for PCT, 7% for TOC, and 11% for H_2O_2 , showed the acceptable prediction of the model.

6.5.3 Estimation of the kinetic parameters of the degradation mechanism for the second target compound (SQX)

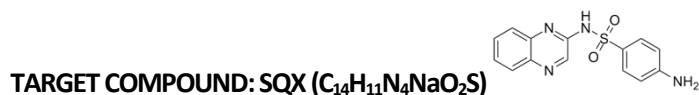
In this step, the experimental data, derived by the assays performed using SQX as model compound, were used to validate the proposed methodology, previously tested with the PCT.

As for the first target, also for SQX the kinetic parameters of the core mechanisms (k_0 , k_1 , k_2 and $k_{\text{elimination}}$) were assumed equal to those previously estimated and shown in Table 6.6, while two kinetic parameters needed to be estimated, namely:

- $k_{\text{target}}^{\text{SQX}}$ [$\text{L}(\text{mmol s})^{-1}$] for the first degradation step of the target compound;
- $k_{\text{fragments}}^{\text{SQX}}$ [$\text{L}(\text{mmol s})^{-1}$] for the following degradation steps of the fragments.

As for PCT, also in this case it was assumed a parameter estimation strategy tuned in order to give priority to a best fitting of TOC and H_2O_2 rather than the target and the specific SQX degradation mechanism and the estimated values of the relative kinetic parameters are summarized in the following Table 6.8.

Table 6.8. Degradation mechanism and estimated values of the relative kinetic for SQX



Degradation mechanism

Formal fragmentation

14→7→3.5→1.75→0.875

TOC value $\text{TOC} = 14 \cdot c_1 + 7 \cdot c_2 + 3.5 \cdot c_3 + 1.75 \cdot c_4$

Number of carbon atoms, NC $\text{NC} = 14$

Number of the consecutive breakage steps, B $\text{B} = 5$

Target specific model parameters

$$k_{\text{target}}^{\text{SQX}} = 0.45\text{E}3 \text{ L mol}^{-1}\text{s}^{-1}$$

$$k_{\text{fragments}}^{\text{SQX}} = 0.35\text{E}3 \text{ L mol}^{-1}\text{s}^{-1}$$

As can be seen, the degradation mechanism is the same however, the number of the consecutive breakage steps changed according to the new number of carbon atoms of the specific molecule to be decomposed.

In this case, the rate of the first degradation step resulted to be similar to the rate of the subsequent degradation steps so showing the formation of intermediate by-products whose degradability is comparable to that of the parent compound.

The degradability of SQX resulted to be obviously less, than the one observed for PCT, because of the greater carbon number, as well as a direct consequence of its structure. Results of TOC and H_2O_2 are presented in the following Figure 6.7 because the main aim was to validate the proposed methodology as a general approach that can be applied in different wastewaters containing single or multiple targets whose quality can be described by a lumped parameter (as it is the TOC).

Hence, the following Figure 6.7 shows the comparison of the simulated and measured data of TOC and H_2O_2 obtained in the case of EXP2_SQX and EXP5_SQX (see Table 6.3). Specifically, these experiments refer to $[\text{SQX}]^0 =$

Advanced Oxidation Process Models for Optimisation and Decision Making support in Water Management

0.08 mmol L⁻¹; corresponding to [TOC]⁰ = 13.72 mg L⁻¹, [Fe²⁺]⁰ = 0.18 mmol L⁻¹; [H₂O₂]⁰ = 5.24 mmol L⁻¹ under dark and irradiated conditions, respectively.

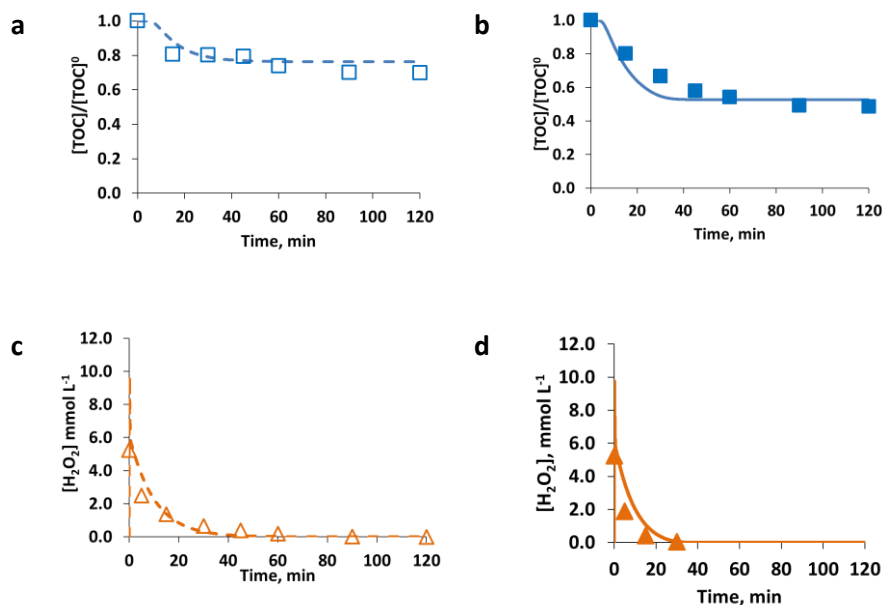


Figure 6.7. Model training results: Comparison of measured (symbols) and simulated (lines) values of TOC (square, **a and b**) presented as normalized values, and H₂O₂ (triangle, **c and d**) presented as concentration values (mmol L⁻¹), obtained for [SQX]⁰ = 0.08 mmol L⁻¹; [Fe²⁺]⁰ = 0.18 mmol L⁻¹; [H₂O₂]⁰ = 5.24 mmol L⁻¹ under dark (empty symbols and dashed lines, **a and c**) and irradiated (solid symbols and lines, **b and d**) conditions

In this case, the enhancement of the process performance promoted by the use of radiation was more evident. In the specific case shown in Figure 6.7, the SQX decayed below the detection limit of the equipment in about 60.0 min under irradiated conditions and in about 90.0 min under dark conditions (experimental results, not shown). Moreover, it can be seen that a 52% final TOC conversion was attained under irradiated conditions conversely a 31% final TOC conversion was reached under dark conditions (experimental results).

Regarding H₂O₂ this was completely consumed under both dark and irradiated conditions, in about 40.0 and 30.0 min, respectively.

The Root Mean Square Error (RSME) values resulting in 17% for SQX, 26% for TOC, 19% for H₂O₂ showed that the model well approximate this system behavior.

The RMSE values slightly increased compared with the previous results obtained using PCT (30% for PCT, 7% for TOC, and 11% for H₂O₂). However, it must be taken into account that a much smaller number of experiments have been used in the case of SQX.

It is important to notice that a minor number of experiments was necessary to validate the model (with SQX) than to train it (with PCT) and this shows a clear advantage of the proposed methodology.

6.5.4 Estimation of the kinetic parameters of the degradation mechanism for the third target compound (FA)

In this step, the experimental data, derived by the assays performed using FA, were used to validate the proposed methodology with a third model compound.

This model compound was selected in order to test the response of the model for the degradation of a very simple molecule. Hence, it represents a different case study than those previously analysed.

First, due to the simplicity of the starting molecule composed by only one carbon atom, it was decided to only follow the TOC evolution, avoiding the HPLC detection of the target. Moreover, for coherence with the methodological approach defined for the first two targets, also in this case it was decided to take into account the attack to the parent compound and the attack to the intermediates originating from it.

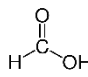
Hence, as for the other targets, also for FA the kinetic parameters of the core mechanisms (k_0 , k_1 , k_2 and $k_{\text{elimination}}$) were assumed equal to those previously estimated and shown in Table 6.6, while the following two kinetic parameters needed to be estimated:

Advanced Oxidation Process Models for Optimisation and Decision Making support in Water Management

- $k_{\text{target}}^{\text{FA}}$ [L(mmol s)⁻¹] for the first degradation step of the target compound
- $k_{\text{intermediates}}^{\text{FA}}$ [L(mmol s)⁻¹] for the following degradation steps of the intermediates

The specific FA degradation mechanism and the estimated values of the relative kinetic parameters are summarized in the following Table 6.9.

Table 6.9. Degradation mechanism and estimated values of the relative kinetic for
FA

TARGET COMPOUND: FA (CH₂O₂) 

Degradation mechanism

Formal fragmentation	1→1
TOC value	TOC= 1·c ₁ +1·c ₂
Number of carbon atoms, NC	NC= 1
Number of the consecutive breakage steps, B	B= 1

Target specific model parameters

$k_{\text{target}}^{\text{FA}} = 0.650 \text{ L mol}^{-1}\text{s}^{-1}$

$k_{\text{intermediates}}^{\text{FA}} = 0.075 \text{ L mol}^{-1}\text{s}^{-1}$

As can be observed, the first step (attack to the parent compound) is characterized by a kinetic parameter of one order magnitude higher than the one describing the subsequent attack to the intermediates originating from the first degradation step. In this case, the parameter estimation suggests that the second degradation step could probably be avoided. However this hypothesis needs to be experimentally confirmed by the evolution of formic acid during the treatment span (HPLC analysis).

The following Figure 6.8 shows the results of TOC and H₂O₂ and particularly the comparison between experimental and simulated data obtained in the case of EXP2_FA and EXP4_FA (see Table 6.4), or rather in the case of [FA]⁰= 0.87 mmol L⁻¹; [Fe²⁺]⁰= 0.09 mmol L⁻¹; [H₂O₂]⁰= 1.76 mmol L⁻¹ under dark and irradiated conditions, respectively.

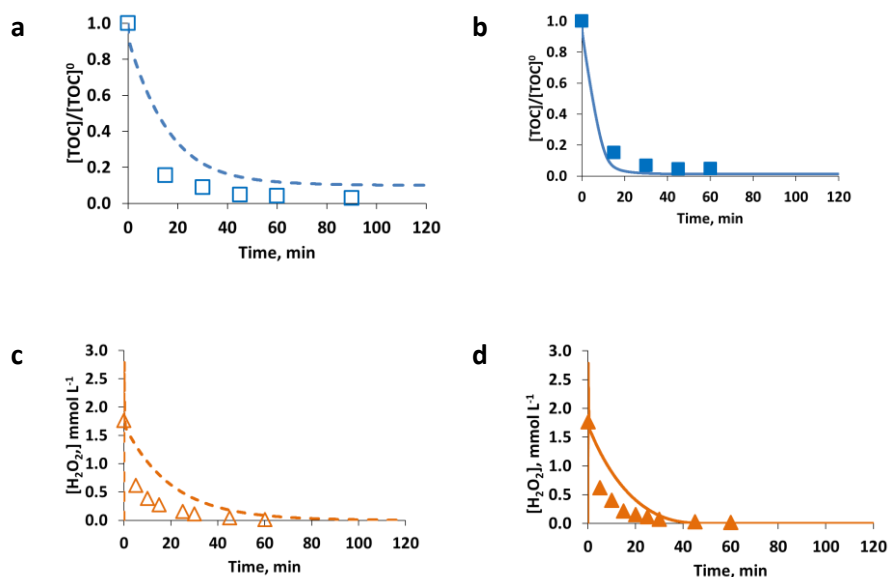


Figure 6.8. Model training results: Comparison of measured (symbols) and simulated (lines) values of TOC (square, **a and b**) presented as normalized values, and H₂O₂ (triangle, **c and d**) presented as concentration values (mmol L⁻¹), obtained for [FA]⁰= 0.87 mmol L⁻¹; [Fe²⁺]⁰= 0.09 mmol L⁻¹; [H₂O₂]⁰= 1.76 mmol L⁻¹ under dark (empty symbols and dashed lines, **a and c**) and irradiated (solid symbols and lines, **b and d**) conditions

As can be observed in Figure 6.8, due to the simplicity of the molecule of the parent compound, the Fenton and photo-Fenton degradation were both very fast. In both cases, experimental results show very similar results starting from the first analysed sample (15.0 min) until the end of the treatment. After 15.0 min, a 80% TOC conversion was attained under both dark and irradiated conditions while a final TOC conversion of about 96% was reached in both cases.

These experimental results suggest that, in order to capture the enhancement due to the use of radiation, more experimental measurements during the first minutes of the reaction, are required. However, the TOC measurements can be performed only each 15.0 min (measuring time of the equipment). Hence, only the detection via HPLC of the target molecule and of the produced intermediates can help to describe the system behavior during the first minutes of the Fenton and photo-Fenton treatment of formic acid.

The model in this case overestimates the enhancement of the process performance due to the use of irradiation, describing the photo-Fenton process as the faster one. This result is probably due, as already observed, to the lack of experimental measurements during the first minutes of the reaction. Moreover, it must be noted that a very low number of experiments (five) was performed to validate the proposed methodology with this third compound.

Finally, also in this case, H_2O_2 is completely consumed under both dark and irradiated conditions in about 45.0 and 60.0 min, respectively.

The Root Mean Square Error (RSME) values resulted in 16% for TOC, 18% for H_2O_2 and highlighted the acceptable prediction of the model.

As can be observed, after the third validation, the RMSE value for TOC decreased while the one related to H_2O_2 remained constant (if compared with the results obtained for the second model compound: 26% for TOC, 19% for H_2O_2) so showing an improvement of the proposed methodology.

Finally, the following Table 6.10 is presented with the aim of summarizing the RMSE values calculated for each of the three model components taken into account (target, TOC, oxidant) and for the three different targets (PCT, SQX, FA).

Table 6.10. RMSE values calculated for each of the three model components taken into account (target, TOC, oxidant) and for the three different targets (PCT, SQX, FA)

ROOT MAIN SQUARE ERROR (NRSME)			
	target compound	TOC	H ₂ O ₂
PCT	30%	7%	11%
SQX	17%	26%	19%
FA	(not measured)	16%	18%

Despite the less number of experiments used to validate the proposed methodology, it was possible to improve the prediction of the target compound. However the RMSE associated with the predictions of TOC and H₂O₂ slightly increased.

The RMSE values although higher than the ones obtained for the conventional modelling approach presented in Chapter 5, can be considered acceptable by considering that a novel approach looking for a generalizable model describing photo-Fenton degradation of various wastewaters that can contain one or multiple target compounds, has been proposed.

6.6 Conclusions

A First Principles Model of medium complexity was proposed and validated for three model compounds, namely PCT, SQX and FA. The model describes the Fenton and photo-Fenton degradation of the model compound as well as TOC and H₂O₂ evolution.

The Direct Computer Mapping based Programmable Structures used to implement the proposed model, showed the following advantages: i) it helped the easy generation and configuration of various model structures in model discovery from the description of a network and from two functional meta-prototypes, ii) it supported the easy and local modification of the locally implementable declarative programs, associated with the state and transition prototypes, and iii) the transition based model representation helped the availability controlled normalized description of competitive fast processes.

The proposed methodology comprises two generally usable modules: i) one for the description of the core mechanism comprising Fenton, photo-Fenton, and the inefficient reactions of the free radicals and another one ii) for the description of the general contaminant degradation mechanism usable for different target compounds.

The module describing the general contaminant degradation mechanism can be algorithmically generated in the knowledge of the carbon number of the target compound, as well as with the knowledge of two kinetic parameters, one for the faster initial rate and the other one describing the subsequent degradation steps.

The Root Mean Square Error (RMSE) values, obtained by validating the methodology with the three different targets, showed the acceptable prediction of the model.

Despite the less number of experiments used to validate the proposed methodology, it was possible to improve the prediction of the target compound and to maintain the prediction of TOC and of the oxidant at acceptable levels.

Hence, the proposed First Principles Model proved to be a causally interpretable and generalized candidate solution for the simulation based analysis and design of photo-Fenton reaction initiated degradation of various wastewaters that can contain one or multiple target compounds (e.g. mixture of organic contaminants).

As further work, the proposed methodology will have to be validated using mixture of organic contaminants. Moreover, another important field of the further work is represented by the modelling of a multi-step fed-batch dosage of H_2O_2 to improve the decontamination ability of the process.

6.7 Acknowledgements

This work was supported by the Spanish “Ministerio de Economía, Industria y Competitividad (MINECO)” and the European Regional Development Fund, both funding the research Project AIMS (DPI2017-87435-R). Francesca Audino, particularly acknowledges the MINECO for the PhD grant [BES-2013-065545].

7 Recipe optimisation

As highlighted in the state of the art section, in the optimisation of batch wise operation of photo-Fenton processes, the hydrogen peroxide dosage strategy plays a crucial role. Because of the activation of inefficient reactions scavenging hydrogen peroxide, the latter represents the most expensive process reactant. Hence, the proposal of proper flexible set of operational conditions (i.e. the recipe) with gradual dosage would allow avoiding or reducing the oxidant consumption.

In the present chapter a systematic dynamic model-based optimisation strategy that takes advantage of the available kinetic models and that is based on both economic and environmental factors, has been explored with

the aim of enabling a practical recipe adjustment in a fast and reliable way, with reduced experimental work.

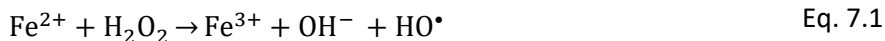
7.1 Introductory perspective

In the last years, research, development and implementation of Advanced Oxidation Processes (AOPs) (Andreozzi et al., 1999), both for industrial and urban wastewaters, have received considerable attention. AOPs have emerged as the only feasible option for the treatment of hardly biodegradable or toxic substances that can resist or damage conventional biological treatments (Oller et al., 2011) and for the treatment of the so-called Contaminants of Emerging Concern (CECs). CECs are a group of chemicals that are being detected in waters in very low concentrations (ng L^{-1} and μL^{-1}) thanks to new and more powerful analytical techniques, and that may be included in future environmental regulations depending on the results of the investigations on their effects on human health and the environment.

Directive 2013/39/EU of the European Parliament and of the Council of 12 August 2013 amending Directives 2000/60/EC and 2008/105/EC tackle the issue of priority substances in the field of water policy, states the importance of CECs monitoring and updates the list of priority substances. According to the European Commission, another important goal will also be the reinforcement of the risk assessment of pharmaceutical products (Ribeiro et al., 2015).

Although AOPs are considered clean technologies for this challenge, they are also expensive due to the consumption of energy and chemical reagents, which increases with treatment time. Hence, the achievement of a practical application of AOPs is required. For that goal, the key issue is the achievement of design and operation approaches providing optimal economic and environmental performance of AOPs.

The photo-Fenton process can be described as an extension of the Fenton process. The Fenton process (Fenton, 1894) occurs by means of addition of hydrogen peroxide to Fe^{2+} salts according to the Equation (7.1):



The photo-Fenton process is based on the use of UV-VIS light irradiation at wavelength higher than 300 nm that allows Fe^{2+} regeneration by the photolysis of Fe^{3+} complexes (Kiwi et al., 1993), (Pulgarin and Kiwi, 1996), as presented in Equation (7.2):



The photo-Fenton process is of added interest among AOPs, for the possibility to develop high efficient and cost effective treatment systems by exploiting solar energy and the combination with biological technologies (Rahim Pouran et al., 2015). Moreover, it has showed to be highly successful for both micropollutants remediation (Miralles-Cuevas et al., 2014) and the treatment of high-strength organic wastewaters (Rahim Pouran et al., 2015). The review by Wang et al., 2016 stressed that the photo-Fenton process has been applied to treat different kinds of wastewaters such as olive-oil mill, textile, pesticide, cosmetic, dye, fermentation brine, green olives, pharmaceutical, cork cooking, pulp mill and phenolic wastewaters.

In the last years a remarkable experimental effort has been made to better understand the photo-Fenton process as a whole. As pointed out in a review by Pignatello et al., 2006, several studies performed at laboratory scale have investigated the role of H_2O_2 consumption, the processing time and the mineralization rate, which are key process efficiency parameters that affect the overall kinetics. Subsequently, Zapata et al., 2010, published an important study, performed at pilot plant scale, evaluating the effect of temperature, dissolved iron concentration, and Dissolved Organic Carbon (DOC) as well as their relationship to such key process efficiency parameters.

More recently, Rahim Pouran et al., 2015 have stressed that a significant number of studies have addressed the investigation of the main factors affecting photo-Fenton performance (percentage of DOC and/or Total Organic Carbon (TOC) removal), such as contaminant loads, Fenton reagents

concentrations, pH and temperature, by the use of multivariate experimental design based on the response-surface methodology.

Conversely, only few studies (Moreno-Benito et al., 2013) have adopted a model-based approach for determining the best operating conditions that can help the development of practical applications.

In the optimisation of batch wise operation of photo-Fenton processes, the hydrogen peroxide dosage strategy plays a crucial role. Experimental results have highlighted the activation of inefficient reactions scavenging hydrogen peroxide, the most expensive process reactant, which can be avoided or reduced by proposing a proper flexible set of operational conditions (i.e. the recipe) with gradual dosage (Yamal-Turbay et al., 2012), (Yamal-Turbay et al., 2013).

According to the literature survey, up until now, the determination of an efficient H_2O_2 dosage profile has been faced mostly following an experimental approach (Prieto-Rodríguez et al., 2011) based on manual H_2O_2 dosing that has led to low process performance or, for control purposes (Ortega-Gómez et al., 2012).

Hence, the main novelty of this work is a systematic dynamic model-based optimisation strategy that takes advantage of kinetic models and enables a practical recipe adjustment in a fast and reliable way, with reduced experimental work and with a novel decision-making focus based on both economic and environmental factors.

The success of an optimisation strategy also depends on the availability of reliable and computationally affordable models.

Regarding photo-Fenton kinetic modelling, two main approaches can be found in literature, such as Empirical Models (Kusic et al., 2006), (Pérez-Moya et al., 2008) that cannot be scaled up and do not address the process dynamics, and First Principles Models (FPMs) (Jeong and Yoon, 2005), (Conte et al., 2012) that are unaffordable even for very simple molecules.

Therefore, a compromise solution was adopted such as the semi-empirical kinetic (shortcut) model by Cabrera Reina et al., 2012 based on simplified photo-Fenton reactions and lumped parameters (for parent compound, intermediates and free radicals). This model was properly adapted to

investigate the effectiveness, efficiency and reliability of a model-based approach in:

- Investigating the interrelations between the main variables that affect the process efficiency, such as processing time, total amount of hydrogen peroxide and final Total Organic Carbon (TOC) removal. Such analysis helps decision making by providing an overview of the best operating conditions, e.g. in terms of total amount of H₂O₂ and processing time to achieve a predetermined final TOC removal.
- Performing the dynamic optimisation of the H₂O₂ dosage profile to drive the process at the minimum processing cost while ensuring operational and environmental constraints such as TOC removal.

The scope of this study is limited to the development of an efficient optimisation strategy for determining the best dosing strategies from a validated and reported model (i.e. (Cabrera Reina et al., 2012)), and further experimental tasks and elaboration of new models is beyond the aim of the work.

To address this problem, a multi-objective optimisation (MO) strategy has been proposed. A direct approach, namely direct simultaneous optimisation method, was applied and developed in the JModelica.org open source platform (Åkesson et al., 2010) for solving the dynamic optimisation problem. Pareto frontiers were built accordingly so that several optimal operating conditions for different treatment configurations can be easily and quickly identified. Besides that, unfeasible operating conditions and unattainable process performances are also recognized and duly mapped.

7.2 Methodological framework and tools

As highlighted in Figure 7.1, the proposed methodology consists of four different steps, such as the kinetic and reactor modelling and the dynamic simulation and optimisation that will be analysed in detail in the following sections.

Advanced Oxidation Process Models for Optimisation and Decision Making support in Water Management

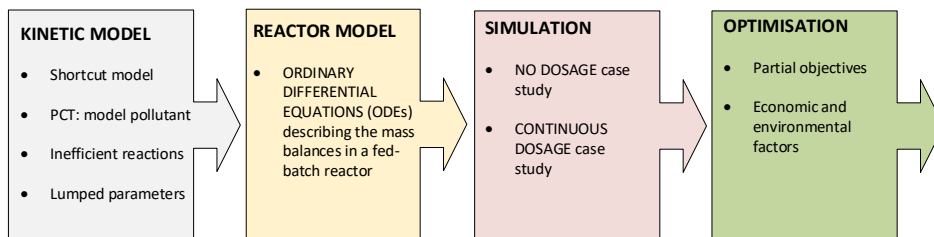


Figure 7.1. Scheme of the proposed methodology consisting of four specific steps: kinetic modelling, reactor modelling, dynamic simulation and dynamic optimisation

7.2.1 Kinetic model and data

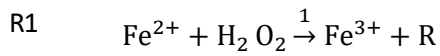
The shortcut model by Cabrera Reina et al., 2012, relying on simplified photo-Fenton process reactions for the prediction of Total Organic Carbon [TOC], hydrogen peroxide [H₂O₂] and dissolved oxygen [DO] concentration evolution, was selected. Cabrera Reina et al., 2012 proposed and fit this model using paracetamol as model pollutant. The model was validated within the following range: a pollutant load range between 4.0 and 25.0 mmol L⁻¹ of TOC, an initial load of Fe²⁺ in a range between 0.09 and 0.44 mmol L⁻¹, an initial H₂O₂ concentration in a range between 9.0 and 45.0 mmol L⁻¹, and a UV irradiance in a range between 13 and 46 W m². Moreover, these authors validated the model also against a new set of experimental data obtained by performing photo-Fenton experiments using an outdoor pilot plant scale for an aqueous solution of a mixture of five commercial pesticides.

The model assumes nine processes and eight states (ferrous and ferric ions Fe²⁺ and Fe³⁺, hydrogen peroxide H₂O₂, free radicals R, dissolved oxygen DO, parent compound M and two partially oxidized organics, such as MX₁ and MX₂). The data and parameter values reported by Cabrera Reina et al., 2012 were also assumed.

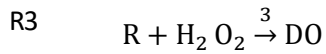
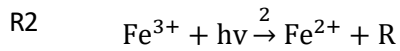
Table 7.1. Kinetic mechanism proposed by Cabrera Reina et al., 2012

ID	Reaction	Description
----	----------	-------------

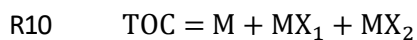
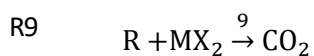
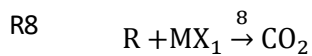
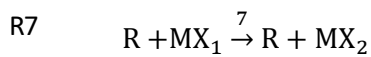
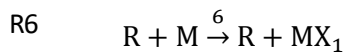
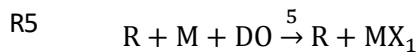
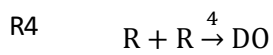
Recipe optimisation



EFFICIENT REACTIONS



INEFFICIENT REACTIONS



The following Figure 7.2 illustrates the simulation of the kinetic model and the capacity to describe the evolution of the concentration of all the components considered ($[\text{C}_i]$ concentration of the generic component i and $[\text{C}_i]^0$ initial concentration of the generic component i).

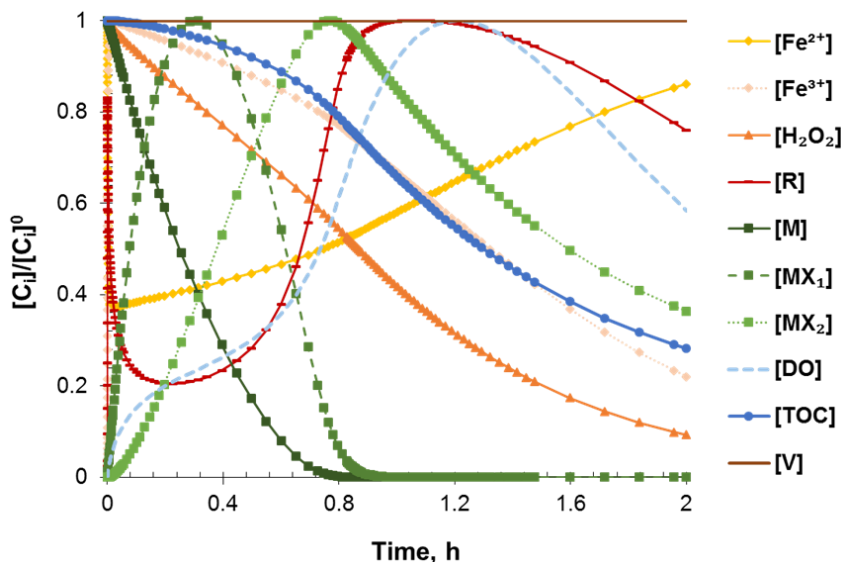


Figure 7.2. Simulation results of the kinetic model proposed by Cabrera Reina et al. (2012) predicting all concentration profiles (initial concentrations are $[H_2O_2]^0 = 35.33 \text{ mmol L}^{-1}$, $[TOC]^0 = 8.33 \text{ mmol L}^{-1}$, $[DO]^0 = 0.21 \text{ mmol L}^{-1}$, $[M]^0 = 8.33 \text{ mmol L}^{-1}$, $[Fe^{2+}]^0 = 0.14 \text{ mmol L}^{-1}$, and zero for the rest)

Especially, such model was selected since it represents an interesting compromise between the complexity of the detailed First Principle Models (Jeong and Yoon, 2005), (Conte et al., 2012) that can ensure rigorousness but at the expense of computational time and the oversimplification of Empirical Models (Kusic et al., 2006), (Pérez-Moya et al., 2008) based on surface response that do not provide information about the process dynamics. Furthermore, the model by Cabrera Reina et al., 2012 was shown to correctly behave for other molecules and mixtures.

The model also allows taking into account the hydrogen peroxide optimisation since it accounts for the inefficient reactions involving H_2O_2 and the free radicals (reactions R3 and R4 in Table 7.1) that lead to an inefficient use of the oxidant, highlighted by an increase in the dissolved oxygen concentration.

In order to check the role of the inefficient reaction $H_2O_2 + HO^\bullet \rightarrow O_2^\bullet$ and of the inefficient reaction $HO^\bullet + HO^\bullet \rightarrow O_2^\bullet$, two additional simulations were

run (based on the same initial concentrations values of the model components) and compared and are shown in Figure 7.3. First, a simulation was run by excluding the inefficient reaction $H_2O_2 + HO^\bullet \rightarrow O_2^\bullet$. Then, only inefficient reaction $HO^\bullet + HO^\bullet \rightarrow O_2^\bullet$ was excluded.

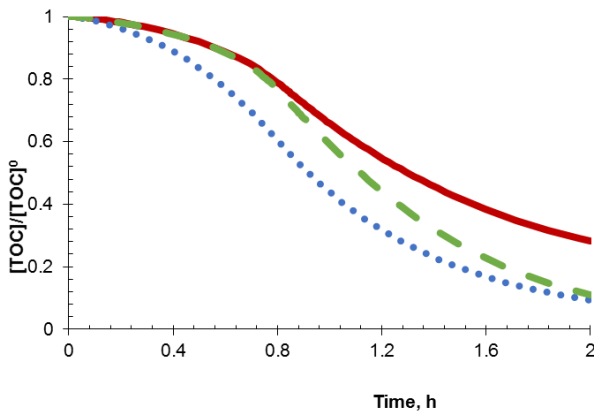


Figure 7.3. Normalized TOC results of three simulations runs **i)** considering the whole set of equations proposed by Cabrera Reina et al. (2012) (solid red line) and disregarding **ii)** only the inefficient reaction $H_2O_2 + HO^\bullet \rightarrow O_2^\bullet$ (dotted yellow line), **iii)** only the inefficient reaction $HO^\bullet + HO^\bullet \rightarrow O_2^\bullet$ (dashed green line)

Figure 7.3 reveals that when the inefficient reaction $H_2O_2 + HO^\bullet \rightarrow O_2^\bullet$ is not considered (dotted yellow line), TOC decreases faster than when the inefficient reaction $HO^\bullet + HO^\bullet \rightarrow O_2^\bullet$ is excluded (dashed green line). This shows that the inefficiency of reaction $H_2O_2 + HO^\bullet \rightarrow O_2^\bullet$ is higher than the inefficiency of reaction $HO^\bullet + HO^\bullet \rightarrow O_2^\bullet$, although both finally converge to a similar performance. As expected, the slowest TOC decrease can be observed for the complete model proposed by Cabrera Reina et al., 2012 (solid red line). This set of simulations reveals once again the deeper insight that can be gained through the exploitation of the kinetic model for facilitating process understanding.

Furthermore, it is also important to notice that an increase in the hydrogen peroxide concentration reduces the process efficiency since it increases the

concentration of radicals [R]. Increasing [R] increases both the rate of oxidation of organic matter and the rate of inefficient production of DO; the latter being more sensitive to [R]. This is modelled by first order efficient reactions (reactions R1 and R2 in Table 7.1, which are linear, $\propto [R]$) and by second order inefficient reactions (reaction R4 in Table 7.1, which is quadratic, $\propto [R]^2$). Thus, while low [R] values favour linear reaction rates over quadratic reaction rates, high [R] values (excess of radicals) favour the rate of inefficient reactions over efficient reactions. The model grasps this trade-off and reveals the subsequent optimisation opportunities.

The use of lumped parameters (for parent compound M, and resulting intermediates, MX_1 and MX_2 , as well as for free radicals R) is also very functional and allows focusing on those easily measurable factors (TOC and DO concentrations, monitored by appropriate sensors), which facilitate the development of real-world applications.

Finally, the selection of paracetamol as model contaminant by Cabrera Reina et al., 2012 has to be acknowledged as a sensible and reported option for preparing recalcitrant synthetic wastewater (Trovó et al., 2008), (Villota et al., 2018). The choice of PCT presents molecular simplicity as well as scarce biodegradability, which favours both the experimental and the modelling tasks.

7.2.2 Reactor model: H_2O_2 Dosage

A reactor model was proposed to consider the H_2O_2 dosage. It is given by a set of Ordinary Differential Equations (ODEs), (Equations (7.3) – (7.12)), describing the mass balances into the fed batch reactor, such as when a reactant dosage is performed:

$$\frac{dV}{dt} = F(t) \quad \text{Eq.7.3}$$

$$\frac{d[H_2O_2]}{dt} = \frac{F(t)}{V} \times ([H_2O_2]^{IN} - [H_2O_2]) - r_1 - r_3 \quad \text{Eq.7.4}$$

$$\frac{d[\text{Fe}^{2+}]}{dt} = \frac{F(t)}{V} \times ([\text{Fe}^{2+}]^{\text{IN}} - [\text{Fe}^{2+}]) - r1 + r2 \quad \text{Eq.7.5}$$

$$\frac{d[\text{Fe}^{3+}]}{dt} = \frac{F(t)}{V} \times ([\text{Fe}^{3+}]^{\text{IN}} - [\text{Fe}^{3+}]) + r1 - r2 \quad \text{Eq.7.6}$$

$$\frac{d[\text{R}]}{dt} = \frac{F(t)}{V} \times ([\text{R}]^{\text{IN}} - [\text{R}]) + r1 + r2 - r3 - (2 \times r4) - r5 - r6 - r7 - r8 - r9 \quad \text{Eq.7.7}$$

$$\frac{d[\text{M}]}{dt} = \frac{F(t)}{V} \times ([\text{M}]^{\text{IN}} - [\text{M}]) - r5 - r6 \quad \text{Eq.7.8}$$

$$\frac{d[\text{MX}_1]}{dt} = \frac{F(t)}{V} \times ([\text{MX}_1]^{\text{IN}} - [\text{MX}_1]) + r5 + r6 - r7 - r8 \quad \text{Eq.7.9}$$

$$\frac{d[\text{MX}_2]}{dt} = \frac{F(t)}{V} \times ([\text{MX}_2]^{\text{IN}} - [\text{MX}_2]) + r7 - r9 \quad \text{Eq.7.10}$$

$$\frac{d[\text{DO}]}{dt} = \frac{F(t)}{V} \times ([\text{DO}]^0 - [\text{DO}]) + (g1_{\text{DO}} \times r3) + (g2_{\text{DO}} \times r4) - (c1_{\text{DO}} \times r5) + (K_{\text{La}} \times ([\text{DO}]^* - [\text{DO}])) \quad \text{Eq.7.11}$$

$$\frac{d[\text{TOC}]}{dt} = \frac{d[\text{M}]}{dt} + \frac{d[\text{MX}_1]}{dt} + \frac{d[\text{MX}_2]}{dt} \quad \text{Eq.7.12}$$

Where:

$$r1 = k_1 [\text{Fe}^{2+}] [\text{H}_2\text{O}_2] \quad \text{Eq.7.13}$$

$$r_2 = k_2 [\text{Fe}^{3+}] [\text{I}] \quad \text{Eq.7.14}$$

$$r_3 = k_3 [\text{R}] [\text{H}_2\text{O}_2] \quad \text{Eq.7.15}$$

$$r_4 = k_4 [\text{R}] [\text{R}] \quad \text{Eq.7.16}$$

$$r_5 = k_5 [\text{R}] [\text{M}][\text{DO}] \quad \text{Eq.7.17}$$

$$r_6 = k_6 [\text{R}] [\text{M}] \quad \text{Eq.7.18}$$

$$r_7 = k_7 [\text{R}] [\text{MX}_1] \quad \text{Eq.7.19}$$

$$r_8 = k_8 [\text{R}] [\text{MX}_1] \quad \text{Eq.7.20}$$

$$r_9 = k_9 [\text{R}] [\text{MX}_2] \quad \text{Eq.7.21}$$

In Equations (7.3)-(7.11), $F(t)$, represents the inlet flowrate (L h^{-1}) that produces a variation in the total volume of the reactor V (L), while $F(t) V^{-1}$ represents the dilution factor due to the continuous addition of hydrogen peroxide solution during reaction time (fed-batch operation).

The symbols $[C_i]^{\text{IN}}$ and $[C_i]$ refer to the concentrations (mmol L^{-1}) in the inlet flowrate and inside the reactor, respectively, for each component. Since the study just considers the hydrogen peroxide dosification, only $[\text{H}_2\text{O}_2]^{\text{IN}}$ is different from zero, while the rest of inlet concentrations are null. Particularly, in all the dosage simulations, a 33% v/w hydrogen peroxide solution was used to calculate $[\text{H}_2\text{O}_2]^{\text{IN}}$ (mmol L^{-1}).

Finally $[\text{DO}]^*$ represents the dissolved oxygen saturation concentration, and $[\text{DO}]^0$ represents the initial dissolved oxygen concentration, both expressed as mmol L^{-1} .

Table 7.2 provides the data given by Cabrera Reina et al., 2012 used in this study:

- the range of the initial concentration for each component ($[C_i]^0$);
- the total and irradiated volume of the reactor (V, V_{IRR});
- the irradiance range ($W\ m^2$);
- the gas–liquid mass transfer coefficient (kla);
- the fitted parameters, such as the kinetic constants (k_1 to k_9) in the reaction rates (r_1 to r_9), and the stoichiometric coefficients ($g_{1DO}, g_{2DO}, c_{1DO}$) in the oxygen balance.

Regarding the values of initial and saturation dissolved oxygen concentrations ($[DO]^0$ and $[DO]^*$), both were set to $0.21\ mmol\ L^{-1}$.

Table 7.2. Kinetic constants, stoichiometric coefficients and initial concentrations ranges by Cabrera Reina et al., 2012

Kinetic parameters ($mmol\ L^{-1}h^{-1}$, with the exception of k_2 expressed as $(W\ m^{-2})^{-1}(mmol\ L^{-1}h^{-1})$ and k_5 expressed as $((mmol\ L^{-1})^2)^{-1}h^{-1}$)								
k_1	k_2	k_3	k_4	k_5	k_6	k_7	k_8	k_9
8.81	5.63	75.8	42798	2643	257	2865	271	107

Stoichiometric coefficients (adimensional except for kla expressed as h^{-1})			
g_{1DO}	g_{2DO}	c_{1DO}	kla
0.75	0.47	0.10	2.70

Advanced Oxidation Process Models for Optimisation and Decision Making support in Water Management

Initial concentrations (mmol L⁻¹) h⁻¹

[Fe ²⁺] ⁰	[Fe ³⁺] ⁰	[H ₂ O ₂] ⁰	[R] ⁰	[M] ⁰	[MX ₁] ⁰	[MX ₂] ⁰	[DO] ⁰	[TOC] ⁰
0.09÷ 0.44	0	9÷ 45	0	4÷ 25	0	0	0.21	9÷ 25

Other parameters

Total volume, V (L)	Irradiated volume, V _{IRR} (L)	Irradiance, I (W m ⁻²)
4.5	2.0	13÷ 46

1* [M]⁰ represents the initial pollutant load expressed as mmol L⁻¹ of TOC, which is equal to the initial concentration of TOC ([TOC]⁰). Once M starts to be oxidized to MX₁ and MX₂, the concentration of TOC is given by the sum of the concentrations of M, MX₁ and MX₂

Furthermore, for the sake of simplicity, nomenclature is completed with the following terms:

- Generic reaction time t, t' and final time τ for the reaction (and the ODEs integration), at which the reaction performance is evaluated;
- Conversion, $\chi(t)$ and $\chi(\tau)$, which is defined by Equation (7.22) and assesses the relative ratio of TOC removal at a given time:

$$\chi(t) = ([\text{TOC}]^0 - [\text{TOC}]^t) / [\text{TOC}]^0 \quad \text{Eq.7.22}$$

Total amount of H₂O₂, A(t), A(τ), which is defined by Equation (7.23) and assesses the total expenditure of H₂O₂, in the batch run, given by the initial amount and the dosed amount:

$$A(t) = A^0 + C \int_0^t F(t') dt' \quad (\text{mmol}) \quad \text{Eq.7.23}$$

7.2.3 Dynamic simulation

Based on such kinetic and reactor models, and data, the dynamic simulation of the photo-Fenton process was carried out for a preliminary study of the behaviour of the system. It highlights the advantages of conveniently managing hydrogen peroxide dosage and consequently, the potential benefits arising from further investigation on photo-Fenton optimisation strategies.

First, a series of dynamic simulations of pure batch runs (no H₂O₂ dosage: H₂O₂ is added by once at the beginning of the process) was performed for the different contaminant loads using different values of the initial concentration of H₂O₂. The purpose was to investigate the system response to a gradual increase in [TOC]⁰ and [H₂O₂]⁰ and to identify the saturation threshold from which inefficient reactions boost and TOC conversion, $\chi(\tau)$, drops.

Moreover, four different case studies were also investigated and compared:

- First, a pure batch case study in which H₂O₂ is added all at once at the beginning of the process (no H₂O₂ dosage profile along the reaction time), was selected as reference in order to highlight the influence of the reactant dosage on the process performance.
- Then, H₂O₂ dosage was analysed by simulating three further fed-batch case studies, considering different H₂O₂ dosage profiles (continuous or stepwise profiles) for different A(t) and for the same A⁰= 0.

The JModelica.org open source platform (Åkesson et al., 2010) was selected as the tool to perform the dynamic simulation of the system under study. The simulation environment uses Assimulo that is a standalone Python package for solving ordinary differential equations (ODEs) and differential algebraic equations (DAEs). Among the different supported solvers, we selected the CVode solver to run the dynamic simulation. The CVode solver (Åkesson et al.,

2010) is a variable-order, variable-step, multi-step algorithm for solving ordinary differential equations of the form shown in Equation (7.24):

$$\frac{dy}{dt} = f(t, y), \quad y(t_0) = y_0 \quad \text{Eq.7.24}$$

It includes the Backward Differentiation Formulas (BDFs), suitable for stiff problems, but also the Adams-Moulton formulas for non-stiff systems.

7.2.4 Dynamic optimisation

Subsequently, the dynamic optimisation of the fed-batch photo-Fenton system was carried out.

The first step was the optimisation study focused on the following partial objectives:

- Maximization of the final TOC removal, $\chi(\tau)$, for a given total amount of H_2O_2 to be dosed, $A(\tau)$, and a fixed final reaction time τ ;
- Minimization of $A(\tau)$ to attain a fixed $\chi(\tau)$ within a given τ .

This study can be used as a sort of sensitivity analysis. Indeed, first $A(\tau)$ and τ , and then $\chi(\tau)$ and τ were changed systematically to assess their effect on the final outcome, $\chi(\tau)$ and $A(\tau)$ respectively. In this way, as in the case of a traditional sensitivity analysis, the identification of critical factors is possible and it attempts to predict alternative outcomes of the same course of action.

Finally, the above described partial objectives were gathered in a single objective function proposed in order to perform a more complex optimisation study aiming at finding the optimal H_2O_2 dosage profile, $F(t)$, and reaction time, τ , that ensure the minimum processing cost while satisfying operational and environmental constraints.

The dynamic optimisation problem includes the definition of the system to be optimized, a cost function (the so-called objective function), a set of constraints (equality and inequality path constraints, equality and inequality

end-point constraints) and controlled variables. It can be generally stated by Equations (7.25)-(7.33) (Biegler, 2007):

$$\min \varphi (z(\tau)) \tag{Eq.7.25}$$

$$z(t), u(t), p$$

$$\text{s. t. } \frac{dz(t)}{dt} = f(z(t), y(t), u(t), p), \quad z(t_0) = z_0 \tag{Eq.7.26}$$

$$g(z(t), y(t), u(t), p) = 0 \tag{Eq.7.27}$$

$$g(z(t)) = 0 \tag{Eq.7.28}$$

$$(z(\tau), y(\tau), u(\tau), p) \leq 0 \tag{Eq.7.29}$$

$$g(z(\tau)) \leq 0 \tag{Eq.7.30}$$

$$y_L \leq y(t) \leq y_U \tag{Eq.7.31}$$

$$u_L \leq u(t) \leq u_U \tag{Eq.7.32}$$

$$z_L \leq z(t) \leq z_U \tag{Eq.7.33}$$

Where $z(t)$ are the differential state variables, $u(t)$ are the control variables, and $y(t)$ are the algebraic variables, all functions of the time $t \in [t_0, \tau]$, while p represents time-independent parameters.

In such problem $z(t)$, $u(t)$, $y(t)$ and p represent the decision variables, while the constraints are represented by the Differential and Algebraic Equations (DAEs) system, given by Equations. (7.26)-(7.30). Particularly, Equations

(7.27) - (7.28) and Equations (7.29) - (7.30), represent equality and inequality path and end-point constraints, respectively. Finally, Equations (7.31) - (7.33) define lower and upper boundaries for algebraic, control and differential state variables, respectively.

Currently, dynamic optimisation problems can be solved by using an indirect approach, based on the first order necessary conditions for optimality obtained from Pontryagin's Maximum Principle, and a direct approach based on various strategies that apply non-linear programming (NLP) solvers to the Ordinary Differential Equations (ODEs) or Differential Algebraic Equations (DAEs) model (Biegler, 2007), (Nocedal et al., 2009). A direct approach, namely direct simultaneous optimisation method, was applied for solving the dynamic optimisation problem. This method is based on orthogonal collocation on finite elements (a fully implicit Runge-Kutta method), and relies on the discretization of both control and state variables by polynomials, whose coefficients become the decision variables of a very large-scale NLP problem.

The dynamic optimisation problem under study was solved by using the same tool adopted to run the dynamic simulation, or rather, the JModelica.org open source platform (Åkesson et al., 2010). The CasADi algorithm based on direct collocation and implemented in Python was used for computing function derivatives and IPOPT (Interior Point Optimizer) solver was used for solving the resulting NLP problem.

7.2.4.1 Optimisation study based on partial objectives

First, the aim of the dynamic optimisation was to study the interaction between $A(\tau)$ and τ . Such interaction affects the process performance, or rather the final TOC removal, $\chi(\tau)$. Hence, an overview of the best operating conditions to achieve a predetermined $\chi(\tau)$ was provided, as a tool aiding decision-making.

Concerning the photo-Fenton process, a particular trade-off appears. Adding all hydrogen peroxide at once (no dosage) results in the need of extra hydrogen peroxide (due to inefficient side reactions), which increases the cost of raw materials. Conversely, a slow gradual dosage of a minimum

amount of hydrogen peroxide results in an increase of time, which increases operational costs (energy, etc.)

This poses a Multi-Objective Optimisation (MO) problem. A MO problem can be formulated as a decision-making problem of simultaneous optimisations of two or more objectives that are conflicting in nature (such as the economic cost of a treatment and desired environmental effect). It can be solved by minimizing an objective function subject to some constraints, and the solution is called Pareto optimal, or a Pareto solution (“A Pareto solution is one for which any improvement in one objective can only take place if at least one other objective worsens”; (Messac et al., 2003), (Pareto V., 1906). The set of Pareto solutions, obtained by systematically varying the constraints to which the objective function is subjected to, is known with the name of Pareto frontier.

Hence, by building Pareto frontiers, by systematically varying $A(\tau)$ and τ , and then $\chi(\tau)$ and τ to determine their effect on $\chi(\tau)$ and $A(\tau)$ respectively, several optimal operating conditions for different treatment configurations can be easily and quickly identified.

Table 7.3.Scenarios selected to perform the preliminary sensitivity analysis of the fed-batch photo-Fenton system (H_2O_2 dosage)

	Objective Function	Decision variables	Constraints
scenario A	Max $\chi(\tau)$	F(t) $[H_2O_2]^0$	τ $A(\tau)$
scenario B	Min $A(\tau)$	F(t) $[H_2O_2]^0$	τ $\chi(\tau)$

Two scenarios (see Table 7.3), all searching for the optimal H_2O_2 dosage profile, F(t), including the starting concentration, $[H_2O_2]^0$ (mmol L⁻¹), were investigated and Pareto frontiers were built.

In scenario A, the objective function to be maximized was the outcome, $\chi(\tau)$, subject to a maximum reaction time, τ (h), and the total amount of H_2O_2 , to be dosed, $A(\tau)$. In scenario B, the objective function to be minimized was $A(\tau)$ subject to a given maximum reaction time and a minimum outcome.

7.2.4.2 Optimisation under economic and environmental considerations

A final problem was to determine both the addition profile of hydrogen peroxide, $F(t)$, and the reaction time τ that maximize the global performance of the photo-Fenton treatment. This also poses a dynamic optimisation problem that turns into a Multi-Objective Problem when economic, environmental, and operational issues are simultaneously considered.

The decision variables were:

- the reaction time, $\tau(h)$ (constrained by a large-enough boundary of 6h);
- the initial concentration of hydrogen peroxide, $[H_2O_2]_0$ (mmo L^{-1}), and
- the dosage profile of hydrogen peroxide, $F(t)(L h^{-1})$.

The constraints are given by the reactor model described in Equations (7.3) – (7.12).

The problem was addressed by formulating a single objective function φ , representing the total cost (€) to be minimized (see Equation (7.34)). The proposed objective function accounts for the cost of hydrogen peroxide, the operational cost, and the environmental cost that results from an incomplete organic matter degradation. It includes the unit cost coefficients for the cost of the reactant C_1 (€ mmol L^{-1}) for the operational cost C_2 (€ h^{-1}) and for the environmental cost C_3 (€ mmol L^{-1}).

$$\varphi = C_1 \cdot A(\tau) + C_2 \cdot \tau + C_3 \cdot V(\tau) \cdot \chi(\tau) \cdot [TOC]^0 \quad \text{Eq.7.34}$$

In this work, the unit cost coefficient C_1 was estimated according to current industrial prices. Conversely, for the sake of illustrative discussion, estimated

values of C_2 in a range between (0-1000 € h⁻¹) and of C_3 (in a range between 0-100 € mmol L⁻¹) were selected and tested with the aim of elucidating the trade-off that arises from different operational and environmental costs. This environmental cost was used for validating the capacity and reliability of the proposed strategy, without loss of generality.

Indeed, other cost functions could be proposed (including concentration or discharge limits). Particularly, operational fixed costs, such as maintenance and amortization, could be easily included in the operational unit cost coefficient C_2 , which is a lumped parameter, and the unit cost coefficient C_3 could be treated as a fine (penalty cost) to be paid per amount of TOC discharged.

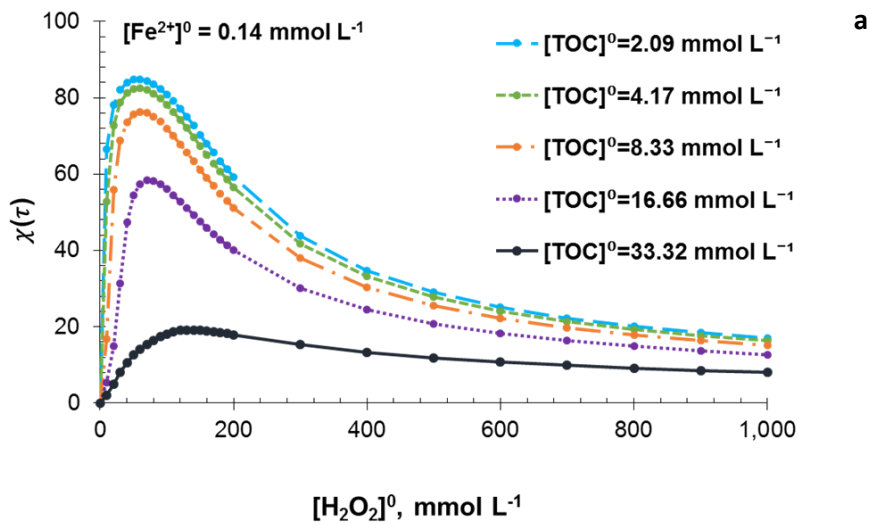
7.3 Results and discussion

7.3.1 Dynamic simulation results

Simulation results in terms of $\chi(\tau)$ for different contaminant loads, $[\text{TOC}]^0$, and different initial concentrations of hydrogen peroxide, $[\text{H}_2\text{O}_2]^0$, are presented in Figure 7.4-a for a fixed reaction time $\tau = 2$ h. Final TOC removal, $\chi(\tau)$, rises as the initial concentration of H_2O_2 increases, until a threshold saturation value is reached, and then $\chi(\tau)$ drops asymptotically. These results are coherent with the experience and the kinetic model and show that too high hydrogen peroxide concentration can revert the process efficiency by increasing the R concentration, which in turn favours the reaction rate of the inefficient second order reactions. The study also shows that by increasing the contaminant load, the peak value of $\chi(\tau)$ reduces from a maximum value of about 85% (for $[\text{TOC}]^0 = 2.09$ mmol L⁻¹) to a minimum value of about 20% (for $[\text{TOC}]^0 = 33.32$ mmol L⁻¹). This behaviour is due to the $\text{Fe}^{2+}/\text{H}_2\text{O}_2$ ratio, that shows to be ineffective for high values of $[\text{TOC}]^0$ (in all previous cases a value of $[\text{Fe}^{2+}]^0 = 0.14$ mmol L⁻¹ was set). This result was then confirmed by running a new simulation for the case of $[\text{TOC}]^0 = 33.32$ mmol L⁻¹ but with an increased value of $[\text{Fe}^{2+}]^0 = 0.14$ mmol L⁻¹ (set equal to 0.28 mmol L⁻¹). Results presented in Figure 7.4-b show that a maximum $\chi(\tau)$ of about 76% can be attained for an initial value of hydrogen peroxide concentration of 120 mmol L⁻¹, so

increasing by more than 50% the final conversion. For the pure batch operation (no dosage after $t=0$ h) three main conclusions arise:

- on one hand, given $[\text{TOC}]^0$ and $[\text{Fe}^{2+}]^0$, an optimum value for the initial concentration of hydrogen peroxide, $[\text{H}_2\text{O}_2]^0$, exists;
- on the other hand, such optimum value for $[\text{H}_2\text{O}_2]^0$ may be insufficient to attain complete mineralization ($\chi(\tau)=100\%$), which indicates that an extra amount of hydrogen peroxide should be subsequently added;
- finally, the amount of iron, $[\text{Fe}^{2+}]^0$, also has a relevant role in the process efficiency and suggests that further work should address the simultaneous optimisation of $[\text{Fe}^{2+}]^0$ and $[\text{H}_2\text{O}_2]^0$ dosage.



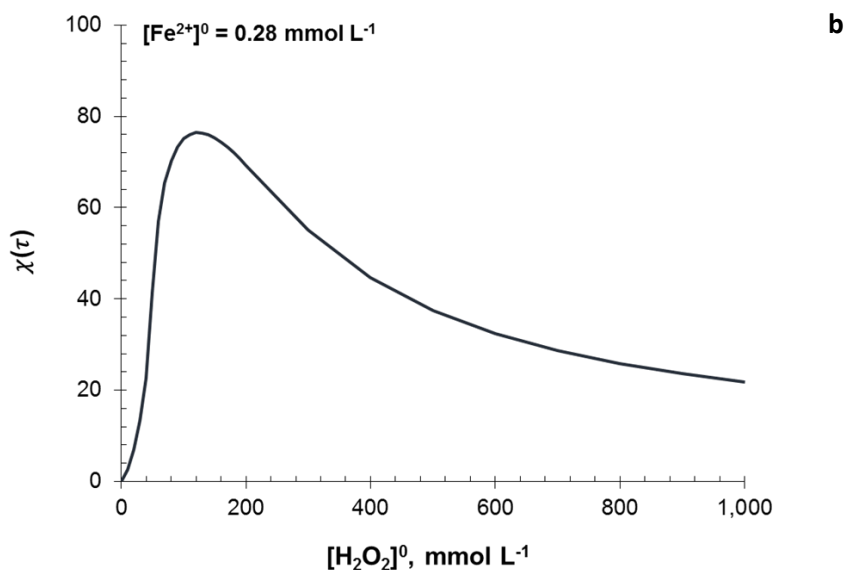
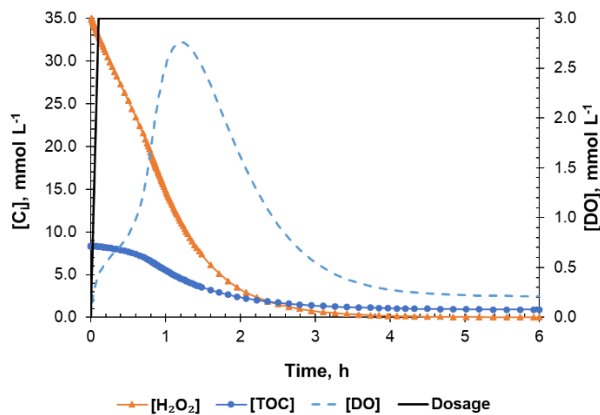


Figure 7.4. Dynamic simulations of pure batch runs (no H_2O_2 dosage) were performed for: **(a)** Different paracetamol loads (corresponding to $[\text{TOC}]^0 = 2.09, 4.17, 8.33, 16.66$ and $33.32 \text{ mmol L}^{-1}$), different values of the initial concentration of hydrogen peroxide (in a range between 0.00 and $1000.00 \text{ mmol L}^{-1}$), and for $[\text{Fe}^{2+}]^0 = 0.14 \text{ mmol L}^{-1}$. **(b)** A given paracetamol load (corresponding to $[\text{TOC}]^0 = 33.32 \text{ mmol L}^{-1}$) and $[\text{Fe}^{2+}]^0 = 0.28 \text{ mmol L}^{-1}$. Final TOC reduction, $\chi(\tau)$ obtained for $\tau = 2 \text{ h}$ is represented for both cases

Conversely, Figure 7.5 (a) - (b) - (c) - (d) show H_2O_2 , DO, and TOC simulated concentration profiles for four different case studies (one pure batch and three fed-batch case studies) that are next discussed. It should be noted that $[\text{DO}]$ is plotted on the secondary axis. Moreover, dosage profile is represented in qualitative terms of accumulated amount (integral) without using any units of measurement. In this way, it is easier to observe the

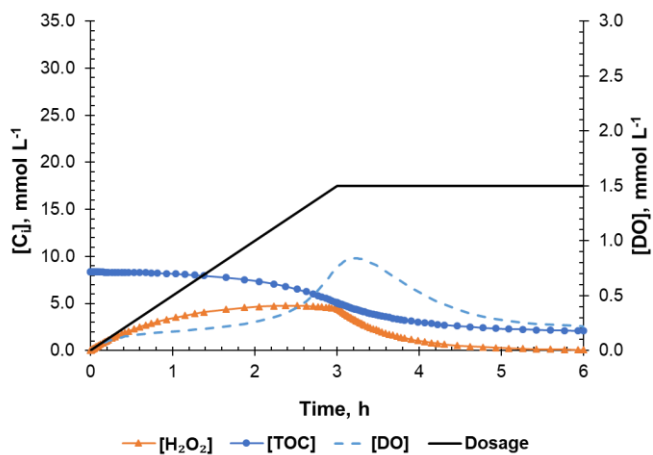
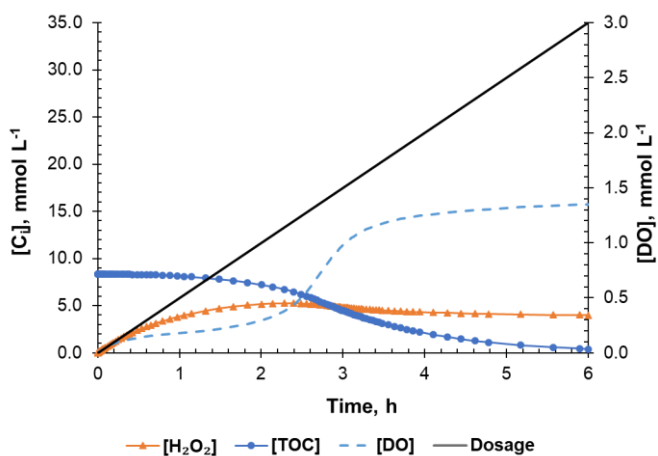
different trends between the various investigated case studies, which are detailed below:

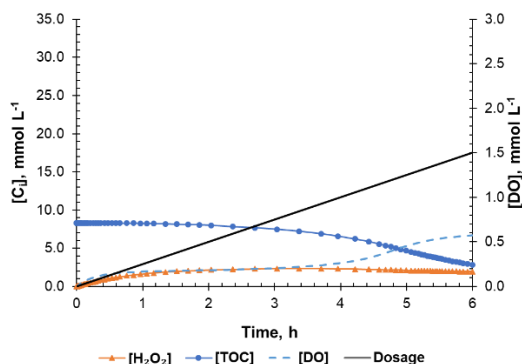
- Case study A: a batch case study with no H_2O_2 dosage and 6 h reaction time. The total amount of H_2O_2 ($A(\tau) = 158.85 \text{ mmol}$) was added at the beginning of the process ($t = 0 \text{ h}$). It is the reference scenario and it is useful to compare and analyze results in terms of reactant dosage and process efficiency improvement.
- Case study B: a fed-batch case study, for which the same total amount of H_2O_2 set for the previous case study A ($A(\tau) = 158.85 \text{ mmol}$) is continuously dosed during the same 6 h reaction time (corresponding to the molar inlet flowrate of hydrogen peroxide of $f_{\text{H}_2\text{O}_2}(t) = 26.48 \text{ mmol h}^{-1}$);
- Case study C: a fed-batch case study, for which half of the same total amount of H_2O_2 set for the previous case study B ($A(\tau) = 79.43 \text{ mmol}$) is continuously released during the first 3 h of the total reaction time of 6 h (corresponding to the molar inlet flowrate of hydrogen peroxide of $f_{\text{H}_2\text{O}_2}(t) = 26.48 \text{ mmol h}^{-1}$);
- Case study D: a fed-batch case study, for which half of the same total amount of H_2O_2 set for the case study B ($A(\tau) = 79.43 \text{ mmol}$) is continuously released during the whole reaction time of 6 h (corresponding to an inlet flowrate of hydrogen peroxide of $f_{\text{H}_2\text{O}_2}(t) = 13.24 \text{ mmol h}^{-1}$).



a

Recipe optimisation





d

Figure 7.5. Comparison of four different dynamic simulation case studies ($\tau = 6$ h): **(a)** Pure batch operation (no H_2O_2 dosage profile) in which H_2O_2 is added all at once at the beginning of the process (158.85 mmol of H_2O_2 corresponding to an initial concentration of $[\text{H}_2\text{O}_2]^0 = 35.33$ mmol L^{-1}); **(b)** Fed-batch operation (H_2O_2 dosage) using the same total amount of H_2O_2 (158.85 mmol), which is continuously dosed until the end; **(c)** Fed-batch operation using half the amount of H_2O_2 (79.43 mmol), which is continuously dosed during half of the time (3 h); **(d)** Fed-batch operation using half the amount of H_2O_2 (79.43 mmol), which is continuously dosed during the whole time horizon (6 h). ² $[\text{DO}]$ is plotted on the secondary axis; the dosage profile is just qualitatively represented without indicating any units of measurement

Figure 7.5-a presents the results for the case study A and reveals a peak in the DO concentration at 1.2 h. The increase in the DO concentration is caused by the inefficient reactions promoted by the excess of free radicals R due to the excess in H_2O_2 concentration. Concerning the H_2O_2 concentration trend, it is possible to observe a steep decrease that leads to its consumption in about 3 h. It is also important to notice that once the H_2O_2 concentration reaches its minimum value (at 3 h), the TOC profile becomes steady and reaches a final value of about 85% . Results in Figure 7.5- b correspond to the case study B. In this case, after a first gradual and slight increase (about 2 h), H_2O_2 concentration reaches a maximum value (about 5.00 mmol L^{-1}) and then it remains almost constant for the rest of the time. A different and lower $[\text{DO}]$ profile can be observed, compared to case study A. This result suggests that a more effective use of the oxidant has been attained but no significant improvement in the final TOC removal could be observed. Then, DO concentration reaches a maximum value (of about 1.20 mmol L^{-1}) at a

reaction time of about 3 h and starting from this point, it remains constant for the whole process. This suggests that the continuous dosage for the whole reaction time of 6 h, cannot be selected as the more effective option. Figure 7.5-c shows the results for the case study C. The H_2O_2 concentration profile has a similar trend compared to the previous case study B. The [DO] profile, presents also a peak but lower and later compared with the previous case studies (about 0.85 mmol L^{-1} and 3.2 h, after the end of the dosage, which reveals the inertia of the system). However, half the amount of H_2O_2 produces a lower performance (lower final TOC removal) compared with case studies A and B. Finally, the results of the last case study are presented in Figure 7.5-d. A lower H_2O_2 concentration profile can be observed due to the selection of a lower initial concentration value. Also in this case, no significant improvement can be reached in the final TOC removal, although the [DO] profile shows an efficient use of the (insufficient) amount of hydrogen peroxide used (a lower peak that is reached with a significant delay). Consequently, the H_2O_2 dosage profile is shown to affect the process performance since it generates different [DO] profiles (in terms of peak and delay) that reveal the extent of inefficient reactions. Furthermore, the simulation of two extreme situations such as case studies A and D reveal existence of an optimum dosage profile attaining the oxidation target with the most efficient use of the oxidant. Hence, a model-based optimisation approach is required in order to propose a systematic methodology allowing for the determination of the optimal H_2O_2 dosage maximizing the process efficiency of any contaminant load. In this regard, the sensitivity analysis was a key point of the present work and relevant considerations can be drawn concerning the more effective way to select the hydrogen peroxide dosage profile to gain a certain TOC removal $\chi(\tau)$ for a specific reaction time τ .

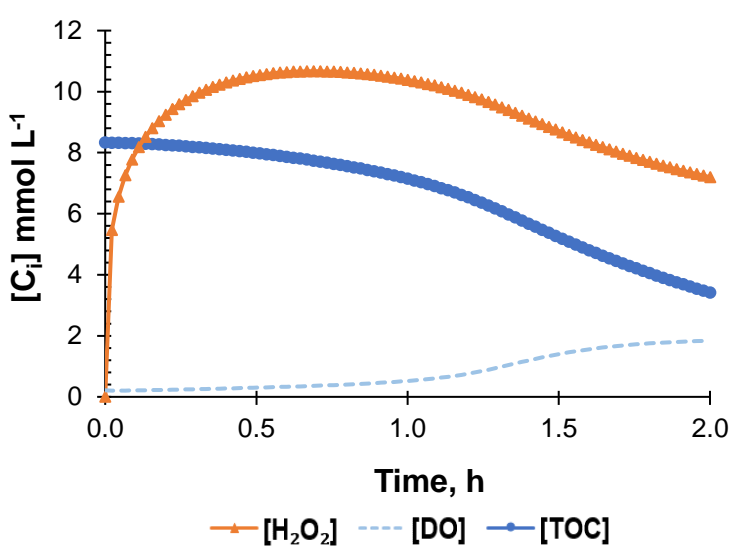
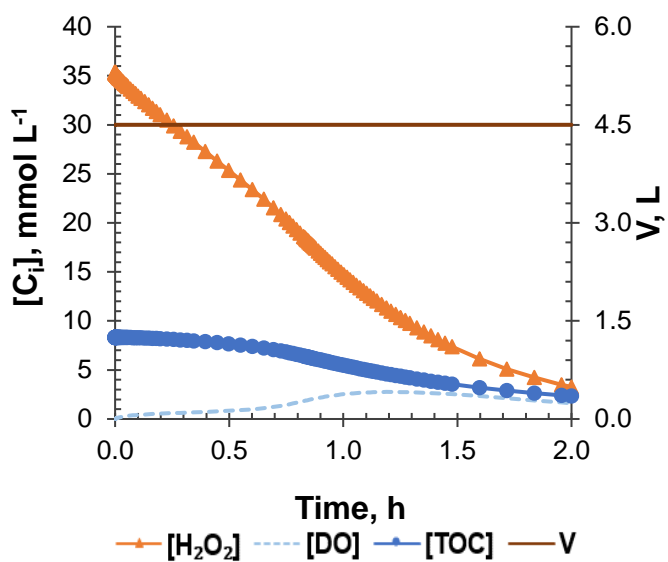
7.3.2 Dynamic optimisation results: optimisation study based on partial objectives

The subsequent step is to address the single dynamic optimisation problem by releasing the dosage profile, $F(t)$, as a control variable and defining a specific objective function to be maximized and a specific set of constraints. The solution is implemented using the JModelica.org open source platform (Åkesson et al., 2010) coupled with Python.

Two scenarios, scenario A and B in Table 7.3, were discussed. For scenario A the objective function is the final TOC removal ($\chi(\tau)$), which needs to be maximized, while the constraints are the reaction time (τ) and the total amount of H_2O_2 ($A(\tau)$) available. Conversely, for scenario B, the objective function is $A(\tau)$, which needs to be minimized, while the constraints are τ and $\chi(\tau)$. In both cases, the control variable is the flowrate of hydrogen peroxide solution, $F(t)$, that is dosed during the reaction time, τ . Thus, the optimisation procedure gives the optimal $F(t)$ (inlet flowrate at each time interval). It also gives the maximum value of TOC removal and of the minimum total amount of H_2O_2 (objective function values for scenario A and B, respectively) for the specific values selected for the constraints (τ and $A(\tau)$ in the case of scenario A, τ and $\chi(\tau)$ in the case of scenario B) of the problem.

An advantage of the proposed optimisation strategy is the computer aided identification of operational opportunities. Therefore, reported experimental results are next compared with the optimal solutions determined under the same conditions. According to Cabrera Reina et al., 2012, by adding the total amount of H_2O_2 all at once ($[\text{H}_2\text{O}_2]^0 = 35.33 \text{ mmol L}^{-1}$), which corresponds to 18.0 mL total volume of H_2O_2 30% and 8823.00 mmol) and setting ($[\text{Fe}^{2+}]^0 = 0.14 \text{ mmol L}^{-1}$), ($[\text{TOC}]^0 = 8.33 \text{ mmol L}^{-1}$), and $I = 32 \text{ W m}^2$, a final TOC removal of about 60% was attained after 2 h of reaction.

First, this situation was simulated (see Figure 7.6-a) and a final TOC removal of about 70% was attained, hence experimental results were reproduced within a 10% error. Next, assuming the minimization of the total amount of hydrogen peroxide, $A(\tau)$, under the same fixed conditions and variable dosage (scenario B), an optimal dosage profile was determined. In this case, as illustrated in Figure 7.6 (b) and (c), the same final TOC removal of about 60% was attained after 2 h, as imposed, but using 14.73 mL of H_2O_2 (corresponding to a total amount of 130.00 mmol of hydrogen peroxide 30%) instead of 18.00 mL. This is a reduction of more than 18% of the H_2O_2 consumption; this may imply a similar cost reduction that is worth to consider. Furthermore, the optimal H_2O_2 profile at each instant in time was also obtained, which could be useful in a perspective of process automatization.



7

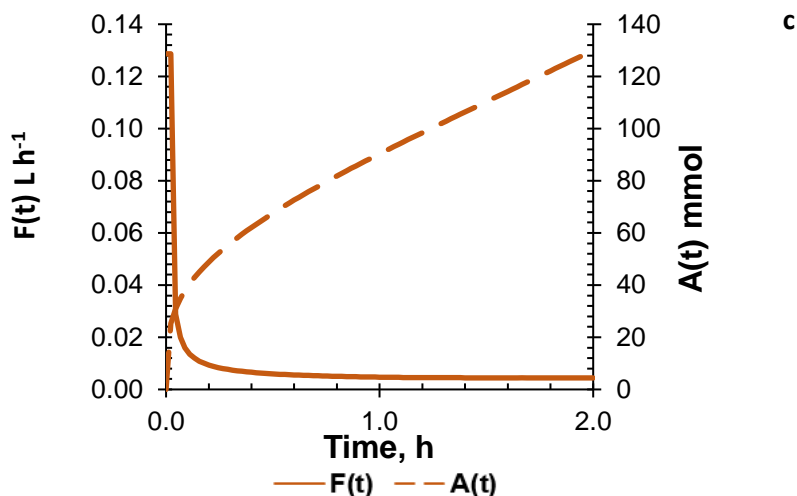


Figure 7.6. Optimisation study: comparison between the optimal solution obtained with the proposed optimisation strategy and the experimental results by Cabrera Reina et al., 2012: **(a)** TOC, H_2O_2 , DO concentration profiles obtained by the dynamic simulation of the system under study in the case of $[Fe^{2+}]^0 = 0.14 \text{ mmol L}^{-1}$, $[H_2O_2]^0 = 35.33 \text{ mmol L}^{-1}$, $[TOC]^0 = 8.33 \text{ mmol L}^{-1}$, $I = 32 \text{ W m}^{-2}$ and $\tau = 2 \text{ h}$. **(b)** TOC, H_2O_2 , DO concentration profiles obtained for the single optimisation problem aiming at the minimization of the total amount of H_2O_2 in the case of $[Fe^{2+}]^0 = 0.14 \text{ mmol L}^{-1}$, $[TOC]^0 = 8.33 \text{ mmol L}^{-1}$, $I = 32 \text{ W m}^{-2}$ and $\tau = 2 \text{ h}$. **(c)** $F(t)$ and $A(t)$ obtained by solving the dynamic optimisation problem described in item b)

Once the optimisation procedures have been developed and tuned, multiple optimisation problems can be systematically solved for scenarios A and B, by varying the values of the constraints. Hence, Pareto frontiers can be built by plotting the calculated value of the objective function, referred to one of the two constraints of the problem, versus the other constraint.

Particularly, the following set of constraints was investigated for the two scenarios:

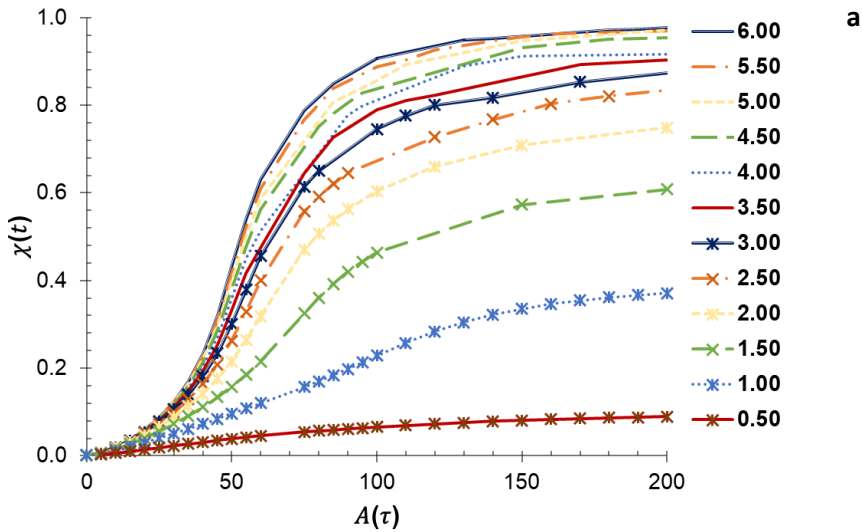
- Scenario A: values between 0 and 6 hours and a set of values ranging between 0 and 200 mmol, were investigated for τ and $A(\tau)$, respectively. Pareto frontiers were

built by combining for a specific value of τ , the optimal values of the final TOC removal obtained for the different values of $A(\tau)$.

- Scenario B: in this case, values between 0 and 3 hours, and a set of values ranging between 0 and 1, were investigated for τ and $\chi(\tau)$, respectively. Pareto frontiers were built by combining, for a specific value of τ , the optimal values of $A(\tau)$, obtained for the different values of the final TOC removal to be achieved.

It is worth noting that in order to improve convergence, it was necessary to set a specific number of finite elements (n_e) and of collocation points (n_cp) in each element, such as to set specific options for the CasADi and collocation-based optimisation algorithm that differ from the default ones. For both scenarios, these values were set equal to 90 and 1, respectively.

Results related to both scenarios are presented in Figure 7.7 (a) – (b)



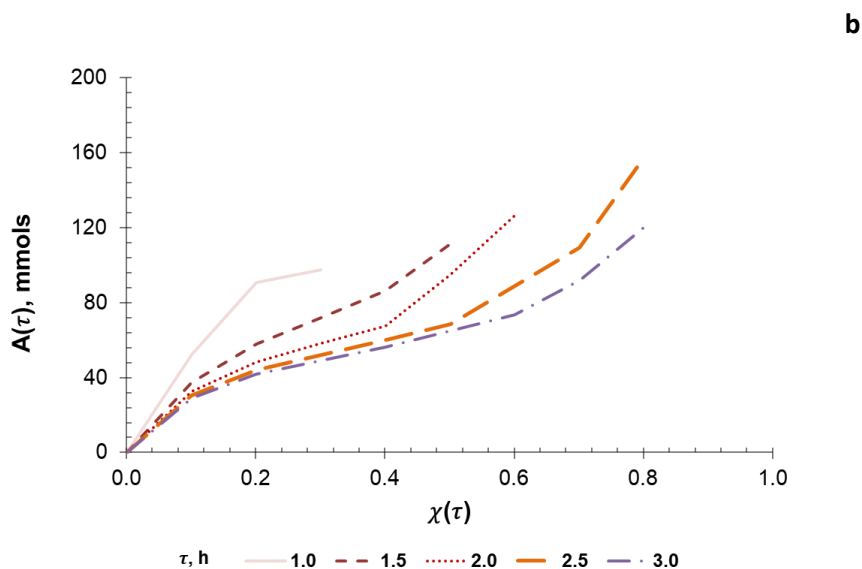


Figure 7.7. Optimisation study based on partial objectives: **(a)** Scenario A, Pareto frontiers built by representing the optimal values of the final TOC removal resulting from different values of the total amount of H_2O_2 (between 0 and 200 mmol) and of the reaction time (between 0 and 6 h); **(b)** Scenario B, Pareto frontiers obtained by plotting the different optimal values of the total amount of hydrogen peroxide, obtained for different values of the final TOCremoval (between 0 and 1) and of the reaction time (between 0 and 3 h)

Pareto frontiers in Figure 7.7-a, show that to achieve a final TOC removal higher than 90%, starting from an initial concentration of TOC equal to 8.33 mmol L^{-1} , at least 4 h are required and an approximate amount of hydrogen peroxide of 200 mmol (that corresponds to a concentration of $44.44 \text{ mmol L}^{-1}$) should be used. Besides, it can be noticed that, starting from a reaction time of 4 h, no significant difference can be detected in the final TOCremoval that can be achieved, neither by increasing the total amount of hydrogen peroxide nor by increasing the reaction time. For example, in 4 h it's possible to reach a final TOC removal of about 90% with a total amount of H_2O_2 of 150 mmol (that corresponds to a concentration of $33.33 \text{ mmol L}^{-1}$). However, for this same value of the total amount of hydrogen peroxide, increasing the reaction time to 5 h produces scarce improvement in the TOC removal. Moreover, it's worth noting that, for a fixed reaction time, a greater

conversion of TOC can be obtained by increasing the amount of H_2O_2 to be dosed, but only up to a certain threshold value (which, in all the cases, it's a value between 150 and 200 mmol), beyond which the conversion does not significantly improve. This is consistent with the kinetics of the process that describes the increasing effect of the inefficient reactions scavenging H_2O_2 and R, caused by the excess of H_2O_2 concentration.

Following and analyzing the results of scenario A, for scenario B the Pareto frontiers were built for a maximum reaction time of 3 h and are shown in Figure 7.7-b. It can be noticed that, for the same initial concentration of TOC equal to 8.33 mmol L^{-1} , in order to reach 80% of TOC removal, a value of the reaction time higher than of 2 h must be selected, regardless of the total amount of hydrogen peroxide added to the reactor. This is due to the increasing effect of the inefficient reactions scavenging TOC and H_2O_2 , as already observed for the previous scenario A. A maximum final TOC removal of about 80% can be attained only for a reaction time of 2.5 and 3.0 h and for a total amount of hydrogen peroxide of about 157 and 120 mmol, respectively. Conversely, for a reaction time of 1 h, very low TOC removal can be reached (a maximum value of 30% with a total amount of H_2O_2 of about 97 mmol). Hence, as expected, the higher is the reaction time to be set and the lower will be the amount of hydrogen peroxide to be dosed to reach the same value of the final TOC removal.

The optimisation study provides both qualitative and quantitative results. It provides a more comprehensive understanding of the process, by investigating the interrelations between the main variables that affect the process efficiency. It also allows for quantifying the optimal hydrogen peroxide profile, the total amount of hydrogen peroxide to be dosed, and the processing time to achieve a specific final TOC removal. Besides, it plays also an important role in decision-making support. It gives an overview of the best operating conditions for different scenarios: the best combination of total amount of hydrogen peroxide and the processing time to achieve a specific final TOC removal, the best combination of processing time, and final TOC removal for a specific value of the total amount of hydrogen peroxide.

For example, once defined the characteristics of the influent to be treated (Chemical Oxygen Demand (COD), Biochemical Oxygen Demand (BOD), Total Organic Carbon (TOC) concentration, toxicity, etc.) and the purpose of the treatment, the information provided by the proposed optimisation strategy

can be used to select the optimal operating conditions. If the photo-Fenton process is needed as pretreatment to increase the biodegradability of the influent by reducing the initial TOC concentration of at least 50% and if the processing time cannot be higher than 2 h, the optimal amount of hydrogen peroxide required is revealed (Figure 7.7-a) to be 100 mmol (corresponding to a concentration of 22.22 mmol L⁻¹). The relative optimal hydrogen peroxide dosage during the 2 hours is also provided.

7.3.3 Dynamic optimisation results: optimisation under economic and environmental considerations

Finally, a different optimisation study was performed by defining an economic objective function (see Equation (7.34)) aimed at determining the addition profile for hydrogen peroxide and the reaction time that optimize the total cost of a fed-batch photo-Fenton process. For this study, the coefficient accounting for the cost of the reactant, C_1 , was estimated according to current industrial prices while a specific set of values has been investigated for unit cost coefficients accounting for the operational and environmental costs, namely C_2 and C_3 respectively, and are shown in Table 7.4:

Table 7.4. Values selected for the unit cost coefficients accounting for H₂O₂, operational and environmental cost, and namely C_1 (€ mmol⁻¹), C_2 (€ h⁻¹) and C_3 (€ mmol⁻¹), respectively

C_1	C_2	C_3
€ mmol ⁻¹	€ h ⁻¹	€ mmol ⁻¹
1E - 4	0	0
	10	10
	50	50
	100	100

500

1000

Hence, by the combination of the different values set for C_2 and C_3 , it was possible to investigate 24 different scenarios. For all of them, the number of finite elements (n_e) and the number of collocation points in each element (n_{cp}) were set to 30 and 1, respectively, in order to improve convergence. The results obtained are presented in Figure 7.8 and 7.9. In Figure 7.8 (a) – (b) a clustered column chart allows to highlight the trade-off between the operational and the environmental cost, with respect to the reaction time that must be set and the final TOC removal that must be achieved, respectively.

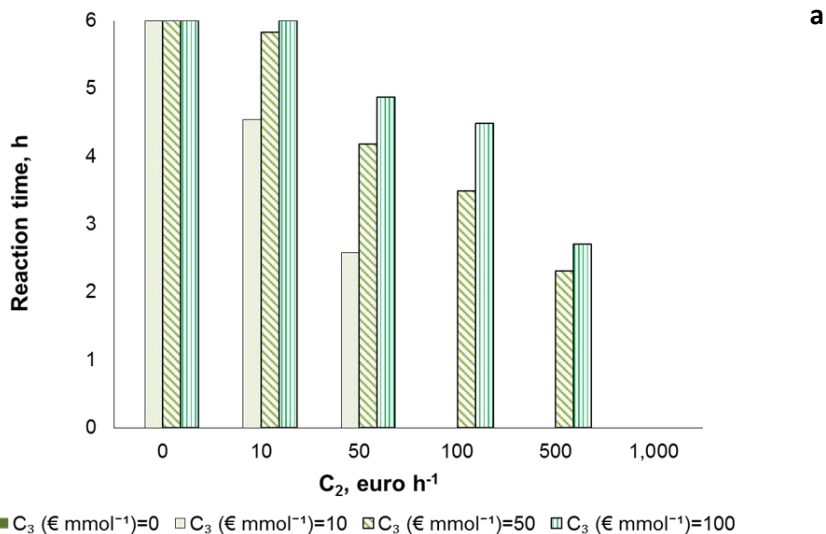
In order to validate the capacity and reliability of the optimisation model, two extreme scenarios were addressed. The first has an environmental unit cost coefficient equal to 0 € mmol^{-1} and the second one where the operational unit cost coefficient is equal to 0 € h^{-1} .

When the environmental unit cost coefficient is equal to zero it is straightforward that there is no need for any treatment and any related expense. As it could be anticipated, the reaction time and the final TOC removal in the optimal solution turn out to be zero, regardless of the value of the operational unit cost coefficient.

Conversely, when an operational cost coefficient equal to zero is set, it can be anticipated that the cheapest solution is the one minimizing other costs (the cost of added peroxide plus the environmental cost) at the expense the operational cost, which will be zero despite the time spent. This is why the optimisation model precisely reveals the maximum available time (set to 6 h as the optimal time).

As expected, for a fixed value of the operational unit cost coefficient, as the environmental unit cost coefficient increases (so becoming more relevant the environmental cost than the operational cost), the reaction time and the TOC removal increase too. It is worth noting that in the case of an operational unit cost coefficient of 100 and 500 € h^{-1} , by increasing the environmental unit cost coefficient from 0 to 10 € mmol^{-1} , no increase in the reaction time

and in TOC removal was recorded. In this case, the reaction time as well as the TOC removal assumed the minimum value (0 h and 0% respectively). The same results can be observed in the case of an operational unit cost coefficient equal to 1000 € h⁻¹, regardless of the value of the environmental unit cost coefficient. This is due to the greater relevance of the operational cost compared to the environmental cost. Thus, in these cases, the best solution is to avoid the process. Hence, the greater is the environmental cost the greater is the need for TOC removal and so the longer will be the process. Finally, for a same value of the environmental unit cost coefficient, the increase in the operational unit cost coefficient produces a decrease in the reaction time and in the TOC removal that can be attained.



Recipe optimisation

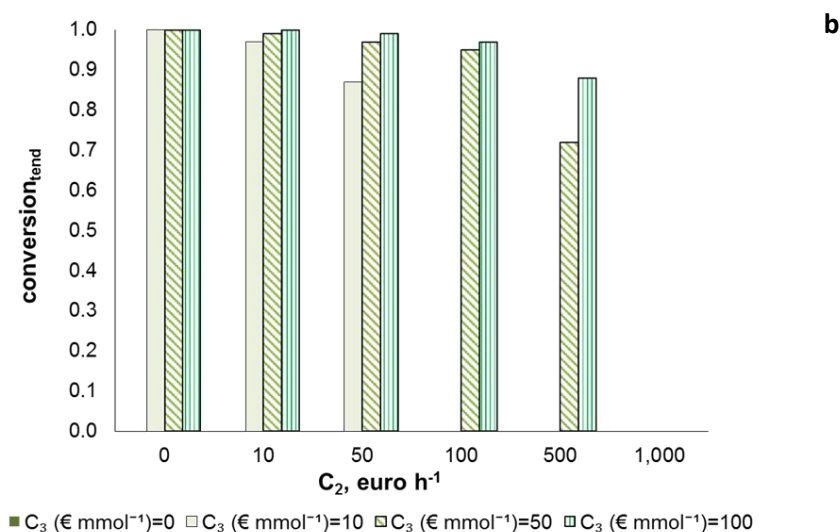


Figure 7.8. Economic optimisation study: **(a)** Clustered column chart representing the reaction time obtained by varying the operational unit cost coefficient (C_2) and the environmental unit cost coefficient (C_3); **(b)** Clustered column chart representing the final percentage of TOC removal, obtained by varying the operational unit cost coefficient (C_2) and the environmental unit cost coefficient (C_3)

Then, a specific case study among the ones above described has been selected in order to analyze the results in terms of cost functions (€), such as environmental, operational, hydrogen peroxide and total cost functions and in terms of total amount of hydrogen peroxide (mmol) added during the processing time.

As a significant example, the scenario corresponding to the following values of C_2 and C_3 was selected:

- $C_2 = 50 \text{ € h}^{-1}$
- $C_3 = 10 \text{ € mmol}^{-1}$

These results are presented in Figure 7.9. As can be noticed, the most relevant cost is represented by the environmental cost that influences the total cost function trend. It is important to notice that with the introduction of the environmental cost, the total cost function starts to decrease, due to the TOC removal and finally tends to a plateau, due to the slower degradation rates characterizing the final steps of the reaction.

Each of these cost values correspond to the objective function value of the best case for each set of cost coefficients, initial values and constraints, but it also corresponds to the optimal dosage profile that causes these costs. Hence, the optimisation study of the model allows identifying the best cost attainable as well as the continuous control action $F(t)$ that allows obtaining it. Thus, for each new situation a new optimisation will produce a new optimal dosage profile that will minimize the operational cost (economic and environmental).

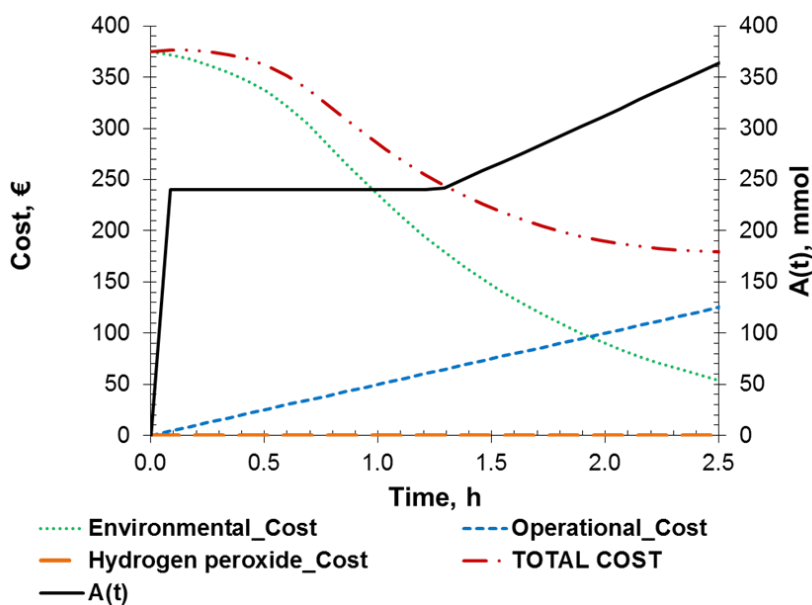


Figure 7.9. Optimisation study based on environmental and economic considerations: representation of the environmental, operational, hydrogen peroxide and total cost functions, as well as the total amount of hydrogen peroxide added during the processing time obtained by setting an operational unit cost coefficient equal to 50 € h^{-1} and an environmental unit cost coefficient equal to 10 € mmol^{-1}

7.4 Conclusions

This work has contributed a model-based optimisation strategy for the efficient photo-catalytic elimination of environmental pollutants such as recalcitrant organic compounds with high TOC load (e.g. industrial wastewaters). While many works in the literature report a great deal of experimental data on Advanced Oxidation Processes, fewer works address the modelling of these processes. Yet, models need to be systematically exploited to identify opportunities and determine efficient operation modes for automated processing.

This work provides a novel multi-objective dynamic optimisation framework for taking advantage of available kinetic models. It has been applied to the photo-Fenton process in order to map the trade-offs involved in its efficient management and determine the best operation recipes in the form of optimal hydrogen peroxide dosage profile. Optimal recipes under different operational, economic and environmental constraints have been found out for the batch-wise photo-Fenton treatment of paracetamol solutions so showing that a fast practical recipe adjustment, based on both economic and environmental factors, was ensured with reduced experimental work.

In particular, a preliminary dynamic simulation showed that a model-based optimisation approach is important for developing a systematic approach to the selection of a H_2O_2 dosage profile enhancing process efficiency while reducing experimental work. It also evidenced the opportunity to attempt the simultaneous optimisation of the $\text{Fe}^{2+}/\text{H}_2\text{O}_2$ ratio in future works.

Hence, a subsequent dynamic optimisation strategy was proposed to determine the optimal dosage profile. Next, a series of optimisation runs allowed for illustrating the different variables affecting process efficiency and system behaviour. It was also possible to show the role of hydrogen peroxide and of reaction time in final TOC removal.

Especially, for the case study addressed, it was possible to reveal that the only way to remove TOC beyond 90%, was to set a reaction time higher than 4 h and a total amount of H_2O_2 comprised between 150 and 200 mmol. The latter range represents a threshold value for the total amount of H_2O_2 that highlights the activation of the inefficient reactions scavenging H_2O_2 and free

radicals. Conversely, very low TOC removal can be achieved for a reaction time lower than 1.5 h.

Pareto frontiers have shown to be a tool providing practical process insight and understanding for sensible decision-making. Furthermore, many other response surfaces could be derived from the model in order to facilitate the analysis of the process for different optimisation objectives.

Finally, an optimisation study accounting for economic as well as environmental factors was presented. A proper objective function was formulated in order to take into consideration the trade-off between the environmental and the operational costs that affects the setting of the reaction time and the final TOC removal to be achieved. The study highlighted a predictable behaviour of the system addressed, thus confirming the reliability and efficiency of the proposed methodology.

7.5 Acknowledgements

This work was supported by the Spanish “Ministerio de Economía, Industria y Competitividad (MINECO)” and the European Regional Development Fund, both funding the research Project AIMS (DPI2017-87435-R). Francesca Audino, particularly acknowledges the MINECO for the PhD grant [BES-2013-065545].

8 Water Supply Chain Modelling and Management

The present chapter addresses the water network optimisation problem aiming at maximizing the total treatment performance while satisfying the required technical, economic, and environmental constraints. The most challenging and innovative task was considering the interrelations between the inlet components and their effect on the wastewater network optimisation, which is one of the major limitations of the approaches reported in the literature. This has been achieved by considering some major types of lumped parameters assessing the quality of water, namely Biological Oxygen Demand (BOD_5), and Chemical Oxygen Demand (COD), jointly with

the study of the combination of the highly expensive Advanced Oxidation Processes (AOPs) with the cheaper conventional biological processes.

8.1 Introduction

The optimisation of wastewater treatment networks has received increasing attention in the last fifty years due to the awareness raising concerning the environmental pollution issues that has led to increasingly stricter environmental regulations.

Since Mishra et al., 1975 it was clear the need of systematic design tools for wastewater treatment systems which has led to an extensive investigation production in this area. Particularly, the first approach assumed a centralized treatment, which implies the treatment of all the different streams (urban and different industrial effluents coming from different production plants) in a common facility.

Subsequently, decentralized wastewater treatments were proposed, in which the different streams were either treated separately or, if necessary, only partially mixed. The solution obtained following a decentralized approach, showed to be the best design option (McLaughlin A.L. et al., 1992) because on one hand it allowed reducing the flowrate to be treated, which turned into a decrease of the investment cost. On the other hand, centralized solutions led to a decrease of the concentration of the contaminant to be removed, resulting from the mixing of the streams, which in turn would lead to an increase of the operational cost.

Most of the several studies that can be found in literature have addressed the optimisation of a wastewater treatment network design by using a graphical representation and techniques on superstructures of alternative designs (Takama et al., 1980), (Wang and Smith, 1994a), (Wang and Smith, 1994b), (Kuo and Smith, 1997). Then, Non Linear Programming (NLP) and Mixed-Integer Non Linear Programming (MINLP) models have generally been proposed for the optimisation of these superstructures.

Moreover, different cases have been explored, such as single pollutant, multiple pollutants and pollutants in different phases (e.g. liquid and solid). Fixed rates for the treatment units and independent components have been usual assumptions (Galan and Grossmann, 1998), (Karuppiah and

Grossmann, 2006). However, an important improvement has recently been presented by Yang et al., 2014 who proposed replacing the traditional fixed recovery treatment units with unit-specific short-cut models, developed for the best available techniques selected for the removal of major pollutant groups.

However, nowadays the investigation is required to face a new modelling and optimisation challenge or rather the modelling and optimisation of a wastewater treatment network that combines conventional biological systems and Advanced Oxidation Processes (AOPs).

Advanced Oxidation Processes (AOPs) have been largely investigated as the only feasible option for the treatment of hardly biodegradable (recalcitrant) as well as toxic substances that can resist or damage, respectively, conventional biological treatments (Oller et al., 2011).

However, with the aim of containing the operational costs mainly due to the energy and reagents consumption, the combination of the AOPs with the cheaper biological systems has been proposed as a potential attractive alternative. Particularly, AOPs can be used as pre-treatments to convert the recalcitrant or toxic contaminants into more biodegradable substances, or as post- treatments to complete the mineralization of the organic matter.

Nonetheless, modelling and optimisation of a wastewater treatment network that combines such two processes, cannot be faced by following a conventional approach. It requires modelling the increase of the biodegradability influent produced by the AOPs.

Hence, in the present work a novel mathematical formulation including the so called BOD₅/COD ratio method was proposed. According to Pagga, 1997, the BOD₅/COD ratio method allows assessing the increase of the biodegradability of an effluent by evaluating the ratio between the Biological Oxygen Demand (BOD₅) and the Chemical Oxygen Demand (COD), characterizing its quality. Specifically, if this ratio results in a value greater than 0.4 the water can be considered biodegradable enough to be sent to a biological subsequent treatment step. Conversely if it is lower than 0.4 it must be pretreated by an AOP.

This has allowed investigating also the interrelations between components and their effect on the wastewater network optimisation, which, to the best knowledge of the authors, is still an open issue.

8.2 Methodological framework

8.2.1 Problem Statement

A formulation based on the general formulation of the design problem of a distributed wastewater network by Galan and Grossmann, 1998, and Karupiah and Grossmann, 2006, was presented.

Particularly, the general problem was stated as follows:

“Given a set of liquid streams, with known flowrates and containing some specific pollutants with known concentrations, and a set of technologies for the removal of each pollutant with known removal efficiencies for each pollutant, the goal is to identify the interconnections of the technologies and their corresponding flowrates and compositions that will meet the discharge composition regulations for each pollutant at minimum total cost”.

Hence, it is possible to distinguish between decision variables and parameters:

- Decision variables: flowrates of the streams as well as their interconnections.
- Parameters: flowrates and concentrations of each inlet stream, discharge composition for each pollutant, efficiency of each treatment unit for the removal of each contaminant, cost coefficients of each treatment unit.

8.2.2 Model formulation (NLP-MINLP)

To solve this problem, a superstructure based on the one proposed by Wang and Smith, 1994a, and Wang and Smith, 1994b, and composed by mixers, splitters and treatment units as well as all the possible interconnections among them was adopted to describe all the possible design alternatives.

The proposed superstructure is shown in Figure 8.1 which also presents the symbols that will be used for streams/connections, and for the corresponding flowrates and concentrations of the inlet contaminants (e.g. BOD₅ and COD).

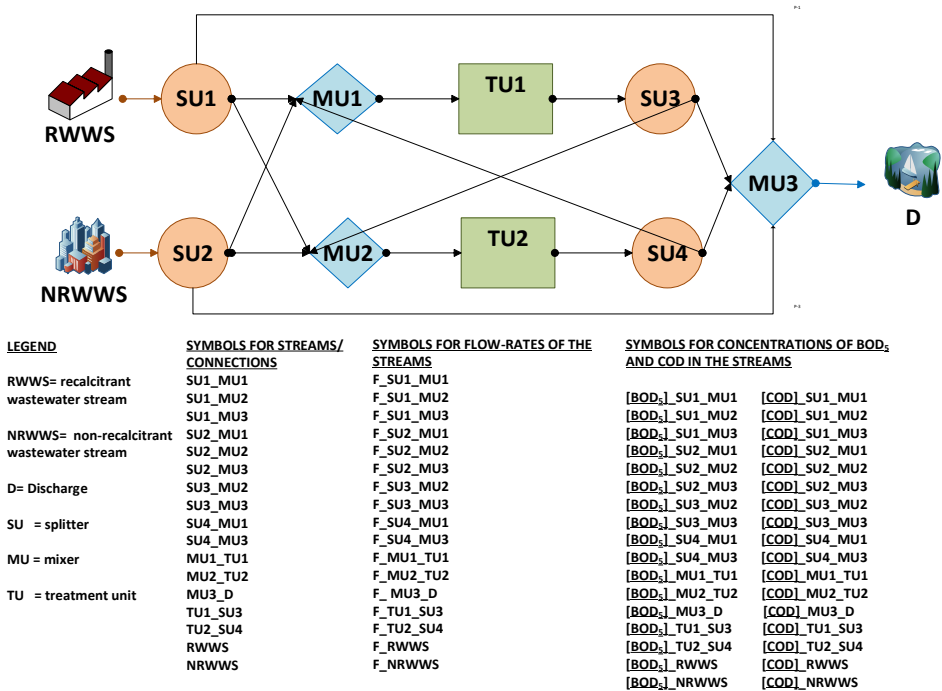


Figure 8.1. General wastewater network superstructure considering two treatment units and two inlet streams

Particularly, two inlet streams and two treatment units were taken into account in the proposed superstructure. In this way, it was possible to face the treatment of both a recalcitrant wastewater indicated as RWWS (that resists biological treatments), and a non-recalcitrant wastewater, indicated as NRWWS, and the combination of the highly expensive Advanced Oxidation Processes (AOPs= TU2) with the cheaper conventional biological systems (biological system= TU1).

Moreover, the interconnections were defined in order to:

- consider the possible direct discharge of the inlet streams (RWWS, NRWWS) to the environment represented by the discharge point (see connections SU1_MU3 and SU2_MU3 in Figure 8.1);
- take into account the possibility of deciding to which treatment unit (TU1 or TU2) the inlet streams must be sent (see connections SU1_MU1 and SU2_MU1 in Figure 8.1);
- consider the possibility of using AOPs and biological systems as pre-treatments (see connections SU3_MU2 and SU4_MU1 in Figure 8.1).

Two types of lumped parameters, namely Biological Oxygen Demand (BOD_5), and Chemical Oxygen Demand (COD), were considered as inlet pollutants entering with the inlet streams.

These lumped parameters were chosen because according to the ratio method described by Pagga, 1997, the value of the $R_p = BOD_5 / COD$ ratio in a stream defines its quality or rather if it is a recalcitrant or a biodegradable wastewater ($R_p < 0.4$ or $R_p \geq 0.4$, respectively).

The general Non Linear Programming (NLP) model by Galan and Grossmann, 1998, and Karuppiah and Grossmann, 2006, based on the total mass balance and the mass balance for each component i , in the splitter, mixer and treatment units, was adopted. However, a novel approach was introduced to describe the efficiency of the treatment units rather than using traditional linear models with constant removal ratios for each component.

8.2.2.1 Mixer units

A mixer $\mu \in MU$ consists of a set of inlet streams j that are specified in the index set m_{IN} , and an outlet stream $k \in m_{OUT}$.

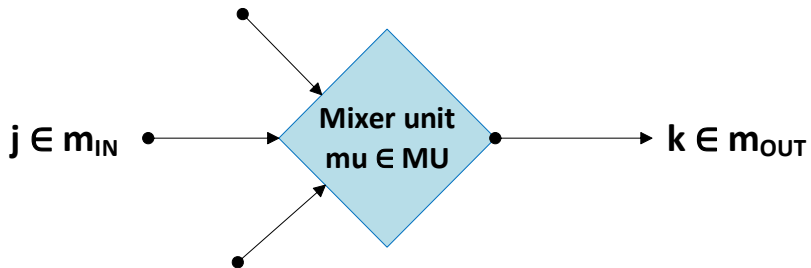


Figure 8.2. Mixer unit

The overall material balance for the mixer $\mu u \in MU$ is given by Equation (8.1) and the mass balances for each contaminant i in that mixer are given in Equation (8.2).

$$F^k = \sum_{j \in m_{IN}} F^j \quad \forall \mu u \in MU, k \in m_{OUT} \quad \text{Eq. 8.1}$$

$$F^k C_i^k = \sum_{j \in m_{IN}} F^j C_i^j \quad \forall i, \forall \mu u \in MU, k \in m_{OUT} \quad \text{Eq.8.2}$$

In the equations above, F^j and F^k represent the total flow of the inlet and outlet streams respectively (in ton h^{-1}), and C_i^j and C_i^k are the concentrations of contaminant i (in mg L^{-1}) in the inlet and outlet streams, respectively.

As can be observed, the individual contaminant balance equations contain a non-convex bilinear terms.

8.2.2.2 Splitter units

A splitter $su \in SU$ consists of an inlet stream $k \in s_{IN}$ and a set of outlet streams j that are specified in the index set s_{OUT} .

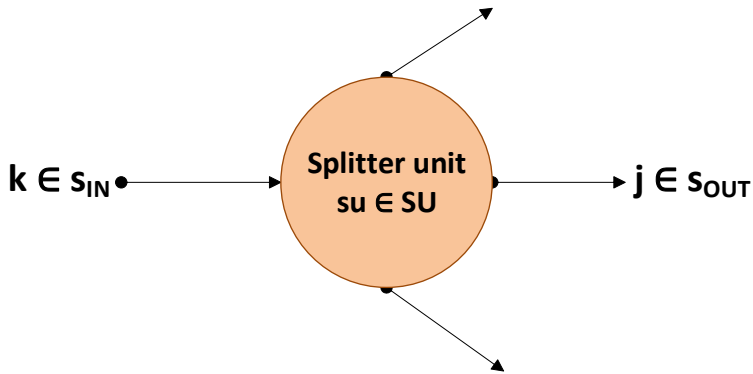


Figure 8.3. Splitter unit

The splitter behavior is modeled by linear equations that state that the contaminant composition of the streams leaving the splitter is equal to the composition of the inlet stream.

$$F^k = \sum_{j \in s_{OUT}} F^j \quad \forall su \in SU, k \in s_{IN} \quad \text{Eq.8.3}$$

$$C_i^j = C_i^k \quad \forall i, \forall su \in SU, \forall j \in s_{OUT}, k \in s_{IN} \quad \text{Eq.8.4}$$

8.2.2.3 Treatment units

A treatment unit $tu \in TU$ has an inlet stream $k \in t_{IN}$ and an outlet stream $j \in t_{OUT}$.

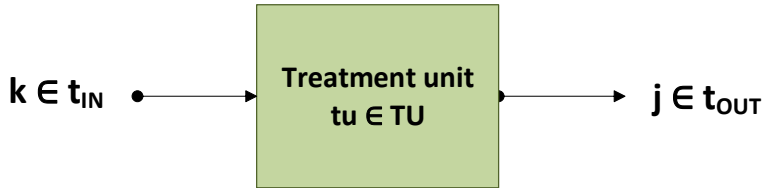


Figure 8.4. Treatment unit

As in the conventional linear models with constant removal ratios for each component, the individual contaminant flow in the outlet stream j is expressed as a linear function of the individual contaminant flow in the inlet stream k in terms of the coefficients β_i^{tu} , that is the removal efficiency of the treatment unit tu for the contaminant i .

$$F^k = F^j \quad \forall tu \in TU, j \in t_{OUT}, k \in t_{IN} \quad \text{Eq.8.5}$$

$$C_i^j = C_i^k \beta_i^{tu} \quad \forall i, \forall tu \in TU, j \in t_{OUT}, k \in t_{IN} \quad \text{Eq.8.6}$$

The novelty of this work states in the proposal of an efficiency removal that depends on the $R_p = BOD_5/COD$ ratio, where BOD_5 and COD are defined as the contaminants (i_1 and i_2) entering with each inlet stream:

$$\beta_i^{tu} \left(R_p = \frac{BOD_5}{COD} \right) \quad \text{Eq.8.7}$$

A continuous piecewise function $\beta = f(R_p)$ integrated by $n = 1, 2, 3 \dots N$ intervals needs to be formulated in math programming terms in order to be introduced in an optimisation model:

$$\beta = f(R_p) = \begin{cases} g_1(R_p) & \text{if } UP_1 \leq R_p < UP_2 \\ g_2(R_p) & \text{if } UP_2 \leq R_p < UP_3 \\ g_3(R_p) & \text{if } UP_3 \leq R_p < UP_4 \\ \dots & \dots \\ g_N(R_p) & \text{if } UP_N \leq R_p < UP_{N+1} \end{cases} \quad \text{Eq.8.8}$$

Such a definition of β is assumed to satisfy $UP_n < UP_{n+1} \quad \forall n$.

In order to proceed, a binary variable x_n is used to indicate whether or not the interval n is considered or not.

Hence, the following equations allow expressing that one and only one interval is selected to define $\beta = f(R_p)$:

$$\beta = \sum_n x_n g_n(R_p) \quad \text{Eq.8.9}$$

$$\sum_n x_n = 1 \quad \text{Eq.8.10}$$

$$x_n \in \{0,1\} \quad \text{Eq.8.11}$$

In particular, for a piecewise linear function:

$$\beta = \sum_n x_n (a_n R_p + b_n) \quad \text{Eq.8.12}$$

and for a two-piece constant function the following expression allows selecting one value out of two:

$$\beta = xb_1 + (1 - x)b_2 \quad \text{Eq.8.13}$$

The next step is constraining the value of the binary variable x_n depending on the value of R_p :

$$x_n = f(R_p) \quad \forall n \quad \text{Eq.8.14}$$

This is done by the following set of constraints:

$$UP_n x_n \leq R_p < UP_{n+1} x_n \quad \forall n \quad \text{Eq.8.15}$$

which can be implemented in an Algebraic Modelling Language by:

$$UP_n x_n \leq R_p \quad \forall n \quad \text{Eq.8.16}$$

$$R_p \leq (UP_{n+1} - \varepsilon) x_n \quad \forall n \quad \text{Eq.8.17}$$

using a small enough value ε to implement the strict inequality if this option is not available in the software tool employed (otherwise, equality will lead to ambiguity and further numerical problems).

Hence, the original NLP model turns into a MINLP model. Moreover, it must be noted that another non linearity, or rather the R_p ratio, is added to the original non-convex bilinear terms contained in the individual component balance equations.

8.2.2.4 Objective function

The water network optimisation problem is aimed at maximizing the total treatment performance. A simple objective function is adopted to define

such a performance as the minimization of the sum of the product of the inlet flow of the streams $i \in TU$ for the specific cost coefficient defined for each treatment unit ($COST_{TU1}$ and $COST_{TU2}$, for the treatment units TU1 and TU2, respectively):

$$\varphi = \sum_{\substack{tu \in TU \\ j \in \text{OUT}}} F^j \text{ COST}^{tu} \quad \text{Eq.8.18}$$

8.3 Case studies

Feasibility and robustness of the model were ensured by testing the model under limit situations (e.g. considering no limits on the discharge composition, and an infinite cost for the TU2= AOPs).

Furthermore, several case studies were addressed with the aim of investigating the potentiality of the proposed methodology and were obtained by:

- changing the values of the cost coefficients;
- changing the discharge composition regulations for each pollutant (namely concentrations of BOD₅ and COD at the discharge point);
- eliminating some interconnections (e.g. possible direct discharge of the inlet streams to the discharge point, or rather connections SU1_MU3 and SU2_MU3 in Figure 8.1);
- changing the concentrations of BOD₅ and COD entering with the inlet streams;
- changing the flowrates of the inlet streams.

All the investigated case studies (CS_1, CS_2,...,CS_8) are summarized in the following Table 8.1:

Water supply chain management

Table 8.1 Case studies to investigate the potentiality of the methodology

	CS_1	CS_2	CS_3	CS_4	CS_5	CS_6	CS_7	CS_8
*[BOD ₅] _{RWWS}	65.0	65.0	65.0	65.0	65.0	65.0	65.0	40.0
*[COD] _{NRWWS}	250.0	250.0	250.0	250.0	250.0	250.0	250.0	133.0
*[BOD ₅] _{RWWS}	150.0	150.0	150.0	150.0	150.0	150.0	150.0	125.0
*[COD] _{NRWWS}	375.0	375.0	375	375	375	375.0	375.0	250.0
*[BOD ₅] _D	≤ 25.0	≤ 25.0	≤ 25.0	≤ 25.0	≤ 25.0	= 25.0	= 25.0	= 25.0
*[COD] _D	≤ 125.0	≤ 125.0	≤ 125.0	≤ 125.0	≤ 125.0	= 125.0	=125.0	=125.0
**F _{RWWS}	30.0	30.0	30.0	30.0	30.0	30.0	50.0	50.0
**F _{NRWWS}	100.0	100.0	100.0	100.0	100.0	100.0	50.0	50.0
***COST _{TU1}	1.0	1.0	1.0	1.0	1.0	1.0	1.0	1.0
***COST _{TU2}	1.0	1.0	10.0	2.0	100.0	100.0	100.0	100.0
SU1 _{MU3}	=0.0	≠0.0	≠0.0	≠0.0	≠0.0	≠0.0	≠0.0	≠0.0
SU2 _{MU3}	=0.0	≠0.0	≠0.0	≠0.0	≠0.0	≠0.0	≠0.0	≠0.0

[BOD₅]_{RWWS} and [COD]_{RWWS}, are the concentrations of BOD₅ and of COD entering with the recalcitrant wastewater

Advanced Oxidation Process Models for Optimisation and Decision Making support in Water Management

[BOD₅]_{NRWWS}, [COD]_{NRWWS}, are the concentrations of BOD₅ and of COD entering with the non-recalcitrant wastewater

[BOD₅]_D and [COD]_D, define the discharge composition for each pollutant or rather the concentrations of BOD₅ and of COD, respectively that are fixed for the discharge point (according to the current law)

F_{RWWS} and F_{NRWWS} are the flowrates defined for the recalcitrant and non-recalcitrant wastewater, respectively

COST_{TU1} cost coefficient of the treatment unit TU1= biological system

COST_{TU2} cost coefficient of the treatment unit TU2= AOP

SU1_MU3 direct discharge of the inlet recalcitrant wastewater to the discharge point

SU2_MU3 direct discharge of the inlet non-recalcitrant wastewater to the discharge point

*all the concentrations are expressed in mg L⁻¹

**all the flowrates are expressed as ton h⁻¹

The limit situations that have been investigated are not reported in Table 8.1. Particularly, the limit situation that assumes no limits on the discharge composition, is the same as CS₂-CS₅ with the only difference that [BOD₅]_D and [COD]_D were set equal to 1000000.0 mg L⁻¹ or rather a value great enough to avoid regulation limits on the discharge composition. The other limit situation is also the same as CS₂-CS₅ but with a COST_{TU2} set to a very high value (e.g. 1000000 € ton¹).

It must be noted that all the case studies addressed the treatment of both a recalcitrant wastewater ($R_p = [BOD_5]_{RWWS}/[COD]_{RWWS} = 65.0/250.0$ and $40.0/133.0 < 0.4$) and a non-recalcitrant wastewater ($R_p = [BOD_5]_{NRWWS}/[COD]_{NRWWS} = 150.0/375.0$ and $125.0/250.0 \geq 0.4$)

Finally, regarding the removal efficiency for each treatment unit and for each component, the values presented in the following Table 8.2 and depending on the R_p (= BOD₅/COD) value have been fixed:

Table 8.2 Values of the efficiency removal defined for each treatment unit (TU1 and TU2) and each component (BOD₅ and COD), expressed as a function of the $R_p = BOD_5/COD$ ratio

Efficiency of treatment unit TU1 (biological process) for the removal of BOD₅ and COD

	if $R_p < 0.40$	if $R_p \geq 0.40$
$\beta_{BOD_5}^{TU1}$	0.00	0.80
β_{COD}^{TU1}	0.20	0.85

Efficiency of treatment unit TU2 (AOP) for the removal of BOD₅ and COD

	if $R_p < 0.40$	if $R_p \geq 0.40$
$\beta_{BOD_5}^{TU2}$	0.70	0.85
β_{COD}^{TU2}	0.75	0.90

8.4 Results and Discussion

Starting from the general superstructure shown in Figure 8.1, the optimisation of the wastewater network has been solved by using the Branch-And-Reduce Optimisation Navigator-BARON solver in GAMS (Tawarmalani and Sahinidis, 2005). This solver was adopted because the bilinear terms (in Equations (8.2) and (8.7)) in the model cause it to be highly non-linear and to have multiple local optima whose presence calls for the application of global optimisation techniques (Liberti et al., 2006).

BARON solver provides a global solution of nonlinear (NLP) and mixed-integer nonlinear programs (MINLP) by implementing deterministic global optimisation algorithms of the branch-and-bound type.

First the limit situations will be analysed and discussed and then the main results of the preliminary novel proposed methodology will be highlighted.

In the case of very permissive limits on the discharge composition, no treatment would be required. Coherently, in this case, the optimal solution sets all flowrates to zero except for the direct discharge to the environment (SU1_MU3 and SU2_MU3), which matches the corresponding inlet flows.

A second limit situation is obtained by setting the AOP treatment cost much higher (1000000 € ton¹) than the one associated to the biological system (1 € ton¹). In this second case, although the cost of the AOP treatment is comparatively very high, the solution requires the AOP treatment because of the constraints on the discharge composition ($[BOD_5]_D \leq 25.0 \text{ mg L}^{-1}$, $[COD]_D \leq 125.0 \text{ mg L}^{-1}$). The same optimal solution is obtained when considering a cost coefficient of 100 € ton¹ (results will be detailed later on) since the discharge composition constraints have to be met despite the cost.

These results prove the robustness of the model at properly describing the system. Starting from this conclusion, several case studies exploring different scenarios, were solved and are discussed below.

Case studies CS_1 and CS_2 have been analysed and compared in order to test the response of the model in the case of allowing also a direct discharge of the wastewater streams, into the environment. As expected, in the CS_2 case the model provides a solution characterized by a lower amount of wastewater to be treated by TU1 and TU2 than the one obtained in the CS_1 case (137.9 ton h⁻¹ against 176.1 ton h⁻¹). This can be explained considering that when direct discharge to the environment is allowed, the regulation limits can be met by allowing lowering the concentration also for dilution with the other streams.

Case studies CS_3, CS_4 and CS_5 were set in order to analyze the response of the model to a gradual increase of the cost coefficients related to the TU2= AOP (while the cost of TU1 was maintained constant). In this case the model gave a coherent and feasible solution. By increasing the cost coefficient, the amount of wastewater to be treated by AOP decreases.

Particularly, first the same solution was obtained in the case of setting $COST_TU2= 1$ and $COST_TU2= 2$. The wastewater to be treated by the AOP in both cases resulted to be 117.1 ton h^{-1} . This shows that the model is not sensitive to low variations in the cost coefficients related to the different treatment units. Conversely, when $COST_TU2= 10$, and $COST_TU2= 100$, the amount of wastewater to be treated by AOP decreased and resulted in a value of 95.1 and 91.9 ton h^{-1} , respectively.

The case study CS_6 was analysed and compared with CS_5 in order to evaluate the response of the model to a variation in the discharge composition regulations for each pollutant.

In the CS_6 case, contrarily to CS_5, a strict limit concentration was set for the BOD₅ ($[BOD_5]_D= 25.0 \text{ mg L}^{-1}$) and COD ($[COD]_D= 125.0 \text{ mg L}^{-1}$). Hence, in the CS_6 case study, the possibility of obtaining a water with a quality higher than the one established by the law (e.g. as in the CS_5 case study setting $[BOD_5]_D \leq 25.0 \text{ mg L}^{-1}$, $[COD]_D \leq 125.0 \text{ mg L}^{-1}$), is not allowed.

In the CS_6 case, as expected, the model gives a solution providing a final outlet characterized by a $[BOD_5]_D= 25.0 \text{ mg L}^{-1}$ and $[COD]_D= 125.0 \text{ mg L}^{-1}$, with a total amount of wastewater to be treated by TU1 and TU2 of 186.4 ton h^{-1} . This amount, as expected, resulted to be lower than the one obtained in the CS_5 case (217.5 ton h^{-1}).

For this reason the subsequent two case studies, or rather CS_7 and CS_8, were solved fixing strict discharge composition regulations ($[BOD_5]_D= 25.0 \text{ mg L}^{-1}$ and $[COD]_D= 125.0 \text{ mg L}^{-1}$).

The case study CS_7 was addressed and compared with the case study CS_6 in order to discuss the effect of the variation in the flowrate of the wastewaters entering the network.

Particularly, Figure 8.5 (a) –(b) shows the graphical solution obtained in the case study CS_7 and CS_6 respectively.

Advanced Oxidation Process Models for Optimisation and Decion Making support in Water Mangement

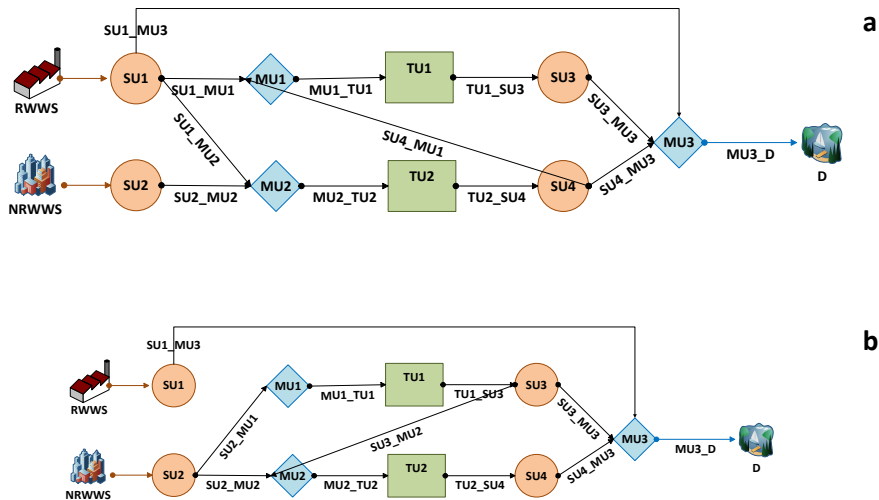


Figure 8.5. Optimal structure of the wastewater network obtained by solving the case studies CS_7 (a) and CS_6 (b)

Particularly the case study CS_7 compared with the case study CS_6, establishes a decrease of the total inlet flowrate (100.0 ton h⁻¹ vs 130 ton h⁻¹), a decrease of the flowrate of the non-recalcitrant wastewater (50.0 ton h⁻¹ vs 100.0 ton h⁻¹) and a slight increase of the flowrate of the recalcitrant wastewater (50.0 ton h⁻¹ vs 30.0 ton h⁻¹).

As can be observed by solving the case study CS_7, the provided solution establishes the mixing of part of the recalcitrant and of the non-recalcitrant wastewater to be treated by the TU2= AOP. Moreover, it also defines the post-treatment via TU1= biological systems of part of the water previously treated with TU2= AOP.

Conversely the optimal solution for the case study CS_6, is a wastewater network in which part of the non-recalcitrant wastewater is sent to TU1 and another part to TU2, while the recalcitrant wastewater is sent to the mixer MU3 and its concentration is lowered for dilution (because of the higher values of the volumes of waters to be treated). Furthermore, in this case the AOP is established to be used as post-treatment for a part of the water previously treated by TU1.

It is important to notice that if it is mandatory to avoid the treatment by dilution the model covers this possibility by fixing equal to 0 the flowrates related to the direct discharge (SU1_MU3 and SU2_MU3).

Hence, as can be noticed, the variation in the flowrate to be treated led to very different solutions.

A table (Tale 8.3) summarizing the results in terms of flowrates of each stream as well as concentrations of the contaminants in each stream, obtained for CS7 and CS_6 is also presented.

Table 8.3 Flowrates of each stream as well as concentrations of the contaminants in each stream corresponding to the optimal structures of the wastewater network obtained by solving the case studies CS_7 (Figure 8.5-a) and CS_6 (Figure 8.5-b)

CASE STUDY CS_7			
	Flowrate	[BOD ₅]	[COD]
	ton h ⁻¹	mg L ⁻¹	mg L ⁻¹
RWWS	50.0	65.0	250.0
NRWWS	50.0	150.0	375.0
SU1_MU1	7.0	65.0	250.0
SU1_MU2	17.6	65.0	250.0
SU1_MU3	25.3	65.0	250.0
SU2_MU1	0.0	/	/

Advanced Oxidation Process Models for Optimisation and Decision Making support in Water Management

SU2_MU2	50.0	150.0	375.0
SU2_MU3	0.0	/	/
MU1_TU1	66.7	41.1	102.8
MU2_TU2	67.6	127.7	342.3
TU1_SU3	66.7	8.2	82.2
TU2_SU4	67.6	38.3	85.5
SU3_MU2	0.0	/	/
SU3_MU3	66.7	8.2	82.2
SU4_MU1	59.7	38.3	85.5
SU4_MU3	7.9	38.30	85.50
MU3_D	130.0	25.0	125.0

CASE STUDY: CS_6

RWWS	30.0	65.0	250.0
NRWWS	100.0	150.0	375.0
SU1_MU1	0.0	/	/
SU1_MU2	0.0	/	/

Water supply chain management

SU1_MU3	30.0	65.0	250.0
SU2_MU1	91.7	150.0	375.0
SU2_MU2	8.2	150.0	375.
SU2_MU3	0.0	/	/
MU1_TU1	91.7	150.0	375.00
MU2_TU2	95.1	40.4	306.5
TU1_SU3	91.7	30.0	300.0
TU2_SU4	95.1	12.10	76.60
SU3_MU2	86.8	30.0	300.0
SU3_MU3	4.8	30.0	300.0
SU4_MU1	0.0	/	/
SU4_MU3	95.1	12.10	76.6
MU3_D	130.0	25.0	125.0

Finally, the case study CS_8 was faced and the obtained optimal solution was compared with the one provided by the case study CS_7 (Figure 8.5-a). The aim was to discuss the effect of the variation in the concentrations of the contaminants of the inlet wastewaters.

Advanced Oxidation Process Models for Optimisation and Decision Making support in Water Management

Figure 8.6 shows the graphical solution obtained by solving CS_8.

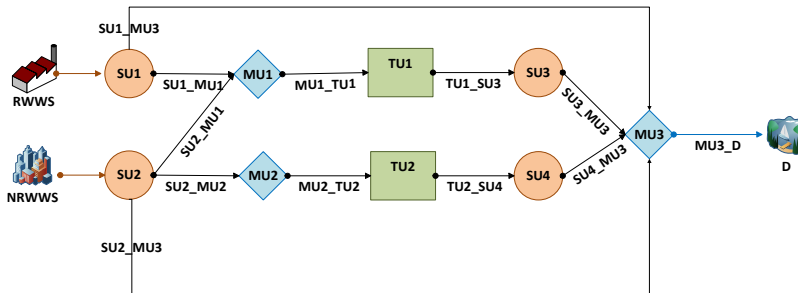


Figure 8.6. Optimal structure of the wastewater network obtained by solving the case study CS_8

Particularly the case study CS_8 compared with the case study CS_7, establishes a decrease of the concentrations of the contaminants entering with the wastewaters to be treated. However, the ratio was maintained about the same so to still consider the treatment of a recalcitrant and a non-recalcitrant wastewater.

In this case, a very different solution was provided establishing only the mixing of part of the non-recalcitrant wastewater with the recalcitrant one to be sent to TU1 and the direct discharge of part of both wastewaters. The use of the AOP as pre-treatment or post-treatment in this case is not taken into account.

Finally Table 8.4 summarizes the corresponding results in terms of flowrates of each stream as well as concentrations of the contaminants in each stream.

Table 8.4 Flowrates of each stream as well as concentrations of the contaminants in each stream corresponding to the optimal structures of the wastewater network obtained by solving the case study CS_8 (Figure 8.6)

CASE STUDY CS_8		
Flowrate	[BOD ₅]	[COD]
ton h ⁻¹	mg L ⁻¹	mg L ⁻¹

Water supply chain management

RWWS	50.0	40.0	133.0
NRWWS	50.0	125.0	250.0
SU1_MU1	43.6	40.0	133.0
SU1_MU2	0.0	/	/
SU1_MU3	6.3	40.0	133.0
SU2_MU1	23.0	125.0	250.0
SU2_MU2	19.2	125.0	250.0
SU2_MU3	7.6	125.0	250.0
MU1_TU1	66.7	69.3	173.4
MU2_TU2	19.2	125.0	250.0
TU1_SU3	66.7	13.8	138.7
TU2_SU4	19.2	18.7	25.0
SU3_MU2	0.0	/	/
SU3_MU3	66.7	13.8	138.70
SU4_MU1	0.0	/	/

Advanced Oxidation Process Models for Optimisation and Decision Making support in Water Management

SU4_MU3	19.2	18.7	25.0
MU3_D	100.0	25.0	125.0

As illustrative example of a solution provided in the case of considering the possibility of obtaining a water with extra quality (not strict regulations on the discharge composition, or rather $[BOD_5]_D \leq 25.0 \text{ mg L}^{-1}$, $[COD]_D \leq 125.0 \text{ mg L}^{-1}$), the graphical solution of the case study CS_5 is shown in Figure 8.7.

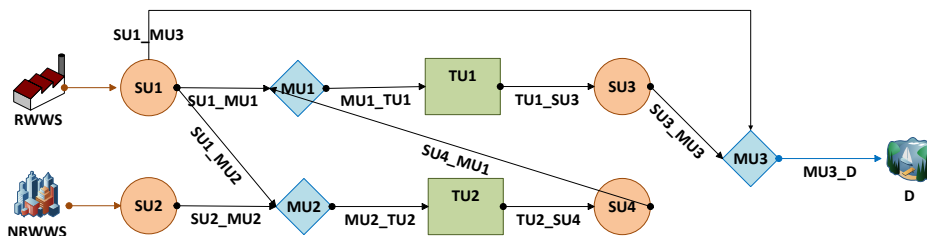


Figure 8.7. Optimal structure of the wastewater network obtained by solving the case study CS_5

A table summarizing the corresponding results in terms of flowrates of each stream and concentrations of the contaminants in each stream, is presented as well.

Table 8.5 Flowrates of each stream as well as concentrations of the contaminants in each stream corresponding to the optimal structures of the wastewater network obtained by solving the case study CS_5 (Figure 8.7)

	Flowrate ton h ⁻¹	[BOD ₅] mg L ⁻¹	[COD] mg L ⁻¹
RWWSS	30.0	65.0	250.0
NRWWS	100.0	150.0	375.0

Water supply chain management

SU1_MU1	16.1	65.0	250.0
SU1_MU2	9.5	65.0	250.0
SU1_MU3	4.3	65.0	250.0
SU2_MU1	0.0	/	/
SU2_MU2	82.4	150.0	375.0
SU2_MU3	0.0	/	/
MU1_TU1	125.6	60.3	150.8
MU2_TU2	91.9	141.2	362.0
TU1_SU3	125.6	12.0	120.6
TU2_SU4	91.9	42.3	90.5
SU3_MU2	0.0	/	/
SU3_MU3	125.6	12.0	120.6
SU4_MU1	91.9	42.30	90.5
SU4_MU3	0.0	/	/
MU3_D	130.0	13.8	125.0

As can be seen in this case the optimal solution model provides a water with a concentration of BOD₅ at the discharge lower than the one established by the law ($13.8 < 25.0 \text{ mg L}^{-1}$). Moreover in this case the water treated by the AOP is totally sent back to the biological system.

8.5 Conclusions

A novel modelling approach including the so called BOD₅/COD ratio method has been proposed for allowing the optimisation of a wastewater treatment combining conventional biological systems and Advanced Oxidation Processes (AOPs). The effect of the interrelations between the different components entering with the inlet streams was also taken into account, as well as the effect of their concentration on the performance of the different treatments.

Feasibility and robustness were demonstrated by solving a series of different case studies addressing different possible behaviors of the wastewater treatment network system.

Despite its simplicity, the proposed model represents a first preliminary approach on one hand in the PSE field of the water network optimisation because it takes into account for the first time the effect of the interrelations between the inlet contaminants on the performance of the treatment units. On the other hand, in the AOPs field, it is the first time, to the best knowledge of the author, that the combination of conventional biological systems and AOPs, is faced following a modelling approach typically followed in the PSE field. Hence, this preliminary modelling proposal opens a new promising research line that will need further investigation effort.

The proposed mathematical formulation will be the starting point for the development of more complex formulations including a greater number of treatment units and technologies, characterized by different operational and investment costs as a function of the treatment units and of the contaminants to be treated. Considering whether or not some treatments should be used, and considering associated fixed costs, would lead to more complex Mixed-Integer Non-Linear formulations (MINLP). These more complex formulations will require the development of a proper solution strategy ensuring the global optimum and the convergence of the model.

Moreover, a formulation that can also take into account the toxicity of the wastewaters (that cannot be treated by dilution) represents a challenge task of future work.

8.6 Acknowledgements

This work was supported by the Spanish “Ministerio de Economía, Industria y Competitividad (MINECO)” and the European Regional Development Fund, both funding the research Project AIMS (DPI2017-87435-R). Francesca Audino, particularly acknowledges the MINECO for the PhD grant [BES-2013-065545].

9 Final remarks and future work

This chapter summarizes the conclusions of the thesis and presents an analysis of further improvements and research lines that may develop from this work.

9.1 Conclusions

Different advanced oxidation processes, namely Fenton, photo-Fenton and VUV photo-oxidation, were investigated and compared for the treatment of

PCT aqueous solution, by evaluating the following performance indicators (KPIs):

- Concentration of the target contaminant ($[C_i]$), measured during an initial time interval until the detection limit is reached;
- Concentration of Total Organic Carbon ([TOC]), measured along the whole treatment span and providing the maximum attainable conversion;
- Cytotoxicity ([TOX]), measured at planned intervals and determining the toxicity of the effluent resulting from the treatment;
- Reaction rate (k), measured as the kinetic constant of the pseudo-first order kinetic model fit to the evolution of the concentration of TOC.

Among the selected AOPs, VUV photo-oxidation and photo-Fenton showed the most promising results:

- VUV photo-oxidation allowed attaining total removal of the target compound and total conversion of TOC. Moreover, no toxicity was detected after the whole treatment span. However, the low reaction rates obtained were shown to be caused by a limited irradiated volume;
- photo-Fenton allowed attaining total removal of the target compound under all the investigated operating conditions. Conversely, the best results in terms of TOC conversion were attained when high concentrations of Fenton reagents were used and by performing the dosage of the oxidant. Hence, it was shown the need of improving the operating conditions for a proper application of the photo-Fenton treatment. Finally, concerning the cytotoxicity, intermediate treatment stages showed higher toxicity than the starting one. Hence [TOX] in the case of the photo-Fenton process resulted to be a key KPI for the evaluation of the feasibility of such process for the treatment of an organic compound.

In addition to the experimental study, the thesis also focused on transforming “data into knowledge” by proposing different modelling approaches. The modelling task was aimed at allowing the subsequent implementation of proper optimisation, control and automation strategies as well as at the modelling and optimisation of general wastewater networks. The modelling effort was focused on Fenton/photo-Fenton processes and on improving their operating conditions.

Accordingly, two practical kinetic models for Fenton and photo-Fenton degradation of organic compounds have been proposed and validated.

- A conventional First Principles Model, based on a line source radiation model with spherical and isotropic emission, was developed for the prediction of Fenton and photo-Fenton degradation of PCT and the oxidant (H_2O_2) consumption. The proposed model was fitted to the experimental data from the pilot plant described in Chapter 3. The proposed model satisfactorily reproduced the system behavior ($\text{RMSE}_{\text{PCT}} = 6.80\%$ and $\text{RMSE}_{\text{H}_2\text{O}_2} = 9.67\%$).
- A non-conventional First Principles Model, describing the photo-Fenton degradation of the target compound and the oxidant consumption together with the TOC evolution, was proposed. This novel approach is based on a contaminant degradation mechanism, depending on the number of carbon atoms in the molecule to be decomposed and that is usable for different target compounds. The proposed model represents a first attempt of implementing a general approach that can describe the Fenton/photo-Fenton degradation of different wastewater systems composed by single or multiple organic contaminants by means of lumped parameters (e.g. TOC) that offer practical characterization of complex mixtures of chemicals. The fitting and validation of the proposed model was performed using three different model compounds and the pilot plant described in Chapter 3. The model provided acceptable predictions of the system behavior with a minimum RMSE value of 7% for the TOC and 11%, for H_2O_2 .

Once a process model has been proposed and validated, it can be systematically exploited to determine efficient operation modes or design alternatives. The thesis has addressed this issue at two different levels: the optimisation of a control recipe and the design of a treatment network.

Regarding control recipes, the thesis proposes a dynamic optimisation framework for taking advantage of available kinetic models and determining the best hydrogen peroxide dosage profile. The simplified model by Cabrera Reina et al., 2012 was adapted to include hydrogen peroxide dosage in a fed-batch operation mode. Economic and environmental objectives and constraints were included to develop a dynamic optimisation problem that was implemented in JModelica and solved using a direct simultaneous optimisation method (IPOPT).

The solution of a series of multi-objective scenarios provided useful understanding of the problem trade-offs, which were mapped and analysed, and demonstrated the potential of the dynamic optimisation framework to provide optimal operating strategies and, particularly, optimal dosage profiles.

Finally, the thesis considered the combination of cheaper conventional biological processes with more expensive Advanced Oxidation Processes (AOPs). A Mixed-Integer Non Linear Programming (MINLP) model for the optimisation of a general wastewater network was proposed based on a superstructure of alternative designs, which was implemented and solved in GAMS.

The model considers the combination of conventional and Advanced Oxidation Processes and introduces the interrelations between components. The BOD₅/COD ratio method, describing the removal efficiency of BOD₅ and COD of a treatment, was introduced for modelling the variation of the biodegradability of the influents. This novel formulation allows determining the extent of the AOP treatments when combined with biological treatments, and solving the trade-off between cost and treatment efficiency.

9.2 Further work

The present work paves the way for new research lines:

- The potentiality of introducing a lumped parameter as a measure of the water quality rather than considering the degradation of a single pollutant (conventional modelling approach) must be further investigated. This is related with the increasing awareness of the importance of considering the potential toxic effects of mixtures of chemicals on the aquatic environment and human health.
- The modelling of the multi-step fed-batch dosage of H₂O₂ must be addressed. On one hand the model can be used to improve the proposed recipe optimisation strategy. On the other hand, it can be developed with the aim of being used for control purposes as well (e.g. connecting the variation of the oxidant concentration with easily measurable variables).
- Finally a more complex formulation for modelling and optimisation of a wastewater network combining conventional and non-conventional treatments must

Final remarks and future work

be developed. Particularly, a greater number of treatment units and technologies with different operational and investment costs, should be considered.

References

- Alfano, O.M., Romero, R.L., Cassano, A.E., 1986. Radiation field modelling in photoreactors—I. homogeneous media. *Chem. Eng. Sci.* 41, 421–444. doi:10.1016/0009-2509(86)87025-7
- Almazan, G., Liu, H.-N., Khorchid, A., Sundararajan, S., Martinez-Bermudez, A.K., Chemtob, S., 2000. Exposure of developing oligodendrocytes to cadmium causes HSP72 induction, free radical generation, reduction in glutathione levels, and cell death. *Free Radic. Biol. Med.* 29, 858–869. doi:10.1016/S0891-5849(00)00384-1
- Andreozzi, R., Carpio, V., Insola, A., Marotta, R., 1999. Advanced oxidation processes (AOP) for water purification and recovery. *Catal. Today* 53, 51–59. doi:10.1016/S0920-5861(99)00102-9
- Andreozzi, R., D’Apuzzo, A., Marotta, R., 2000. A kinetic model for the degradation of benzothiazole by Fe³⁺-photo-assisted Fenton process in a completely mixed batch reactor. *J. Hazard. Mater.* 80, 241–257. doi:10.1016/S0304-3894(00)00308-3
- Antunes, S.C., Freitas, R., Figueira, E., Gonçalves, F., Nunes, B., 2013. Biochemical effects of acetaminophen in aquatic species: edible clams *Venerupis decussata* and *Venerupis philippinarum*. *Environ. Sci. Pollut. Res.* 20, 6658–6666. doi:10.1007/s11356-013-1784-9
- Arslan-Alaton, I., 2007. Degradation of a commercial textile biocide with advanced oxidation processes and ozone. *J. Environ. Manage.* 82, 145–154. doi:10.1016/j.jenvman.2005.12.021
- Audino, F., Conte, L.O., Schenone, A.V., Pérez-Moya, M., Graells, M., Alfano, O.M., 2019. A kinetic study for the Fenton and photo-Fenton paracetamol degradation in an annular photoreactor. *Environ. Sci. Pollut. Res.* 26, 4312–4323. doi:10.1007/s11356-018-3098-4

- Babuponnusami, A., Muthukumar, K., 2012. Advanced oxidation of phenol: A comparison between Fenton, electro-Fenton, sono-electro-Fenton and photo-electro-Fenton processes. *Chem. Eng. J.* 183, 1–9. doi:10.1016/j.cej.2011.12.010
- Badawy, M.I., Ghaly, M.Y., Gad-Allah, T.A., 2006. Advanced oxidation processes for the removal of organophosphorus pesticides from wastewater. *Desalination* 194, 166–175. doi:10.1016/j.desal.2005.09.027
- Baran, W., Adamek, E., Ziemiańska, J., Sobczak, A., 2011. Effects of the presence of sulfonamides in the environment and their influence on human health. *J. Hazard. Mater.* 196, 1–15. doi:10.1016/j.jhazmat.2011.08.082
- Bautista, P., Mohedano, A.F., Gilarranz, M.A., Casas, J.A., Rodriguez, J.J., 2007. Application of Fenton oxidation to cosmetic wastewaters treatment. *J. Hazard. Mater.* 143, 128–134. doi:10.1016/j.jhazmat.2006.09.004
- Bautitz, I.R., Nogueira, R.F.P., 2007. Degradation of tetracycline by photo-Fenton process—Solar irradiation and matrix effects. *J. Photochem. Photobiol. A Chem.* 187, 33–39. doi:10.1016/j.jphotochem.2006.09.009
- Beamon, B.M., 1998. Supply chain design and analysis: *Int. J. Prod. Econ.* 55, 281–294. doi:10.1016/S0925-5273(98)00079-6
- Benatti, C.T., Tavares, C.R.G., Guedes, T.A., 2006. Optimization of Fenton's oxidation of chemical laboratory wastewaters using the response surface methodology. *J. Environ. Manage.* 80, 66–74. doi:10.1016/j.jenvman.2005.08.014
- Bianco, B., De Michelis, I., Vegliò, F., 2011. Fenton treatment of complex industrial wastewater: Optimization of process conditions by surface response method. *J. Hazard. Mater.* 186, 1733–1738. doi:10.1016/j.jhazmat.2010.12.054
- Biegler, L.T., 2007. An overview of simultaneous strategies for dynamic optimization. *Chem. Eng. Process. Process Intensif.* 46, 1043–1053. doi:10.1016/j.cep.2006.06.021

References

- Boix, M., Montastruc, L., Pibouleau, L., Azzaro-Pantel, C., Domenech, S., 2011. A multiobjective optimization framework for multicontaminant industrial water network design. *J. Environ. Manage.* 92, 1802–1808. doi:10.1016/j.jenvman.2011.02.016
- Bossmann, S.H., Oliveros, E., Göb, S., Siegwart, S., Dahlen, E.P., Payawan, L., Straub, M., Wörner, M., Braun, A.M., 1998. New Evidence against Hydroxyl Radicals as Reactive Intermediates in the Thermal and Photochemically Enhanced Fenton Reactions. *J. Phys. Chem. A* 102, 5542–5550. doi:10.1021/jp980129j
- Boxall, A.B.A., 2004. The environmental side effects of medication. *EMBO Rep.* 5, 1110–1116. doi:10.1038/sj.embor.7400307
- Braun, A.M., Jakob, L., Oliveros, E., do Nascimento, C.A.O., 2007. Up-Scaling Photochemical Reactions. pp. 235–313. doi:10.1002/9780470133491.ch3
- Brillas, E., Calpe, J. C., Casado, J., 2000. Mineralization of 2,4-D by advanced electrochemical oxidation processes. *Water Res.* 34, 2253–2262. doi:10.1016/S0043-1354(99)00396-6
- Cabrera Reina, A., Santos-Juanes Jordá, L., García Sánchez, J.L., Casas López, J.L., Sánchez Pérez, J.A., 2012. Modelling photo-Fenton process for organic matter mineralization, hydrogen peroxide consumption and dissolved oxygen evolution. *Appl. Catal. B Environ.* 119–120, 132–138. doi:10.1016/j.apcatb.2012.02.021
- Cabrera Reina, A., Santos-Juanes, L., García Sánchez, J.L., Casas López, J.L., Maldonado Rubio, M.I., Li Puma, G., Sánchez Pérez, J.A., 2015. Modelling the photo-Fenton oxidation of the pharmaceutical paracetamol in water including the effect of photon absorption (VRPA). *Appl. Catal. B Environ.* 166–167, 295–301. doi:10.1016/j.apcatb.2014.11.023
- Cassano, A.E., Martin, C.A., Brandi, R.J., Alfano, O.M., 1995. Photoreactor Analysis and Design: Fundamentals and Applications. *Ind. Eng. Chem. Res.* 34, 2155–2201. doi:10.1021/ie00046a001

- Catalkaya, E.C., Kargi, F., 2007. Color, TOC and AOX removals from pulp mill effluent by advanced oxidation processes: A comparative study. *J. Hazard. Mater.* 139, 244–253. doi:10.1016/j.jhazmat.2006.06.023
- Chen, R., Pignatello, J.J., 1997. Role of Quinone Intermediates as Electron Shuttles in Fenton and Photoassisted Fenton Oxidations of Aromatic Compounds. *Environ. Sci. Technol.* 31, 2399–2406. doi:10.1021/es9610646
- Commission Implementing Decision (EU) 2015/495 of 20 March 2015 establishing a watch list of substances for Union-wide monitoring in the field of water policy pursuant to Directive 2008/105/EC of the European Parliament and of the Council (notified under document C(2015) 1756) Text with EEA relevance Official Journal L 78, 24.3.2015, p. 40–42 (URL: <https://publications.europa.eu/en/publication-detail/-/publication/a90868de-d1f9-11e4-9de8-01aa75ed71a1/language-en> accessed 04/05/2019)
- Conte, L.O., Farias, J., Albizzati, E.D., Alfano, O.M., 2012. Photo-Fenton Degradation of the Herbicide 2,4-Dichlorophenoxyacetic Acid in Laboratory and Solar Pilot-Plant Reactors. *Ind. Eng. Chem. Res.* 51, 4181–4191. doi:10.1021/ie2023228
- Conte, L.O., Schenone, A. V., Alfano, O.M., 2016. Photo-Fenton degradation of the herbicide 2,4-D in aqueous medium at pH conditions close to neutrality. *J. Environ. Manage.* 170, 60–69. doi:10.1016/j.jenvman.2016.01.002
- Csukás, B., Balogh, S., Kováts, S., Aranyi, A., Kocsis, Z., Bartha, L., 1999. Process design by controlled simulation of the executable structural models. *Comput. Chem. Eng.* 23, S569–S572. doi:10.1016/S0098-1354(99)80140-9
- Csukás, B., Varga, M., Miskolczi, N., Balogh, S., Angyal, A., Bartha, L., 2013. Simplified dynamic simulation model of plastic waste pyrolysis in laboratory and pilot scale tubular reactor. *Fuel Process. Technol.* 106, 186–200. doi:10.1016/j.fuproc.2012.07.024
- da Rocha, O.R.S., Dantas, R.F., Duarte, M.M.M.B., Duarte, M.M.L., da Silva, V.L., 2010. Oil sludge treatment by photocatalysis applying black and white light. *Chem. Eng. J.* 157, 80–85. doi:10.1016/j.cej.2009.10.050

References

- da Rocha, O.R.S., Dantas, R.F., Bezerra Duarte, M.M.M., Lima Duarte, M.M., da Silva, V.L., 2013. Solar photo-Fenton treatment of petroleum extraction wastewater. *Desalin. Water Treat.* 51, 5785–5791. doi:10.1080/19443994.2013.792136
- Dalgic, G., Turkdogan, I., Yetilmezsoy, K., Kocak, E., 2016. Treatment of real paracetamol wastewater by fenton process. *Chem. Ind. Chem. Eng. Q.* 32–32. doi:10.2298/CICEQ150831032D
- Dalgic, G., Turkdogan, I., Yetilmezsoy, K., Kocak, E., 2017. Treatment of real paracetamol wastewater by Fenton process. *Chem. Ind. Chem. Eng. Q.* 23, 177–186. doi:10.2298/CICEQ150831029D
- Daughton, C.G., Ternes, T.A., 1999. Pharmaceuticals and personal care products in the environment: agents of subtle change? *Environ. Health Perspect.* 107, 907–938. doi:10.1289/ehp.99107s6907
- De Gusseme, B., Vanhaecke, L., Verstraete, W., Boon, N., 2011. Degradation of acetaminophen by *Delftia tsuruhatensis* and *Pseudomonas aeruginosa* in a membrane bioreactor. *Water Res.* 45, 1829–1837. doi:10.1016/j.watres.2010.11.040
- De la Cruz, N., Dantas, R.F., Giménez, J., Esplugas, S., 2013. Photolysis and TiO₂ photocatalysis of the pharmaceutical propranolol: Solar and artificial light. *Appl. Catal. B Environ.* 130–131, 249–256. doi:10.1016/j.apcatb.2012.10.003
- De Laurentiis, E., Prasse, C., Ternes, T.A., Minella, M., Maurino, V., Minero, C., Sarakha, M., Brigante, M., Vione, D., 2014. Assessing the photochemical transformation pathways of acetaminophen relevant to surface waters: Transformation kinetics, intermediates, and modelling. *Water Res.* 53, 235–248. doi:10.1016/j.watres.2014.01.016
- Directive 2000/60/EC of the European Parliament and of the Council of 23 October 2000 establishing a framework for Community action in the field of water policy Official Journal L 327 , 22/12/2000 P. 0001 - 0073 (URL: <https://eur-lex.europa.eu/legal-content/EN/TXT/?uri=CELEX%3A32000L0060> accessed 04/05/2019)

Directive 2455/2001/EC, DECISION N° 2455/2001/EC OF THE EUROPEAN PARLIAMENT AND OF THE COUNCIL of 20 November 2001 establishing the list of priority substances in the field of water policy and amending Directive 2000/60/EC Official Journal L 331, 15.12.2001, p. 1-5 (URL: <https://publications.europa.eu/en/publication-detail/-/publication/309e2a94-6831-4bac-b15b-a9cac54cbae0> accessed 04/05/2019)

Directive 2008/105/EC of the European Parliament and of the Council of 16 December 2008 on environmental quality standards in the field of water policy, amending and subsequently repealing Council Directives 82/176/EEC, 83/513/EEC, 84/156/EEC, 84/491/EEC, 86/280/EEC and amending Directive 2000/60/EC of the European Parliament and of the Council Official Journal L 348, 24.12.2008, p. 84–97 (URL: <https://eur-lex.europa.eu/legal-content/GA/TXT/?uri=CELEX:32008L0105> accessed 04/05/2019)

Directive 2013/39/EU of the European Parliament and of the Council of 12 August 2013 amending Directives 2000/60/EC and 2008/105/EC as regards priority substances in the field of water policy Text with EEA relevance Official Journal L 226, 24.8.2013, p. 1–17 (URL: <https://eur-lex.europa.eu/LexUriServ/LexUriServ.do?uri=OJ:L:2013:226:0001:0017:EN:PDF> accessed 04/05/2019)

DOGC núm.3894, DECRET 130/2003, de 13/05/2003, (29.5.2003). (URL: <http://www.gencat.cat/diari/3894/03127147.htm>, accessed 04/05/2019)

Dorota Napierska, Isabella Sanseverino, Robert Loos, Livia Gómez Cortés, Magdalena Niegowska and Teresa Lettieri, Modes of action of the current Priority Substances list under the Water Framework Directive and other substances of interest, EUR 29008 EN, Publications Office of the European Union, Luxembourg, 2018, ISBN 978-92-79-77301-3, doi:10.2760/226911, JRC110117 (URL:[http://publications.jrc.ec.europa.eu/repository/bitstream/JRC110117/jrc_tech_report_moa_final__31may2018\(8\).pdf](http://publications.jrc.ec.europa.eu/repository/bitstream/JRC110117/jrc_tech_report_moa_final__31may2018(8).pdf) accessed 04/05/2019)

EC COM(2012) 252. Communication from the Commission to the council. The combination effect of chemicals Chemical mixtures. Brussels, 31.5.2012.EFSA (European Food Safety Authority), 2008. Opinion of the

References

- Scientific Panel on Plant Protection Products and their 169 Residues to evaluate the suitability of existing methodologies and, if appropriate, the identification of new approaches to assess cumulative and synergistic risks from pesticides to human health with a view to set MRLs for those pesticides in the frame of Regulation (EC) 396/2005. The EFSA Journal 2008, 704, 1-85.
- European Chemical Industry Council-CEFIC, 2018. LANDSCAPE OF THE EUROPEAN CHEMICAL INDUSTRY 2018 (URL <https://www.chemlandscape.cefic.org/wpcontent/uploads/combined/fullDoc.pdf> accessed 04/05/2019).
- European Commission, 2012a, Commission Staff Working Document, European Overview (1/2) Accompanying the Document: “Report From the Commission to the European Parliament and the Council on the Implementation of the Water Framework Directive (2000/60/EC) River Basin Management Plans”.
- Eykhoff, P., 1974. System Identification-Parameter and State Estimation. London: Wiley-Interscience.
- Farias, J., Rossetti, G.H., Albizzati, E.D., Alfano, O.M., 2007. Solar Degradation of Formic Acid: Temperature Effects on the Photo-Fenton Reaction. Ind. Eng. Chem. Res. 46, 7580–7586. doi:10.1021/ie0700258
- Feng, X., Bai, J., Wang, H., Zheng, X., 2008. Grass-roots design of regeneration recycling water networks. Comput. Chem. Eng. 32, 1892–1907. doi:10.1016/j.compchemeng.2007.10.006
- Fenton, H.J.H., 1894. LXXIII.—Oxidation of tartaric acid in presence of iron. J. Chem. Soc., Trans. 65, 899–910. doi:10.1039/CT8946500899
- Flash Eurobarometer 344, ATTITUDES OF EUROPEANS TOWARDS WATER – RELATED ISSUES, TNS Political & Social at the request of Directorate General for Environment, 2012. (URL: http://ec.europa.eu/commfrontoffice/publicopinion/flash/fl_344_summary_en.pdf accessed 04/05/2019)
- Fotakis, G., Timbrell, J.A., 2006. In vitro cytotoxicity assays: Comparison of

LDH, neutral red, MTT and protein assay in hepatoma cell lines following exposure to cadmium chloride. *Toxicol. Lett.* 160, 171–177. doi:10.1016/j.toxlet.2005.07.001

Galan, B., Grossmann, I.E., 1998. Optimal Design of Distributed Wastewater Treatment Networks. *Ind. Eng. Chem. Res.* 37, 4036–4048. doi:10.1021/ie980133h

Gallard, H., de Laat, J., 2000. Kinetic modelling of Fe(III)/H₂O₂ oxidation reactions in dilute aqueous solution using atrazine as a model organic compound. *Water Res.* 34, 3107–3116. doi:10.1016/S0043-1354(00)00074-9

García-Montaño, J., Torrades, F., García-Hortal, J.A., Domènech, X., Peral, J., 2006. Degradation of Procion Red H-E7B reactive dye by coupling a photo-Fenton system with a sequencing batch reactor. *J. Hazard. Mater.* 134, 220–229. doi:10.1016/j.jhazmat.2005.11.013

Giannakis, S., Gamarra Vives, F.A., Grandjean, D., Magnet, A., De Alencastro, L.F., Pulgarin, C., 2015. Effect of advanced oxidation processes on the micropollutants and the effluent organic matter contained in municipal wastewater previously treated by three different secondary methods. *Water Res.* 84, 295–306. doi:10.1016/j.watres.2015.07.030

Göb, S., Oliveros, E., Bossmann, S.H., Braun, A.M., Nascimento, C.A.O., Guardani, R., 2001. Optimal experimental design and artificial neural networks applied to the photochemically enhanced Fenton reaction. *Water Sci. Technol.* 44, 339–345. doi:10.2166/wst.2001.0321

Gonzalez, M.C., Braun, A.M., 1995. VUV photolysis of aqueous solutions of nitrate and nitrite. *Res. Chem. Intermed.* 21, 837–859. doi:10.1163/156856795X00512

Gulkaya, I., Surucu, G., Dilek, F., 2006. Importance of H₂O₂/Fe²⁺ ratio in Fenton's treatment of a carpet dyeing wastewater. *J. Hazard. Mater.* 136, 763–769. doi:10.1016/j.jhazmat.2006.01.006

Heberer, T., Duennbier, U., Reilich, C., Stan, H.-J., 1997. Detection of Drugs and Drug Metabolites in Ground Water Samples of a Drinking Water Treatment Plant. *Fresenius Environ. Bull.* 6, 438–443.

References

- Heberer, T., Reddersen, K., Mechlinski, A., 2002. From municipal sewage to drinking water: fate and removal of pharmaceutical residues in the aquatic environment in urban areas. *Water Sci. Technol.* 46, 81–88. doi:10.2166/wst.2002.0060
- Heragu, S.S., 2006. *Facilities Design*, 2nd Edition.
- Hoff, R.B., Meneghini, L., Pizzolato, T.M., Peralba, M. do C.R., Díaz-Cruz, M.S., Barceló, D., 2014. Structural Elucidation of Sulfaquinoxaline Metabolism Products and Their Occurrence in Biological Samples Using High-Resolution Orbitrap Mass Spectrometry. *Anal. Chem.* 86, 5579–5586. doi:10.1021/ac501132r
- Hoigné, J., Bader, H., 1983. Rate constants of reactions of ozone with organic and inorganic compounds in water—I. *Water Res.* 17, 173–183. doi:10.1016/0043-1354(83)90098-2
- Huston, P.L., Pignatello, J.J., 1999. Degradation of selected pesticide active ingredients and commercial formulations in water by the photo-assisted Fenton reaction. *Water Res.* 33, 1238–1246. doi:10.1016/S0043-1354(98)00330-3
- Ince, N.H., 1999. “Critical” effect of hydrogen peroxide in photochemical dye degradation. *Water Res.* 33, 1080–1084. doi:10.1016/S0043-1354(98)00295-4
- ISO 6332:1988. Water quality — Determination of iron — Spectrometric method using 1, 10-phenanthroline (URL: <https://www.iso.org/standard/12630.html> accessed 04/05/2019)
- Jeong, J., Yoon, J., 2005. pH effect on OH radical production in photo/ferrioxalate system. *Water Res.* 39, 2893–2900. doi:10.1016/j.watres.2005.05.014
- Ji, F., Li, C., Zhang, J., Deng, L., 2011. Heterogeneous photo-Fenton decolorization of methylene blue over LiFe(WO₄)₂ catalyst. *J. Hazard. Mater.* 186, 1979–1984. doi:10.1016/j.jhazmat.2010.12.089
- Jones, O.A.H., Green, P.G., Voulvoulis, N., Lester, J.N., 2007. Questioning the

Excessive Use of Advanced Treatment to Remove Organic Micropollutants from Wastewater. *Environ. Sci. Technol.* 41, 5085–5089. doi:10.1021/es0628248

Jordá, L.S.-J., Martín, M.M.B., Gómez, E.O., Reina, A.C., Sánchez, I.M.R., López, J.L.C., Pérez, J.A.S., 2011. Economic evaluation of the photo-Fenton process. Mineralization level and reaction time: The keys for increasing plant efficiency. *J. Hazard. Mater.* 186, 1924–1929. doi:10.1016/j.jhazmat.2010.12.100

Joss, A., Keller, E., Alder, A.C., Göbel, A., Mc Ardell, C.S., Ternes, T., Siegrist, H., 2005. Removal of pharmaceuticals and fragrances in biological wastewater treatment. *Water Res.* 39, 3139–3152. doi:10.1016/j.watres.2005.05.031

Jung, Y.J., Kim, W.G., Yoon, Y., Kang, J.-W., Hong, Y.M., Kim, H.W., 2012. Removal of amoxicillin by UV and UV/H₂O₂ processes. *Sci. Total Environ.* 420, 160–167. doi:10.1016/j.scitotenv.2011.12.011

Kang, N., Lee, D.S., Yoon, J., 2002. Kinetic modeling of Fenton oxidation of phenol and monochlorophenols. *Chemosphere* 47, 915–924. doi:10.1016/S0045-6535(02)00067-X

Karuppiah, R., Grossmann, I.E., 2006. Global optimization for the synthesis of integrated water systems in chemical processes. *Comput. Chem. Eng.* 30, 650–673. doi:10.1016/j.compchemeng.2005.11.005

Kiwi, J., Pulgarin, C., Peringer, P., Grätzel, M., 1993. Beneficial effects of homogeneous photo-Fenton pretreatment upon the biodegradation of anthraquinone sulfonate in waste water treatment. *Appl. Catal. B Environ.* 3, 85–99. doi:10.1016/0926-3373(93)80070-T

Klamerth, N., Malato, S., Agüera, A., Fernández-Alba, A., 2013. Photo-Fenton and modified photo-Fenton at neutral pH for the treatment of emerging contaminants in wastewater treatment plant effluents: A comparison. *Water Res.* 47, 833–840. doi:10.1016/j.watres.2012.11.008

Koleva, M.N., Polykarpou, E.M., Liu, S., Styan, C.A., Papageorgiou, L.G., 2015. Synthesis of Water Treatment Processes using Mixed Integer Programming. pp. 1379–1384. doi:10.1016/B978-0-444-63577-8.50075-9

References

- Kolpin, D.W., Furlong, E.T., Meyer, M.T., Thurman, E.M., Zaugg, S.D., Barber, L.B., Buxton, H.T., 2002. Pharmaceuticals, Hormones, and Other Organic Wastewater Contaminants in U.S. Streams, 1999–2000: A National Reconnaissance. *Environ. Sci. Technol.* 36, 1202–1211. doi:10.1021/es011055j
- Kuo, W.-C.J., Smith, R., 1997. Effluent treatment system design. *Chem. Eng. Sci.* 52, 4273–4290. doi:10.1016/S0009-2509(97)00186-3
- Kusic, H., Koprivanac, N., Bozic, A., Selanec, I., 2006. Photo-assisted Fenton type processes for the degradation of phenol: A kinetic study. *J. Hazard. Mater.* 136, 632–644. doi:10.1016/j.jhazmat.2005.12.046
- Kušić, H., Lončarić Božić, A., Koprivanac, N., 2007. Fenton type processes for minimization of organic content in coloured wastewaters: Part I: Processes optimization. *Dye. Pigment.* 74, 380–387. doi:10.1016/j.dyepig.2006.02.022
- Langford, K.H., Thomas, K. V., 2009. Determination of pharmaceutical compounds in hospital effluents and their contribution to wastewater treatment works. *Environ. Int.* 35, 766–770. doi:10.1016/j.envint.2009.02.007
- Lapworth, D.J., Baran, N., Stuart, M.E., Ward, R.S., 2012. Emerging organic contaminants in groundwater: A review of sources, fate and occurrence. *Environ. Pollut.* 163, 287–303. doi:10.1016/j.envpol.2011.12.034
- Liberti, L., Di Milano, P., Zza, P., Da Vinci, L., 2006. Introduction to global optimization.
- Lopez, A., Mascolo, G., Detomaso, A., Lovecchio, G., Villani, G., 2005. Temperature activated degradation (mineralization) of 4-chloro-3-methyl phenol by Fenton's reagent. *Chemosphere* 59, 397–403. doi:10.1016/j.chemosphere.2004.10.060
- Manan, Z.A., Wan Alwi, S.R., Ujang, Z., 2006. Water pinch analysis for an urban system: a case study on the Sultan Ismail Mosque at the Universiti Teknologi Malaysia (UTM). *Desalination* 194, 52–68.

doi:10.1016/j.desal.2005.11.003

McLaughlin, L. A.; McLaugh, H. J.; Groff, K. A., 1992. Develop an effective wastewater treatment strategy. *Chem. Eng. Prog.* 1992, 88 (Sept), 34.

Messac, A., Ismail-Yahaya, A., Mattson, C.A., 2003. The normalized normal constraint method for generating the Pareto frontier. *Struct. Multidiscip. Optim.* 25, 86–98. doi:10.1007/s00158-002-0276-1

Miklos, D.B., Remy, C., Jekel, M., Linden, K.G., Drewes, J.E., Hübner, U., 2018. Evaluation of advanced oxidation processes for water and wastewater treatment – A critical review. *Water Res.* 139, 118–131. doi:10.1016/j.watres.2018.03.042

Miralles-Cuevas, S., Audino, F., Oller, I., Sánchez-Moreno, R., Sánchez Pérez, J.A., Malato, S., 2014. Pharmaceuticals removal from natural water by nanofiltration combined with advanced tertiary treatments (solar photo-Fenton, photo-Fenton-like Fe(III)–EDDS complex and ozonation). *Sep. Purif. Technol.* 122, 515–522. doi:10.1016/j.seppur.2013.12.006

Mishra, P.N., Fan, L.T., Erickson, L.E., 1975. Application of mathematical optimisation techniques in computer aided design of wastewater treatment systems. *AIChE Sym. Ser.* 71, 136–153.

Moctezuma, E., Leyva, E., Aguilar, C.A., Luna, R.A., Montalvo, C., 2012. Photocatalytic degradation of paracetamol: Intermediates and total reaction mechanism. *J. Hazard. Mater.* 243, 130–138. doi:10.1016/j.jhazmat.2012.10.010

Moles, C.G., Mendes, P., Banga J.R., 2003. Parameter Estimation in Biochemical Pathways: A Comparison of Global Optimization Methods. *Genome Res.* 13, 2467–2474. doi:10.1101/gr.1262503

Moreno-Benito, M., Yamal-Turbay, E., Espuña, A., Pérez-Moya, M., Graells, M., 2013. Optimal recipe design for Paracetamol degradation by advanced oxidation processes (AOPs) in a pilot plant. pp. 943–948. doi:10.1016/B978-0-444-63234-0.50158-5

Mosmann, T., 1983. Rapid colorimetric assay for cellular growth and survival: Application to proliferation and cytotoxicity assays. *J. Immunol. Methods* 65, 55–63. doi:10.1016/0022-1759(83)90303-4

References

- Muir, N., Nichols, J.D., Stillings, M.R., Sykes, J., 1997. Comparative bioavailability of aspirin and paracetamol following single dose administration of soluble and plain tablets. *Curr. Med. Res. Opin.* 13, 491–500. doi:10.1185/03007999709113322
- Murov, S.L.; Carmichael, I.; Hug, G.L., 1993. *Handbook of Photochemistry*, 2nd ed. ed. New York.
- National Research Council. 2003. *Beyond the Molecular Frontier: Challenges for Chemistry and Chemical Engineering*. Washington, DC: The National Academies Press. <https://doi.org/10.17226/10633>.
- Nichela, D.A., Berkovic, A.M., Costante, M.R., Juliarena, M.P., García Einschlag, F.S., 2013. Nitrobenzene degradation in Fenton-like systems using Cu(II) as catalyst. Comparison between Cu(II)- and Fe(III)-based systems. *Chem. Eng. J.* 228, 1148–1157. doi:10.1016/j.cej.2013.05.002
- Nocedal, J., Wächter, A., Waltz, R.A., 2009. Adaptive Barrier Update Strategies for Nonlinear Interior Methods. *SIAM J. Optim.* 19, 1674–1693. doi:10.1137/060649513
- Nogueira, R., Oliveira, M., Paterlini, W., 2005. Simple and fast spectrophotometric determination of H₂O₂ in photo-Fenton reactions using metavanadate. *Talanta* 66, 86–91. doi:10.1016/j.talanta.2004.10.001
- Novo, A., André, S., Viana, P., Nunes, O.C., Manaia, C.M., 2013. Antibiotic resistance, antimicrobial residues and bacterial community composition in urban wastewater. *Water Res.* 47, 1875–1887. doi:10.1016/j.watres.2013.01.010
- Oller, I., Malato, S., Sánchez-Pérez, J.A., Gernjak, W., Maldonado, M.I., Pérez-Estrada, L.A., Pulgarín, C., 2007a. A combined solar photocatalytic-biological field system for the mineralization of an industrial pollutant at pilot scale. *Catal. Today* 122, 150–159. doi:10.1016/j.cattod.2007.01.041
- Oller, I., Malato, S., Sánchez-Pérez, J.A., Maldonado, M.I., Gassó, R., 2007b. Detoxification of wastewater containing five common pesticides by

solar AOPs–biological coupled system. *Catal. Today* 129, 69–78.
doi:10.1016/j.cattod.2007.06.055

Oller, I., Malato, S., Sánchez-Pérez, J.A., Maldonado, M.I., Gernjak, W., Pérez-Estrada, L.A., Muñoz, J.A., Ramos, C., Pulgarín, C., 2007c. Pre-industrial-scale Combined Solar Photo-Fenton and Immobilized Biomass Activated-Sludge Biotreatment. *Ind. Eng. Chem. Res.* 46, 7467–7475.
doi:10.1021/ie070178v

Oller, I., Malato, S., Sánchez-Pérez, J.A., 2011. Combination of Advanced Oxidation Processes and biological treatments for wastewater decontamination—A review. *Sci. Total Environ.* 409, 4141–4166.
doi:10.1016/j.scitotenv.2010.08.061

Oppenländer, T., Baum, G., Egle, W., Hennig, T., 1995. Novel vacuum-UV- (VUV) and UV-excimer flow-through photoreactors for waste water treatment and for wavelength-selective photochemistry. *Proc. Indian Acad. Sci. - Chem. Sci.* 107. doi:10.1007/BF02869955

Oppenländer, T., 1997. Photochemische Methoden der Wasserbehandlung mit Excimer-Durchflußphotoreaktoren und Vakuum-UV-Oxidation eines Eisen-EDTA-Komplexes. *Chemie Ing. Tech.* 69, 1782–1786.
doi:10.1002/cite.330691221

Oppenländer, T., Gliese, S., 2000. Mineralization of organic micropollutants (homologous alcohols and phenols) in water by vacuum-UV-oxidation (H₂O-VUV) with an incoherent xenon-excimer lamp at 172 nm. *Chemosphere* 40, 15–21. doi:10.1016/S0045-6535(99)00222-2

Ortega-Gómez, E., Moreno Úbeda, J.C., Álvarez Hervás, J.D., Casas López, J.L., Santos-Juanes Jordá, L., Sánchez Pérez, J.A., 2012. Automatic dosage of hydrogen peroxide in solar photo-Fenton plants: Development of a control strategy for efficiency enhancement. *J. Hazard. Mater.* 237–238, 223–230. doi:10.1016/j.jhazmat.2012.08.031

Ortega-Gómez, E., Esteban García, B., Ballesteros Martín, M.M., Fernández Ibáñez, P., Sánchez Pérez, J.A., 2013. Inactivation of *Enterococcus faecalis* in simulated wastewater treatment plant effluent by solar photo-Fenton at initial neutral pH. *Catal. Today* 209, 195–200.
doi:10.1016/j.cattod.2013.03.001

References

- Ortiz de la Plata, G.B., Alfano, O.M., Cassano, A.E., 2010. Decomposition of 2-chlorophenol employing goethite as Fenton catalyst. I. Proposal of a feasible, combined reaction scheme of heterogeneous and homogeneous reactions. *Appl. Catal. B Environ.* 95, 1–13. doi:10.1016/j.apcatb.2009.12.005
- Pablos, C., Marugán, J., van Grieken, R., Serrano, E., 2013. Emerging micropollutant oxidation during disinfection processes using UV-C, UV-C/H₂O₂, UV-A/TiO₂ and UV-A/TiO₂/H₂O₂. *Water Res.* 47, 1237–1245. doi:10.1016/j.watres.2012.11.041
- Pagga, U., 1997. Testing biodegradability with standardized methods. *Chemosphere* 35, 2953–2972. doi:10.1016/S0045-6535(97)00262-2
- Pal, A., Gin, K.Y.-H., Lin, A.Y.-C., Reinhard, M., 2010. Impacts of emerging organic contaminants on freshwater resources: Review of recent occurrences, sources, fate and effects. *Sci. Total Environ.* 408, 6062–6069. doi:10.1016/j.scitotenv.2010.09.026
- Pareto, V., 1906. *Manuale di Economica Politica*, Societa Editrice Libreria. Milan.
- Pérez-Moya, M., Graells, M., del Valle, L.J., Centelles, E., Mansilla, H.D., 2007. Fenton and photo-Fenton degradation of 2-chlorophenol: Multivariate analysis and toxicity monitoring. *Catal. Today* 124, 163–171. doi:10.1016/j.cattod.2007.03.034
- Pérez-Moya, M., Graells, M., Buenestado, P., Mansilla, H.D., 2008. A comparative study on the empirical modeling of photo-Fenton treatment process performance. *Appl. Catal. B Environ.* 84, 313–323. doi:10.1016/j.apcatb.2008.04.010
- Pérez-Moya, M., Mansilla, H.D., Graells, M., 2011. A practical parametrical characterization of the Fenton and the photo-Fenton sulfamethazine treatment using semi-empirical modeling. *J. Chem. Technol. Biotechnol.* 86, 826–831. doi:10.1002/jctb.2595
- Pham, T.T.H., Brar, S.K., Tyagi, R.D., Surampalli, R.Y., 2010. Optimization of Fenton oxidation pre-treatment for *B. thuringiensis* – Based production

of value added products from wastewater sludge. *J. Environ. Manage.* 91, 1657–1664. doi:10.1016/j.jenvman.2010.03.007

Pignatello, J.J., 1992. Dark and photoassisted iron(3+)-catalyzed degradation of chlorophenoxy herbicides by hydrogen peroxide. *Environ. Sci. Technol.* 26, 944–951. doi:10.1021/es00029a012

Pignatello, J.J., Liu, D., Huston, P., 1999. Evidence for an Additional Oxidant in the Photoassisted Fenton Reaction. *Environ. Sci. Technol.* 33, 1832–1839. doi:10.1021/es980969b

Pignatello, J.J., Oliveros, E., MacKay, A., 2006. Advanced Oxidation Processes for Organic Contaminant Destruction Based on the Fenton Reaction and Related Chemistry. *Crit. Rev. Environ. Sci. Technol.* 36, 1–84. doi:10.1080/10643380500326564

Pintor, A.M.A., Vilar, V.J.P., Boaventura, R.A.R., 2011. Decontamination of cork wastewaters by solar-photo-Fenton process using cork bleaching wastewater as H₂O₂ source. *Sol. Energy* 85, 579–587. doi:10.1016/j.solener.2011.01.003

Prieto-Rodríguez, L., Oller, I., Zapata, A., Agüera, A., Malato, S., 2011. Hydrogen peroxide automatic dosing based on dissolved oxygen concentration during solar photo-Fenton. *Catal. Today* 161, 247–254. doi:10.1016/j.cattod.2010.11.017

Prieto-Rodríguez, L., Oller, I., Klamerth, N., Agüera, A., Rodríguez, E.M., Malato, S., 2013. Application of solar AOPs and ozonation for elimination of micropollutants in municipal wastewater treatment plant effluents. *Water Res.* 47, 1521–1528. doi:10.1016/j.watres.2012.11.002

Pulgarin, C., Kiwi, J., 1996. Overview on Photocatalytic and Electrocatalytic Pretreatment of Industrial Non-Biodegradable Pollutants and Pesticides. *Chimia (Aarau)*. 50.

Rabiet, M., Togola, A., Brissaud, F., Seidel, J.-L., Budzinski, H., Elbaz-Poulichet, F., 2006. Consequences of Treated Water Recycling as Regards Pharmaceuticals and Drugs in Surface and Ground Waters of a Medium-sized Mediterranean Catchment. *Environ. Sci. Technol.* 40, 5282–5288. doi:10.1021/es060528p

References

- Rad, L.R., Irani, M., Divsar, F., Pourahmad, H., Sayyafan, M.S., Haririan, I., 2015. Simultaneous degradation of phenol and paracetamol during photo-Fenton process: Design and optimization. *J. Taiwan Inst. Chem. Eng.* 47, 190–196. doi:10.1016/j.jtice.2014.10.014
- Rahim Pouran, S., Abdul Aziz, A.R., Wan Daud, W.M.A., 2015. Review on the main advances in photo-Fenton oxidation system for recalcitrant wastewaters. *J. Ind. Eng. Chem.* 21, 53–69. doi:10.1016/j.jiec.2014.05.005
- Ramirez, J.H., Costa, C.A., Madeira, L.M., 2005. Experimental design to optimize the degradation of the synthetic dye Orange II using Fenton's reagent. *Catal. Today* 107–108, 68–76. doi:10.1016/j.cattod.2005.07.060
- Ribeiro, A.R., Nunes, O.C., Pereira, M.F.R., Silva, A.M.T., 2015. An overview on the advanced oxidation processes applied for the treatment of water pollutants defined in the recently launched Directive 2013/39/EU. *Environ. Int.* 75, 33–51. doi:10.1016/j.envint.2014.10.027
- Rivas, F.J., Beltrán, F.J., Gimeno, O., Alvarez, P., 2003. Optimisation of Fenton's reagent usage as a pre-treatment for fermentation brines. *J. Hazard. Mater.* 96, 277–290. doi:10.1016/S0304-3894(02)00217-0
- Ross, A.B., Farhataziz, A., 1977. Selective specific rates of reactions of transients in water and aqueous solutions. Part III. Hydroxyl radical and perhydroxyl radical and their radical ions. *Natl. Stand. Ref. Data Ser., U S A Natl. Bur. Stand.* 59, 1–22.
- Rubio-Castro, E., Ponce-Ortega, J.M., Serna-González, M., El-Halwagi, M.M., 2012. Optimal reconfiguration of multi-plant water networks into an eco-industrial park. *Comput. Chem. Eng.* 44, 58–83. doi:10.1016/j.compchemeng.2012.05.004
- Salazar, C., Ridruejo, C., Brillas, E., Yáñez, J., Mansilla, H.D., Sirés, I., 2017. Abatement of the fluorinated antidepressant fluoxetine (Prozac) and its reaction by-products by electrochemical advanced methods. *Appl. Catal. B Environ.* 203, 189–198. doi:10.1016/j.apcatb.2016.10.026

- Santos-Juanes, L., Sánchez, J.L.G., López, J.L.C., Oller, I., Malato, S., Sánchez Pérez, J.A., 2011. Dissolved oxygen concentration: A key parameter in monitoring the photo-Fenton process. *Appl. Catal. B Environ.* 104, 316–323. doi:10.1016/j.apcatb.2011.03.013
- Shafiei, S., Domenech, S., Koteles, R., Paris, J., 2004. System closure in pulp and paper mills: network analysis by genetic algorithm. *J. Clean. Prod.* 12, 131–135. doi:10.1016/S0959-6526(02)00188-9
- Shokry, A., Audino, F., Vicente, P., Escudero, G., Moya, M.P., Graells, M., Espuña, A., 2015. Modeling and Simulation of Complex Nonlinear Dynamic Processes Using Data Based Models: Application to Photo-Fenton Process. pp. 191–196. doi:10.1016/B978-0-444-63578-5.50027-X
- Silva, A.M.T., Zilhão, N.R., Segundo, R.A., Azenha, M., Fidalgo, F., Silva, A.F., Faria, J.L., Teixeira, J., 2012. Photo-Fenton plus *Solanum nigrum* L. weed plants integrated process for the abatement of highly concentrated metalaxyl on waste waters. *Chem. Eng. J.* 184, 213–220. doi:10.1016/j.cej.2012.01.038
- Simunovic, M., Kusic, H., Koprivanac, N., Bozic, A.L., 2011. Treatment of simulated industrial wastewater by photo-Fenton process: Part II. The development of mechanistic model. *Chem. Eng. J.* 173, 280–289. doi:10.1016/j.cej.2010.09.030
- Soriano-Molina, P., García Sánchez, J.L., Alfano, O.M., Conte, L.O., Malato, S., Sánchez Pérez, J.A., 2018. Mechanistic modeling of solar photo-Fenton process with Fe³⁺-EDDS at neutral pH. *Appl. Catal. B Environ.* 233, 234–242. doi:10.1016/j.apcatb.2018.04.005
- Sun, J.-H., Sun, S.-P., Fan, M.-H., Guo, H.-Q., Lee, Y.-F., Sun, R.-X., 2008. Oxidative decomposition of p-nitroaniline in water by solar photo-Fenton advanced oxidation process. *J. Hazard. Mater.* 153, 187–193. doi:10.1016/j.jhazmat.2007.08.037
- Sun, Y., Pignatello, J.J., 1993a. Photochemical reactions involved in the total mineralization of 2,4-D by iron(3+)/hydrogen peroxide/UV. *Environ. Sci. Technol.* 27, 304–310. doi:10.1021/es00039a010
- Sun, Y., Pignatello, J.J., 1993b. Organic intermediates in the degradation of

References

- 2,4-dichlorophenoxyacetic acid by iron(3+)/hydrogen peroxide and iron(3+)/hydrogen peroxide/UV. *J. Agric. Food Chem.* 41, 1139–1142. doi:10.1021/jf00031a025
- Takama, N., Kuriyama, T., Shiroko, K., Umeda, T., 1980. Optimal water allocation in a petroleum refinery. *Comput. Chem. Eng.* 4, 251–258. doi:10.1016/0098-1354(80)85005-8
- Tawarmalani, M., Sahinidis, N. V., 2005. A polyhedral branch-and-cut approach to global optimization. *Math. Program.* 103, 225–249. doi:10.1007/s10107-005-0581-8
- Tekin, H., Bilkay, O., Ataberk, S., Balta, T., Ceribasi, I., Sanin, F., Dilek, F., Yetis, U., 2006. Use of Fenton oxidation to improve the biodegradability of a pharmaceutical wastewater. *J. Hazard. Mater.* 136, 258–265. doi:10.1016/j.jhazmat.2005.12.012
- Teodosiu C.; Barjoveanu G.; Teleman D., 2003. Sustainable Water Resources Management 1. River Basin Management and the EC Water Framework Directive. *Environ. Eng. Manag. J.* 2, 377–394.
- Ternes, T.A., 1998. Occurrence of drugs in German sewage treatment plants and rivers1Dedicated to Professor Dr. Klaus Haberer on the occasion of his 70th birthday.1. *Water Res.* 32, 3245–3260. doi:10.1016/S0043-1354(98)00099-2
- Tokumura, M., Katoh, H., Katoh, T., Znad, H.T., Kawase, Y., 2009. Solubilization of excess sludge in activated sludge process using the solar photo-Fenton reaction. *J. Hazard. Mater.* 162, 1390–1396. doi:10.1016/j.jhazmat.2008.06.026
- Tokumura, M., Morito, R., Hatayama, R., Kawase, Y., 2011. Iron redox cycling in hydroxyl radical generation during the photo-Fenton oxidative degradation: Dynamic change of hydroxyl radical concentration. *Appl. Catal. B Environ.* 106, 565–576. doi:10.1016/j.apcatb.2011.06.017
- Tokumura, M., Morito, R., Kawase, Y., 2013. Photo-Fenton process for simultaneous colored wastewater treatment and electricity and hydrogen production. *Chem. Eng. J.* 221, 81–89.

doi:10.1016/j.cej.2013.01.075

- Toro Santamaria, J.; Egner M.; Hirth, S.T.b.; Del Valle Mendoza, L.J.; Audino, F.; Pérez-Moya, M., 2017. Photo Induced Advanced Oxidation of Relevant Pollutants in Water without Additives, in: Proceedings of the 5th European Conference on Environmental Applications of Advanced Oxidation Processes, Prague, Czech Republic, 25–29 June 2017 (Ed.), .
- Trovó, A.G., Melo, S.A.S., Nogueira, R.F.P., 2008. Photodegradation of the pharmaceuticals amoxicillin, bezafibrate and paracetamol by the photo-Fenton process—Application to sewage treatment plant effluent. *J. Photochem. Photobiol. A Chem.* 198, 215–220. doi:10.1016/j.jphotochem.2008.03.011
- Trovó, A.G., Pupo Nogueira, R.F., Agüera, A., Fernandez-Alba, A.R., Malato, S., 2012. Paracetamol degradation intermediates and toxicity during photo-Fenton treatment using different iron species. *Water Res.* 46, 5374–5380. doi:10.1016/j.watres.2012.07.015
- Varga, M., Balogh, S., Csukas, B., 2016. An extensible, generic environmental process modelling framework with an example for a watershed of a shallow lake. *Environ. Model. Softw.* 75, 243–262. doi:10.1016/j.envsoft.2015.10.022
- Varga, M., Csukas, B., 2017. Generation of extensible ecosystem models from a network structure and from locally executable programs. *Ecol. Modell.* 364, 25–41. doi:10.1016/j.ecolmodel.2017.09.014
- Varga, M., Prokop, A., Csukas, B., 2017. Biosystem models, generated from a complex rule/reaction/influence network and from two functionality prototypes. *Biosystems* 152, 24–43. doi:10.1016/j.biosystems.2016.12.005
- Vilar, V.J.P., Moreira, F.C., Ferreira, A.C.C., Sousa, M.A., Gonçalves, C., Alpendurada, M.F., Boaventura, R.A.R., 2012. Biodegradability enhancement of a pesticide-containing bio-treated wastewater using a solar photo-Fenton treatment step followed by a biological oxidation process. *Water Res.* 46, 4599–4613. doi:10.1016/j.watres.2012.06.038
- Villegas-Guzman, P., Giannakis, S., Rtimi, S., Grandjean, D., Bensimon, M., de Alencastro, L.F., Torres-Palma, R., Pulgarin, C., 2017. A green solar

References

- photo-Fenton process for the elimination of bacteria and micropollutants in municipal wastewater treatment using mineral iron and natural organic acids. *Appl. Catal. B Environ.* 219, 538–549. doi:10.1016/j.apcatb.2017.07.066
- Villota, N., Lomas, J.M., Camarero, L.M., 2018. Kinetic modelling of water-color changes in a photo-Fenton system applied to oxidate paracetamol. *J. Photochem. Photobiol. A Chem.* 356, 573–579. doi:10.1016/j.jphotochem.2018.01.040
- von Wedel, L., Marquardt, W., 2000. Rome: A repository to support the integration of models over the lifecycle of model-based engineering processes. *Comput. Aided Chem. Eng.* doi:10.1016/S1570-7946(00)80091-7
- Walling, C., Goosen, A., 1973. Mechanism of the ferric ion catalyzed decomposition of hydrogen peroxide. Effect of organic substrates. *J. Am. Chem. Soc.* 95, 2987–2991. doi:10.1021/ja00790a042
- Wang, Y.P., Smith, R., 1994a. Wastewater minimisation. *Chem. Eng. Sci.* 49, 981–1006. doi:10.1016/0009-2509(94)80006-5
- Wang, Y.-P., Smith, R., 1994b. Design of distributed effluent treatment systems. *Chem. Eng. Sci.* 49, 3127–3145. doi:10.1016/0009-2509(94)E0126-B
- Wang, Y.P., Smith, R., 1995. Wastewater minimization with flowrate constraints. *Chem. Eng. Res. Des.* 73, 889–904.
- Wang, N., Zheng, T., Zhang, G., Wang, P., 2016. A review on Fenton-like processes for organic wastewater treatment. *J. Environ. Chem. Eng.* 4, 762–787. doi:10.1016/j.jece.2015.12.016
- Yamal-Turbay, E., Graells, M., Pérez-Moya, M., 2012. Systematic Assessment of the Influence of Hydrogen Peroxide Dosage on Caffeine Degradation by the Photo-Fenton Process. *Ind. Eng. Chem. Res.* 51, 4770–4778. doi:10.1021/ie202256k
- Yamal-Turbay, E., Jaén, E., Graells, M., Pérez-Moya, M., 2013. Enhanced

photo-Fenton process for tetracycline degradation using efficient hydrogen peroxide dosage. *J. Photochem. Photobiol. A Chem.* 267, 11–16. doi:10.1016/j.jphotochem.2013.05.008

Yamal-Turbay, E., Ortega, E., Conte, L.O., Graells, M., Mansilla, H.D., Alfano, O.M., Pérez-Moya, M., 2015. Photonic efficiency of the photodegradation of paracetamol in water by the photo-Fenton process. *Environ. Sci. Pollut. Res.* 22, 938–945. doi:10.1007/s11356-014-2990-9

Yang, L., Salcedo-Diaz, R., Grossmann, I.E., 2014. Water Network Optimization with Wastewater Regeneration Models. *Ind. Eng. Chem. Res.* 53, 17680–17695. doi:10.1021/ie500978h

Zapata, A., Oller, I., Rizzo, L., Hilgert, S., Maldonado, M.I., Sánchez-Pérez, J.A., Malato, S., 2010. Evaluation of operating parameters involved in solar photo-Fenton treatment of wastewater: Interdependence of initial pollutant concentration, temperature and iron concentration. *Appl. Catal. B Environ.* 97, 292–298. doi:10.1016/j.apcatb.2010.04.020

Zhang, Y., Pagilla, K., 2010. Treatment of malathion pesticide wastewater with nanofiltration and photo-Fenton oxidation. *Desalination* 263, 36–44. doi:10.1016/j.desal.2010.06.031

Appendix A: Scientific production

A. Journals publications

- Francesca Audino, Gerard Companya; Moisès Graells; Antonio Espuña; Montserrat Pérez-Moya, 2019, Systematic Optimisation Approach for the Efficient Management of the Photo-Fenton Treatment Process. *Science of the Total Environment*, Volume 646, Pages 902-913. DOI: <https://doi.org/10.1016/j.scitotenv.2018.07.057>.
- F. Audino, L. O. Conte, A. Schenone, M. Pérez-Moya, M. Graells, and O. M. Alfano, 2019, A Kinetic Study for the Fenton and photo-Fenton Paracetamol Degradation in an Annular Photoreactor with an Explicit Assessment of Local Volumetric Rate of Photon Absorption. *Environmental Science and Pollution Research (ESPR) Journal of the Photo-Fenton Treatment Process*, Volume 26, Issue 5, Pages 4312–4323. DOI: <https://doi.org/10.1007/s11356-018-3098-4>.
- Francesca Audino, Jorge Mario Toro Santamaria, Luis Javier Del Valle Mendoza, Moisès Graells Sobre, Montserrat Pérez-Moya, 2019, Removal of Paracetamol Using Effective Advanced Oxidation Processes. *International Journal of Environmental Research and Public Health*, 16, 505. DOI: <https://doi.org/10.3390/ijerph16030505>.

B. Journals publications published before starting the PhD

- S.Miralles-Cuevas, F.Audino, I.Oller, R.Sánchez-Moreno, J.A.Sánchez Pérez, S.Malato, 2014, Pharmaceuticals removal from natural water by nanofiltration combined with advanced tertiary treatments (solar photo-Fenton, photo-Fenton-like Fe(III)–EDDS complex and ozonation). *Separation and Purification Technology*, Volume 122, Pages 515-522. DOI: <https://doi.org/10.1016/j.seppur.2013.12.006>.

C. Conference proceedings

- Ahmed Shokry, Francesca Audino, Patricia Vicente, Gerard Escudero, Montserrat Perez Moya, Moisès Graells, Antonio Espuña, 2015, Modelling and Simulation of Complex Nonlinear Dynamic Processes Using Data Based Models: Application to Photo-Fenton Process. *Computer Aided Chemical Engineering*, Volume 37, Pages 191-196. DOI: <https://doi.org/10.1016/B978-0-444-63578-5.50027-X>.
- Francesca Audino, Sergio Medina Gonzalez, Moisès Graells, Montserrat Pérez-Moya, Antonio Espuña, Carlos Alberto Méndez, 2017, Optimisation of a Distributed Wastewater Treatment Network Considering Lumped Parameters Interrelations. *Computer Aided Chemical Engineering*, Volume 40, Pages 2701-2706. DOI: <https://doi.org/10.1016/B978-0-444-63965-3.50452-9>.
- Francesca Audino, Leandro Conte, Agustina Schenone, Montserrat Pérez-Moya, Moisès Graells, Orlando Mario Alfano, 2017, A Kinetic Study for the Fenton and Photo-Fenton Paracetamol Degradation in a Pilot Plant Reactor. *Computer Aided Chemical Engineering*, Volume 40, Pages 301-306. DOI: <https://doi.org/10.1016/B978-0-444-63965-3.50052-0>.
- Francesca Audino, Mónica Varga, Montserrat Pérez-Moya, Moisès Graells, Antonio Espuña, Béla Csukás, 2018, Experiments and Direct Computer Mapping Based Model for Photo-Fenton Process. *Computer Aided Chemical Engineering*, Volume 43, Pages 223-228. DOI: <https://doi.org/10.1016/B978-0-444-64235-6.50040-1>.

D. Presentations in Conferences

- Poster presentation: Ahmed Shokry, [Francesca Audino](#), Patricia Vicente, Gerard Escudero, Montserrat Perez Moya, Moisès Graells, and Antonio Espuña. Modelling and Simulation of Complex Nonlinear Dynamic Processes Using Data Based Models: Application to Photo-Fenton Process. 12th PSE and 25th ESCAPE Joint Event Copenhagen, Denmark, 31st May – 4th June 2015.
- Oral presentation: F. Audino, G. Companya, M. Graells, A. Espuña, [M. Pérez-Moya](#), Dynamic Simulation and Optimisation of a Fed-Batch Photo-Fenton Process. VIII Meeting on Environmental Application of Advanced Oxidation Processes VIII EPOA, and II Iberoamerican Congress of Advanced Oxidation Technologies II CIPOA, Belo Horizonte, Brazil, 3rd - 6th November 2015.
- Poster presentation: [Carlos Jiménez-Moreno](#), Francesca Audino, Moisès Graells, Kinetic modelling of the photo-Fenton reaction and parameter fitting: a

comparative study. 22th International Congress of Chemical and Process Engineering (CHISA), Prague, Czech Republic, 27th -31st August 2016.

- Poster presentation: Francesca Audino, Javier Yus Cobo, Noemí Fradejas Rojo, Montserrat Pérez Moya, Kinetic modelling of the photo-Fenton reaction and parameter fitting: a comparative study. 5th European Conference on Environmental Applications of Advanced Oxidation Processes (EAAOP5), Prague, Czech Republic, 25th -29th June 2017.
- Poster presentation: Toro Santamaria, J. M., Egner, S., Hirth, T., Del Valle Mendoza, L. J., Audino, F., Perez-Moya, M., Photo Induced Advanced Oxidation of Relevant Pollutants in Water Without Additives. 5th European Conference on Environmental Applications of Advanced Oxidation Processes (EAAOP5), Prague, Czech Republic, 25th -29th June 2017.
- Oral presentation: Audino F., Sanz J., Parrellada E., Graells M., and Pérez-Moya M., Influence of Fenton Reagent Ratios and of Hydrogen Peroxide Dosage on the Photo-Fenton Process Efficiency. 15th International Conference on Environmental Science and Technology (CEST2017), Rhodes, Greece, 31st August -2nd September 2017.
- Poster presentation: Audino F., Conte L. O., Schenone A., Pérez-Moya M., Graells M., Alfano O. M., A Kinetic Study for the Fenton and Photo-Fenton Paracetamol Degradation in a Pilot Plant Reactor. 27th European Symposium on Computer Aided Process Engineering – ESCAPE 27, Barcelona, Spain, 1st -5th October 2017.
- Poster presentation: Audino F., Medina-González S., Graells M., Pérez-Moya M., Espuña A., Méndez C., Optimisation of a Distributed Wastewater Treatment Network Considering Lumped Parameters Interrelations. 27th European Symposium on Computer Aided Process Engineering – ESCAPE 27, Barcelona, Spain, 1st -5th October 2017.
- Poster and short oral presentation: F. Audino, L. Conte, A. Schenone, M. Pérez-Moya, M. Graells, M.A. Orlando, A Kinetic Study for the Fenton and photo-Fenton Paracetamol Degradation in an Annular Photoreactor Involving LVRPA. 3rd Iberoamerican Conference on Advanced Oxidation Technologies (III CIPOA) and 2nd Colombian Conference on Advanced Oxidation Processes (II CCPAOX), Medellín (Guatapé), Colombia, 14th -17th October 2017.

Advanced Oxidation Process Models for Optimisation and Decision Making support in Water Management

- Poster presentation: Francesca Audino, Mónica Varga, Montserrat Pérez-Moya, Moisés Graells, Antonio Espuña, and Béla Csukás, Experiments and Direct Computer Mapping Based Model for Photo-Fenton Process. 28th European Symposium on Computer Aided Process Engineering –ESCAPE28, Graz, Austria, 10th - 13th June 2018.
- Oral presentation: Audino Francesca. Varga Mónica. Csukás Béla. Pérez-Moya Montserrat. Graells Moisés. Espuña Antonio, Toward a Generalized, Simplified, First Principles Model for Photo-Fenton Process Based Degradation of Harmful Contaminants (CECs). The 10th European meeting on Solar Chemistry and Photocatalysis: Environmental Applications (SPEA10), Almería, Spain, 4th -8th June 2018.
- Poster presentation: Audino F., Toro Santamaria J. M., Graells M., Egner S., Hirth T., Pérez-Moya M., Removal of Paracetamol by Photo-induced Advanced Oxidation without Additives. The 10th European meeting on Solar Chemistry and Photocatalysis: Environmental Applications (SPEA10), Almería, Spain, 4th -8th June 2018.

E. Attendance to Workshops, Meetings and Summer Schools

- 13th Mediterranean Congress of Chemical Engineering. SEQUI, FIRA BARCELONA, EXPOQUIMIA. Barcelona, Spain, 30th September-3rd October 2014.
- 20th Conference of the International Federation of Operational Research Societies (IFORS). EURO (The Association of European Operational Research Societies), SEIO (Spanish Society of Statistics and Operations Research), UPC (Universitat Politècnica de Catalunya - Barcelona Tech), FIB (Facultat d'Informàtica de Barcelona). Barcelona, Spain, 13th -18th July 2014.
- 1st Summer School on Environmental applications of Advanced Oxidation Processes . European PhD School on Advanced Oxidation Processes, University of Salerno, Department of Civil Engineering (Italy). Salerno, Italy, 15th -19th June 2015.
- Canada-Spain Workshop on AOPs, AOPs and Ozone Fundamentals Updates and Current Industrial Applications. Universitat de Barcelona, CIEMAT-PSA. Barcelona, Spain, 7th -8th July 2016.

- IV Reunión Nacional de Grupos de Fotocatálisis. Universitat de Extremadura. Badajoz, Spain, 22nd -23rd September 2016.
- Escuela de verano de Ingeniería de Procesos. Universitat Politècnica de Catalunya. Barcelona, Spain, 18th -20th July 2018.

F. Investigation projects:

- Centre d'enginyeria de processos, energia i medi ambient, 2014 SGR 1092. Agència de Gestió d'Ajuts Universitaris i de Recerca- AGAUR.
- Sistema integrado de la gestión de la energía y los recursos ambientales para procesos industriales económicamente sostenibles, DPI2012-37154-C02-01. Ministerio de Economía, Industria y Competitividad-MINECO.
- Sistema integrado de la gestión de la energía y los recursos ambientales para procesos industriales económicamente sostenibles, DPI2012-37154-C02-01. Ministerio de Economía, Industria y Competitividad-MINECO.
- Advanced Integration Methods for Efficient Symbiosis in Process Networks, DPI2017-87435-R. Ministerio de Ciencia, Innovación y Universidades-MICINN.

G. Scholarships

- Estancias Breves en Centros I+D (Predoctorales) 2014. EEBB-I-15-10301. Ministerio de Economía, Industria y Competitividad-MINECO.
- Estancias Breves en Centros I+D (Predoctorales) 2016 EEBB-I-17-12418. Ministerio de Economía, Industria y Competitividad-MINECO.
- Ayudas para Contratos Predoctorales. BES-2013-065545. Ministerio de Economía, Industria y Competitividad-MINECO.

H. Stays

Advanced Oxidation Process Models for Optimisation and Decision Making support in Water Management

- Investigation centre, University: Universidad Nacional del Litoral (UNL)-
Instituto de Desarrollo Tecnológico para la Industria Química (INTEC)-Consejo Nacional
de Investigaciones Científicas y Técnicas (CONICET) Santa Fe

Director: Carlos Alberto Méndez

Place: Santa Fe (Argentina)

Date: 28th July-04th December 2015

- Investigation centre, University: Universidad Nacional del Litoral (UNL)-
Instituto de Desarrollo Tecnológico para la Industria Química (INTEC)-Consejo Nacional
de Investigaciones Científicas y Técnicas (CONICET) Santa Fe

Director: Orlando Mario Alfano

Place: Santa Fe (Argentina)

Date: 04th February-04th June 2017